

Blind Benchmark Predictions of the NACOK Air Ingress Tests Using the CFD Code FLUENT

by

Marie-Anne V. Brudieu

Diplome d'Ingenieur
Ecole Polytechnique, France 2005

Submitted to the Department of Nuclear Engineering
In partial fulfillment of the requirements for the degrees of

Master of Science in Nuclear Engineering

at the

MASSACHUSETTS INSTITUTE OF TECHNOLOGY

February, 2007

Copyright © 2007 Massachusetts Institute of Technology. All Rights Reserved.

Author.....

Department of Nuclear Engineering
January 15, 2007

Certified by.....

Professor of the Practice of Nuclear Engineering **Andrew C. Kadak**
Thesis Supervisor

Certified by

Assistant Professor **Jacopo Buongiorno**
Thesis Reader

Accepted by.....

Associate Professor **Jeffrey A. Coderre**
Chairman, Department Committee on Graduate Students

[This page is left intentionally blank]

Blind Benchmark Predictions of the NACOK Air Ingress Tests Using the CFD Code FLUENT

by

Marie-Anne V. Brudieu

Submitted to the Department of Nuclear Science and Engineering
on January 15, 2006, in partial fulfillment of the
requirements for the degree of
Master of Science in Nuclear Science and Engineering

Abstract

The JAERI and NACOK experiments examine the combined effects of natural convection during an air ingress event: diffusion, onset of natural circulation, graphite oxidation and multicomponent chemical reactions. MIT has been benchmarking JAERI tests using the FLUENT code for approximately three years [1]. This work demonstrated that the three fundamental physical phenomena of diffusion, natural circulation and then chemical reactions can be effectively modeled using computational fluid dynamics.

The latest series of tests conducted at the NACOK facility were two graphite corrosion experiments: The first test consisted of an open chimney configuration heated to 650C with a pebble bed zones of graphite pebbles and graphite reflectors. The second test is a similar test with a cold leg adjacent to the hot channel with an open return duct below the hot channel. Natural circulation, diffusion and graphite corrosion were studied for both tests. Using and adapting previous computational methods, the FLUENT code is used to blind benchmark these experiments. The objective is to assess the adequacy of the modeling method used in this blind benchmarking analysis by comparing these blind test predictions to the actual data and then modify the model to improve predictive capability. Ultimately, the objective is to develop a benchmarked analysis capability that can be used for real reactors calculations, and to improve the understanding of the physical phenomena taking place during an air ingress event.

This thesis presents the modeling process of these experiments, the blind model results and the comparison of the blind computed data with experimental data. Sensitivity studies provide a good understanding of the different phenomena occurring during an air ingress event. The blind benchmarking demonstrates the ability of FLUENT to model satisfactorily in full scale the NACOK air ingress experiment. The blind models are then improved to successfully model air ingress events. An important finding of this work is that there is great variability in graphite corrosion data and that good qualification of specific graphite used is vital to predicting the effects of an air ingress event.

Thesis Supervisor: Professor Andrew C. Kadak, Professor of the Practice

Acknowledgments

I would like to express my deep gratitude to Prof. Andrew Kadak for all his help and support during these 18 months. His kindness and positive views were a real motivation.

Financial support for this thesis was provided by Westinghouse Nuclear. They also showed great interest in the thesis which was a an amazing reward and motivation for further work.

I would like to acknowledge the great help of Rachel Morton and Wenfeng Liu who supported me with patience through FLUENT technical difficulties. I am grateful to Prof Buongiorno for reading this thesis through all the typos and mistakes and I am fondly acknowledging Nicephore and all my friends who offered a compassionate ear to my complaints.

I would like to express all my love to my family back in France, who never doubted of my success. I am deeply thankful for Eric and the Walkers who became my family on this side of the pond and offered me love and support.

Contents

1	Introduction	1
1.1	Context	1
1.2	The Pebble Bed Modular Reactor (PBMR) [5]	3
1.3	The air ingress accident	7
1.3.1	Description of the phenomena	7
1.3.2	Past experiments and Benchmarks	10
2	The NACOK experiments (Naturzug im Core mit Korrosion)	18
2.1	NACOK	18
2.2	The new air ingress experiments	21
2.2.1	Description of the Open Chimney Test (March 2004)	21
2.2.2	Description of the Return-Duct Test (July 2004)	26
2.3	Materials and graphite	28
2.3.1	The reflector graphite: ASR-1RS	28
2.3.2	The matrix pebble graphite: A3-3	29
2.4	Visualisation of the NACOK experiment	29
3	Modeling NACOK with FLUENT	33
3.1	Validation of a Computational Fluid Dynamics Code [10], [11]	33
3.2	Procedure followed for the blind benchmarking of the NACOK experiments	35

3.3	Detailed description of the general FLUENT model used in NACOK computations, [12], [26]	37
4	Chemistry models in the event of an air ingress accident	47
4.1	Chemistry in an air ingress event	47
4.1.1	Reactions	47
4.1.2	Mechanisms and Regimes of graphite corrosion	49
4.2	Modeling chemistry in FLUENT	51
4.2.1	Species transport	51
4.2.2	Chemistry model [12]	52
4.3	Graphite corrosion reaction rates	53
4.4	Reaction rates input in FLUENT	56
4.4.1	Correlations chosen for the NACOK graphite oxidation modeling	56
4.4.2	Carbon monoxide oxidation reaction rate	58
4.4.3	Boudouard reaction rate	59
4.4.4	Stoichiometry variation of the graphite oxidation reaction with temperature	59
4.4.5	Importance of the burn-off on graphite oxidation rate	61
5	Sensitivity studies	62
5.1	Pressure loss in the pebble beds	62
5.2	Modeling the reflector as a porous media	67
5.3	Modeling diffusion mass transfer	70
5.4	Modeling steady state flow for the return duct chimney	74
5.5	Chemistry Sensitivity studies	76
6	Results of the Benchmarking of the Open Chimney Test, March 2004	84
6.1	The Blind Benchmark Model	85

6.1.1	Description	85
6.1.2	First estimate of graphite loss	85
6.1.3	Results	87
6.1.4	Further analysis of the experimental results	93
6.2	Other models and runs	97
6.2.1	Temperature of 900C	97
6.2.2	Modified chemistry model	97
7	Results of the Benchmarking of the Return Chimney Test, July 2004	103
7.1	Stage one of Blind Benchmarking : the diffusion process and onset of natural convection	105
7.1.1	The transient diffusion model	106
7.1.2	Results	107
7.2	Stage two of Blind Benchmarking: Steady state calculation of the hot channel final state	109
7.2.1	The steady state model	109
7.2.2	Results	110
7.3	The modified model	113
8	Conclusions and Future Work	117
8.0.1	Future work	119
9	Summary of the main variables in FLUENT models	120
	Nomenclature Table	121
	Appendices	127

List of Figures

1-1	PBMR power conversion cycle	4
1-2	PBMR plant diagram	5
1-3	Fuel pebbles	6
1-4	Natural circulation process after a break in a coaxial pipe . .	8
1-5	Air ingress accident stages in a pebble bed reactor	9
1-6	Interaction between air ingress event parameters	10
1-7	The JAERI experimental configuration	12
1-8	The JAERI mesh, 490 hexahedral cells and 1850 mixed cells	13
1-9	Mole Fraction of N2 Benchmarking of the Isothermal JAERI Experiment	14
1-10	Comparison of mole fraction change of nitrogen between the gas sampling positions H-1 and C-1 in the thermal experiment	15
1-11	Example of good agreement between simulation and experi- ment on JAERI multi-component experiment at H3 measure point. At time 100 min, one can observe the onset of natural convection	16
2-1	Overall set up of the NACOK experimental facility	19
2-2	Photo of the set up of the NACOK experimental facility[13]	20
2-3	Open chimney experiment drawing [13]	23
2-4	Lower channel experimental setting for open chimney exper- iments[13]	24

2-5	Mesh of the lower channel, when reflectors are modeled in detail	25
2-6	Plans and picture of arrangement for the 96 channels reflectors and lower reflector. Top left: top view of the lower reflectors. Top right and bottom left: top view of the fine reflectors. Bottom right: picture of the fine reflectors.	26
2-7	Global experimental setting for return duct experiments	27
2-8	Initial temperature distribution in the return duct experiment	28
2-9	Lower channel set up	30
2-10	Reflectors. On the left, before the experiment, on the right, after the experiment [13]	31
2-11	Entry chamber, with four graphite columns. On the left, before the experiment, on the right, after the experiment [13]	31
2-12	60 mm diameter pebbles. The cables are linked to temperature and species measurement devices located in the lower chimney and pebble bed	32
3-1	Zones name in the FLUENT model	38
4-1	Corrosion Regimes	50
4-2	Comparison of the graphite oxidation and Boudouard reaction rates $(\widetilde{R}_{C,r})$	54
4-3	Various correlations of stoichiometry coefficient ratio evolution with respect to the temperature	60
5-1	5 m high pebble bed pressure drop (Pa) vs. air flow velocity (m/s) as input in FLUENT, Kuhlmann correlation and power law equation	64
5-2	Comparison between Ex (Experiments) and Co (Computations) for the natural convection NACOK test: superficial velocity option	66

5-3	Comparison between Ex (Experiments) and Co (Computations) for the natural convection NACOK test: physical velocity option	66
5-4	Detailed 96 channels reflector as modeled for the sensitivity studies	69
5-5	Comparison of the pressure loss at different flow velocities for a detailed reflector model and simplified porous media model	69
5-6	Comparison between theoretical curves as calculated by PBMR [33] and FLUENT kinetic model of the diffusion in a vertical tube	72
5-7	Model configuration for diffusion sensitivity analysis	73
5-8	Evolution of the mass fraction of helium in an open horizontal tube (in the center of the square) in a volume filled with nitrogen. Red (dark) corresponds to a mass fraction of helium = 1 and blue (light) to a mass fraction of helium = 0	73
5-9	Temperature distribution in Kelvins in the hot and cold leg	74
5-10	Mass flow rate with respect to time steps. A steady state is reached for a mass flow rate of $4.3g.s^{-1}$	75
5-11	Chemistry sensitivity studies model	76
5-12	Evolution of the species molar fraction with respect to time	78
6-1	Mesh of the lower part of the experiment	86
6-2	Estimate of the maximum graphite loss in 8 hours	88
6-3	Flow Temperature distribution in the open chimney test	89
6-4	Computed molar fractions in the open chimney test. Experimental data not available	90
6-5	Mass fractions of CO_2 on the left, CO in the middle and O_2 on the right	91
6-6	Velocity distribution in the lower part of the channel in $m.s^{-1}$	92

7-1	Geometry and mesh and of the main channel, return ducts and surroundings	106
7-2	Diffusion process in the return duct experiment at 80 seconds and 163 min. The scale represents the nitrogen mass fraction.	107
7-3	Diffusion process in the return duct experiment at 4.4 hours and onset of natural convection. The scale represents the nitrogen mass fraction.	108
7-4	Temperature Experimental conditions of the external walls of the main channel	111
7-5	Experimental Gas Temperature at different height levels. hXXX corresponds to the height in mm and the names refer to the instruments in the return duct experiment.	112
7-6	Comparison of computed and experimental temperatures for the blind FLUENT return duct experiment at 8 hours	114

List of Tables

1.1	PBMR design parameters	4
2.1	ASR-1RS properties [9]	29
3.1	Mixture properties [12]	43
4.1	Chemical reactions taking place during an air ingress event .	48
5.1	Stoichiometry sensitivity study	79
5.2	Corrosion reaction rates sensitivity study for same flow rates and initial temperatures of 923 K	80
5.3	Boudouard reaction sensitivity analysis	81
5.4	Stoichiometry sensitivity study with UDF	82
6.1	Open chimney computation and experiment key results . . .	88
6.2	Graphite corrosion location for the blind model	96
6.3	Comparison of computed and experimental temperatures for the adapted and blind FLUENT open chimney model	99
6.4	Graphite corrosion location for the blind and adapted model	100
7.1	Comparison of computed and experimental temperatures for the blind FLUENT return duct experiment	113
7.2	Comparison of computed and experimental temperatures for the blind FLUENT return duct experiment	115

7.3	Graphite corrosion location for the adapted model of the return duct experiment	116
9.1	Modifiable variables in FLUENT models	120

Chapter 1

Introduction

1.1 Context

The United States of America and more generally the world, is experiencing times of great change in the energy market, consumption and production. The Generation IV initiative [7] was launched to answer the challenges raised by this new growing demand for clean energy. There are different designs of Generation IV reactors undergoing current research and development. One of these reactors, the Very High Temperature Reactor, utilizes graphite for moderation and helium for coolant. Its core can be either prismatic or a pebble bed. The electricity production of this reactor comes from more efficient Brayton cycles, with coolant outlet temperatures ranging from 850C to 950C. The high temperatures produced by these types of reactors provide the possibility to use them for many other applications, including Hydrogen production.

This thesis focuses on the safety of Pebble Bed reactors during an hypothetical air ingress accident. The Pebble Bed Modular Reactor, (PBMR) is being developed in the Republic of South Africa by PBMR, Pty Limited. Another version of a pebble bed reactor is also being developed in China. The first PBMR is scheduled to be operated by 2012 by ESKOM, the South African government owned electrical utility. Westinghouse is currently working to provide design expertise for the ESKOM utility's Pebble-Bed Modular Reactor and prepare for future licensing in the United

States. The safety of High Temperature Gas-Cooled Reactors, is recognized as a significant attribute of this type of reactor. Indeed, one of the most interesting features of these reactors lies in the fact that they do not need complex emergency cooling systems. In all accident situations, the heat can be removed by natural circulation without active core cooling systems. An other significant advantage is that this type of reactor is inherently safe, and as a result, it can not melt down.

An important accident scenario that some raise as a concern about graphite moderated reactors, is the issue of the potential for graphite corrosion and the possibility of a fire caused by air ingress events. In this type of accident, a break in the primary circuit, for instance a coaxial pipe between the reactor vessel and the power conversion system, allows the ingress of surrounding air in the reactor core. The air reacts with the graphite of the reflector as well as the graphite of the fuel pebbles in a complex set of exothermic and endothermic reactions. The species produced during these reactions are mainly CO (carbon monoxide) and CO_2 (carbon dioxide). Therefore, the key issue in this accident scenario is to be able to predict what damage will be done to the graphite, the overall reactor structure and the fuel. It is also essential to know temperatures reached and estimate the amount of CO produced as well as the amount of oxygen available in the reactor to determine whether burning occurs. Once these parameters are known and understood, an estimate can be made on the risk of graphite burning and damage to the core.

Various experimental and computational studies of the overall problem were performed over many years. [1], [2], [3], [4]. These studies attempted to take into account the key parameters of the accident and several complex effects: fluid dynamics, species diffusion, onset of natural circulation, temperature distribution, heterogeneous and homogeneous chemical reactions depending on temperature and species distributions, heat transfer and removal, chemical species and mass transport. The work presented in this thesis is part of the general effort to improve understanding and modeling of air ingress events. More particularly, the main goal of this thesis is to benchmark a computational fluid dynamics code, FLUENT, to air ingress experiments run at the NACOK facility located at the Jülich Center in Germany. The benchmarking is blind, meaning that the physical FLUENT models were developed

without access to the experimental results data. This benchmarking of the code confirms that the methods used in FLUENT can be used to understand and study the events of air ingress in the reactor. The secondary goal for this thesis is to develop a better understanding of the phenomena taking place during the air ingress accident and the interactions between various parameters. It is hoped that this improved understanding will be used to identify key factors affecting the progression of the event and to take appropriate mitigating measures.

This introductory chapter presents the PBMR design, the air ingress accident and a summary of past analysis performed on the issue at MIT .

1.2 The Pebble Bed Modular Reactor (PBMR) [5]

Design Description

The PBMR reactor is designed to produce 165 MWe using 400 MWth, which makes it a small reactor, adaptable to many different types of markets due to its modularity and high temperature. The PBMR is a direct Brayton gas cycle plant schematically shown on Figure 1-1:

1. Helium gas is passed into the reactor and flow through the pebble bed where heat is produced. The gas is heated up to 900C at a pressure of 69 bar.
2. The gas flows through the turbine which drives a generator
3. Helium goes then through a recuperator where it is reheated.
4. The gas then goes through stages of recuperator, inter cooling, recooling and compression before re-entering the core at 540C.

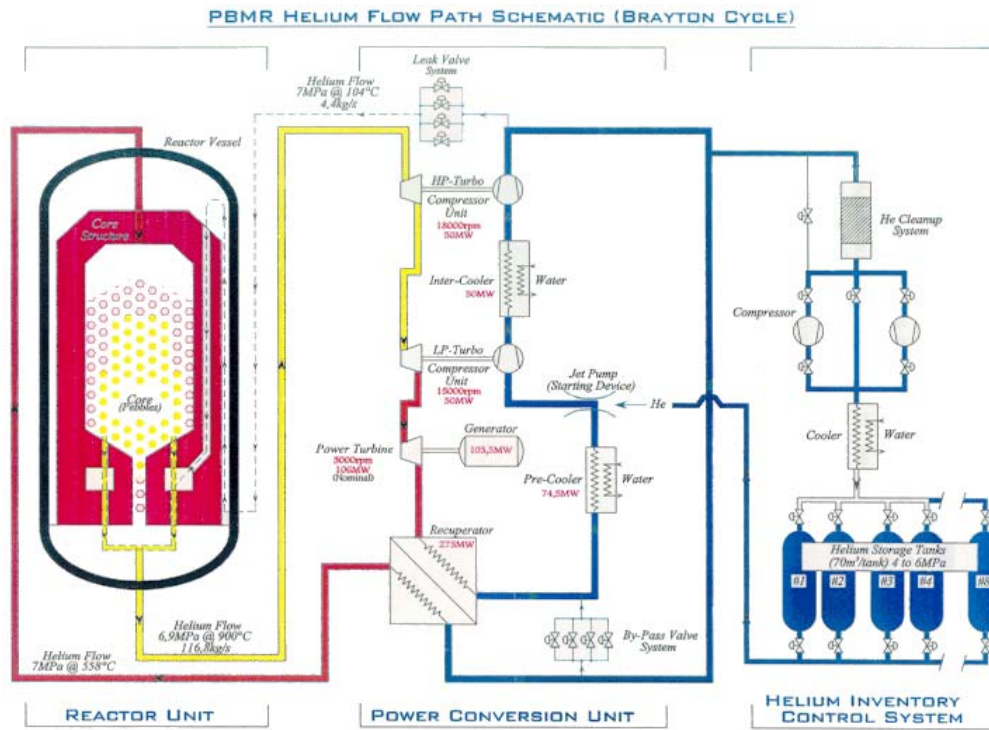


Figure 1-1: PBMR power conversion cycle

Table 1.1 summarizes the main design parameters and Figure 1-2 presents the overall layout of the key power turbine conversion elements of the plant:

Table 1.1: PBMR design parameters

450 000 spheres
Pressure vessel: 6.2 m diameter and 27 m high
Outer reflector: 1 m thick graphite blocks
Inlet core coolant: 540C, Outlet core coolant: 900C
Inlet turbine coolant: 900C, Outlet turbine coolant: 500C
Core pressure: 9 Mpa
Turbine outlet pressure: 2.6Mpa
Thermal efficiency: 40

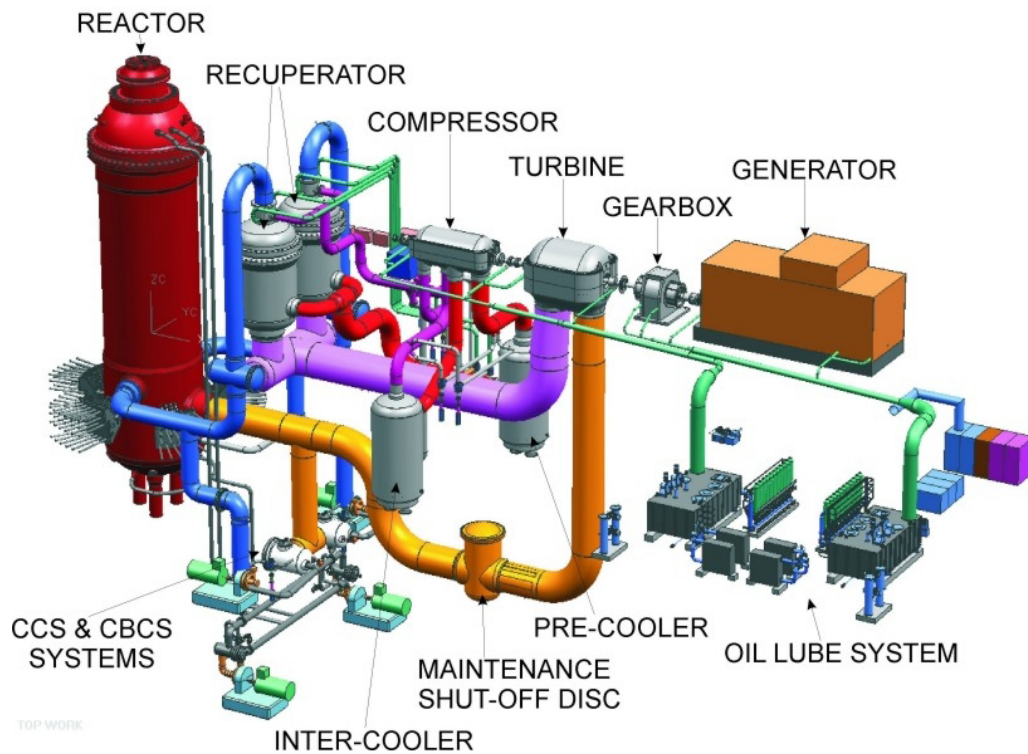


Figure 1-2: PBMR plant diagram

Fuel

The PBMR does not have a pressure tight containment to prevent leakage of the radioactive materials from the primary pressure boundary. This function is provided by the silicon carbide coated fuel micro sphere contained in the pebbles, designed to contain fission products during accidents and transients. Approximately 11 000 coated fuel particles are contained in a single graphite pebble which also has an outer graphite shell as shown on Figure 1-3. The reactor is loaded with 440 000 spheres, a fourth of them being simple graphite unfueled moderator spheres. The PBMR operates with an online refueling system, pebbles being added to the core from the top and removed at the bottom. Depending on the amount of uranium left in the sphere, it is either sent to storage or reloaded in the core. The storage of the pebbles is easier than standard fuel, since the used pebbles can be stored in casks in air cooled rooms in the basement of the reactor building due to the overall lower decay heat produced by each pebble.

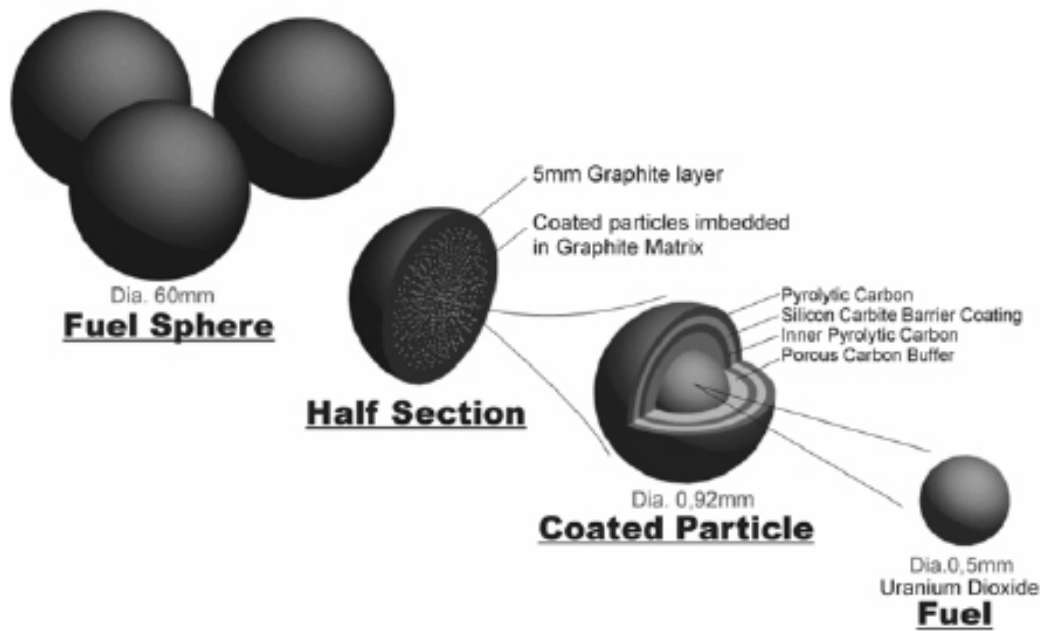


Figure 1-3: **Fuel pebbles**

Safety Features

The micro sphere fuel particles can be degraded at temperatures higher than 1800C. The inherent safety design of the reactor keeps the temperature below 1600C under most severe conditions. The core is designed such that it has a high surface area to volume ratio. In addition, the core configuration relies on conduction to transfer heat out of the core to the vessel. The heat can be effectively removed through the reactor vessel surface by conduction and convection to the reactor cavity. As a result, meltdown can not occur in the event of a loss of coolant accident. [5]

The coolant, helium, is an inert gas, both chemically and radiologically if impurities are minimized. It does not react with oxides and will not cause corrosion of parts of the core. Moreover, this allows the use of a direct cycle, since even in the case of leakage of helium, little or no radioactivity will escape.

1.3 The air ingress accident

1.3.1 Description of the phenomena

Massive air ingress accidents have a very low occurrence probability but can have severe consequences. Therefore, it is an issue that will be carefully reviewed during the licensing process of the PBMR in the Republic of South Africa and in the USA.

An important aspect of the design bases of the plant is to establish credible accident scenarios that must be addressed by the designer. The establishment of these design bases accidents will be based on regulatory decisions informed by probabilistic risk analysis on the likelihood of failures causing air ingress. For light water reactors, double ended guillotine breaks is a standard design bases accidents. For the purpose of describing a worst case (but not credible) loss of coolant accident (LOCA) scenario, a double ended guillotine break is analyzed for pebble bed reactors as well. In the event of a double end pipe break or other type of LOCA, the first stage of the accident is a loss of helium with depressurization. This occurs until atmospheric conditions are reached. In the mean time, there is a rise in the core temperature. This rise is slow due to the fact that graphite has a high heat capacity, that is, a high capability to store and transfer heat. There is no air ingress in the core as long as the helium pressure in the reactor vessel remains higher than the outside atmospheric pressure. Once the outside and inside pressures are at equilibrium, air being heavier than helium, it enters the core very slowly by molecular and thermal diffusion. reactor vessel remains higher than the outside atmospheric pressure. Once the outside and inside pressures are at equilibrium, air being heavier than helium, it enters the core very slowly by molecular and thermal diffusion.

This process can take a long time, depending on the location of the break and overall reactor condition [8]. As air enters in contact with hot graphite, chemical exothermic and endothermic oxidation reactions occur. Multidimensional localized natural convection will enhance species transport. Due to the reactions, the temperature of the incoming gas rises and its density therefore decreases. Buoyancy forces increase with the temperature gradient. This leads, at some point, to the onset of

natural circulation (Figure 1-4). In the case of a coaxial pipe break, this physical mechanism leads to air entering the reactor core, rising up to the top and going out through the breach of the outer tube of the coaxial pipe .

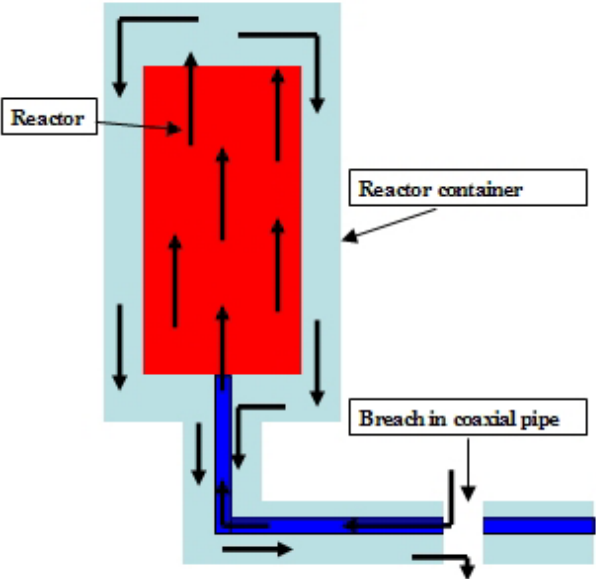


Figure 1-4: **Natural circulation process after a break in a coaxial pipe**

The circulation of air also provides a cooling function for the core. (passive cooling system). However, it also brings a supply of fresh air with oxygen, allowing more oxidation of the graphite to occur, which raises the temperature due to the dominance of exothermic oxidation reactions. A major issue is then to determine the temperature increase of the core as a combination of the heat stored in graphite, the energy deposited or removed by the endothermic and exothermic chemical reactions and the heat removed by convection. Knowing the temperatures in the core will help determine air ingress velocities, the concentrations of CO and CO₂ and ultimately whether the graphite might burn.

The other important feature is the corrosion of the structural graphite. It is vitally important to be able to predict the location and mass loss along with the total corrosion. The integrity of the structure as well as the evolution of its mechanical and thermal properties will strongly depend on how the structural graphite is chemically reacted and structurally affected.

The stages of an air ingress accident are shown on Figure 1-5. The first figure on the left shows the depressurization stage in which helium exits the core until atmospheric pressure is reached. The middle figure shows the slow diffusion stage, when air enters by diffusion through the core. The third figure shows the natural convection stage, when air circulates through the core.

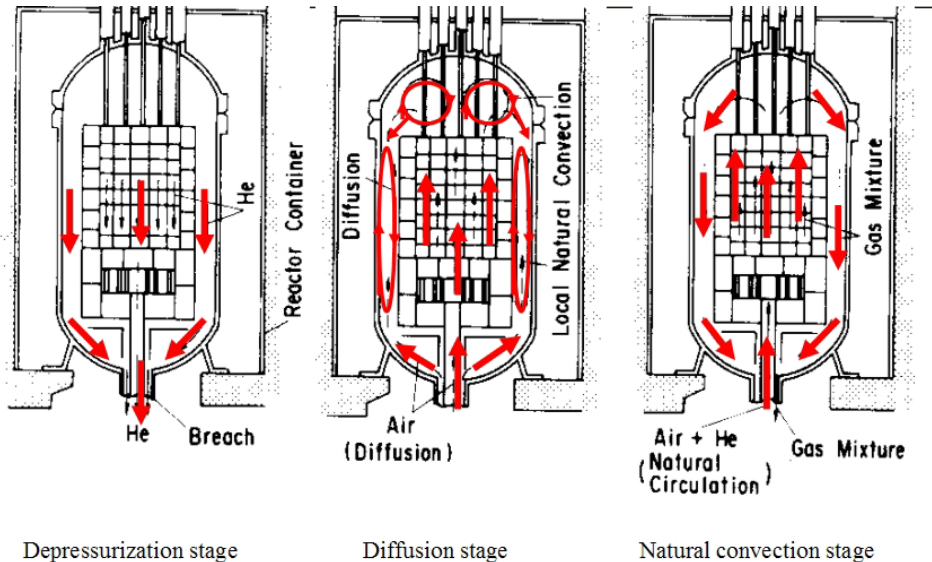


Figure 1-5: Air ingress accident stages in a pebble bed reactor

To understand the air ingress phenomena, it is necessary to be able to predict the following parameters:

- The speed at which air diffuses in the helium cooled core.
- The time of onset of natural convection.
- The oxidation rate of the graphite of the reflector and pebbles.
- The temperature distribution in the reactor core. The balance between the cooling due to air ingress and the temperature rise due to decay heat and graphite corrosion.
- The amount of graphite corroded and its location (preservation of the integrity of the reactor).

- The velocity of air in different locations of the core and the air mass flow rate.

Several parameters and features interact with each other in a complex manner to determine air ingress accident progression. Figure 1-6 presents a diagram showing the interactions between several parameters. For instance, one can see that the temperature distribution will affect the corrosion reactions, the Boudouard endothermic reaction (reaction of CO_2 with graphite) and the mass flow rate. The temperature is going to be affected by the geometrical layout of the core and piping as well as the type of graphite. Figure 1-6 shows therefore the complexity of correlations between several structural and physical characteristics of the core during an air ingress event.

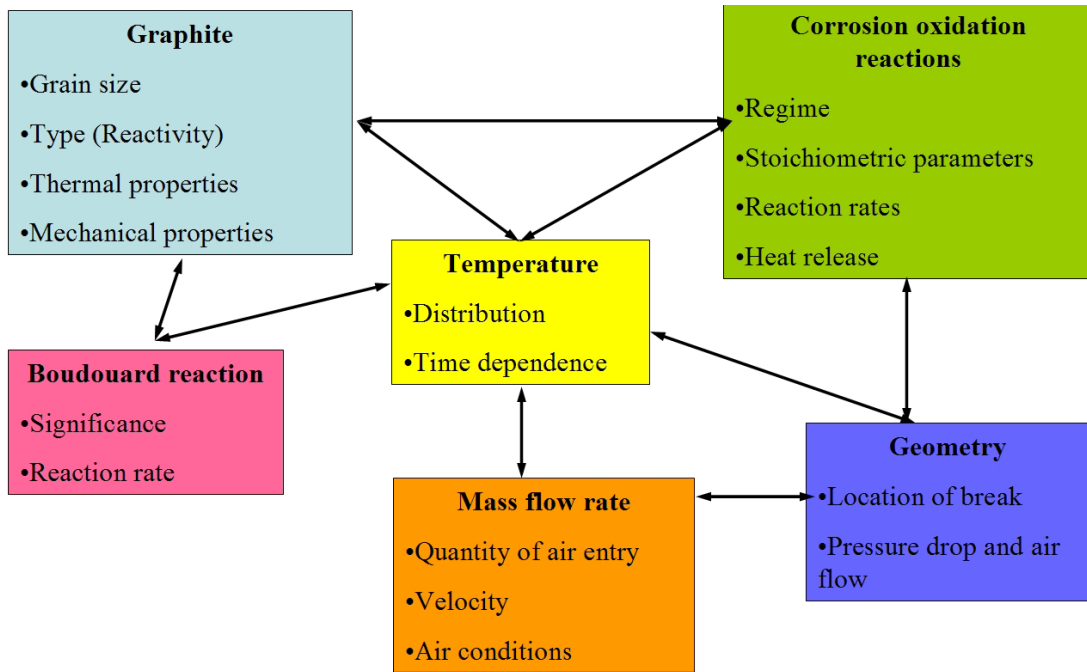


Figure 1-6: Interaction between air ingress event parameters

1.3.2 Past experiments and Benchmarks

The Japan Atomic Research Energy Institute has hosted a series of experiments designed to study the parameters and phenomena taking place during air ingress [4]. Three basic experiments were performed by JAERI, included separate study of diffusion, onset of natural convection and a complete multicomponent air ingress simulation with graphite and air. MIT has benchmarked FLUENT using these three

JAERI air ingress experiments [1], [6]. The experimental apparatus consisted of a reverse U-shaped tube and a gas tank as shown on Figure 1-7. A temperature gradient could be applied to the tube creating a hot and cold leg. A graphite tube could be inserted in the heated pipe section to simulate a reflector flow channel. The experiments simulated were each focused on a different phenomenon. The first experiment, called isothermal experiment, was designed to study the diffusion of nitrogen in helium in an isothermal environment. The second experiment studied the onset of natural circulation. The reverse U tube was heated on one side and a natural convection flow took place from the hot leg to the cold leg. Finally, a multi-component experiment with a graphite tube inserted simulating an air ingress event was studied. Molecular diffusion, natural convections and corrosion were studied in this experiment. The modeling approach presented in this thesis follows the same approach used by the scientists at JAERI namely different phenomena were studied separately (diffusion, flow, chemistry). Once well understood, they were combined. Indeed, a very good insight on the phenomena and their sensitivity to different parameters can be gained from this method.

A complete model was developed with FLUENT to model the JAERI experiments in 2003 [1]. Results and comparison with experimental data were very satisfying for diffusion, thermal and multi-component simulations. This work showed that the FLUENT model and methodology is able to predict each separate physical phenomena occurring during air ingress accidents in a simple geometry. Not only were the chemical reactions well modeled as a function of time but also the onset of natural circulation was well predicted. FLUENT ability to simulate air ingress accidents was also investigated by Lim and No [2], [3]. They successfully benchmarked the CFD code on small scale experiments with simple geometries and protocols (two bulbs diffusion experiment, annular flow tube Takahashi experiment, Circular flow tube Ogawa experiment and the JAERI experiments). This proves the ability of FLUENT to model separate effects of air ingress events in small configurations.

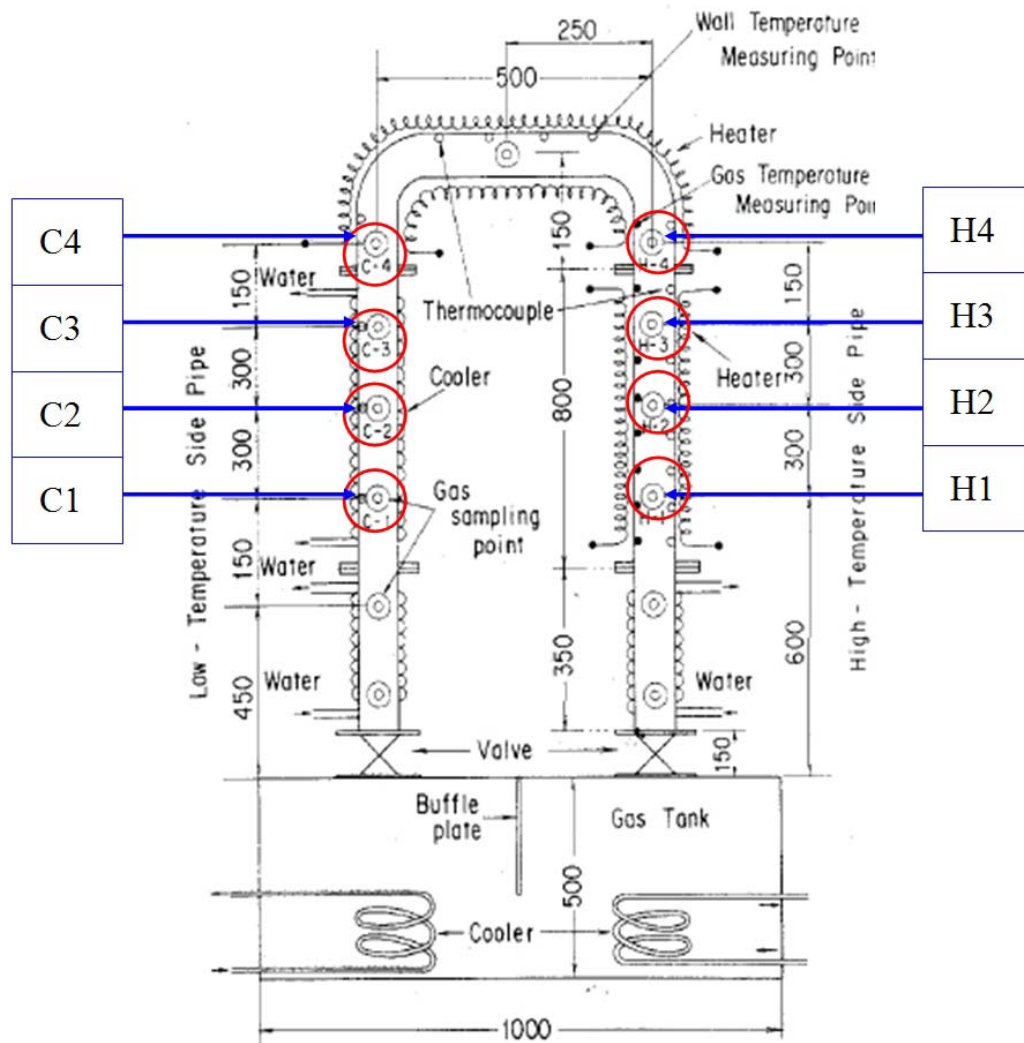


Figure 1-7: The JAERI experimental configuration

The MIT benchmarking of the JAERI diffusion experiment [1]

The boundary condition in this experiment is that all the wall temperatures are equal to the environment temperature, 18 C. Before opening of the isolation valves, there is 100% He in the pipe region and 100% N₂ in the gas tank region. No disturbance is involved in this pure diffusion process. Figure 1-8 shows the geometry and mesh developed by Zhai. The properties of He and N₂, such as the specific heat, conductance, density and viscosity, were all from the ideal gas database of FLUENT.

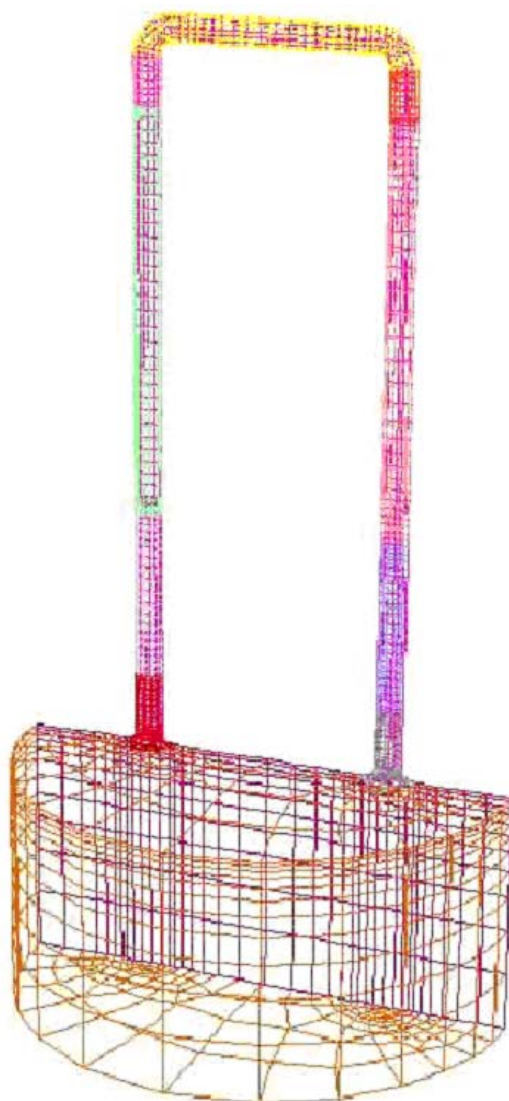


Figure 1-8: **The JAERI mesh, 490 hexahedral cells and 1850 mixed cells**

Figure 1-9 shows the experimental and calculated mole fraction changes of N₂ at various gas sampling positions for the isothermal experiment. H1, H2, H3, H4 refer to 4 points monitored in the hot leg, and C1, C2, C3, C4 refer to 4 points monitored in the cold leg. The calculation is in good agreement with the experiment in which diffusion is the only phenomenon occurring. This benchmarking showed that the modeling procedure applied in FLUENT can be used to model the diffusion stage of air ingress.

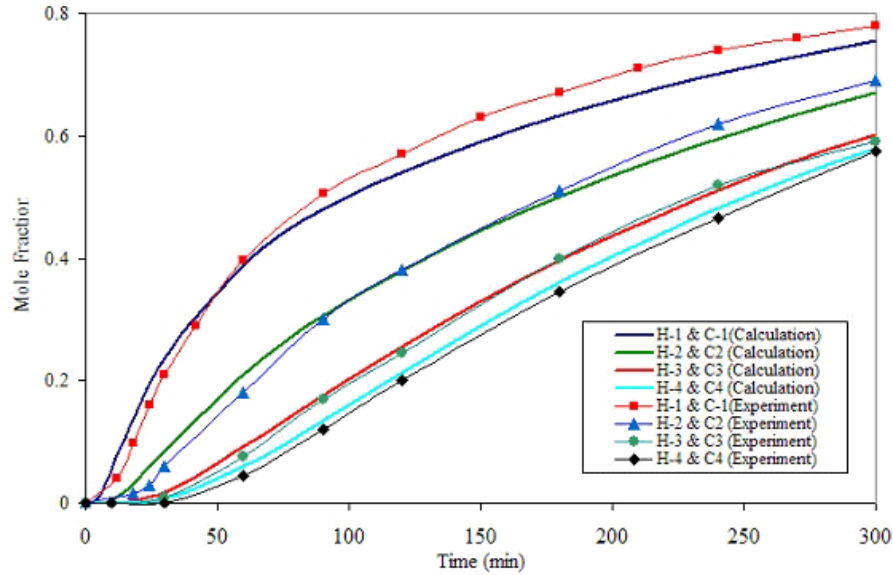


Figure 1-9: Mole Fraction of N2 Benchmarking of the Isothermal JAERI Experiment

The MIT benchmarking of the JAERI thermal experiment [1]

The purpose of this experiment is to provide a temperature gradient between the hot and cold legs to assess the onset of natural circulation. Thus, in this experiment, diffusion of nitrogen in helium is enhanced by the temperature difference and the density difference in the hot and cold legs which ultimately produces natural circulation. For the thermal experiment, the same facility as in the diffusion experiment is used, but the hot leg is heated 256C and the cold leg is maintained at 20C.

The mole fraction change of N2 and the initiation time of the natural circulation of pure nitrogen is shown on Figure 1-10. As can be seen, the agreement of the FLUENT calculation with the experiment is very good, demonstrating the ability to model the second phase of the air ingress phenomenon using the CFD tool.

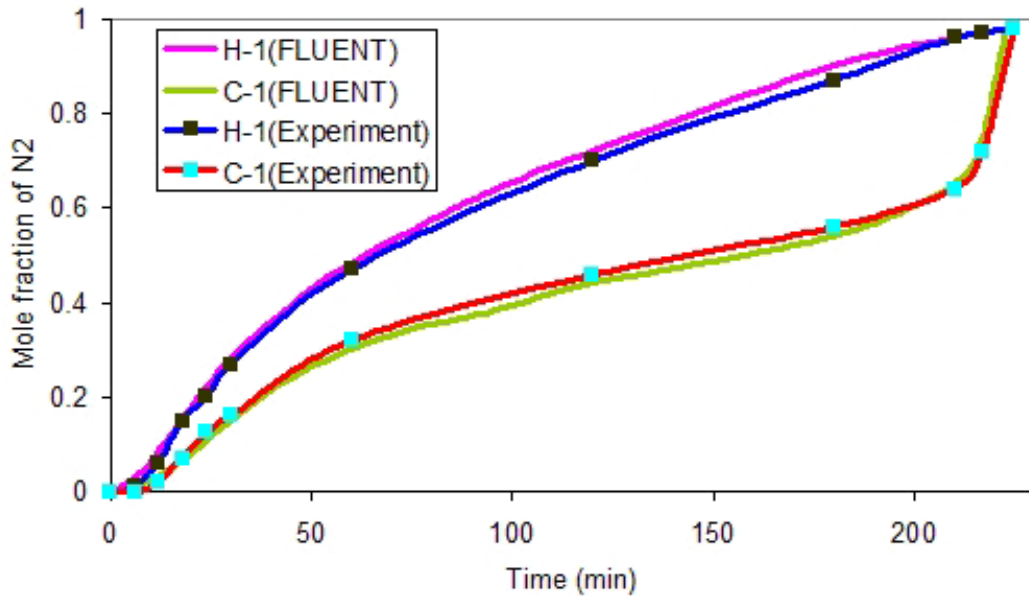


Figure 1-10: Comparison of mole fraction change of nitrogen between the gas sampling positions H-1 and C-1 in the thermal experiment

The MIT benchmarking of the JAERI multi component experiment [1]

The multi-component experiment was set up to investigate the integrated phenomena of molecular diffusion and natural convection with graphite oxidation in a multi-component gas system. The objectives of the multi-component experiment is to investigate the basic features of the flow behavior of the multi-component gas mixture, consisting of He, N₂, O₂, CO, CO₂, etc. This experiment tests all major phenomena in an air ingress event for prismatic reactors. 100% Helium is injected into the tube and air is injected into the gas tank. The high-temperature side pipe and the connecting pipe are heated from about 400C to 800C. The initial conditions for the multi-component experiment are as follows: the total pressure in the system is set equal to the atmospheric pressure, no gas flow exists before the opening of both valves. A time equals zero, both valves are open simultaneously and air is allowed to diffuse into the test chamber. An integrated transient multi-component chemical model was used to simulate diffusion, natural circulation as well as chemical reactions.

The results show quite good agreement with experimental data at the measured points for O₂, CO and CO₂ mole fractions as can be seen on Figure 1-11. Using the model developed for this experiment, the FLUENT code also shows excellent agreement on the onset of natural circulation. Natural circulation occurs in the multi-component experiment when the buoyancy produced by density difference between the hot and cold leg is high enough to overcome the friction in the flow path. Almost all the oxygen was consumed during the diffusion stage, but in natural circulation stage, most of the oxygen escaped from the graphite section of the test assembly. Moreover, the dominant reaction production is CO₂, not CO due to the rapid CO oxidation rate and high oxygen concentration, while most of the immediate product at the graphite surface is CO. This benchmarking performed by Zhai demonstrated that their modeling of air ingress process was valid.

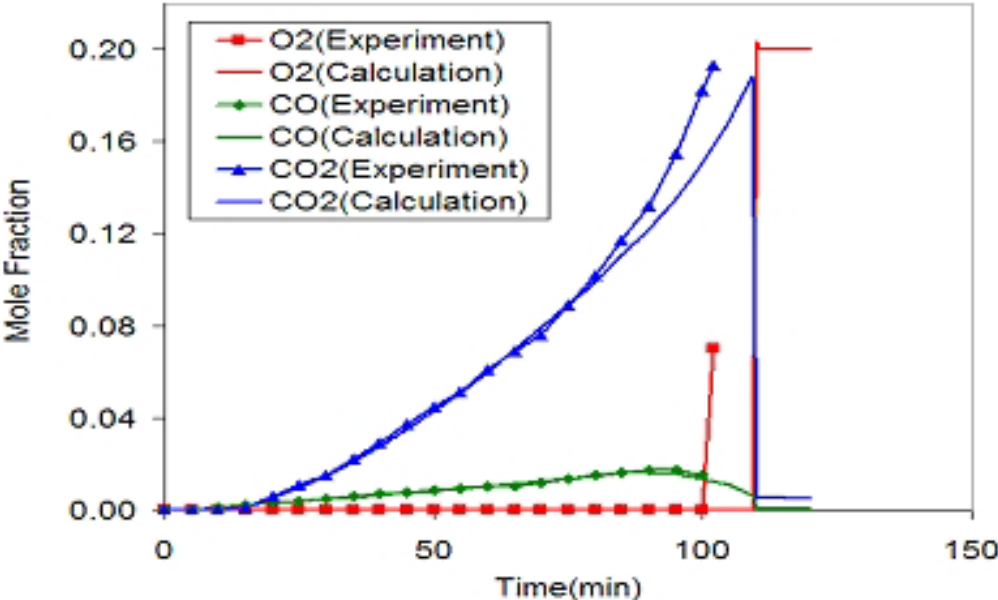


Figure 1-11: **Example of good agreement between simulation and experiment on JAERI multi-component experiment at H3 measure point. At time 100 min, one can observe the onset of natural convection**

One should bear in mind that the JAERI experiments were done to investigate an air ingress accident in a prismatic reactor. Therefore, further work was needed on pebble bed reactor. To do so, the Jülich Forschungszentrum in Jülich, Germany, built the NACOK facility. NACOK stands, for Natural Convection and Corrosion

in the Core. These experiments feature a full scale complex investigation of an air ingress accident in a pebble bed reactor. They are presented in detail in the following chapter.

Chapter 2

The NACOK experiments (Naturzug im Core mit Korrosion)

2.1 NACOK

The NACOK experimental facility was built more than 13 years ago at the Jülich Research Center in Germany to study the effects of airflow driven by natural convection in the event of the complete rupture of the coaxial hot gas duct. The main goals of the facility are to determine:

- The natural convection air mass flow and its dependence on temperatures and geometrical parameters.
- The time of onset of natural convection, that is the time between the break of the coaxial duct and the start of major air inflow.
- The locally dependent corrosion of graphite.
- The formation of gases and aerosols (dust).
- The temperature distribution and heat generated by exothermic reactions.

The other goal of the experimental set up is also to collect sufficient data to allow the benchmarking of several codes, such as TINTE, THERMIX-DIREKT and in our case, FLUENT.

The overall experimental arrangement can be seen on Figure 2-1 and 2-2.

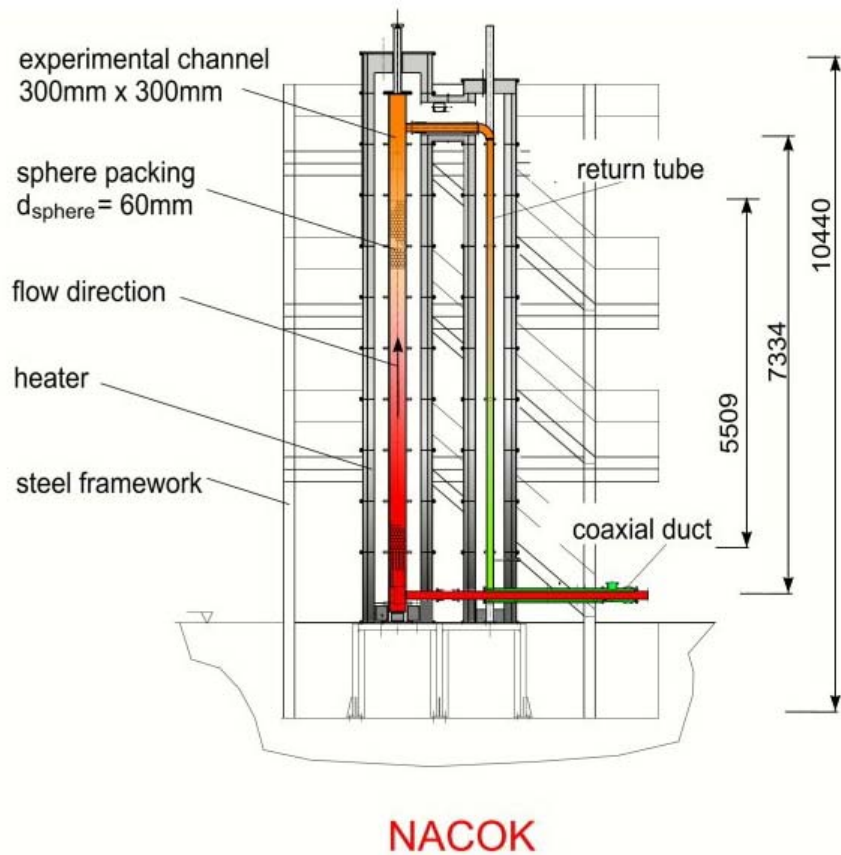


Figure 2-1: Overall set up of the NACOK experimental facility

The main features are:

- A chimney of 7.3 m high.
- A return duct
- Different sections in the main channel : bottom reflector, sphere packing and top reflector.
- Measurement devices for temperature, pressure and species composition.
- External variable heaters and temperature controls set up for different sections of the experimental channel and return duct.



Figure 2-2: **Photo of the set up of the NACOK experimental facility**[13]

Several series of experiments have been run at this facility in the past. The first tests to be thoroughly documented were performed in 1999 and reported by Kuhlmann [8]. The first series of tests were to study natural circulation in a hot and cold leg (return duct set-up). The second test was an open chimney corrosion test simulating the lower reflector and graphite pebbles. These early experiments were not designed to supply exact data relevant to multicomponent experiments. As a result of these tests, additional questions were raised: determination of reaction rates or species transfer mechanisms, temperature attained in the corrosion zone, location of the corrosion, variation of the mass flow depending on the gas atmosphere, influence of various parameters on corrosion and mass flow and in leakage to the experimental apparatus. For all these reasons, these early tests were not able to provide reliable quantitative data in order to assess the impact of chemical reactions

on graphite mass loss and temperature distribution. The qualitative results are however of high interest for a blind benchmarking analysis. They allow us to check whether the qualitative and quantitative computational results make sense.

Available public information on past experiments provide the following data:

- The temperature can go up to 1500C in the HTR and up to 1200C in the NACOK. [8]
- The mass flow rates in the NACOK are in the gram range (between $1g.s^{-1}$ and $15g.s^{-1}$)
- The time of onset of natural convection is in the hour range. For a specific setup, it was of about 8 hours.

This information allows the reader to have a better feeling of the size and functioning of the NACOK experiment. Such informations were also valuable for a qualitative evaluation of the first blind computational results.

2.2 The new air ingress experiments

The most recent series of tests were performed in March 2004 and July 2004 for PBMR. After making modifications to the NACOK facility addressing the concern of earlier tests and to allow for the collection of reliable data upon which to benchmark codes for future analysis. The first test was the open chimney corrosion test and the second, a return duct corrosion test. These tests are not completely documented at this time, and it is the purpose of this section, to give an outline of their experimental configuration and procedures.

2.2.1 Description of the Open Chimney Test (March 2004)

Configuration

The NACOK facility was configured to allow the hot leg to vent to the atmosphere as shown on Figure 2-3. The hot leg was heated to a uniform temperature of 650C. The test fluid is nitrogen. This temperature is maintained by wired heaters around

the chimney during the experiment. The heated internal walls are then maintained at this minimum temperature during the entire air ingress experiment. The interior of the lower part of the chimney consists almost entirely of graphite. The lowest part of the channel is the reflector. It is composed of two sets of ASR-1RS graphite blocks with vertical cylindrical holes of 40 mm and then 16 mm diameter. The properties of this graphite are very similar to the IG-110 used in Japan. Above the reflectors, there are two different beds of pebbles (60mm and 30 mm diameter) made of A3-3 matrix graphite of 350 mm and 600 mm heights respectively. The porosity of the pebble beds is 0.395. The porosity is the ratio of pores volumes over total volume:

$$Porosity = \frac{VolumePores}{TotalVolume} = 0.395 \quad (2.1)$$

The lower bed is made of the bigger pebbles. Above the pebble beds lies a long empty zone until the top of the chimney, at a height of 8316mm. A flow measurement device at the entrance of the channel induces a pressure drop that would not exist in natural conditions. The experimental set up is shown on Figure 2-3, 2-4, 2-5 and 2-6.

Experimental procedure

Nitrogen at 650C is initially blown into the experimental apparatus for a sufficiently long time to ensure that all components are at thermal equilibrium equal to 650C. Once this equilibrium is established, the pressure is equalized with atmospheric pressure. At the time $t = 0s$, the entrance duct is opened and air from the building is allowed to enter. Outside temperature and humidity as well as the inlet flow are recorded. These parameters were stable over the duration of the experiment (Relative humidity of 29% and temperature of 22C). Temperature sensors and gas composition analysis devices are placed in the experimental channel at different radius values for data recording. Data also recorded at various heights temperature values and species fractions. This data was not made available to this study prior to the analysis.

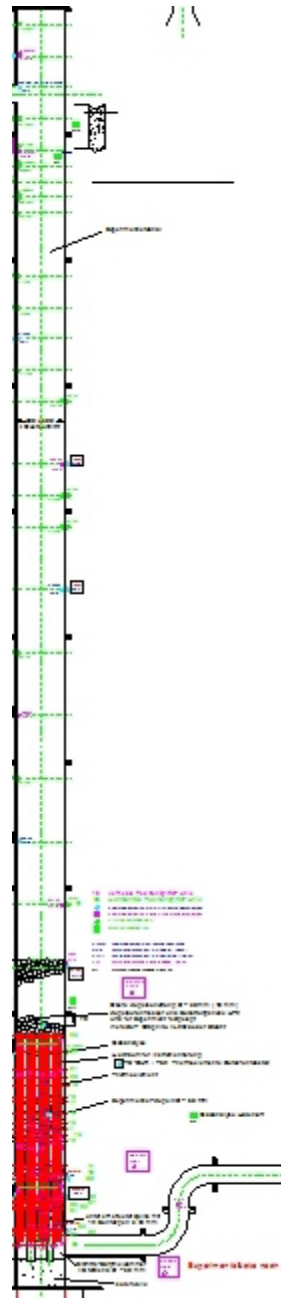


Figure 2-3: Open chimney experiment drawing [13]

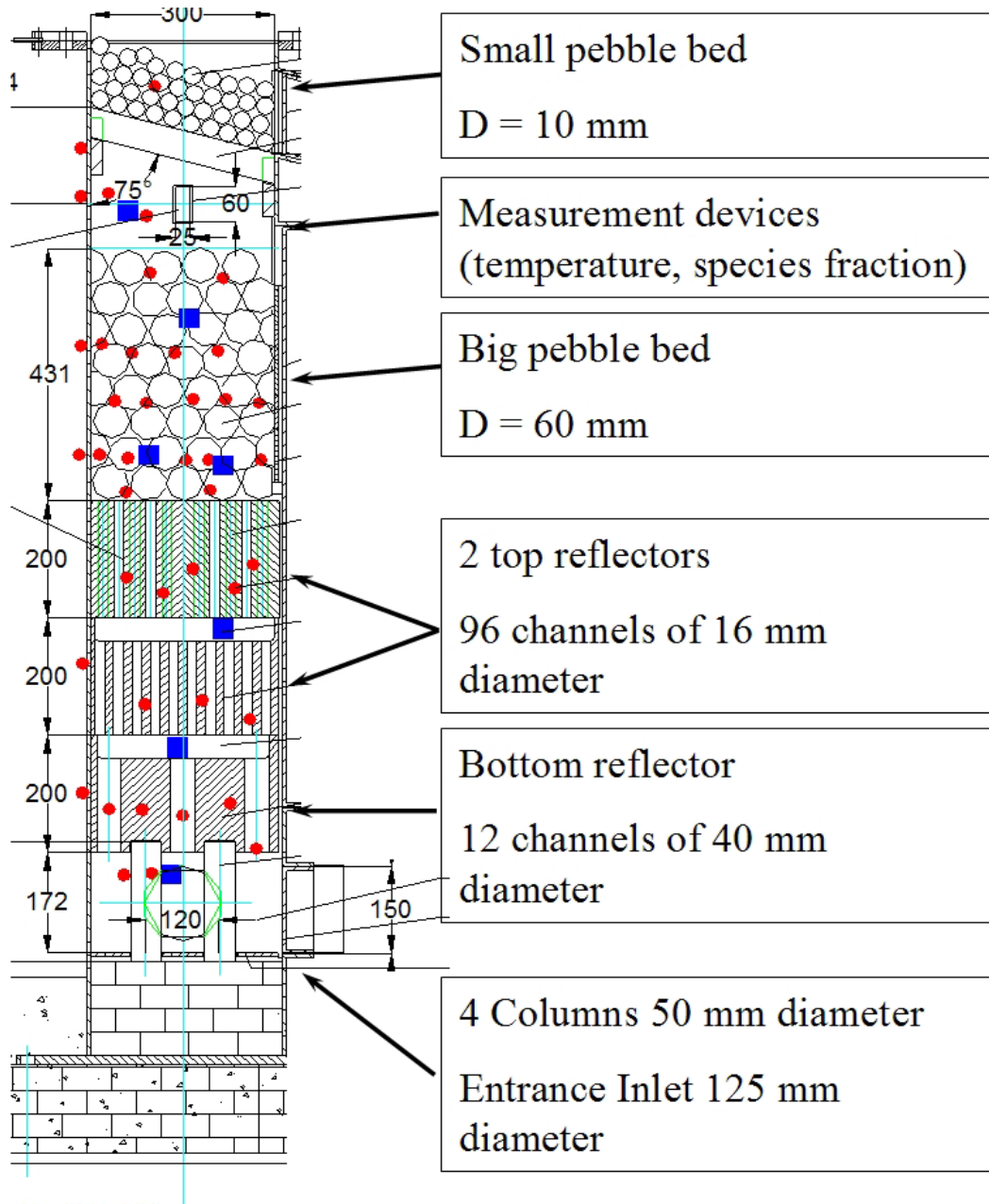


Figure 2-4: Lower channel experimental setting for open chimney experiments[13]

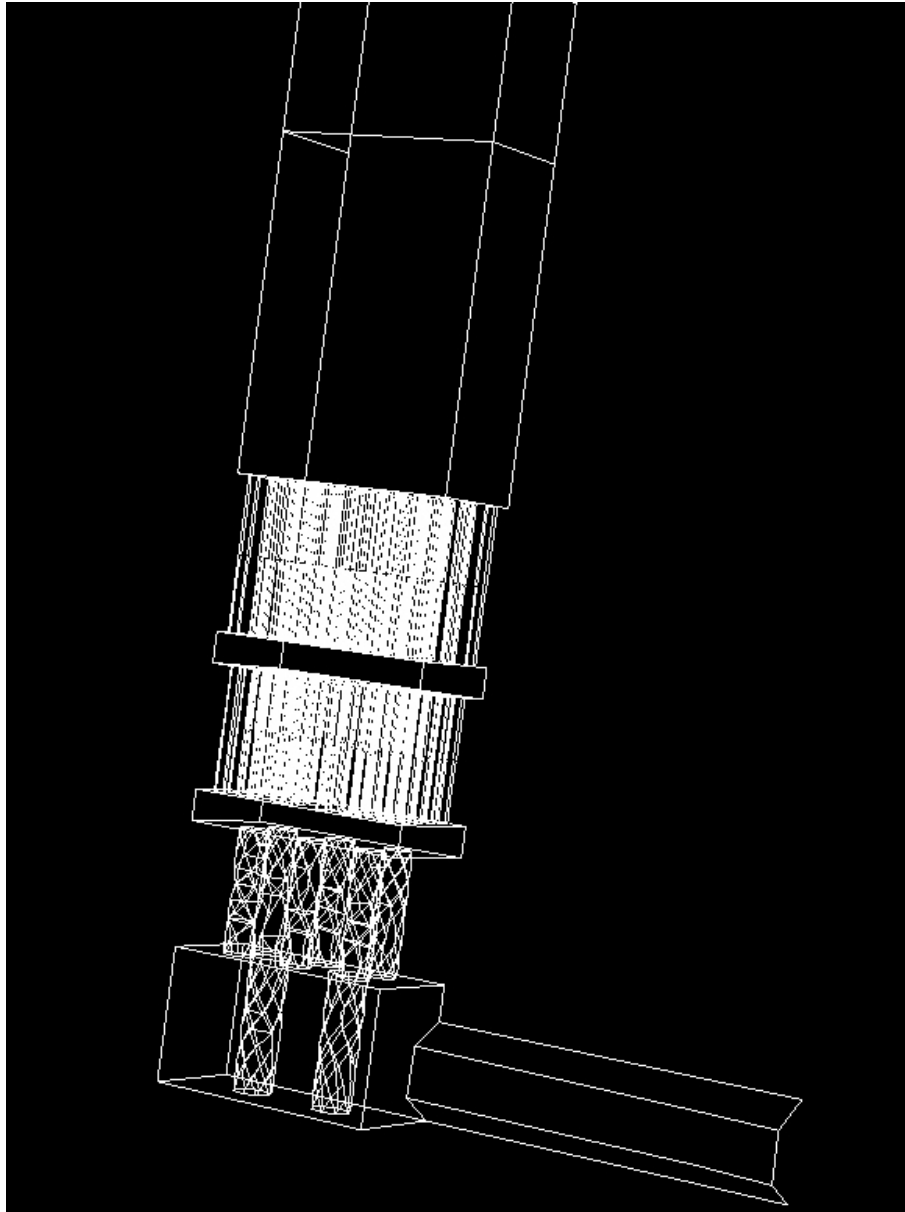


Figure 2-5: Mesh of the lower channel, when reflectors are modeled in detail

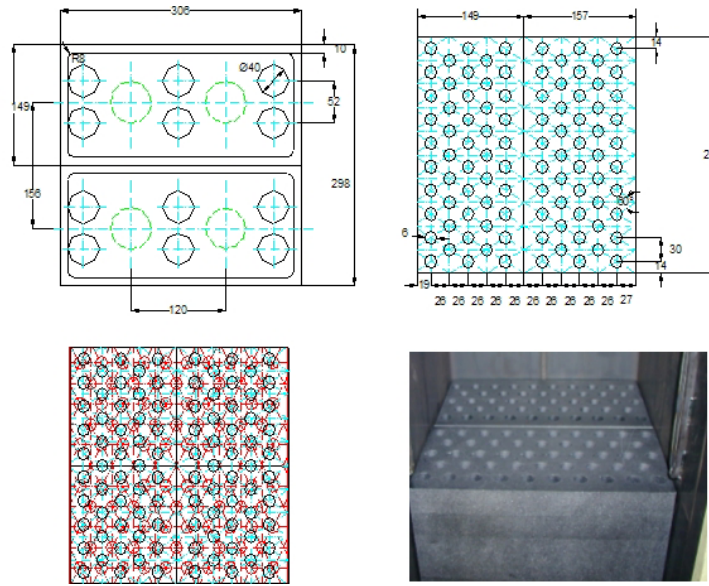


Figure 2-6: **Plans and picture of arrangement for the 96 channels reflectors and lower reflector. Top left: top view of the lower reflectors. Top right and bottom left: top view of the fine reflectors. Bottom right: picture of the fine reflectors.**

2.2.2 Description of the Return-Duct Test (July 2004)

Configuration

The overall experimental setting is very similar to the previous one. However, in these experiments, the top of the chimney is closed and the return duct of 125 mm diameter is set up as shown on the Figure 2-7. The inlet and outlet ducts drawn are not properly shown since in the NACOK facility they are in the same plane. The height of the large pebbles bed is reduced to 280 mm from 350 mm which reduces the pressure loss. The configuration of inlet and outlet ducts is of particular importance since it affects the diffusion and flow processes before the onset of natural convection.

Experimental procedure

The channel is heated using 850C nitrogen under light pressure to a temperature of 850C. It is then filled with helium and electrically heated to maintain an 850C initial condition. The pressure is equalized before the inlet duct and outlet duct are

opened simultaneously to start the experiment. The top of the cold leg is maintained at a temperature between 175C and 200C. We assume in our analysis 180C as in shown in Figure 2-8. The lower part of the return duct does not have any specific temperature externally maintained. Figure 2-8 shows the temperature distribution as modeled in FLUENT.

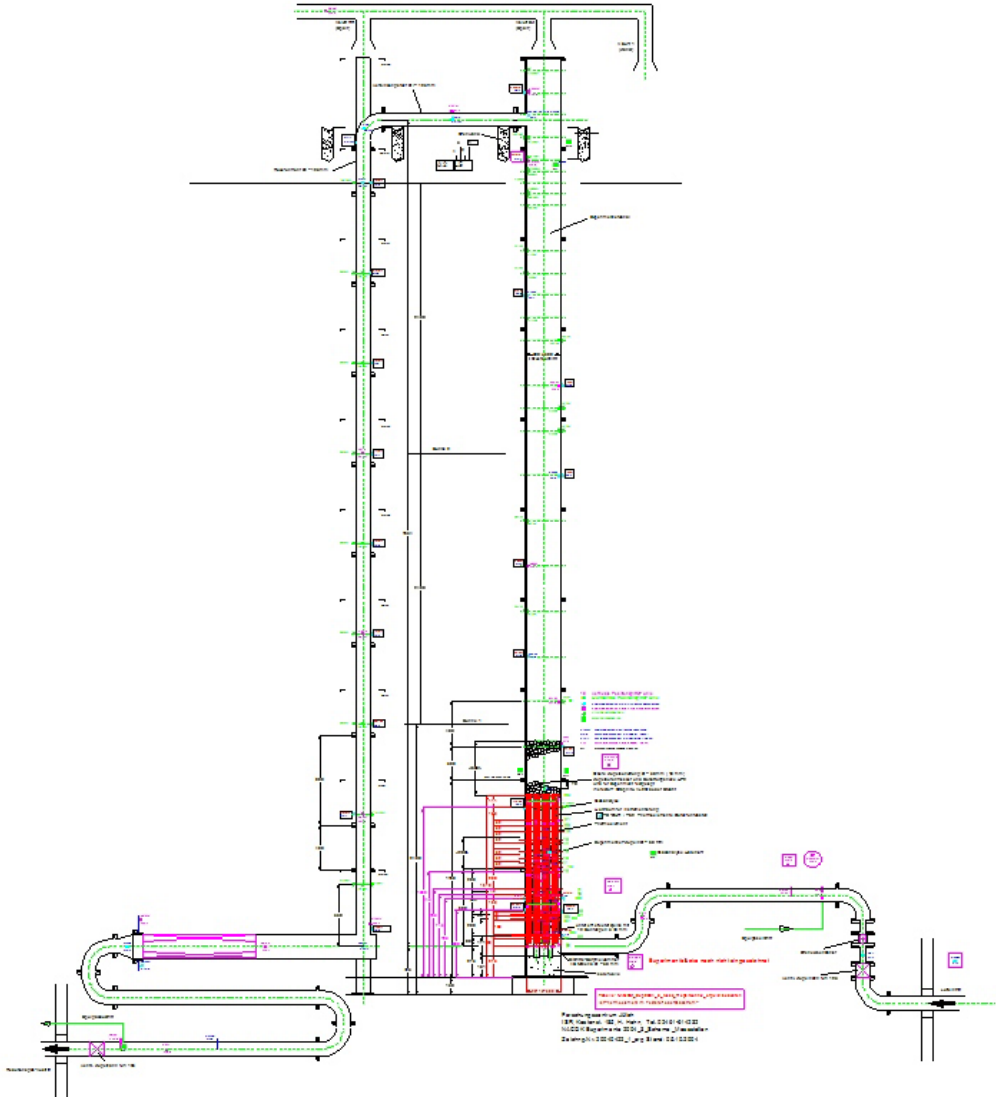


Figure 2-7: Global experimental setting for return duct experiments

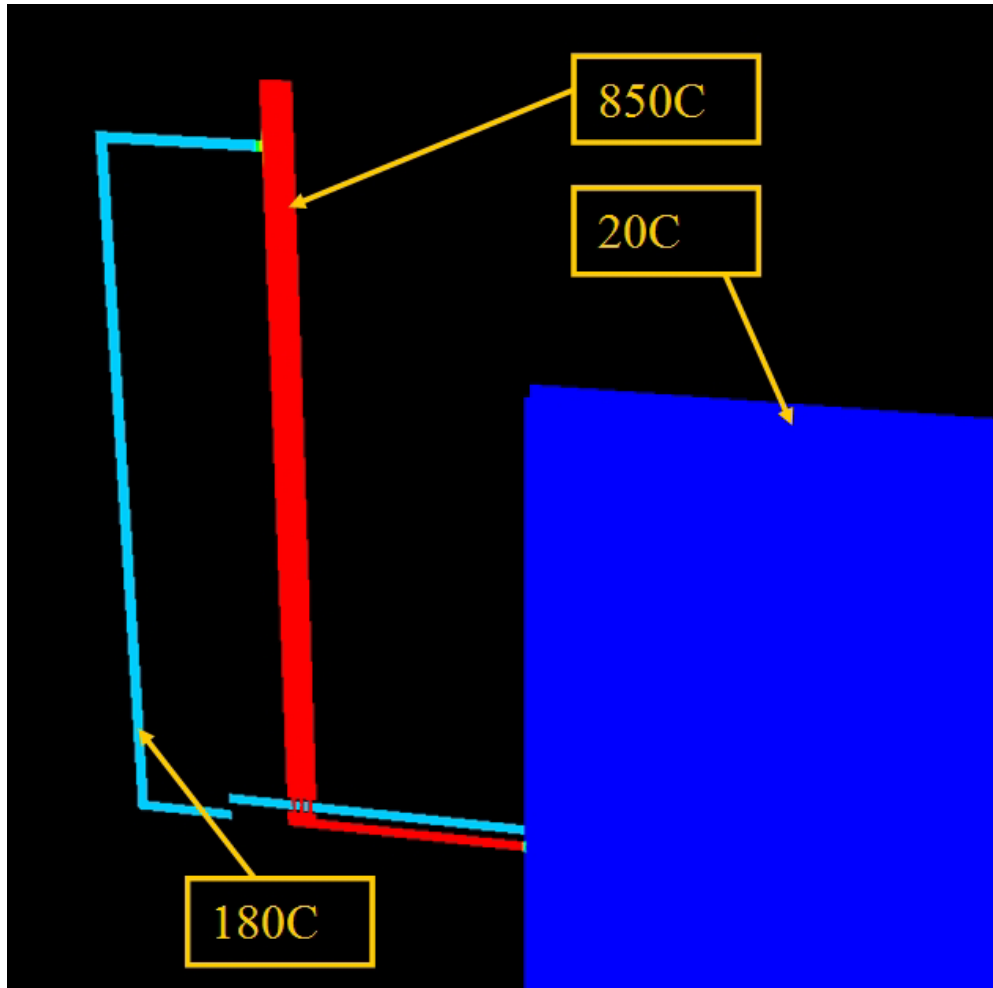


Figure 2-8: Initial temperature distribution in the return duct experiment

2.3 Materials and graphite

No precise information was provided on the type of materials used in the 2004 experimental runs. It is therefore assumed that they were similar to those described by Kuhlmann in the 2001 experiments report [8].

2.3.1 The reflector graphite: ASR-1RS

The reflector graphite is assumed to be ASR-1RS which was used in previous NA-COK experiments. The material properties are shown on Table 2-1. The graphite in

the reflector must be able to survive high mechanical stresses, display a good degree of purity and a low anisotropy. This graphite is produced by mixing and pressing together a filler (pitch coke, *grainsize* $\leq 120\mu m$) and a binder (hard coal). The final grains have a diameter of less than 1mm. Therefore, the graphite has a high density and little ash and volatile components. The graphite is heat treated at high temperatures, above 2800C.

Table 2.1: **ASR-1RS properties [9]**

Density	$1780kg.m^{-3}$
Heat conductivity	$125W.m^{-1}.K^{-1}$ at 40C
Specific Heat Capacity	$710J.Kg^{-1}K^{-1}$
Ash content	390 ppm

2.3.2 The matrix pebble graphite: A3-3

Graphite varieties that are used as matrix materials for the pebbles must meet the requirements for mechanical strength, temperature, stability and good heat conductivity. The maximum temperature for thermal treatment is restricted to about 1950C. This is due to possible microsphere fuel degradation at these temperatures. It is of less importance in the process of modeling the NACOK experiment to have information on this graphite since only a small amount of oxygen is expected to reach the pebble zone. Knowledge of pebble graphite corrosion could be important however in actual air ingress events in reactors since it must be shown that fuel degradation would be limited. Therefore, no reaction would occur on graphite except for the Boudouard reaction that will be negligible at the NACOK temperatures.

2.4 Visualisation of the NACOK experiment

In order to clarify the actual configuration of the experiment, pictures taken at the Jülich research center by NACOK scientists are presented in Figure 2-9, 2-10 and 2-11 and 2-12.

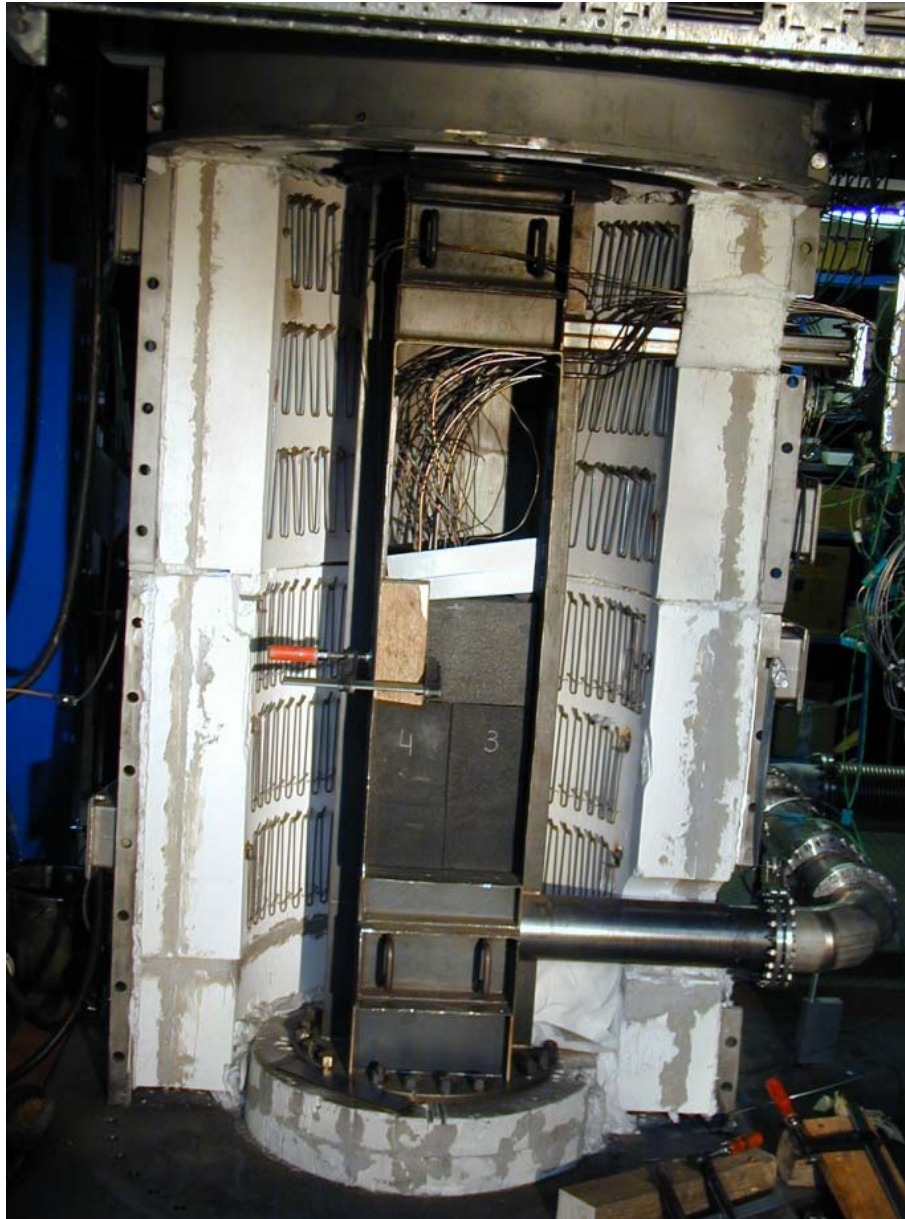


Figure 2-9: Lower channel set up



Figure 2-10: Reflectors. On the left, before the experiment, on the right, after the experiment [13]



Figure 2-11: Entry chamber, with four graphite columns. On the left, before the experiment, on the right, after the experiment [13]



Figure 2-12: 60 mm diameter pebbles. The cables are linked to temperature and species measurement devices located in the lower chimney and pebble bed

Chapter 3

Modeling NACOK with FLUENT

3.1 Validation of a Computational Fluid Dynamics Code [10], [11]

In order to understand some of the procedures in this thesis, the processes, requisites and methods used in CFD modeling, this section presents a tutorial on Computational Fluid Dynamics modeling. Computational Fluid Dynamics (CFD) is a very powerful tool used for the analysis of fluid flows with varying complexity. The reliability on the CFD results tool depends on the number of phenomena modeled, the complexity of the physical processes modeled, the numerical sub-models used, the user expertise. CFD softwares provide approximate solutions of the equations that govern fluid flow, which are, in the NACOK experiment case:

- The mass conservation equation
- The momentum conservation equation
- The energy conservation equation
- The species conservation equations

In addition to these equations, the user needs to provide boundary conditions for a specific application. The solver is then launched with a numerical method whose accuracy will depend on the grid precision, the discretization method, the algorithm used to solve equations. Some of these inputs are provided by the user, in which

case results depend on the user's judgment. Other inputs, such as the discretization method, are part of the characteristics of the method used.

The blind benchmarking of the NACOK experiments is being done in this spirit. Benchmarking is one way of validating a code by comparing the CFD computed results to reliable experimental data that usually consists of simplified test cases. Typically, a few simple experiments are run in order to prove that the physical phenomena (flow, buoyancy, chemical reaction, etc.) can be represented by the code. Then, sensitivity studies can be done numerically to study the impact of several parameters in simple cases. This step is important to provide insights on the range of uncertainty of inputs and their impact on the output. Once the physical phenomena are well understood, the model needs to be benchmarked on more complex geometry and cases. Due to the difficulties of performing experiments on large scale that assess such complex phenomena such as those that occur in an air ingress event, only a few experimental tests were run. Therefore, it was decided to proceed to a **blind benchmarking** approach to test the modeling method for general application. This means that no experimental data was received before the creation and execution of the FLUENT NACOK model.

A short overview of the issues that need to be tackled with during code validation is presented. [11]

The problem definition

Some parameters must be defined in order to set up the problem. The user must choose, among others, a compressible vs incompressible flow, steady vs transient flow, laminar vs turbulent flow, isothermal vs non-isothermal, buoyant vs non-buoyant, reacting vs non reacting, two dimensional vs three dimensional flow and the extent of the computational model. Boundary conditions and initial conditions must be given and their choice explained in order to justify the simulation of a well-posed realistic model.

The numerical methods

Different methods that can be found in commercial softwares are the finite volume method or the finite element method. Numerical discretization, used to translate the mathematical equations into a computer code, induces approximations and thus, errors. A very frequent error which occurs is numerical diffusion, leading to an over prediction of mixing. In order to avoid this, high order schemes must be selected. Unfortunately, these usually lead to divergence.

Solution control and convergence are a major part of the convergence procedure of a model. Once algebraic equations have been defined based on the grid and numerical scheme, they must be solved with iterative algorithms. Therefore, the user has to provide the code/software with convergence criteria or decide when to stop the iterative process. In conclusion to this short overview of CFD modeling, one ought to remember, as it was said by Versteeg and Malalsekera in 1995 [11]:

"In solving fluid flow problems, we need to be aware that the underlying physics is complex and the results generated by a CFD code are at best as good as the physics embedded in it and at worst as good as its operator"

3.2 Procedure followed for the blind benchmarking of the NACOK experiments

The blind benchmarking of the NACOK experiments followed the outlines presented above, with adjustments to the specifics of this case. The open chimney case was developed first and next modified for the return chimney experiment. The steps in the blind benchmarking of the NACOK experiments are as follows:

1. Identifying the physical and chemical phenomena taking place in an air ingress event. This includes among other things, the natural circulation, the chemical reactions, species transport, heat exchanges.
2. Bringing together information on the NACOK experiments. At first, vague

plans, procedures and facility descriptions were received. Details were then investigated further by ways of communication with the Jülich center in Germany. A good understanding and knowledge of the experimental configuration and test procedures was eventually reached.

3. Verification of FLUENT capabilities to model the physical phenomena occurring in an air ingress event. This was done with the help of FLUENT's documentation and service center, as well as small computations modeling various processes in simple geometries.
4. Development of a geometry and grid corresponding to the actual experimental setting. Simplification of this geometry and mesh in order to diminish the computational time. Rough sensitivity study was conducted to assess the impact of the grid precision.
5. Development of several FLUENT models for complete and simplified geometries, focusing on separate effects. Benchmarking of these models was achieved based on previous experiments when possible (natural circulation and pressure loss in pebble beds).
6. Adaptations of these models to shorten computational time (simpler geometries and pressure loss adapted to the FLUENT model, etc...).
7. Creation of a complete model, executed steady state and transient analysis for the open chimney. Comparison of the results with data provided by the JULICH center and PBMR Inc.
8. Sensitivity studies runs on simple geometries to modify the complete model based on comparisons made with the experimental data.
9. Creation of a better FLUENT model benchmarking the NACOK experiments, a detailed explanation of these models and suggestions to modify the methodology to PBMR modeling.

3.3 Detailed description of the general FLUENT model used in NACOK computations, [12], [26]

In the development of the model, geometry and mesh choices were made to limit the computational time. The detailed model files are presented in Appendices. However, it is believed that the explanation of certain parameter choices deserves explanation.

Preprocessing

The preprocessing, that is, creation of the geometry and grid that need to be input in FLUENT, was conducted with GAMBIT 2.2.30. The geometry was created based on information received by the Jülich center. The xOz symmetry plane was chosen as to divide by two the size of the model. There are a total of 10 fluid zones and 1 solid zone: inlet, low entry (columns area), lowref (first reflector), interef (space between reflector 1 and 2), ref2 (second reflector), interef2, ref3, peb1 (60 mm diameter pebble bed), intpeb (space between the pebble beds), peb2, chimney, return and solid. The zones location are shown on Figure 3-1.

Inlet tube: length, bending and area variations are not well known. For the open chimney experiment, the full length of the inlet tube(>3m) was not modeled due to lack of adequate knowledge of the real configuration. The model would gain in precision if this was modeled. The inlet is therefore modeled as a tube of 125 mm diameter and of 500 mm length. This length is adequate to model the flow path in the inlet tube and the diffusion phenomenon. The inlet boundary condition is a pressure inlet condition. A porous-jump zone is modeled after the inlet to account for the flow meter device as well as the pressure loss induced by the tubing. The inlet was meshed with Hex/Wedge elements, Cooper type with a spacing of 20mm between each element with a total of 600 elements in the volume.

For the return duct experiment however, the diffusion and therefore the length of tubing determines the onset of natural convection. The inlet channel was modeled as a rectangular inlet of side 110 mm, which conserves the flow area. Then, the tube length was fully modeled based on best interpretation of different plans provided for the configuration.

Entry zone: The entry zone contains 2 (taking in account the symmetry, 4 otherwise) graphite columns. Both the entry space where air is flowing and the columns (solid) are meshed with Tet/Hybrid elements Tgrid type. A size function was used in order to provide a coarser mesh in the bottom entry section and a finer mesh close to the top reflector flow zone.

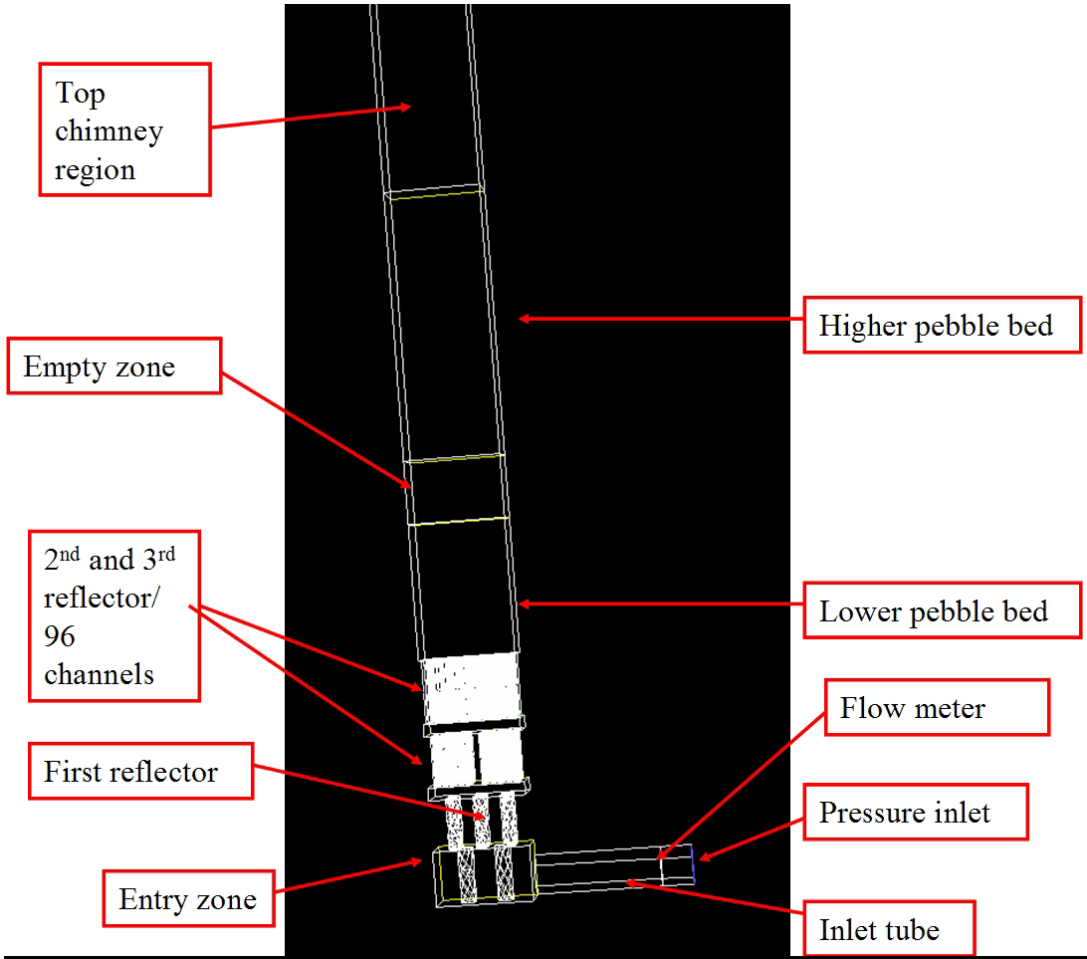


Figure 3-1: Zones name in the FLUENT model

First reflector: Modeled as channels with graphite walls. For meshing, the channel zone was unified with the empty flow space above. This zone was meshed in a similar way as the entry.

Second and Third Reflectors: Several models were created, with detailed geometry and with the reflector of 96 channels modeled as a porous media. In this latter case, the porous media is a rectangular, meshed with Hex/Wedge elements

type cooper. The porous media approximation is further described in Chapter 5.

Top chimney region: Divided in the following zones with Hex/Wedge elements Cooper type: small pebbles bed (378 elements), empty zone (252 elements), big pebble bed zone (504 elements), top chimney (4032 element). The pebble zones were modeled as a porous media.

Return duct: The duct is modeled as a rectangular pipe of same flow area as the real tube. The same uncertainties in the actual geometry for the outlet pipe apply as for the inlet pipe configuration.

Solver

The segregated solver formulation was selected to model the NACOK experiments. This solver solves fundamental equations sequentially. It works well for mildly compressible flows and does not use much memory. The segregated solver is also the only solver that offers the physical velocity formulation in porous media (discussed below). The discretization scheme for the convection terms of each governing equation chosen is the first order upwind scheme with the segregated solver. This choice is made to better reach convergence. With this scheme, quantities at the cell face are equal to cell quantities, calculated by assuming that the cell center value is a cell average. Once convergence is reached, the second order upwind scheme is turned on. Values at cell face are computed using a multidimensional linear reconstruction. The third order MUSCL scheme adds the central differencing scheme to the previous one and can be used to obtain even better accuracy. It was used when time permitted, mainly for sensitivity studies.

The body-force weighted scheme is activated for the pressure interpolation scheme, as recommended in the case of large body forces. The second order scheme would have been a good option had it not been inconsistent with the porous media approach. The density interpolation scheme is set to the first order upwind scheme, since the flow does not undergo shocks. The derivatives in the flow equations are evaluated with the node based gradient option. Compared to the cell based one, it allows a better accuracy for unstructured triangular mesh, which is used for the most critical locations.

The PISO pressure-velocity coupling method is chosen. It is recommended for transient runs with large time steps as well as highly skewed mesh. For steady state runs, PISO with skewness correction is used. If the convergence is too slow, the SIMPLE method can be used, but care is needed where the mesh is highly skewed, which is easily the case when complex rectangular and circular geometrical features interact.

The physical velocity porous media velocity method is activated. The porous media formulation is described in Chapter 5. The superficial velocity is based on the volumetric flow rate, which does not take in account the increase of velocity due to the pores. The chemical reaction rates are defined by the in-pore diffusion, which depend strongly on the velocity of the fluid at the surface of the reacting graphite. Therefore, using the physical velocity option yields more accurate chemistry results. The two resistance coefficients in the porous media formulation are derived in using the superficial velocity. FLUENT assumes that the inputs for these resistance coefficients are based upon well-established empirical correlations that are usually based on superficial velocity. Therefore, the inputs for the resistance coefficients are converted into those that are compatible with the physical velocity formulation. This allows one to properly account for the pressure drop across the porous zone for the same mass flow rate and the same resistance coefficients as for the superficial velocity option.

The setting of the under relaxation factors (URF) is one of the most complex tasks in the achievement of stable convergence. The under relaxation reduces the change of scalar variable quantity produced at each iteration. The larger the under relaxation factors, the larger the change in the value of the variable at each iteration. The solution converges faster but might also be unstable. The smaller the URF, the slower the convergence will be. In these experiments, the dependency of the flow on light buoyancy forces sets the need for a very cautious approach. Using the PISO skewness coupling methods induces the need to set the under-relaxation factors for momentum and pressure so that they sum to 1. The momentum URF is the most sensitive one and therefore is usually set between 0.1 and 0.5 at start of

the computation. For further precision, it can be taken down to 0.001 if the solution gets unstable. The pressure URF is set from 0.9 to 0.5. The species URF are set between 0.1 and 0.5. The energy URF is set to 0.3. The density and body forces URFs are set to 0.6.

Convergence judgment

Convergence is monitored primarily by watching residuals decrease and specific parameters stabilize (mass flow rate, species concentrations). Instability is observed when residuals start to oscillate. In these computations the residuals are chosen mainly as an index of stability and for convergence screening of the energy equation. In order to judge convergence, the mass flow rate and species concentration at different places of the experiment are monitored. Convergence is reached when these values have not been changing for a significant number of iterations. In unsteady computations, it is recommended by FLUENT users manual to choose the time step so as to obtain convergence in 5 to 10 iterations. However, when convergence is too slow because of small URFs, it is accepted that convergence of the step can be attained in more iterations, for instance fifty.

Other FLUENT parameters

Other major parameters that can be subject to variations and have an impact on the outcome of the computations are presented here.

Space: The problem modeled features of three dimensional phenomena and is therefore modeled in three dimensions. Some 2D simulations were used to develop a fundamental understanding of the solver and software as well as for the sensitivity studies on solver options, flow options, chemical reactions models, mesh sizes and geometries, pressure drop correlations and species transport.

Time: It is believed that steady state can be reached for both the open chimney and hot and cold leg experiments. However, to confirm this assumption, the transients models need to be run for a long enough time to show steady state is approached. Once it has been shown that the transient case is approximating the steady state, steady state calculations can be used for benchmarking.

The transient models are run using the Frozen Flux Formulation in order to accelerate the convergence. The first Order Implicit scheme is used. The adaptive time stepping method is used with the following parameters: Elapsed time of 24H, minimum time step size of 0.001 s, 10 iterations per step and a minimum step change factor of 0.1. The start of the experiment can be run with a few accelerated time steps (up to 5 s). Likewise, when the flow stabilizes, longer time steps are imposed and a return to short time steps allows a stabilization in the convergence residuals. Another way to accelerate the run without leading to divergence is to have longer initial time step and allowing a small minimum step size change so that FLUENT can automatically change back very quick to very small time steps.

Different gross estimates for the computational times with one 3.06GHz processor and 2 Gb of RAM are given here. For a flow only steady state calculation, good convergence is reached in less than 10 hours. For the same multicomponent calculation, up to one week is needed to reach with confidence convergence in the second degree order. For a transient with only diffusion and no reactions modeled computation, a week also is needed to reach an experimental time of 10 hours. Finally, a full multicomponent transient calculation for the return chimney experiment can take up to a month with time steps of 0.5s to compute 8 hours of experiment. By comparison, a small sensitivity study typically reached convergence in less than 5 minutes.

Viscosity: The calculated Reynolds number of the flow reaches a maximum of 95, far from turbulence limit. Thus, the model can be run in laminar mode. However, the chemistry depends on small scale localized vortices. Therefore, two models were compared: one with the laminar flow option, associated with the finite rate chemistry (base model) and the other one with the standard k-epsilon turbulence model with full buoyancy effects turned on and the Finite rate/Eddy Dissipation turbulence/chemistry interaction. No significant differences in the chemistry behavior of the system for the flow formulation (laminar and turbulent) were observed due most probably to the fact that steady vortices are not turbulent.

Species modeling

Species modeling is one the most complex issues to model in FLUENT. Therefore, several sensitivity studies and models were investigated and are presented in following chapters.

Material properties The mixture properties, composed of 7 different species, are summarized on table 3-1.

Table 3.1: Mixture properties [12]

Specie/Properties	C_{solid}	N_2	O_2	CO_2	CO	H_2O	He
C_p $J.Kg^{-1}.K^{-1}$	1220	1040	919.31	840.37	1043	2014	5193
Thermal conductivity $W.m^{-1}.K^{-1}$	0.0454	0.0242	0.0246	0.0145	0.025	0.0261	0.152
Viscosity $*10^{-5} Kg.m^{-1}.s^{-1}$	1.75	1.66	1.91	1.37	1.75	1.34	1.99
Lennard-Jones characteristic length \dot{a}	2	3.621	3.458	3.941	3.59	2.605	2.57
Lennard-Jones energy parameter C	-263	-175	-165	-78	-163	299	10.2
Standard enthalpy $J.Kgmol^{-1}$	-101	0	0	$-3.35*10^{-8}$	$-0.15*10^{-8}$	$-2.4*10^{-8}$	-3117
Standard state entropy $KJ.Kgmol^{-1}.K^{-1}$	5.731	191.4	205	213.7	197.5	188.6	126

Description of the boundary conditions

Pressure outlet: The pressure in FLUENT includes the hydrostatic head and requires $P_{gauge} = P - \rho * g * z$ where P is the pressure. The gauge pressure given as an input must therefore be

$$P_{GaugeOpenchimney} = -27.4Pa$$

$$P_{GaugeReturnDuct} = 0Pa$$

respectively for the open chimney outlet duct and the return chimney experiment outlet duct. Since the outside of the chimney was not modeled in the open chimney

experiment, in order to avoid a back flow of cold air, the return flow temperature was fixed to be the heated wall temperature.

Pressure inlet: The gauge pressure at the inlet is zero. The inlet temperature is 300K. The mass composition of air entry is 23% oxygen, 0.0043% water vapor (based on hygrometric charts for 30% humidity at 20C) and 76.57% N_2 .

Pebble bed: The porosity of the pebble beds was set to be 0.395. The wall side effects do not exist due to the configuration of the pebble bed. As described later in Chapter 5 the FLUENT porosity pressure loss model was used, as an adaptation from the Khulmann correlation [8]. The pressure loss is the integration over the length of the pebble bed of the momentum sink source. S is the momentum sink term in the momentum conservation equation. C_0 and C_1 correspond here to the pressure loss coefficients in the pebble bed modeled as a porous media :

$$S = -C_0|v|^{C_1} \quad (3.1)$$

The values of C_0 and C_1 were obtained by sensitivity studies described in Chapter 5. The 60 mm diameter pebbles induce a pressure loss with $C_0 = 36.668$ and $C_1 = 1.7599$, a surface to volume ratio of 60.35. The smaller pebbles of 10 mm diameter, induce a pressure loss with $C_0 = 341$ and $C_1 = 1.6107$, a surface to volume ratio of 363.

96 channel reflectors: The small reflectors were chosen to be either modeled in detail or as a porous medium. In both cases, different approximations were used to diminish the complexity of the mesh. The two options were studied in a sensitivity analysis. In the detailed model, the solid graphite surrounding the channel is not modeled and the approximation lies in the fact that the temperature of the walls needs to be fixed. Therefore, the only the gas will heat up, with no heat transfer to the wall. In the second option, the reflector is modeled as a porous media with the correct surface to volume ratio and pressure loss. ($C_0 = 63$ and $C_1 = 1.72$, surface to volume ratio of 53.58) In that case, the approximation lies in the geometrical dispersion of the heat produced by the chemical reactions. This second approximation was used in the blind models.

Flow meter: It was mentioned by the Jülich center that the flow meter at the inlet of the experimental setting induced a significant pressure drop. No specific

information was given on the latter except for the dependence of the pressure loss on the square of the velocity. Therefore, based on former Jülich theoretical studies, a pressure loss was developed as a fan boundary condition. The theoretical study from Jülich gives a pressure loss of $\Delta P = 25.52Pa$ and a mass flow rate of $3.5g.s^{-1}$ for the open chimney and $\Delta P = 7.25Pa$ and $1.6g.s^{-1}$ for the return duct experiment [13]. The pressure loss in a Fan boundary condition is going to be dependent on the velocity as: $\Delta P = \Sigma f_n * v^{n-1}$. The velocity, in the inlet tube of $125mm$ diameter with a density of $1.22kg.m^{-3}$ is:

$$v = \frac{\dot{m}}{\rho * A}$$

As a result,

$$f_3 = \frac{\Delta P * (\rho * A)^2}{\dot{m}^2}$$

For the open chimney experiment, $f_3 = 446$ and for the return duct one, $f_3 = 606$. f_0 and f_1 are both equal to zero since the theoretical study from Jülich [13] shows that the pressure loss is proportional to the square of the velocity.

Wall treatment: The standard FLUENT wall functions are used, without dealing with moving walls or wall roughness. This is an approximation since graphite surface can be quite rough. However, this assumption should not affect significantly the phenomena modeled. The thermal conditions for the external walls of the channel are as follows: fixed temperature (650C or 850C), no wall thickness and heat generation rate. One of the material used for walls is aluminum, with a density of $2719kg/m^3$, $C_p = 871 J/kg-K$ and thermal conductivity = $202.4 W/m-K$. The other type of wall material is graphite. The graphite data from PBMR was used [9]: density of $2240 kg/m^3$, $C_p = 710 J/kg-K$ and a thermal conductivity of $168 W/m-K$. The material which is used in the outer structure of the NACOK experiment is a non oxydable alloy modeled as Aluminum. If the wall is at the interface of a graphite block and a flow channel, the coupled thermal option is switched on. In that case, the temperature depends on the graphite block temperature. The potential heating of the wall is not considered. This approximation can be justified by the fact that the chemical reactions depend on the flow cell temperature, not the wall temperature. In addition, since the flow is constant for the steady state case, we can expect the decrease of temperature due to the graphite heat absorption not to have a major impact on the flow temperature. Therefore, the fluid temperature

will be compared to the data and not the wall temperature. The species boundary conditions is a zero diffusive flux through the wall. If the wall is made of graphite, the reaction mechanism is switched on.

Chapter 4

Chemistry models in the event of an air ingress accident

The moderator in a high temperature gas reactor is graphite and the coolant is helium. These two materials do not react with each other, even at very high temperatures. However, in the event of an air ingress accident, several chemical species will be produced in the reactor. The mixture entering the reactor is composed of Oxygen (O_2), Water Vapor (H_2O), Nitrogen (N_2) and other species in negligible amounts. The O_2 will react with the graphite (C) producing several other species that will take part in other chemical reactions. It is therefore very important to understand the reactions taking place and their mechanisms. The purpose of this chapter is to describe the chemical reactions taking place and a short literature review of papers on this issue. The models used in FLUENT are then presented.

4.1 Chemistry in an air ingress event

4.1.1 Reactions

The oxidation reactions taking place in the reflector or the pebble bed of the reactor are described below [14]:

Table 4.1: **Chemical reactions taking place during an air ingress event**

1: $C + \frac{1}{2}O_2 \rightarrow CO$	$\Delta H = -111kJ/mol$
2: $C + O_2 \rightarrow CO_2$	$\Delta H = -394kJ/mol$
3: $C + CO_2 \rightarrow 2CO$	$\Delta H = 172kJ/mol$
4: $C + H_2O \rightarrow CO + H_2$	$\Delta H = 131kJ/mol$
5: $CO + 0.5O_2 \rightarrow CO_2$	$\Delta H = -283kJ/mol$

A positive enthalpy means that the reaction is endothermic, and a negative one means that the reaction is exothermic. These reactions can combine with each other, have different energy of activation and reaction rates. The reaction of oxygen with carbon is exothermic and favored thermodynamically. However, graphite is not corroded at ambient temperatures, since the graphite oxidation rate is temperature dependent. This means that kinetics are of great importance to determine which reactions are favored as a function of temperature. The oxidation of graphite is going to be significant from $T \geq 600C$. In high temperature reactors and more specifically in the NACOK experiments, the system will be in the range of 500C to 1200C, where graphite oxidation occurs.

The second major reaction can be seen as the conjunction of reactions 1 and 5. One could say that the reaction producing carbon monoxide maximizes the amount of carbon removed by a given mass of oxygen and the reaction producing carbon dioxide maximizes the amount of heat produced by oxidizing a given mass of carbon.

The third reaction, called the Boudouard reaction, starts to have a significant impact on the chemical system at $T \geq 850C$.

Concerning the reaction of water vapor with graphite, at $T = 850C$ and $P = 0.1atm$, oxygen reacts 10 000 times faster. Therefore, this reaction will not be taken into account in this analysis. Water vapor however, needs to be accounted for in the species mixture, since it affects the oxidation of carbon monoxide.

4.1.2 Mechanisms and Regimes of graphite corrosion

The oxidation mechanisms are very complex and can vary depending on the system conditions. In case of absence of catalysts, the typical scheme is the following [14], [15]:

1. Transportation of the oxidant to the surface of the graphite
2. Adsorption of the oxidant on the graphite surface (physiosorption)
3. Formation of C-O bonds (chemisorption)
4. Breaking of C-C bonds
5. Desorption of CO or CO_2
6. Transport of reaction products from the graphite surface.
7. Reaction of resulting gases with Oxygen or graphite

The reaction rates depend on the rate of each of these steps. This gives an understanding of the parameters on which the reaction rates depend, that is : rate at which the oxidant has access to the surface, the partial pressure of the oxidant (step 1-3), the surface area available to the oxidant for reaction (step 3), the catalytic impurities or in-pore deposit present in the pores of the graphite (step 2-3), the temperature (step 3-4), the rate of removal of reaction products (step 5-6), the effective diffusion coefficient (step 1-2).

There are three different regimes depending on the temperature of the system as shown on Figure 4-1. Temperature ranges are given as representative and depend on experimental conditions. Moreover, the transition between regimes does not depend only on the temperature but also on the flow rate for regime II to III and on the material dimensions for regime I to II. The gas pressures will also have an influence.

- **Regime I: Chemical controlled regime, $T \leq 600C$**

This regime occurs at low temperatures and therefore at low reaction rates. The oxidant concentration is going to be homogenized in the depth of the

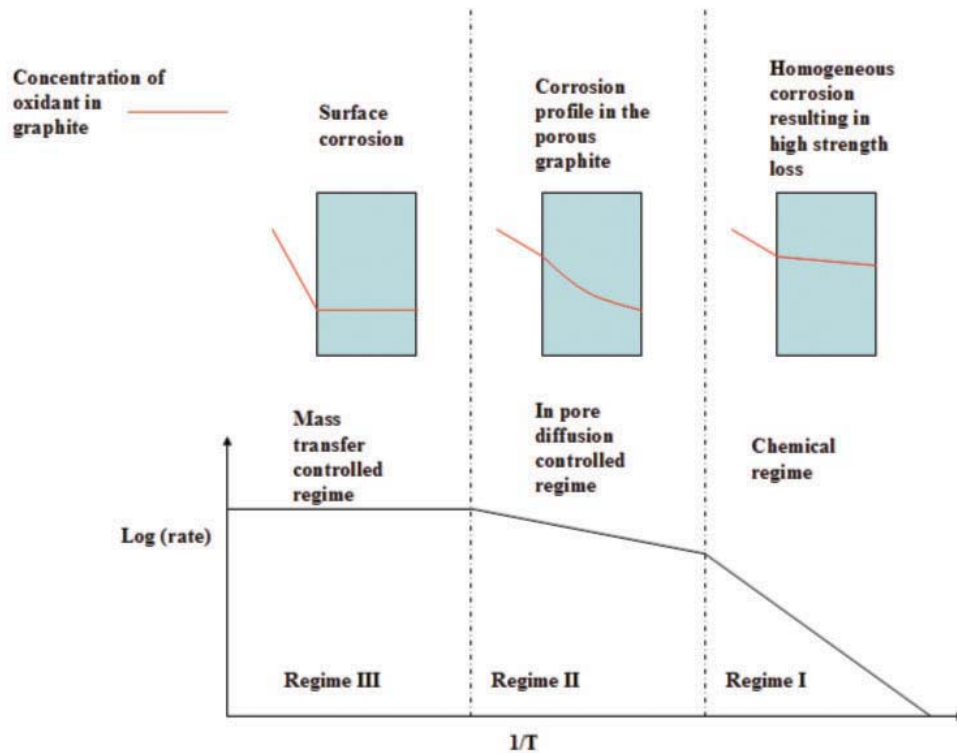


Figure 4-1: Corrosion Regimes

graphite. Therefore, oxidation occurs also "inside" the graphite. This will lead to a strong loss of mechanical strength and can produce up to 10% burn-off. Burn-off is the percentage of graphite that has reacted over the graphite that can react. The reaction rate in that case is limited by the internal activity of the graphite, that is the ability to physiosorption and desorption.

- **Regime II: In pore diffusion controlled regime, $600C \leq T \leq 900C$**

Since the reaction rate becomes higher at this temperature, the diffusion in the graphite pores will control the reaction rate (transport of oxidant). The oxidation corrosion becomes smaller in depth of the material and as a burn off profile is formed. The kinetic expressions should then include diffusion coefficient for graphite, and by comparison to regime I, the activation energy is divided by half.

- **Regime III: Mass transfer regime, $T \geq 900C$**

The reaction rate at the surface of the graphite is so high that most of the oxi-

dant that penetrates the laminar sublayer of gas flowing past the hot graphite is immediately consumed. The reaction rate in that case can be expressed in terms of the superficial graphite area (not taking in account the pore area) ($kg.m^{-2}.s^{-1}$) and depends on external mass transfer.

4.2 Modeling chemistry in FLUENT

FLUENT has the ability to model mixing, transport and reaction of chemical species. The solver solves conservation and diffusion equations as well as reaction sources for each species. The conservation equation for the species molar quantity X takes the following form[12]:

$$\frac{\partial}{\partial t}(\rho X) + \nabla(\rho \vec{v} X) = -\nabla \vec{J} + R_X + S_X \quad (4.1)$$

where

- R_X the net rate of production of the specie X
- S_X the rate of creation by other means
- J the diffusion flux of specie X due to concentration gradients.

Reactions can be modeled to occur in the bulk phase, in porous regions and on walls.

4.2.1 Species transport

In order to model species transport several parameters and data must be input in FLUENT. First, a "mixture" must be created, with all species available in the chemical system. This list of components composes the fluid. The mixing laws dictating how mixture properties are going to be derived must be chosen. Finally, diffusion coefficients must be input. Zhai [1] in his work found that the kinetic model applies well to this reaction system ,and that the "Full Multicomponent diffusion", although very expensive computationally, gives accurate results. The species parameters are calculated according to this theory using the Lennard-Jones potentials [20]. These diffusion parameters are going to be used in the full multicomponent diffusion model

in FLUENT. The Fickian diffusion model cannot be used since we are far from having one main species once the reactions have started producing CO and CO₂, and in the return duct experiment, the flow is actually diffusion driven before the onset of natural convection.

4.2.2 Chemistry model [12]

There are several ways to deal with chemical reactions using FLUENT. The most suitable is the FLUENT finite rate model. In this model, FLUENT treats the information given on reaction rates as species source terms. The reaction rates are expressed using an Arrhenius model, and the inputs are calculated in order to have the best possible match between the experimental correlations and the Arrhenius models. The flow in NACOK is laminar, and the turbulent mixing of species was not modeled. This is an approximation since there are necessarily small localized turbulences in the corners and geometrical complexities of the experimental configuration.

The net mass source (variation) of chemical species R due to the molar reaction source \widetilde{R}_r (the molar variation of quantity of a species over time) is computed as the sum of the Arrhenius reaction sources over the reactions in which the species X participates.

$$R_{X,mass} = M * \Sigma \widetilde{R}_{X,r} \quad (4.2)$$

$$\widetilde{R}_{X,r} = \nu * \left(k_{f,r} \prod_{N_r}^{j=1} [C_{j,r}]^{\eta_{f,j,r}} - k_{b,r} \prod_{N_r}^{j=1} [C_{j,r}]^{\eta_{b,j,r}} \right) \quad (4.3)$$

The Arrhenius expression gives

$$k_{f,r} = A_r T^\beta e^{-\frac{E_A}{8.314T}} \quad (4.4)$$

The units are as follows::

- R in $kg.s^{-1}$
- A_r , the rate constant
- $\widetilde{R}_{x,r}$ in $kgmol.s^{-1}$

- E_A in $J.kmol^{-1}$ and in that case, $R = 8314.4J.kgmol^{-1}K^{-1}$
- M is the molecular weight of specie X in $g.mol^{-1}$
- $k_{f,r}$ is the forward rate and $k_{b,r}$ is the backward reaction rate in $kgmol.s^{-1}$.
- $\eta_{j,r}$ is the rate exponent for each reactant and product
- ν is the overall stoichiometric coefficient of X in reaction r
- $C_{j,r}$ is the molar concentration of the species r in the reaction j
- T the temperature is in K
- β is a constant specific to the reaction

It can be seen that the reaction rate temperature dependence is an exponential. Figure 4-2 shows the evolution of the graphite oxidation and Boudouard reaction rate with respect to the temperature.

4.3 Graphite corrosion reaction rates

There are many research papers written over the last fifty years on graphite oxidation. They usually describe a new correlation developed in the case of specific experimental conditions, or present sensitivity studies on a specific parameter such as burn off dependence, temperature dependence, water vapor concentration influence etc... Two different models that apply to graphite corrosion in regime II in HTR and applicable to the NACOK will be presented in this section.

Arrhenius model correlations

The Arrhenius model is based on the principle that for the reactants to react, they need to acquire enough energy to overcome the energy barrier in order to become an activated complex. This energy needed is the activation energy, E_A . The energy available for the species system is based on the temperature which can be calculated with Maxwell-Boltzmann statistical physics. Therefore, the proportion of molecules that can react is proportional to $e^{-\frac{E_A}{RT}}$. The proportionality constant is the reaction

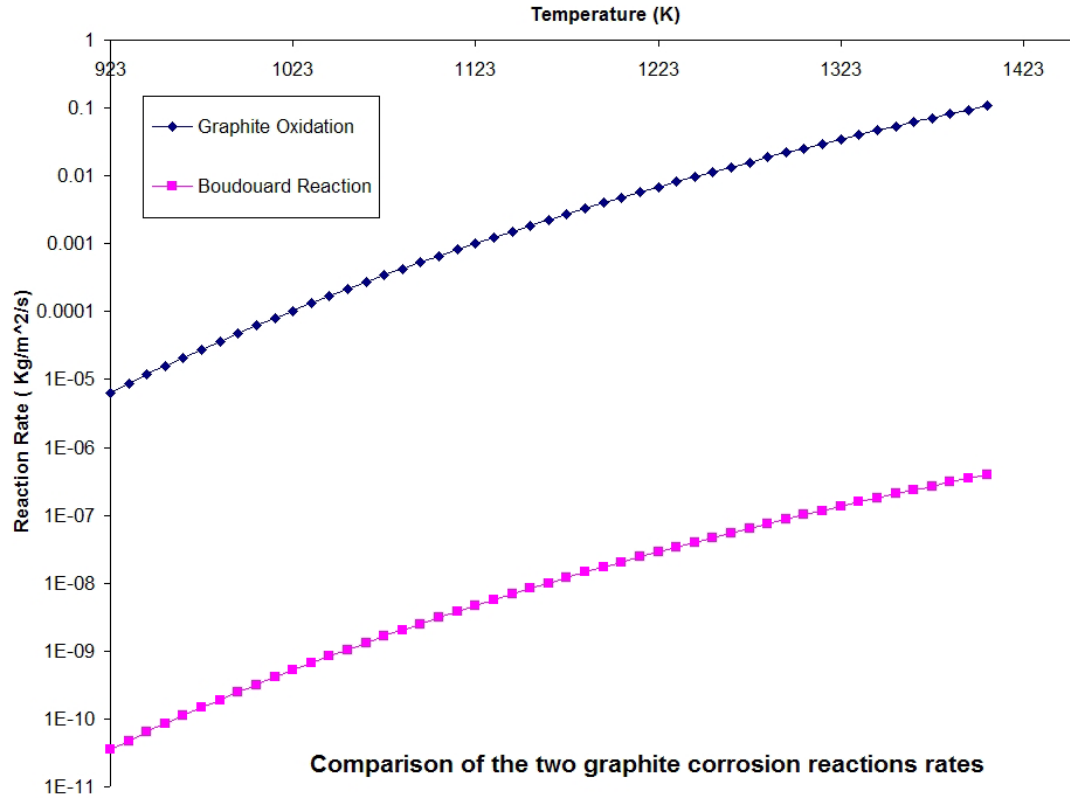


Figure 4-2: Comparison of the graphite oxidation and Boudouard reaction rates ($\widetilde{R}_{C,r}$)

rate constant, k . It can be seen that increasing the temperature will increase the rate of reaction.

$$r = k * e^{-\frac{E_A}{RT}} \quad (4.5)$$

The Arrhenius model can give a very good approximation of the reaction rates but is rarely exact. However, its simple expression allows for the use of multiple correlations. This model will be used in FLUENT for our chemistry modeling.

Hinshelwood-Langmuir correlation

In order to have a good insight on the complexity of the development of reaction rates correlation, the Hinshelwood-Langmuir model is presented. This correlation is the most appropriate kinetic model for the kind of surface reaction occurring in graphite oxidation and takes into account the inhibition by reaction products, the

diffusion in the graphite pores and the burn-off. The HL model is a superposition of second's Ficks law and the rate equation of regime I that follows an Arrhenius kinetic model [15].

$$r_{regimeI} = k_I * e^{-\frac{E_A}{RT}} * [O_2] * f_{regimeI}(B) \quad [mol.m^{-3}.s^{-1}] \quad (4.6)$$

$$r_{regimeII} = k_{II} * e^{-\frac{E_A}{2RT}} * [O_2]^{\frac{n+1}{2}} * f_{regimeII}(B) \quad [mol.m^{-3}.s^{-1}] \quad (4.7)$$

and for regime II, the rate constant is going to depend on the burn-off and the effective diffusion in the pores of the graphite.

$$k_{II}(B = 0) = \sqrt{k_{regimeI} * D_{eff}} * \frac{2}{n + 1} \quad (4.8)$$

In these equations:

- k_0 is the kinetic Arrhenius rate constant
- E_A is the activation energy in $J.kmol^{-1}$
- R is the universal gas constant in $J.kgmol^{-1}K^{-1}$
- $[O_2]$ is the oxygen concentration in $mol.m^{-3}$
- $f_{regimeI}$ is a function giving the dependence on graphite burn-off for regime I
- $f_{regimeII}$ is a function giving the dependence on graphite burn-off for regime II
- D_{eff} is the effective gas diffusivity within the graphite in $m^2.s^{-1}$

The values and correlations of the different parameters were established experimentally and therefore have important uncertainties due to the experimental conditions in which they were obtained and can be only applied to very specific experimental conditions. However, this model provides a good insight on the complexity of the reaction rate and the dependence on several parameters. The values for the rate equations can vary for different materials by a factor of 20 for the rate constant k_0 and by a factor of 2 for the activation energy E_A .

4.4 Reaction rates input in FLUENT

4.4.1 Correlations chosen for the NACOK graphite oxidation modeling

The Jülich center in Germany was not able to provide specific accurate data on the type of graphite used in their experimental runs of March and July 2004. However, the very complete Kuhlmann report details the type of graphite set up in the NACOK chimney. Unfortunately, the analytical reaction rates used for this first NACOK study are based on the VELUNA experiments, that aimed at developing graphite corrosion rate correlations for pebble packed beds. These correlations are integrated and take in account all diffusion processes and flow patterns and therefore cannot be used as input in a FLUENT model since the software calculates this phenomena. It would induce a repetition when taking in account some phenomena such as diffusion, mass transfers etc. Therefore, a new approach was needed. [8] [16] [17]

Correlation model I, used by Lim and No [2] [3]

Lim and No performed similar studies on the JAERI and SANA experiments as the ones described in this thesis. They developed a correlation for graphite IG-110 oxidation. The graphite IG-110 has been extensively studied in the literature and has properties close to the ASR-1RS. The reaction rate as expressed by Lim and No is:

$$r_{C-O_2} = 7500e^{-\frac{218000}{RT}} P_{O_2}^{0.75} \quad (4.9)$$

and the dissipation/generation rates for each species are expressed as:

$$R_{O_2} = \nu_{O_2} * r_{C-O_2} * \frac{M_{O_2}}{M_C} \quad kg.m^{-2}.s^{-1} \quad (4.10)$$

$$R_{CO} = \nu_{CO} * r_{C-O_2} * \frac{M_{CO}}{M_C} \quad kg.m^{-2}.s^{-1} \quad (4.11)$$

$$R_{CO_2} = \nu_{CO_2} r_{C-O_2} * \frac{M_{CO_2}}{M_C} \quad kg.m^{-2}.s^{-1} \quad (4.12)$$

where

- ν_{O_2} is the stoichiometric coefficient of O_2
- M the molar mass of each species in $kg.kmol^{-1}$
- P the pressure is in Pa

This correlation is expressed as a function of the O_2 partial pressure. Therefore, adaptation of the parameters must be calculated in order to input them in FLUENT which requires a reaction rate as a function of the concentration.

FLUENT reaction rate = experimental correlation reaction rate, and therefore, based on the Arrhenius FLUENT expression of the reaction rate:

$$k_{FLUENT}[O_2]^{0.75} = \frac{k_{experimental}P_{O_2}^{0.75}}{M_C} \quad (4.13)$$

and we know the ideal gas law: $PV = nRT$ with $R = 8314 \text{ J.kgmol}^{-1}K^{-1}$, $[O_2]$ in $kgmol.m^{-3}$

$$k_{FLUENT} = \frac{k_{experimental}(RT)^{0.75}}{M_C} \quad (4.14)$$

For this correlation, the values are:

$$\nu_{O_2} = 0.77$$

$$k_{experimental} = 7500, k_{FLUENT} = (8314 * T)^{0.75} * k_{experimental} * \frac{1}{12}.$$

$$\text{For } T = 650C, k_{FLUENT} = 9.113 * 10^7.$$

$$\text{For } T = 850C, k_{FLUENT} = 1.05610^8$$

$$\text{The activation energy is: } E_A = 2.1810^8 \text{ J.kgmol}^{-1}$$

Correlation model II, used by Takeda and Hishida [4]

Takeda and Hishida performed air ingress experiments at the JAERI facilities. They had a very good insight on the choice of reaction rates for graphite corrosion by oxygen since they could actually do some related experiments on the graphite they used. The correlations developed by Takeda and Hishida are as follow:

$$r_{C-O_2} = 360 * e^{-\frac{2.09*10^5}{RT}} P_{O_2} s^{-1} \quad (4.15)$$

with R in $kJ.mol^{-1}K^{-1}$ and the dissipation/generation rates for each species are expressed as:

$$R_{O_2} = \nu_{O_2} * r_{C-O_2} * \frac{\rho_C}{M_C} * M_{O_2} \quad kg.m^{-3}.s^{-1} \quad (4.16)$$

$$R_{CO} = \nu_{CO} * r_{C-O_2} * \frac{\rho_c}{M_C} * M_{CO} \quad kg.m^{-3}.s^{-1} \quad (4.17)$$

$$R_{CO_2} = \nu_{CO_2} * r_{C-O_2} * \frac{\rho_c}{M_C} * M_{CO_2} \quad kg.m^{-3}.s^{-1} \quad (4.18)$$

If we do the same calculations as previously, we obtain:

$$k_{FLUENT} = k_{experimental} * RT * \frac{M_{O_2}\rho_C}{M_C} \quad (4.19)$$

For this correlation, the values to put in FLUENT are therefore:

$$\nu_{O_2} = 0.88$$

$$E_A = 2.09 * 10^8 J.kgmol^{-1}$$

$$\text{for } T = 650C, k_{FLUENT} = 3.517 * 10^{11}$$

$$\text{for } T = 850C, k_{FLUENT} = 4.28 * 10^{11}.$$

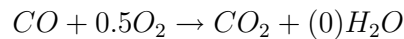
It appears that the oxidation rate recommended by Takeda and Hishida is much faster than the one recommended by Lim and No. This can be explained by different experimental conditions and sizes of experiments as well as by the different types of graphite used.

Both correlations were applied to the NACOK model as a guidance to first results. A correlation more adapted to this graphite was then developed based on the first benchmarking results.

4.4.2 Carbon monoxide oxidation reaction rate

The reaction rate of this reaction can be found in FLUENT's database. It is described as two reactions in order to take into account the water vapor concentration impact on the rate. The inputs are therefore:

Reaction A :



$$E_A = 1.674 * 10^8 J.kgmol^{-1}$$

$$k = 2.24 * 10^{12}$$

Reaction B:



$$E_A = 1.674 * 10^8 J.kgmol^{-1}$$

$$k = 4.5 * 10^7$$

4.4.3 Boudouard reaction rate

The Boudouard reaction rate proposed here is the one known for the corrosion of A3-3 type graphite.

$$R_C = -\frac{0.145 * e^{-25000/T} * P_{CO_2}}{1 + 3.4 * 10^{-5} * e^{7000/T} * P_{CO_2}^{0.5}} \text{ kg.m}^{-2}.\text{s}^{-1} \quad (4.20)$$

4.4.4 Stoichiometry variation of the graphite oxidation reaction with temperature

Reactions 1 and 2 combined together can be written with stoichiometry coefficients that vary with the temperature. At high temperatures, the oxidation reactions are going to be fast, and as a result, the concentration of oxidant at the graphite surface is very low. Since there is not enough oxidant, CO is going to be the main product and only a few percentage of the CO will react with the few oxygen left again to produce CO₂ before accessing the free stream transport zone.



. with $\frac{x}{y} = A(T)$ and therefore:

$$x = \frac{A}{(A + 1)} \quad (4.22)$$

$$y = \frac{A + 2}{2(A + 1)} \quad (4.23)$$

$$z = \frac{1}{(A + 1)} \quad (4.24)$$

It is generally accepted that $A(T)$ has an Arrhenius like dependence of T .

$$A = k_A * e^{-\frac{E}{RT}} \quad (4.25)$$

The values of k_A and E vary for different graphites. Even for the same graphite, experimentalists have produced different results. However, the values of the different reaction rate parameters have a strong impact on the temperature distribution in the NACOK experiment. Indeed, if more CO is produced, a highly exothermic oxidation of CO will lead to a rise in temperature.

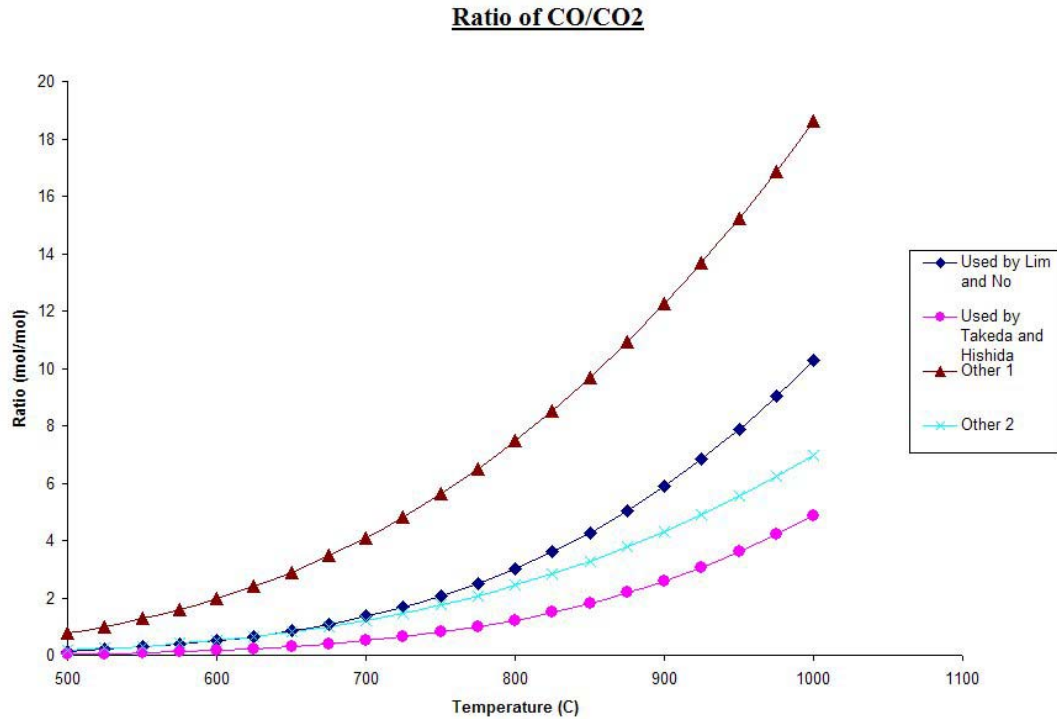


Figure 4-3: **Various correlations of stoichiometry coefficient ratio evolution with respect to the temperature**

Figure 4-3 presents the variation of the ratio of $\frac{CO}{CO_2}$ with the temperature. It appears that for the low range of temperatures where these correlations apply, the results are comparable. The differences widen with higher temperatures. In order to

be conservative, it is recommended to use the correlation provided by Lim and No. Its values are on the higher range of the average, and this will give an overestimation of the amount of CO. The highest ratio is not chosen since it is very briefly described in Takeda and Hishida and its range of application is unknown. Sensitivity studies are presented in Chapter 5 on the choice of the ratio of CO and CO_2 correlation.

4.4.5 Importance of the burn-off on graphite oxidation rate

Activation energy values and Arrhenius rate constants vary with the graphite burn-off at temperature higher than $600C$. Below $600C$, there is not enough burn-off to take this issue in account, even though the burn-off profile in the graphite is constant in depth. This means that there will be very little oxidation propagating in depth of the graphite, perpendicular to its surface.

In regime II, due to the in-pore diffusion, the burn-off will vary exponentially in depth, giving rise to a variation of reaction rates. The variation in oxidation rate is due to the change of total surface reaction. This can be explained by the fact that the reaction occurs at the wall of the pores. When the microstructure of the material changes, closed pores open and micropores become greater, the reaction surface increases, leading to an increase in reaction rate. At some point, the available reaction surface will reach a maximum, at approximately 40% burn-off. Beyond this maximum, the pore walls join together and the surface available will decrease, leading to a decrease in the reaction rate.

In regime III, the oxidation rate will decrease over time due to the reduction of the surface reaction since the oxidation attack at the surface will cause a geometry change of the graphite specimen. [22]

With this understanding of the phenomena taking place with burn-off, the variations of the Arrhenius rate parameters are more understandable. The Arrhenius rate constant, A , is going to decrease, due to a smaller temperature dependence of the rate with burn off. The activation energy is also going to decrease, due to the increase of surface reaction. This factor was only considered as an integrated effect which comes from experimental measurements of corrosion rate data.

Chapter 5

Sensitivity studies

5.1 Pressure loss in the pebble beds

Thermodynamically, the pebble bed is considered as a packed bed, meaning that the pebbles are not in motion. In a pebble bed, a large amount of heat transfer can occur in a small volume. For example, in the PBMR or other high temperature gas reactors, the fuel pebble or fuel compact is at a high temperature and generates decay heat. This is a major heat source. This is not the case in the NACOK, since the pebbles are made of graphite or ceramics. The pebbles without fuel do not generate any heat but store a considerable amount of energy. The pebbles help keep the temperature in the chimney at the reference temperature of the experiment. The flow in a packed bed is very complex, enhancing mixing and creating complex flow patterns. Moreover, the fluid will follow a longer path along the pebbles than if the flow pipe were empty. This deviation of the flow path induces a pressure loss. There are two major ways to describe the pressure loss in a pebble bed. The first one by considering the flow around each pebble and the second one by introducing a hydraulic diameter. Many pressure drop correlations have been developed for particles of different shapes and sizes and for different packing densities.

Jülich work on pressure drop

Kuhlmann, at the Jülich center in Germany, developed a pressure drop correlation based on the previous KTA report and experiments. [8] [21]. This correlation was

applied to FLUENT and the flow model benchmarked to the experiments described in the Khulmann report.

The Khulmann correlation [8]

The pressure loss ΔP prescribed by KTA is :

$$\frac{\Delta P}{\Delta H} = \psi * \frac{1 - \epsilon}{\epsilon^3} * \frac{1}{d} * \frac{1}{2\rho} * \left(\frac{\dot{m}}{A}\right)^2 \quad (5.1)$$

And the parameter ψ , for the NACOK experiment was found to be such that :

$$\psi = \frac{505}{Re/(1 - \epsilon)} + \frac{0.1}{(Re/(1 - \epsilon))^{0.1}} \quad (5.2)$$

These equations can be better understood when linked to the more general pressure loss equation:

$$\Delta P = \xi * \frac{h}{d} * \frac{\rho}{2} * v^2 \quad (5.3)$$

In these equations,

h or ΔH are the height of the pebble bed in m

ϵ is the porosity (0.395)

d is the pebble diameter in m

A is the flow cross section area in m^2

\dot{m} is the mass flow rate in $g.s^{-1}$

v is the flow velocity in $m.s^{-1}$

Re is the Reynolds number with $Re = \frac{(\dot{m}/A)*d}{\eta}$ with η the fluid dynamic viscosity

$\xi = \psi * \frac{1-\epsilon}{\epsilon^3}$ is a constant of the configuration

ρ is the gas density

This pressure loss cannot directly be input in FLUENT.

The pressure loss in a porous media in FLUENT can be modeled as an isotropic phenomenon, following a power law pressure drop [12]:

$$S = -C_0 * |v|^{C_1} \tag{5.4}$$

S is a source term in the momentum equation. S being constant in the pebble bed, $\Delta P = h * S$. Average values for the viscosity and density were chosen, and the power law was fit to the Kuhlmann correlation. It can be seen on the Figure 5-1 that the power law model allows a good approximation of the complex Kuhlmann correlation.

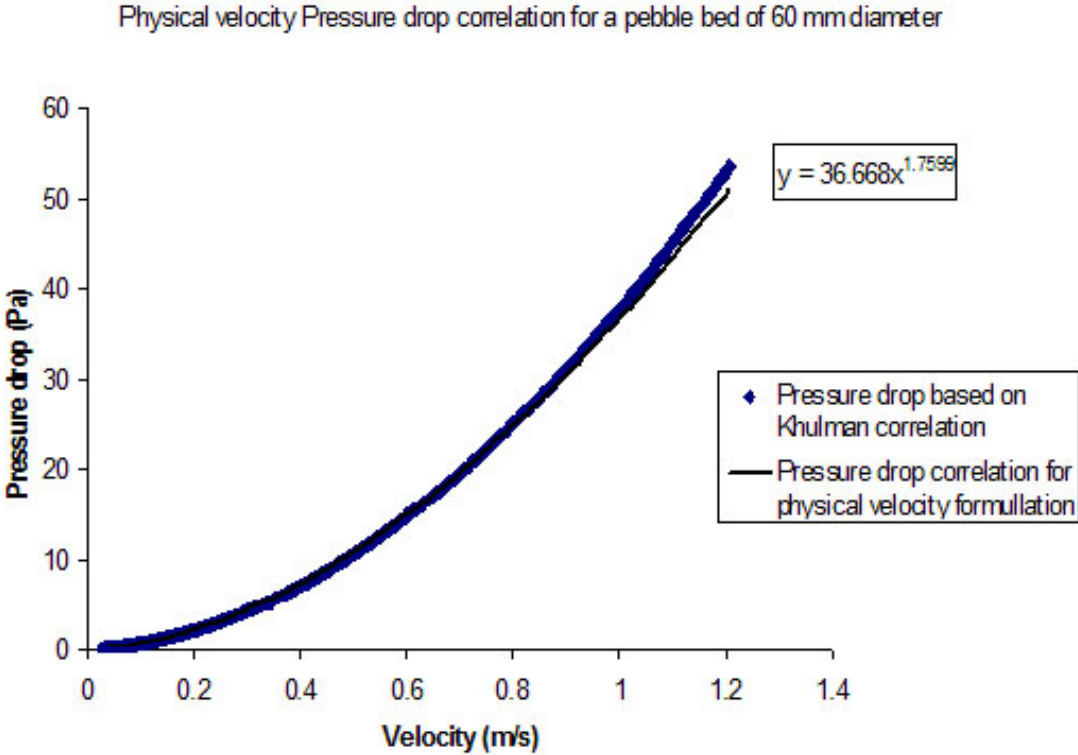


Figure 5-1: 5 m high pebble bed pressure drop (Pa) vs. air flow velocity (m/s) as input in FLUENT, Kuhlmann correlation and power law equation

Physical velocity vs. superficial velocity

FLUENT calculates the velocity in the porous media using the volumetric flow rate. Therefore, the computed velocity, called superficial velocity is proportional to the real velocity, called physical velocity. The physical velocity is the velocity of the gas flowing past the actual pebble.

$$v_{superficial}^{\vec{}} = \epsilon v_{physical}^{\vec{}} \quad (5.5)$$

where ϵ is the porosity of the media defined as the ratio of the volume occupied by the fluid to the total volume. There is an increase of the real velocity in the porous region, due to a smaller flow area available around the real pebbles. Since we are interested by the real velocity of air across the pebbles, it is important in our case to take in account this increase by selecting the physical velocity option in FLUENT. Indeed, the chemical reactions particularly depend on diffusion and transport of species, which is highly dependent on the velocity. Choosing this option adds some complexity in the adaptation of the pressure loss correlation, since the empirical correlations are usually based on superficial velocity. FLUENT automatically converts the pressure loss coefficients into those compatible with the physical velocity option when this option is turned on. Since the Kuhlmann correlation is based on real velocity, its parameters were modified in order to have the right pressure loss with the real velocity. The mass flow rates computed with physical velocity and superficial velocity are very close, as can be seen on Figures 5-2 and 5-3. This gives confidence in the simplification of the complex reflector geometry by developing porous media correlations. However, it appears that the superficial velocity option calculations gave slightly better results than the physical velocity option calculations. This can be explained by the fact that the parameters for the physical velocity option were adapted to match mainly the range of mass flow rate in which the NACOK experiments lie.

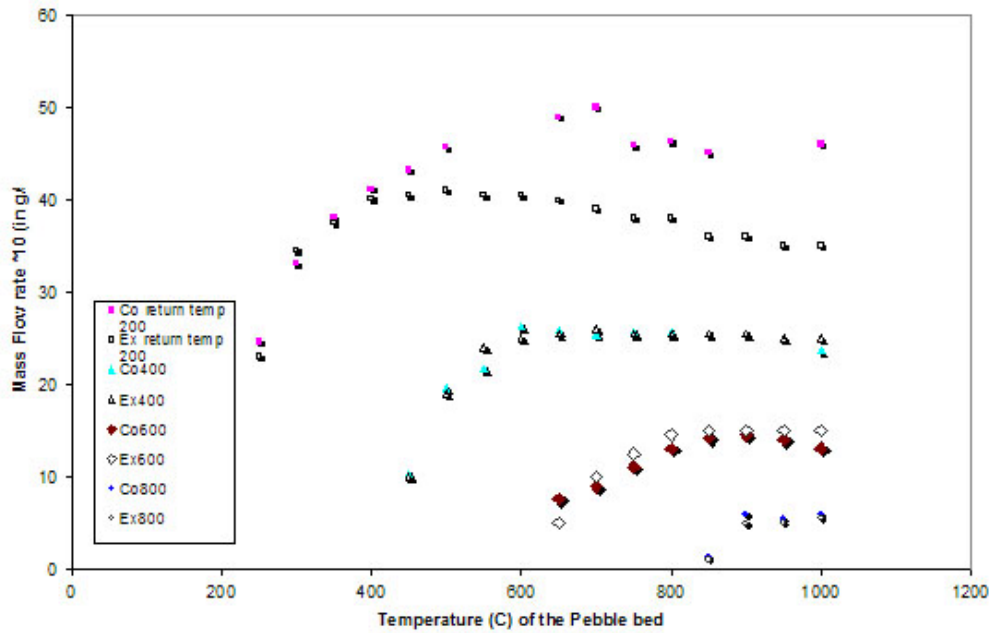


Figure 5-2: Comparison between Ex (Experiments) and Co (Computations) for the natural convection NACOK test: superficial velocity option

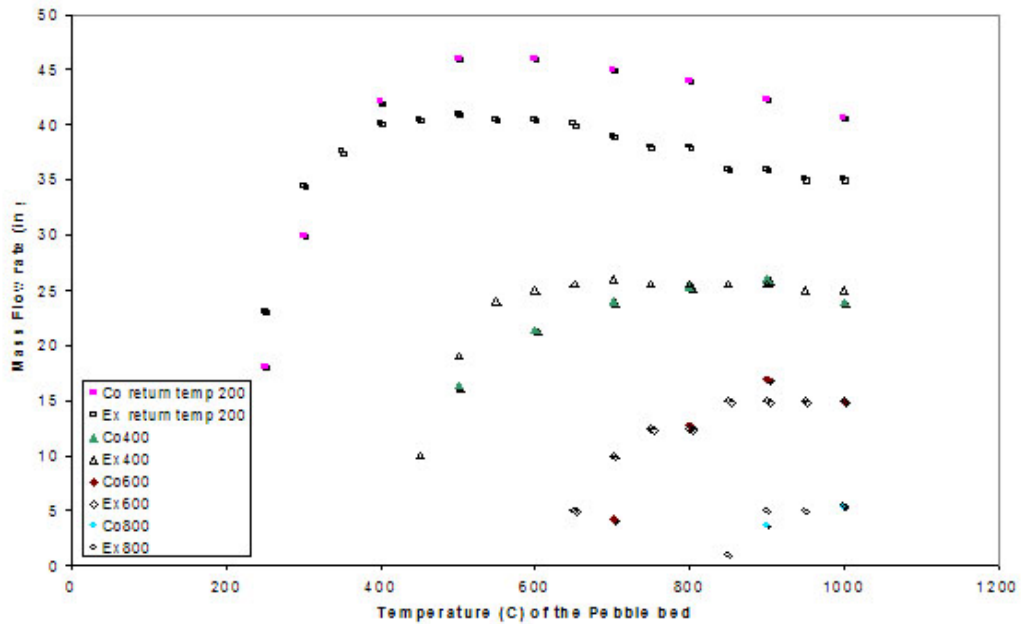


Figure 5-3: Comparison between Ex (Experiments) and Co (Computations) for the natural convection NACOK test: physical velocity option

Benchmarking of the natural flow in the NACOK experiment

In order to check the capacity of FLUENT to model natural convection flow and pebble bed induced pressure drop, the natural flow experiments run in 2001 [8] were used to benchmark the flow model. The pressure drop model presented needed to be benchmarked since it was different than the one developed by Zhai [1] in that it uses the physical velocity option instead of the superficial velocity for porous media and that it adapts the Kuhlmann correlation to a power law model.

Test Configuration: The height of the pebble pile was $h=5\text{m}$; the total height of the test stand, critical for the lift, was $H = 7.3\text{m}$. To create the broadest possible data base, four temperature steps were chosen for the return pipe at an interval of 200 K each, up to the maximum temperature of 800C. The temperature in the experimental channel was at least 50 K higher and was then increased in 50 K steps up to the maximum heating temperature. As expected, the convection flow developed due to the balance between the buoyancy forces (density driven) and the pressure drop in the pebble bed (function of the dynamic viscosity).

The FLUENT model used the physical velocity formulation based on the Kuhlman pressure drop correlation for the pebble bed modeled as a porous media. Temperature dependence of the density and the viscosity were taken in account using the ideal gas law and the kinetic theory. Figures 5-2 and 5-3 show a good agreement between the experiments and the simulation, when comparing the physical and superficial velocity, especially for lower mass flow rates. The discrepancy in the higher mass flow rates might be due to the loss of flow reported in this experiment and turbulences in the flow that were not modeled. However, the latest NACOK experiments are in the range of mass flow rates where the model is in good agreement.

5.2 Modeling the reflector as a porous media

The NACOK experiments have three types of graphite reflectors. The smaller ones have ninety-six 16 mm diameter channels. Creating the geometry and the mesh for this level of detail when modeling a full scale experiment is computationally time

consuming. In addition to that, due to the difference of scales (16 mm vs 200 mm height), the mesh created tends to be skewed and unreliable. Therefore, it was decided to develop a model to deal with fine reflectors as a porous media. The issues raised by this method are the establishment of the correct pressure loss, maintaining the correct surface to volume ratio and calculating the correct porosity in the media considered. Even though it appeared that the NACOK experiment could be run in steady state with the full detailed reflector geometry, the porous assumption for the fine reflector allows a faster and easier development of a model for a full scale reactor with a little less accuracy.

The surface to volume ratio was calculated to be $53.58m^{-1}$, based on basic geometrical considerations in the NACOK experiment. The porosity of the media, also based on geometrical considerations, was calculated to be 0.13. The pressure loss is more complex to define. Since no specific experiment was conducted on finding the pressure loss induced by the reflector, a correlation was established using FLUENT to FLUENT benchmarking. This is not a procedure that can be used for full results or benchmarking of a code. However, in this case, we only consider part of the experiment and aimed at simplifying the model using the same code. The reflector was modeled in detail and the pressure loss was computed for different velocities and mass flow rates at the range of viscosities (temperatures) of the NACOK experiment. Based on this data, a pressure loss following the power law FLUENT model was fitted. The reflector was then modeled as a porous media with this correlation and the flow rate for different experimental conditions was compared with the detailed reflector model. The detailed reflector structure is shown on Figure 5-4

The pressure loss correlation developed is, for the NACOK fine 96 holes reflector: $S = 63|v|^{1.72}$, with S the momentum pressure loss source term and v the velocity. Figure 5-5 shows the comparison of the pressure loss for a detailed reflector model and simplified porous media model.

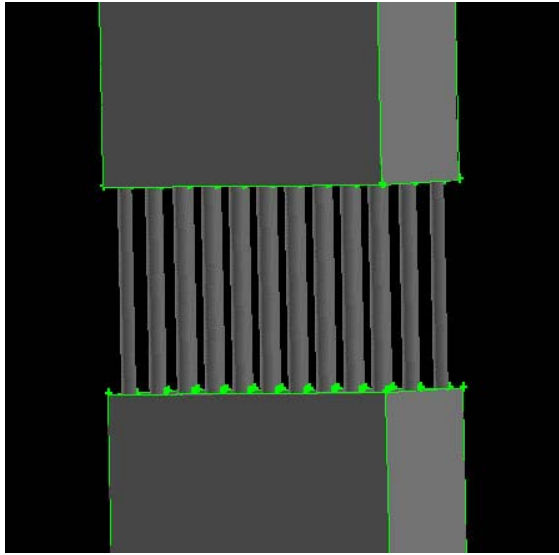


Figure 5-4: Detailed 96 channels reflector as modeled for the sensitivity studies

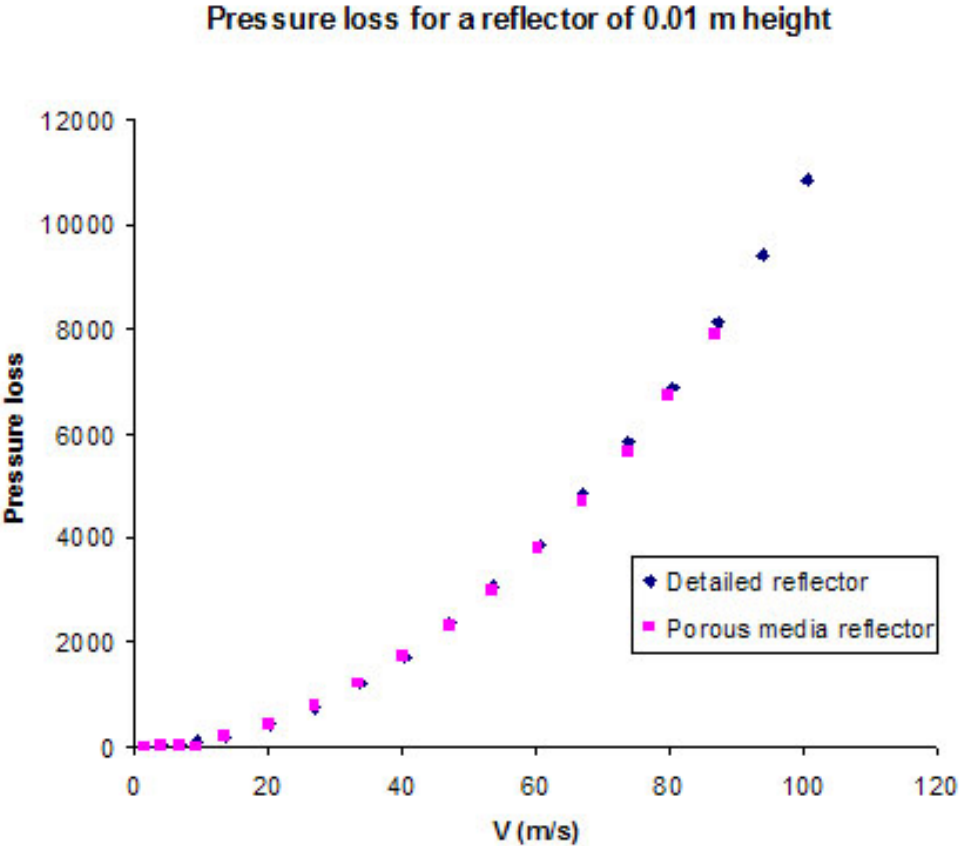


Figure 5-5: Comparison of the pressure loss at different flow velocities for a detailed reflector model and simplified porous media model

5.3 Modeling diffusion mass transfer

Theory

Heat is transferred when there is a temperature difference in a system. The species diffusion phenomenon is similar to the heat transfer by diffusion phenomenon. For species, if there is a difference in the concentration of some chemical species in a mixture, mass transfer will occur to establish an equilibrium. The species are going to be displaced to compensate the concentration gradient. Eventually, this gradient will be null. No effect of thermophoresis was considered in this study. For the transfer of a species A in a binary mixture composed of species A and B, Fick's law gives :

$$\vec{j}_A = -\rho * D_{AB} * \nabla m_A \quad (5.6)$$

, where

- j_A is the mass flux of species A in $kg.s^{-1}.m^2$
- ρ is the density of the mixture in $kg.m^{-3}$
- D_{AB} is the mass diffusivity in $m^2.s^{-1}$
- m_A is the species mass fraction

Fick's law is strictly valid when the total mixture composition is not changing, that is when the system is not open. For Ficks law to be valid, the diffusion coefficient must not be dependent on the species concentration, which is the case in a highly dilute mixture. However, the NACOK experiments are a non dilute system. Therefore, the use of the Fickian law would be only an approximation. However, FLUENT has the ability to model the full multicomponent diffusion in a laminar flow. The software uses the Maxwell Stefan equations, leading to a generalized Fick's law applicable for multiple species. This method is more computationally expensive but should be more accurate for the NACOK experiments. The kinetic theory model in FLUENT provides a calculation of the diffusion coefficients suitable for a complex mixture such as the one found in the NACOK experiments. [12]

Benchmarking the FLUENT diffusion model

In order to feel confident in the choice of the diffusion model and options, a small model was developed to benchmark the diffusion process with a multicomponent mixture comparable to the one used in the NACOK experiments. The system considered here is a vertical tube of 2 m high and 125 mm diameter. The top half is filled with helium and the bottom half is filled with nitrogen. Theoretical calculations for the diffusion process over time were made at PBMR [33]. A model of this system was solved by FLUENT using the kinetic theory model and multicomponent diffusion. It appears on Figure 5-6 that the diffusion process modeled by FLUENT gives satisfying results. PBMR modeled the diffusion by using a User Defined Function with the species diffusion equations. This gives a better fit of the theoretical curves. However, using this theoretical approach does not allow FLUENT to take in account other side effects such as wall effect (due to viscosity) or variations of the coefficients due to temperature, etc. These factors might account for the small discrepancy between the FLUENT model and the theoretical calculations. In conclusion, this benchmarking model shows that the FLUENT diffusion model can be used to model diffusion in the NACOK computational benchmarking.

Description of diffusion and flow features in the return duct experiment

As it has been described in Chapter 2, the inlet and outlet tubes to the channels of the NACOK experiments are horizontal and at the same level. At $t=0s$, they are filled with helium. When both ducts are simultaneously opened to the atmosphere, the helium in the horizontal tubes escapes through the openings due its low density. The horizontal ducts then fill up quickly with air. The process taking place vertically in the rest of the chimney is of a different nature and driven by both diffusion and natural convection. Computations and sensitivity studies were done in order to model this phenomena correctly. The boundary inlet and outlet conditions used for the open chimney experiments were inadequate to model this flow sequence. The pressure inlet boundary condition and outlet pressure boundary condition assume the "outside" gas condition. FLUENT can not model correctly the boundary species distribution with these boundary conditions since the species concentrations cannot change at these boundaries. Sensitivity studies showed the necessity to add a volume

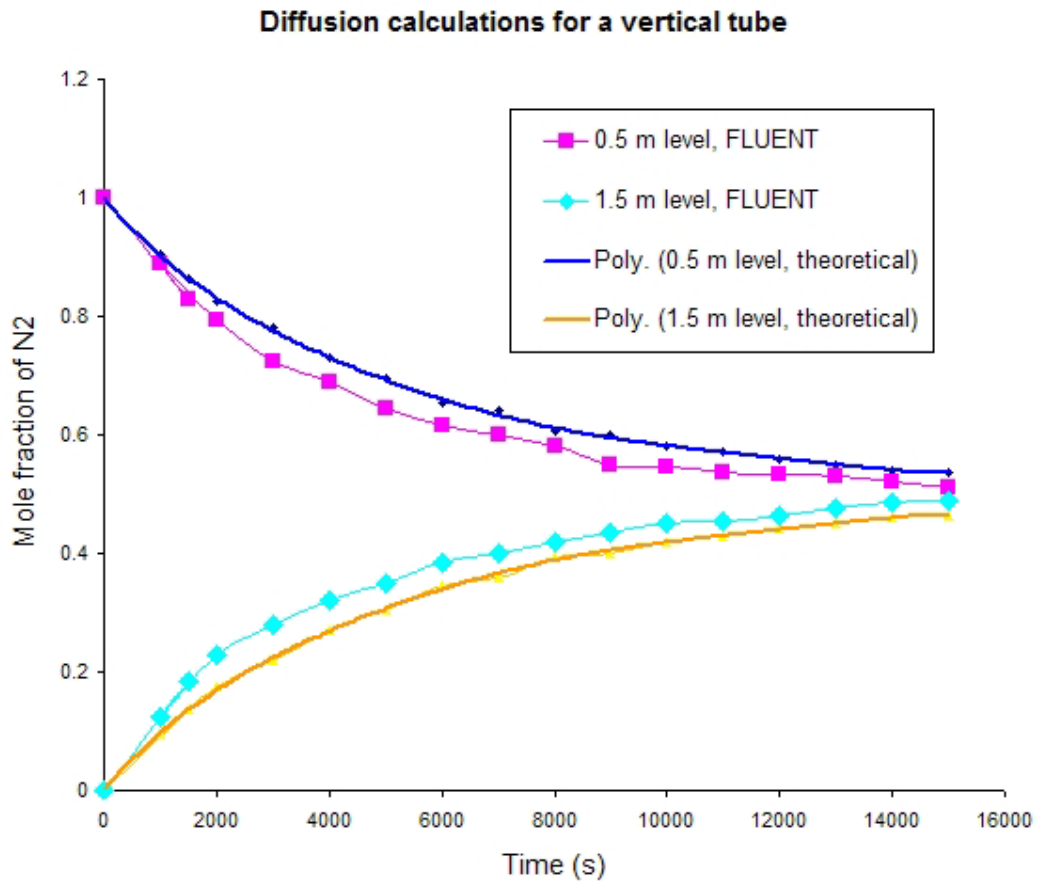


Figure 5-6: Comparison between theoretical curves as calculated by PBMR [33] and FLUENT kinetic model of the diffusion in a vertical tube

outside the channel from which air comes from and in which helium can flow. The final model and conditions are described more specifically in Chapter 6. Figure 5-7 shows the model configuration. Figure 5-8 shows the evolution over a few seconds of the outflow of helium from a horizontal tube open on both ends on a larger volume filled with nitrogen. The helium escapes the tube rapidly and in a few seconds, the equilibrium is reached. The process should take a longer time in the return duct chimney since the horizontal ducts are opened only on one end, but the overall phenomenon is similar and lasts a few minutes.

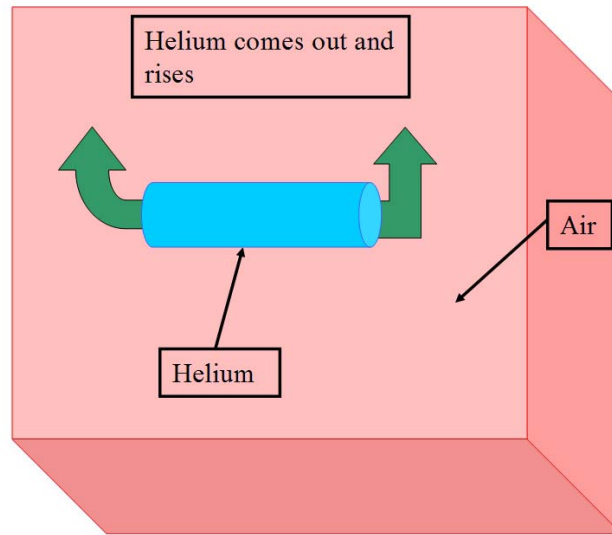


Figure 5-7: Model configuration for diffusion sensitivity analysis

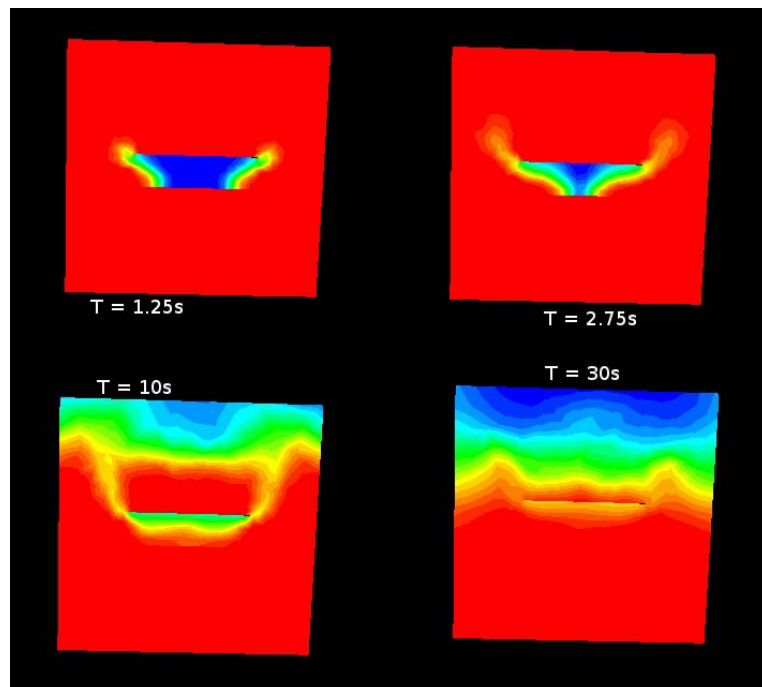


Figure 5-8: Evolution of the mass fraction of helium in an open horizontal tube (in the center of the square) in a volume filled with nitrogen. Red (dark) corresponds to a mass fraction of helium = 1 and blue (light) to a mass fraction of helium = 0

5.4 Modeling steady state flow for the return duct chimney

The procedure followed to model the return duct experiment is divided in several stages:

- The diffusion process is modeled time dependent. The chemical reactions are inactivated.
- The natural circulation stage is modeled steady state with the chemical reactions activated.

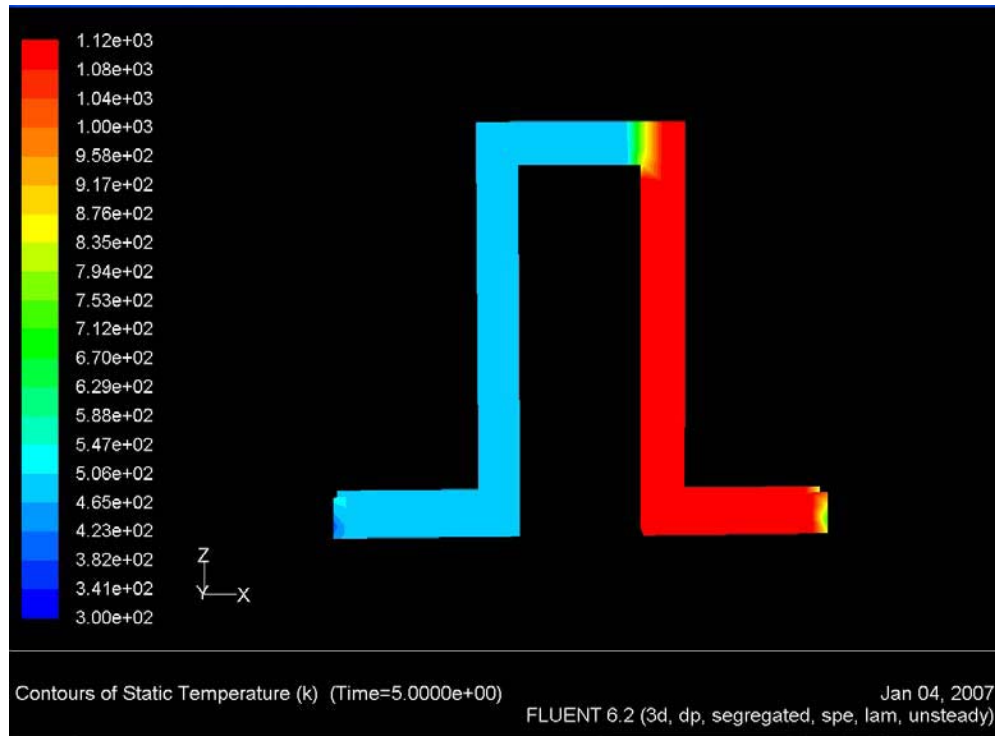


Figure 5-9: **Temperature distribution in Kelvins in the hot and cold leg**

It is therefore of importance to validate this procedure, and more specifically, to check whether a steady state is reached while modeling the transient diffusion and onset of natural circulation. Figure 5-9 represents the model used. A hot and cold leg of 500mm high and 2500mm^2 cross section are heated at respectively 1123 K and 500 K . Both legs are initially filled up with helium and the outside of the ducts

is nitrogen. At $t=0s$, the valves are open and nitrogen is let in. The time step is equal to 1s. The diffusion process takes place during 127s until natural circulation occurs. The mass flow rate at the pressure inlet is recorded over time.

Figure 5-10 presents the evolution of the mass flow rate at the pressure inlet as a function of time. The diffusion process is characterized by an unstable flow since this one is quite low and the pressure inlet boundary condition does not facilitate convergence for this process. At $t = 127s$, the mass flow rates jumps to $4.3g/s$ and stabilized in approximately 30 s. A steady state is then reached. The same model is then run steady state, with the hot and cold leg initially filled up with nitrogen. The computed mass flow rate is then $4.29 g/s$. This validates the procedure followed, namely, modeling the diffusion process time dependently and the natural circulation in steady state.

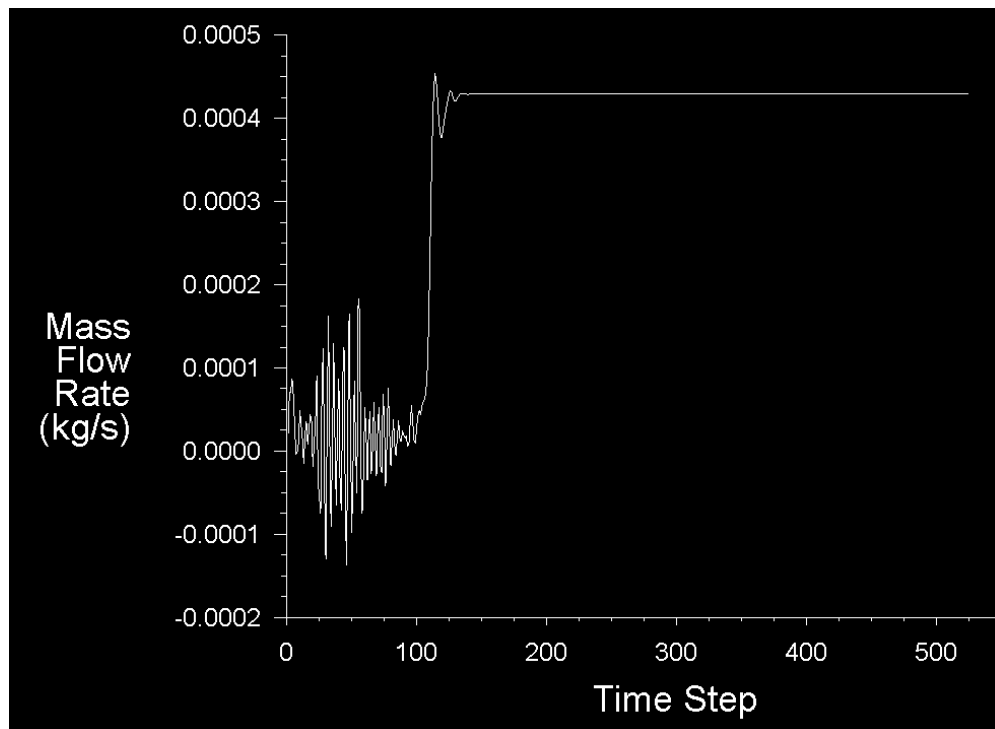


Figure 5-10: Mass flow rate with respect to time steps. A steady state is reached for a mass flow rate of $4.3g.s^{-1}$

5.5 Chemistry Sensitivity studies

This section presents sensitivity studies on chemistry parameters, such as time dependence, stoichiometry and reaction rates. The impact on the modeled system of the variation of some critical parameters such as Arrhenius constant or stoichiometric coefficients of the chemical modeling are investigated. The sensitivity studies on chemical reactions presented in this section were all based on the same geometrical mesh and model. A section of the 96 channel reflector of 16 mm diameter holes similar to the upper NACOK reflectors was studied. Only one single channel was modeled with a mass inflow of $0.03541g.s^{-1}$ at 650C going upwards as shown on Figure 5-11. The inflow is composed of 5% oxygen, 0.0043% water vapor and nitrogen. This composition was chosen to represent approximately the composition of the mixture reaching the higher reflectors. The composition of the inflow can be modified depending on the features investigated. Several variations of models and reactions rates are then applied to develop a better understanding of the phenomena taking place during these reactions and how the FLUENT model deals with them. These models are presented in the following sections.

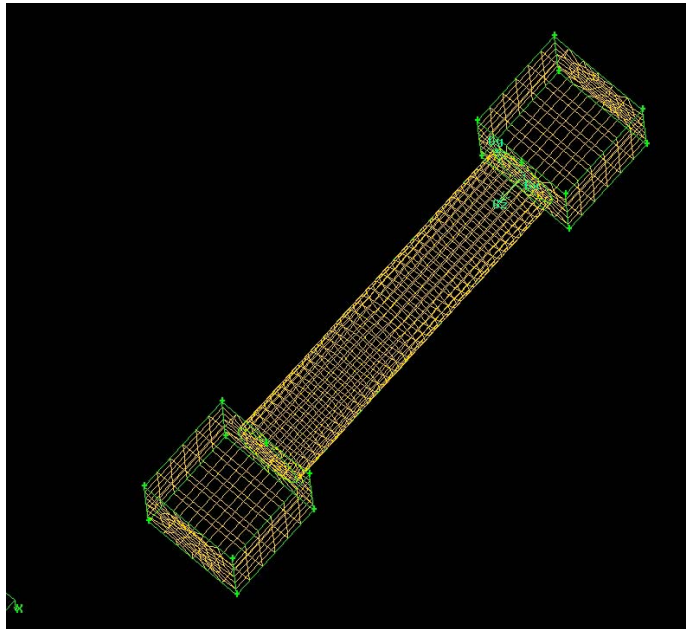


Figure 5-11: **Chemistry sensitivity studies model**

Transient model of chemical reactions

In general, steady state is reached when all physical parameters are constant over time. In this chemistry study, steady state is reached when the species concentrations do not vary over time. The corrosion of the graphite and carbon monoxide oxidation reach a steady state if the experimental conditions become steady and if there is enough supply of graphite. However, the concentrations or mass fractions of the different species present in the system are necessarily changing in the early part of the experiment and before the steady state is reached. It is very computationally expensive to model the transient chemical phenomena in the entire experiment. Therefore, in order to develop a good understanding of the time dependence of reactions taking place and the evolution of the species mass fractions, a simple transient model was investigated. In order to check whether a steady state is reached, only the slowest reaction was modeled, that is, the graphite corrosion due to oxygen. The reaction of carbon monoxide with oxygen being much faster, its effects are close to instantaneous. In this sensitivity study, the evolution of species fractions was recorded over time. It appears that a time step of 0.1s is sufficient to assure convergence of the chemistry model.

The evolution of the volume average of the species molar fraction with respect to time in the single channel is shown on Figure 5-12. One can see that a steady state is reached after 15 seconds of flow through the channel. This confirms therefore that sensitivity studies run in steady state mode give meaningful results and that transient simulations are not necessary to compute the end state of a system. Moreover, the ratio of carbon monoxide with respect to carbon dioxide is constant over time. Any changes from this ratio in more complete models can therefore be attributed without doubt to the reaction of oxygen with carbon monoxide and the Boudouard reaction.

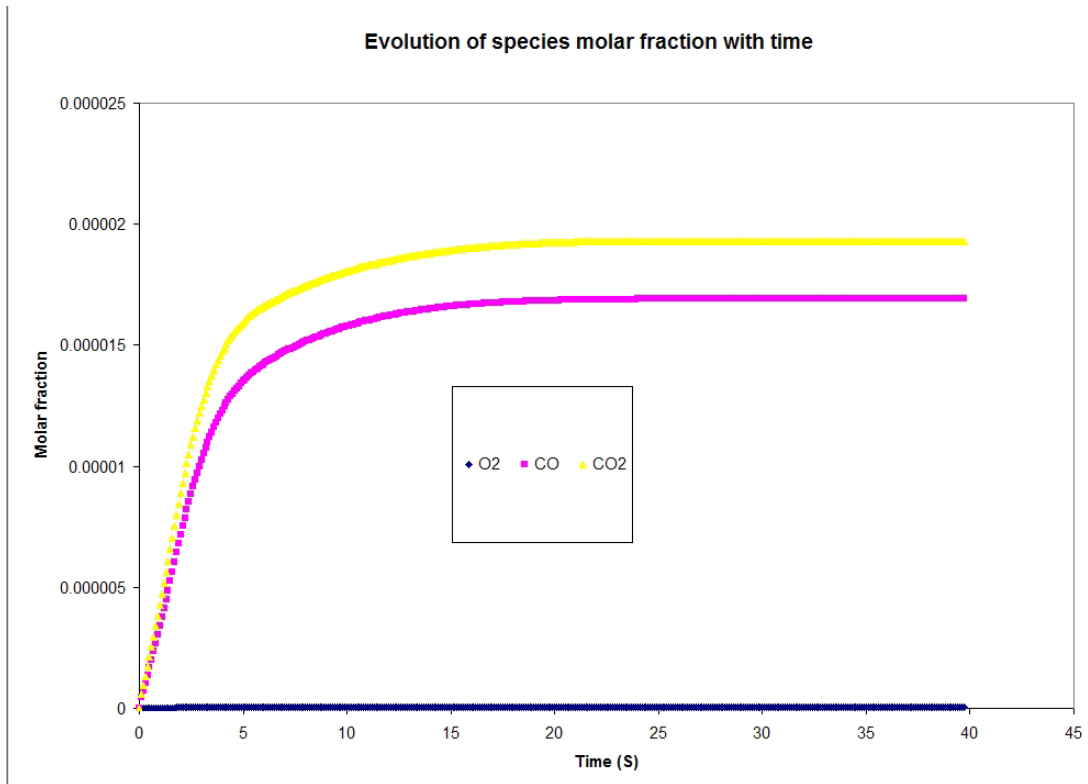


Figure 5-12: Evolution of the species molar fraction with respect to time

Temperature and the stoichiometric coefficients

The dependence and different correlations for the stoichiometric coefficients as a function of temperature were described in the Chapter 4. It is also important to realize that the stoichiometry of the reaction will have a strong impact on the temperature, due to the different heat produced by the corrosion reactions and the carbon monoxide oxidation. A small sensitivity study was conducted to explore this question. The stoichiometry of the graphite corrosion reaction was varied and the final state data of the system were compared for the simple configuration. The results are presented on Table 5-1.

One can see here that the variation of the initial stoichiometry greatly affects on this model the end state. The computed final temperature rises when there is more carbon dioxide produced. This makes sense since the heat emitted during the production of carbon dioxide is more than three times the heat emitted during the

production of carbon monoxide by graphite corrosion. In addition to that, the final molar ratio of species in the channel follow the logical evolution of the stoichiometric initial ratios. However, it appears that the more carbon dioxide is produced, the less it will be present proportionally to the initial conditions. This can be explained by the fact that there is less oxygen available when there is more carbon dioxide produced, and therefore, less carbon monoxide will react with oxygen to form carbon dioxide. This can reach a point where few carbon monoxide molecules will react with oxygen, inducing a slowdown in the rise of temperature with the variation of initial stoichiometric parameters.

Table 5.1: **Stoichiometry sensitivity study**

Input ratio of $\frac{CO}{CO_2}$	2.69	2.09	0.85
Computed final temperature in the channel	1120C	1260C	1300C
Computed final ratio of $\frac{CO}{CO_2}$ in the mixture	1.9	1.57	1.38
Computed final ratio / Initial input stoichiometry ratio	1.55	1.33	0.61

Corrosion Reaction rates

In order to study the impact on the final system of different graphite corrosion reaction rates, a sensitivity study was conducted using the single channel model at a mean initial temperature of 923 K (650C). The main variation in reaction rate is due to the Arrhenius constant. The activation energy is known to be of the order of $10^8 \text{ kgmol} \cdot \text{J}^{-1}$ but the range for the Arrhenius constant goes from 10^7 to 10^{13} [2] [4] [15]. Therefore, the sensitivity studies were run with a variation only on the Arrhenius constant. The higher this constant, the faster the graphite corrosion that takes place. The results are presented on Table 5-2.

Table 5.2: Corrosion reaction rates sensitivity study for same flow rates and initial temperatures of 923 K

Arrhenius constant as input in FLUENT	10^7	10^9	10^{11}	10^{13}
Computed maximum final temperature in the channel	924K	1310K	2100K	2520K
Computed average final temperature in the channel	923.5K	1130K	1537K	1780K
Computed average surface mass loss in the channel ($kg.s^{-1}.m^{-2}$)	$1.78 * 10^{-4}$	0.0178	1.78	178

It appears here clearly that the Arrhenius constant and thus the reaction rate has a large impact on the final state of the system. The major change in end state temperatures in these models is due to the type of computational experiment run (small channel and a lot of oxygen available). The range of differences will be smaller in full size real life air ingress conditions experiments since less oxygen should reach these reflectors. However, this extreme model clarifies the response of the system to a change in reaction rate and confirms that the knowledge of corrosion reaction rate of the graphite is of major importance in being able to predict other physical parameters of the system such as temperature and mass loss.

Boudouard reaction

The Boudouard reaction was described in Chapter 3. It is an endothermic reaction, that can help the cooling of the system where corrosion take place. A sensitivity study was run with the one channel model described at the beginning of this section. For this sensitivity study, the channel was set at 850C. One model was run with the Boudouard reaction activated, the other without. The results are presented on Table 5.3.

Table 5.3: Boudouard reaction sensitivity analysis

Boudouard reaction activation	On	Off
Computed final maximum temperature in the channel	1840K	1850K
Computed average final temperature in the channel	1437K	1455K
Computed average surface mass loss in the channel ($kg.s^{-1}.m^{-2}$)	2.280	2.281

The results of this sensitivity study confirm the cooling impact of the Boudouard reaction. Similarly to the graphite corrosion by oxygen, the Boudouard reaction rate is not specifically known for these experimental conditions. Therefore, it is of interest to see what are the impact of changes in the Boudouard reaction rate. A similar model was run with a Boudouard reaction rates with the Arrhenius factor = 1000. The final computed average temperatures is 1437K instead of 1455 K without the Boudouard reaction. Therefore, in a 1123K environment, the Boudouard reaction will not affect the end state temperature of the system but will provide additional cooling.

Stoichiometry as a function of temperature

Various stoichiometry coefficients correlations and the dependence of the stoichiometry coefficients on the temperature were presented in Chapter 4. The FLUENT model use fixed stoichiometry coefficients, based on the main temperature of the experiment, namely 650C and 850C. However, since the temperatures changes due to air cooling and heat production by exothermic reactions, the stoichiometry coefficients in the graphite oxidation reaction are also changing. Therefore, a User Defined Function (UDF) was created in order to take in account this phenomena. This UDF is given in the Appendix 4.

FLUENT chemistry option is not set up to have a variation of stoichiometry coefficients with temperature even with the use of UDFs. Therefore, the following

procedure was used:

- Create 15 reactions of graphite oxidation in the FLUENT chemistry model. The reactions are named r650, r675, ..., r900 as a reference to the temperature at which they take place. For each reaction, the stoichiometry coefficient are the ones from the Lim and No correlation on Figure 4-2
- A UDF is created that affects the surface reaction rates. For the reaction, the rate is set to the graphite oxidation rate from the Lim and No correlation (Section 4.4.1) if the temperature is in the range of T-25 and T+25. The rate is set to zero otherwise.
- As a result, at each iteration, the UDF is applied to each cell. Only the reaction with the stoichiometric coefficients corresponding to the right temperature range has a non zero rate.

Table 5.4: **Stoichiometry sensitivity study with UDF**

Model	UDF	without UDF
Mole fraction of O_2	$9.15 * 10^{-5}$	$9.146 * 10^{-5}$
Mole fraction of CO	0.087	0.088
Mole fraction of CO_2	0.901	0.901
Average temperature	850 C	850 C

The standard sensitivity analysis model described in this section was run steady state with a low reaction rate in order to be able to observe the impact of a UDF without having results taken to an extreme by the heat generation due to an important quantity of oxygen introduced. Therefore, the Arrhenius factor was artificially set to 10^9 . This way, only the impact of the use of a UDF on the graphite mass loss is studied and not the heat production. The first one is run without the UDF using FLUENT input stoichiometry of Lim and No at 850C [2] [3], the second one with the user defined function activated. Table 5-4 shows the values of interest to compare the impact of the UDF on the final state of the system. It appears that there is no major difference in the species distribution or in the temperature

distribution in the channel. Therefore, the use of UDF could reduce uncertainty in the computational results. However, using fixed stoichiometric coefficients does not jeopardize the accuracy of the results.

Chapter 6

Results of the Benchmarking of the Open Chimney Test, March 2004

The open chimney experiment was thoroughly described in Chapter 2. Therefore, a very short overview of the experiment is given here. The FLUENT main model used to model these experiments was thoroughly described in Chapter 3. Unless mentioned otherwise, the results presented in this chapter were obtained with this main model.

The NACOK open chimney experiment is made of an open chimney heated to a uniform temperature of 650C. The lowest part of the channel is the reflector made of graphite. Above the reflectors are two pebble beds of different size and material. One is made of ceramic with a 10 mm diameter, while the other one is made of graphite with a 60 mm diameter. The experiment proceeds as follows: initially, nitrogen at 650C is blown into the experimental apparatus for a sufficiently long time to ensure that all components are at a thermal equilibrium of 650C. Once this occurs, the pressure is equalized at atmospheric pressure. At the time $t = 0s$, the entrance duct is open and air from the building is let in. Sensors and measurement devices analyze the flow, the temperature and the distribution of species all along the chimney.

This benchmarking of the open chimney experiment being blind, the main results presented here come from the first blind run of the open chimney experiment. The results of this run were then compared to information and data received from the

Jülich center in Germany and from PBMR in the Republic of South Africa. Several sensitivity studies on the chemical reactions presented in Chapter 5 were inspired by these results. Based on these sensitivity studies and the result comparisons, several revisions to the model are also proposed.

6.1 The Blind Benchmark Model

6.1.1 Description

The basic model mainly corresponds to the various parameters and configurations that have been described in the previous chapters (Chapter 3 and 4). The chemistry model for this run was based on Takeda and Hishida [2] [3]. This model was chosen since Takeda and Hishida had performed benchmarking using FLUENT. The Boudouard reaction was not taken in account at first, since its impact is negligible at these temperatures. The small channels reflectors were modeled as porous media. Figure 6-1 shows the FLUENT mesh of the model. The model was run steady state. This can be justified by the transient chemistry studies on small reflectors presented in Chapter 5 which showed that steady state is reached in a relatively short time. Indeed, one can see the evolution of the gas species concentration graphs (Figure 5-9). It appears that at constant mass flow, a species concentration steady state is reached. The experiments at the NACOK facility lasted for 480 min. In order to shorten the computational time and benchmark the experiment, the model was run steady state and the results compared to the steady state (after 300 min) to experimental data. Chapter 9 shows the key variables of the model.

6.1.2 First estimate of graphite loss

In order to obtain a preliminary estimate of the mass flow rate and velocity in the NACOK experiments, simulations were run without the chemical reactions option in FLUENT activated. This implies that no heat was being added by the graphite corrosion and the temperature stayed at 650 degrees Celsius. The mass flow rate calculated is in the right order of magnitude, since it was shown in the Kuhlmann experiments [8] that a delta temperature of 600 C induces only a multiplication by

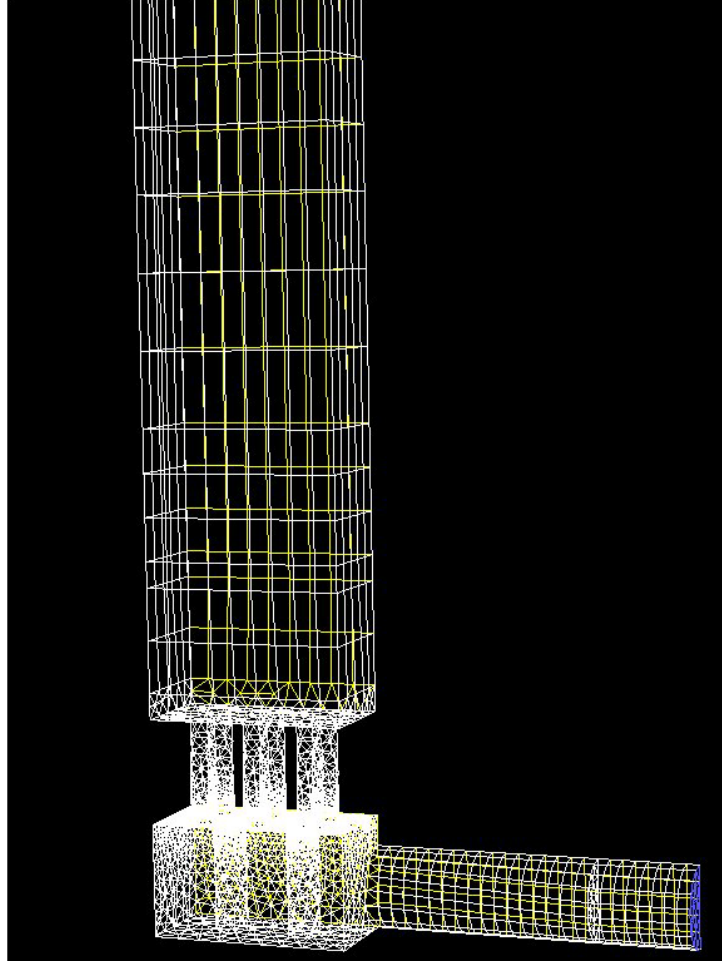


Figure 6-1: Mesh of the lower part of the experiment

3 of the mass flow rate. Therefore, the good range of mass flow rate is known. According to the specifications on the NACOK experimental setting, temperature is limited to 1500 C. Therefore the experimental flow rate should be in the same range as the one computed even without taking in account any heat production.

For the open chimney, at a temperature of 650 C without chemical reactions, the mass flow rate computed is approximately, after convergence of the steady state, $3.54g.s^{-1}$. Over 480 min, the quantity of air entering the channel is:

$$Q_{air} = \frac{\dot{m} * T}{M_{air}} \quad (6.1)$$

Where $M_{air} = 29g.mol^{-1}$ is the molar mass of air at 20C, $T = 480 * 60 = 28800s$ and $\dot{m} = 3.54$. The quantity of air entering during the experiment is 3515 mol. The

air entering is composed of 23% mass of O₂. Therefore, the total quantity of oxygen entering the channel is $Q_{O_2} = 808 \text{ mol}$. In order to make a very conservative estimate of the maximum mass of graphite corroded during the experiment, one can consider that all the oxygen will react with the graphite with a stoichiometric coefficient of 0.77 (Chapter 3). Therefore, the graphite loss will be of 1049 mol, which corresponds to a mass loss of $Q_{\text{graphite}} = M_C * 808 = 12.5 \text{ kg}$. The high estimate of graphite that can be corroded in 480 minutes is 12.5 kg. This way to predict an over estimate of the mass of graphite corroded is very convenient. Indeed, without having to run a complex chemistry model with high uncertainties, a good conservative estimation of the loss of graphite can be found. It is strongly recommended to use this method before running any complete model. The graph on Figure 6-2 shows a quick estimate of the maximum graphite loss in 480 minutes, that is 8 hours as a function of the temperature and the air ingress mass flow rate. One has to bear in mind that this is the maximum estimate, and that the overestimation is even larger at higher temperatures. Moreover, this estimate is in the right range if the mass flow rate computed is correct. In case of high uncertainties on the mass flow rate due to poor knowledge of the flow configuration, this method would provide an estimate of the graphite mass loss that could be off by a factor 3.

6.1.3 Results

This section presents the results obtained for the open chimney experiment. Further analysis of the discrepancies and interpretations are in the following section.

Presentation

The results are compared with the data provided by the JULICH center after the analysis was complete. The data provided included axial temperature at different axial locations, mass flow rates and gross mass loss. Table 6.1 provides key parameters of interest in air ingress events: mass flow rates, graphite loss and outlet species fraction. The interpretation of the results helps understanding where the discrepancies come from and will be done using raw data provided by PBMR.

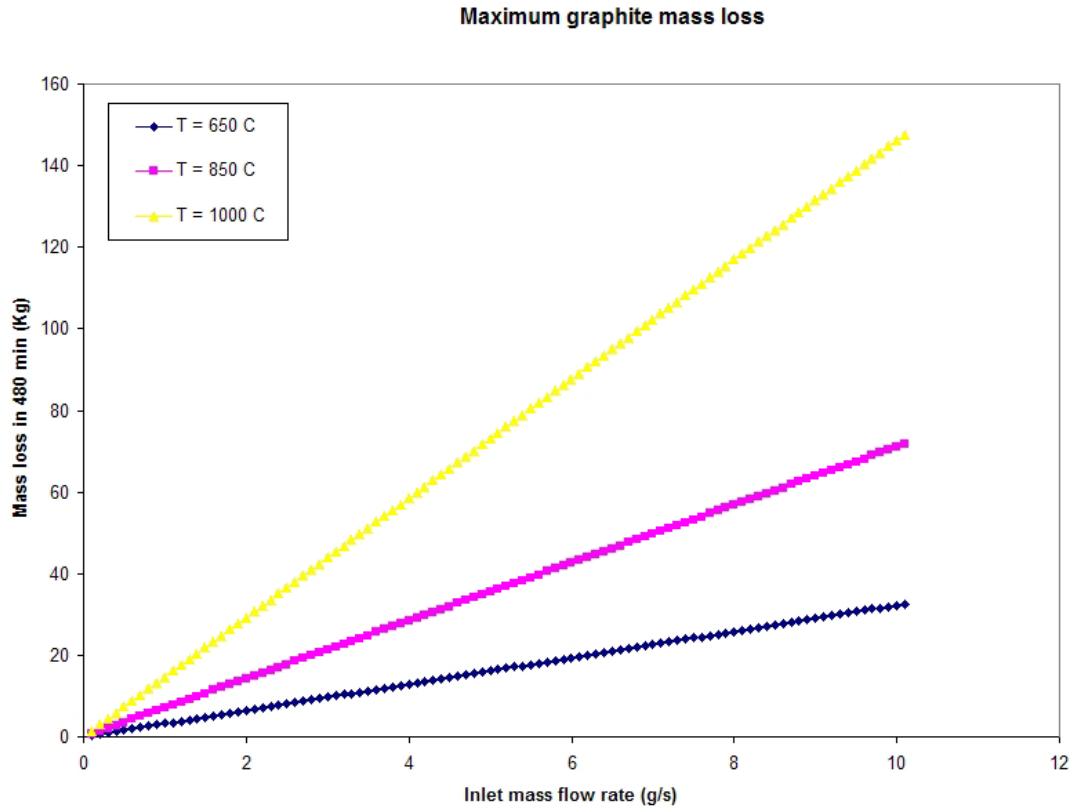


Figure 6-2: Estimate of the maximum graphite loss in 8 hours

Table 6.1: Open chimney computation and experiment key results

Parameter	FLUENT run	NACOK
Time (min)	480	480
Mass flow rate ($g.s^{-1}$)	3.54	3.4
Air entry (Kmol)	3.416	3.515
Graphite Loss (Kg)	9.302 kg	9.05 kg
Outlet O_2 molar fraction	0.005	< 0.1
Outlet CO molar fraction	0.01	< 0.1
Outlet CO_2 molar fraction	0.206	0.21

There is an excellent agreement with the mass flow rate and the amount of graphite corroded.

Temperature distribution

Figure 6-3 shows the distribution of temperature varying vertically in the chimney. Please note that the scale on the figure is about 2 meters. There is no change of temperature or species concentrations within the last 5 m of the channel. There is a good qualitative agreement for the distribution of temperature and the absolute values. The maximum temperature for the FLUENT blind model recorded at a sensor point is 920 C. The experimental maximum temperature is 870C. There is therefore a discrepancy of 50C. The FLUENT model overestimates the maximum temperature and can therefore provide a conservative evaluation of the distribution of heat produced.

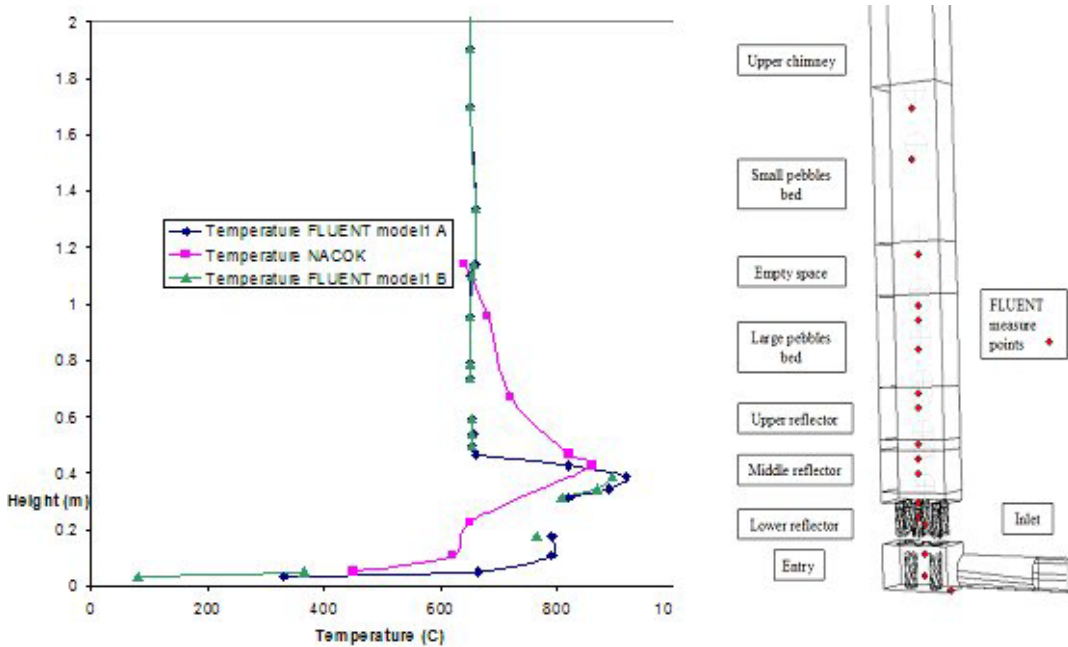


Figure 6-3: Flow Temperature distribution in the open chimney test

Species distribution

Figures 6-5 and 6-4 show the FLUENT calculated distribution of species mass fractions in the channel. One can see that the majority of the oxygen is consumed in the lower reflector, either by the graphite corrosion reaction or the CO oxidation. FLUENT computations show also a small increase in the molar fraction of CO at the outlet. This can be explained by the Boudouard reaction, very slow at this tem-

perature, that produces a small amount of CO. This CO can not react with oxygen since all of it is consumed in the lower parts of the channel.

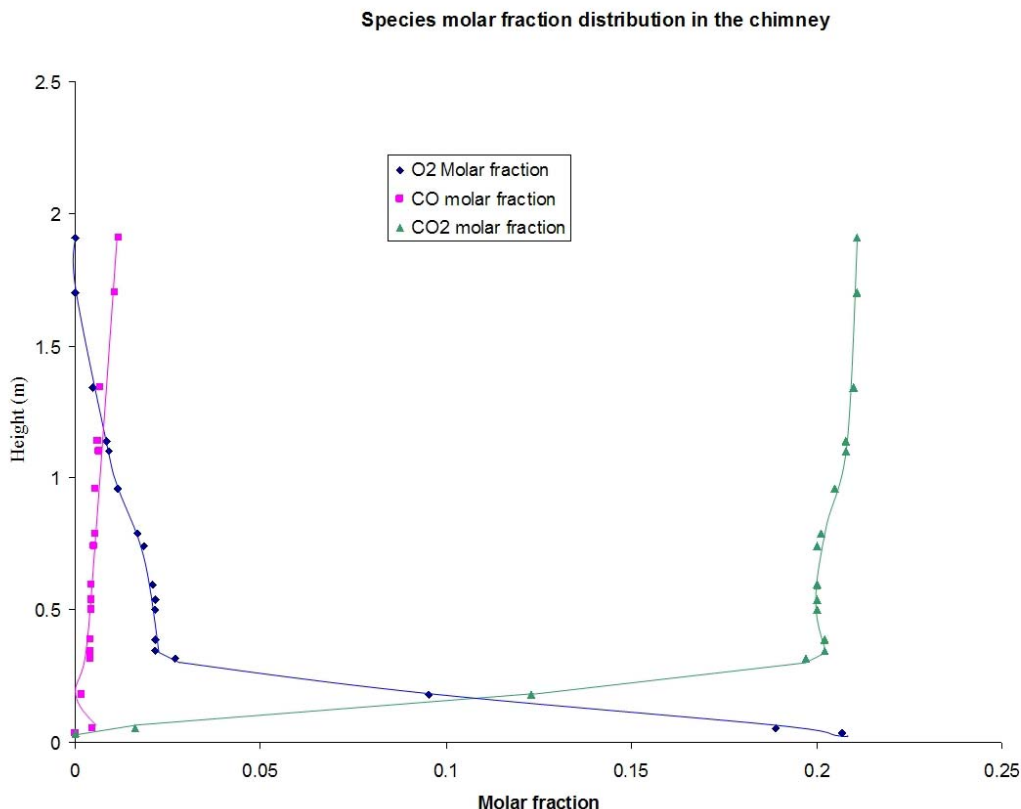


Figure 6-4: **Computed molar fractions in the open chimney test. Experimental data not available**

Velocity

An overview of the velocity distribution in the channel is interesting. The species transport and diffusion in the graphite pores will depend on the speed at which the air flows. The maximum velocity does not exceed $1.5m.s^{-1}$ and the maximum Reynolds number does not exceed 1200. This confirms that the flow is globally laminar at these mass flow rates. However, it is likely that some small turbulences will take place at major changes of geometry, at the entrance of the reflectors and the pebbles. The small turbulences will have an impact on the reactions at the boundary layer of the graphite since the reaction rate is limited by the transfer of

species to the graphite . This layer was not meshed in detail in this model since its thickness is of the order of the millimeter.

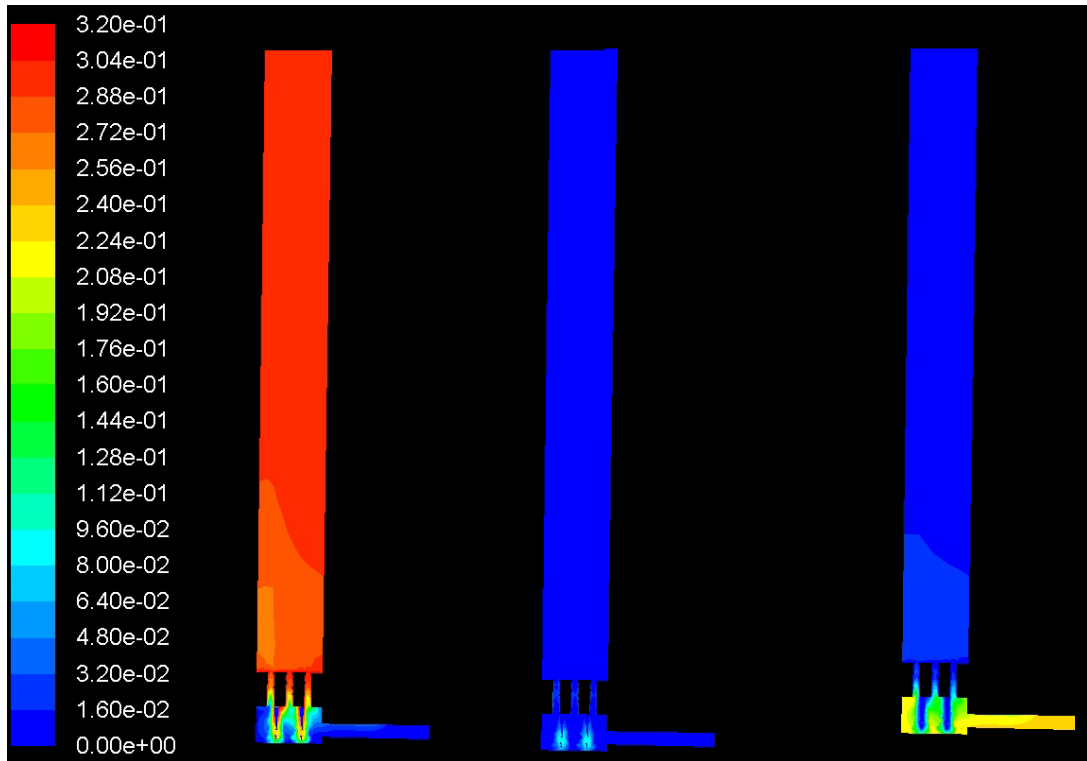


Figure 6-5: Mass fractions of CO_2 on the left, CO in the middle and O_2 on the right

Figure 6-6 shows the velocity vectors and the Reynolds number distribution in steady state calculations for the open chimney experiment.

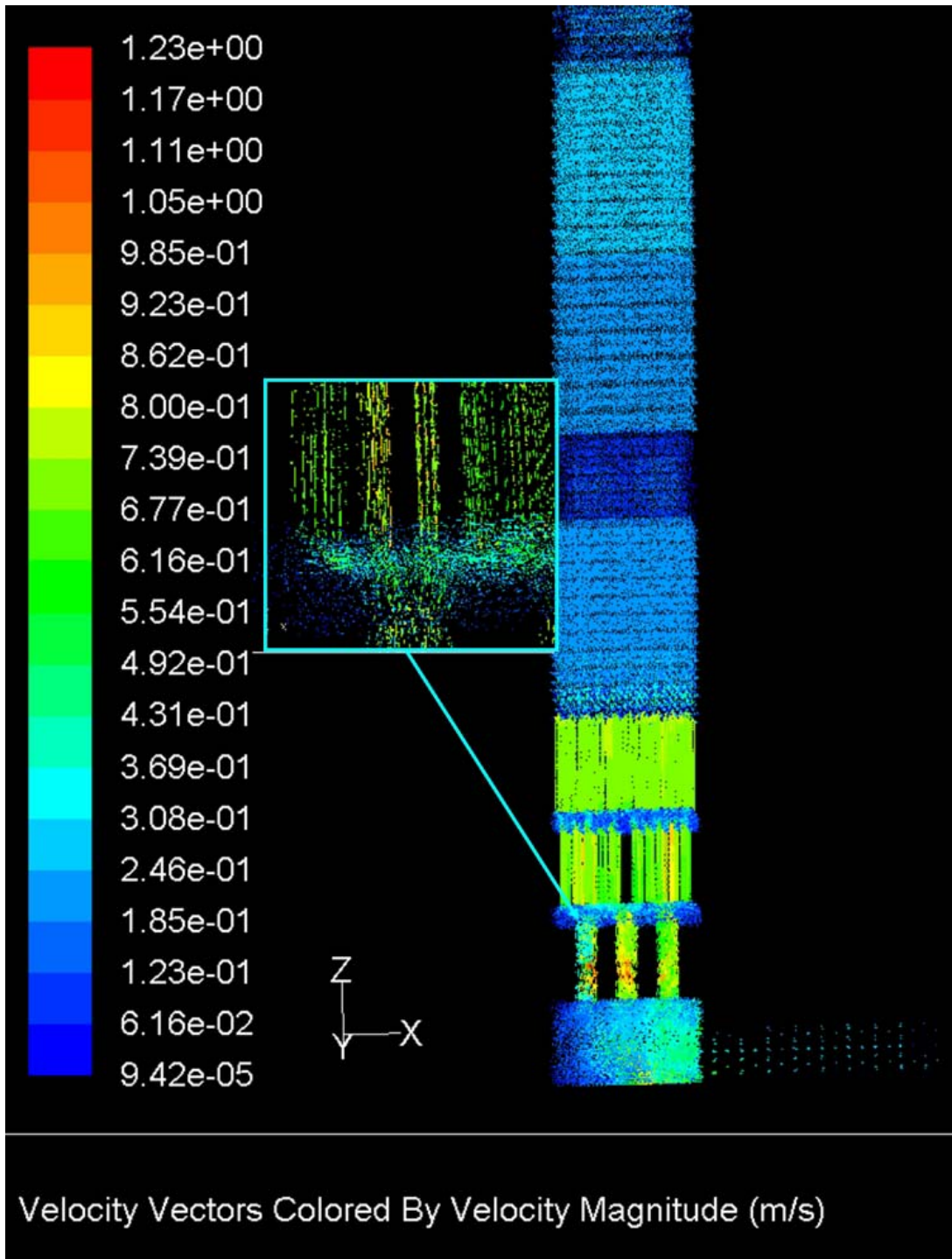


Figure 6-6: Velocity distribution in the lower part of the channel in $m.s^{-1}$

6.1.4 Further analysis of the experimental results

The results are very good considering the conditions (blind benchmarking) under which the model was created.

Flow modeling

The mass flow rate is off only by 4.1%. Apart from the blind benchmark model whose results were described in the previous section, a natural convection flow model with detailed reflectors was run to compare the mass flow rate. This detailed model gave similar results for the flow properties. The mass flow rate computed with this detailed reflector model is $33.8g.s^{-1}$. This confirms that the method developed to model detailed reflectors and pebble beds by porous media work not only on the separate effects as the sensitivity studies in Chapter 4 showed, but also on integral models such as the whole NACOK experiment. This results will allow future simplicity in the development of models for the Pebble Bed Reactor.

A good estimate of the mass flow rate was known based on calculations provided by the Jülich center [13]. These studies done at the Jülich center predicted an exact mass flow rate of $34.4g.s^{-1}$. Moreover, the flow model on the pebble bed was benchmarked based on the Khulmann report [8] as described in Chapter 4. These two parameters allowed good confidence in the flow model before the blind results were compared with experimental data.

Temperature distribution

The FLUENT model overestimates the temperature distribution.

- At first inspection, it appears that the graphite reaction rate assumed was too high, which resulted in the heat accumulating in the lower part of the reflector which would explain the discrepancy in the temperature distribution in the lower part of the channel. More precisely, if the reactions occurred more slowly, the total amount of heat produced would be the same, but oxygen would have time to travel further up the chimney before reacting with the graphite. Therefore the heat generated would be "diluted" and spread out higher in the

chimney. The chemical models were modified as described in the following sections in order to obtain a better agreement. The chemistry of the reactions was thoroughly described in previous chapters as well as several sensitivity studies.

It is suggested that the Arrhenius factor in the graphite corrosion rate equation [Equation 4-5] was over estimated. The value used at the blind benchmarking in the FLUENT model was $3.6 * 10^{12}$. A more appropriate value should be in the range of $[10^8 \text{ to } 10^{11}]$. This problem can be solved for further complete modeling with some specifically designed benchmarking corrosion experiments that will provide applicable Arrhenius factors or more complex reaction rate correlation models. Global gross correlations for the PBMR should be developed on simple models. For instance, this could be done by recording the mass of graphite of a reflector corroded at a specific temperature when exposed to oxygen. A better understanding and modeling of the chemistry taking place in this event could be done using atomic multi scale modeling and microscopic modeling. The complexity of the reactions and the multiplicity of parameters call indeed for a combination of first principle modeling and experiments.

An example of an experiment to run to obtain the parameters necessary to model the corrosion reactions in FLUENT could be to have a pebble bed (6*6*6 pebbles), a small channel (16 mm diameter) and a larger channel (40 mm diameter) at fixed temperature (ranging from 650 to 1000C) in a closed environment. Air should be blown on these structures and species concentration recorded at the exit of the experiment. After 60 min, which is a long enough time to obtain a thorough corrosion of the experiments, the amount of graphite loss should be calculated by weighing the pieces. Putting together data of graphite mass loss, and species concentration evolution over time, Arrhenius equation parameters E_A , A and n can be obtained for these experimental conditions by fitting the species concentration evolution over the following equations:

$$r_{C-O_2} = k * e^{-\frac{E_A}{RT}} * P_{O_2}^n \quad (6.2)$$

$$\frac{d[O_2]}{dt} = \nu_{O_2} * r_{C-O_2} * \frac{\rho_C}{M_C} * M_{O_2} \quad kg.m^{-3}.s^{-1} \quad (6.3)$$

$$\frac{d[CO]}{dt} = \nu_{CO} * r_{C-O_2} * \frac{\rho_c}{M_C} * M_{CO} \quad kg.m^{-3}.s^{-1} \quad (6.4)$$

$$\frac{d[CO_2]}{dt} = \nu_{CO_2} * r_{C-O_2} * \frac{\rho_c}{M_C} * M_{CO_2} \quad kg.m^{-3}.s^{-1} \quad (6.5)$$

In order to have different correlations for reflector grade graphite and pebble graphite, the experiment would have to be separated and done twice, once with the reflectors and ceramic pebbles, the other one with ceramic reflectors and graphite pebbles.

- A second explanation for the slight inaccuracy in temperature distribution as well as the overestimate of maximum temperature could be the under estimate of the ratio of carbon monoxide over carbon dioxide. If there is more carbon dioxide produced, more heat is generated since this reaction is the most exothermic one (3 times more heat produced than for the production of carbon monoxide by graphite corrosion). This aspect however is balanced by the fact that with less carbon monoxide, the oxidation of the carbon monoxide will take place less extensively. This reaction being highly exothermic, the amount of heat produced will be lower and counterbalance the amount of extra heat produced by a higher ratio of carbon dioxide produced.
- This blind FLUENT model of the NACOK open channel experiment was created without considering heat losses occurring in the experimental facility. Since the entire channel is initially at a uniform temperature of 650 C, this modeling of the heat storage and transfer in the graphite or aluminum walls is not essential. The heat transfer from the reacting graphite to the gas is however modeled. The experimental conditions are rarely idealistic and there could be discrepancies between the theoretical and real initial temperature distributions. Therefore, in order to treat this uncertainty, one would have to modify over time the boundary conditions of the model based on actual experimental data.

The overall result on the graphite mass loss is very good since it is off only by 1.5%. The Jülich center scientists also considered the crumbly pieces found at the bottom of the chimney as a graphite loss. Since the graphite mass loss is computed from surface mass loss in FLUENT, the crumbly pieces at the bottom of the channel

should not be accounted for in the mass loss to compare results. In that case, the NACOK mass loss is 9.05 kg. The computational results are off then by 2.8%.

The location distribution of the corrosion is not as satisfying. It appears, as can be seen on Table 6-2, that the reactions in the NACOK occur higher than expected from FLUENT computations. This confirms the previous hypothesis that the reactions rates used were too high. However, the good agreement on the overall mass loss confirms that the stoichiometry is right. An additional explanation for this discrepancy is the idealized experimental conditions modeled. FLUENT inputs a wall temperature of 650C from the very bottom of the channel. However, in reality, the heating wires might not go this low and the temperature at the entrance is lower at the beginning of the experiments. This factor might also contribute to this discrepancy in mass loss location. Finally, one should notice that there is a mass loss of .788 kg in the pebble area. This means that the oxygen was able to reach the pebbles. It confirms that the reactions are slow enough to let time for the air to rise up to this level.

Table 6.2: **Graphite corrosion location for the blind model**

Location	FLUENT mass loss (Kg)	NACOK mass loss (Kg)
lower columns	2.585	0.16
Lower reflector	4.84	0.29
Middle reflector	0.89	5.724
Upper reflector	0.984	2.346
Pebbles	0.0027	0.788
Crumbly pieces	NA	0.258
Total	9.307	9.05

6.2 Other models and runs

6.2.1 Temperature of 900C

The chemical reactions are highly dependent on the temperature. As described in the previous section, a higher temperature leads to a higher fraction of carbon monoxide produced during graphite corrosion, which leads to a rise in the amount of heat produced. Sensitivity studies have been described in Chapter 5, but it is of interest to assess the impact on the temperature distribution on the full scale model. The higher temperatures will lead to a higher flow rate, which by negative feedback will induce a cooling of the channel. This additional cooling is somehow counter balanced by the extra heat produced due to the extra O_2 entering the channel. A computational model similar to the blind model for an open chimney was run for an initial channel temperature of 900C (instead of 650C).

The mass flow rate calculated is $3.81g.s^{-1}$, that is, a rise of 12% over the 650 C mass flow rate. An approximate run (convergence reached only on a first order basis) gives a maximum temperature of 1150C. Despite an increase of 250C in the core structure, the temperature rise over the 650C case was only of 300C suggesting that the cooling effect of higher air ingress is effective, limiting the temperature rise in the pebble bed.

6.2.2 Modified chemistry model

The analysis of the blind model showed the following imperfections in the blind assumptions:

- Over estimate of the maximum temperature in the chimney.
- Inaccurate location of this maximum temperature in the experimental channel.
- Inaccurate distribution of the graphite mass loss locations

It is postulated that the main reasons for these discrepancies lie in the chemistry model. Therefore, in order to show that the model can be modified to provide a better match of the experimental data, a new model was developed at steady state.

This model was developed by running several models with different reaction rate parameters. The results were then compared to the experimental data and the rate parameters accordingly modified. The modified model is identical to the blind model except for the chemistry formulation. In order to reach a better match of experimental and computational data, this model was run with a fixed mass flow rate of $3.4g.s^{-1}$. Once a better match of data was reached, the model was run again with free flow to check the overall consistency of the modified model.

Modifications in the chemistry

After several runs and trials, it appears that a more accurate (but still not perfect) chemical modeling of the graphite should be as follows:

$$k = 10^{11}$$

$$\frac{n_{CO}}{n_{CO_2}} = 1.86$$

where k represents the Arrhenius factor in equation 6.2. As a reminder, in the blind model, k was chosen to be

$$k_{blind} = 3.6 * 10^{12}$$

and

$$\frac{n_{CO}}{n_{CO_2}}_{blind} = .86$$

. Therefore, for this modified model, the reaction rate is slower and there is more carbon monoxide produced, as suggested in the interpretations of the blind results. The ratio of carbon monoxide and carbon dioxide stoichiometric coefficients is changed by 112%. This can seem quite high. However, as explained in Chapter 4, it is still in the range for this ratio. Indeed, this range goes from 0.6 to 6 depending on the correlation considered.

Temperature distribution results

The temperature distribution of this modified model is compared with the experimental data. The comparison is presented in Table 6-3. The experimental data were taken at specific points. In some part of the experimental channel, the temperature

variations over a small distance can be of several degrees Celsius and several dozen of degrees in different parts of a same channel reflector. This is due to the high gradient of temperature between the wall (at fixed temperature) and the flow in the lower parts of the channel. In order to avoid additional discrepancies between computational and experimental data that would be due to a different location of the temperature sensor, the computed temperature presented in the table are the averaged temperatures over the specified volume. The experimental data is still point specific.

Table 6.3: Comparison of computed and experimental temperatures for the adapted and blind FLUENT open chimney model

Location	FLUENT blind tem- perature (C)	FLUENT adapted tem- perature (C)	NACOK temperature (C)
lower columns	506 C	502 C	450 C
Lower reflector	920 C	762 C	650 C
Middle reflector	651 C	844 C	870 C
Upper reflector	650 C	740 C	720 C
Pebbles	650 C	660 C	690C
Upper Channel	650 C	650 C	650 C

The maximum temperature is no longer over estimated and the maximum point is correctly localized in the middle reflector. There is still a slight over estimate of the overall average temperature. There are some discrepancies in the values of the temperature due to the fact that the computed values are average based and the experimental ones a point measure. There is however a much better prediction of the temperature distributions except for the lower reflector. The temperature increase is too low in the channel compared to the experimental results. An explanation for this phenomena is proposed in the interpretation section.

Graphite corrosion results

The graphite corrosion distribution obtained with the adapted model is presented in Table 6-4.

Table 6.4: **Graphite corrosion location for the blind and adapted model**

Location	FLUENT blind mass loss (Kg)	FLUENT adapted mass loss (Kg)	NACOK mass loss (Kg)
lower columns	2.585	0.882	0.16
Lower reflector	4.84	1.986	0.29
Middle reflector	0.89	2.46	5.724
Upper reflector	0.984	2.02	2.346
Pebbles	0.0027	1.4	0.788
Crumbly pieces	NA	NA	0.258
Total	9.307	8.78	9.05

Similarly to the temperature distribution, the agreement between computational and experimental data is better for the adapted model than the blind model. There is a slight under prediction of the total mass loss of graphite (2.9%) due to the change in the ratio of CO and CO_2 stoichiometry coefficients. This discrepancy lies in the range of the computational and experimental uncertainty range (estimated to be about 10%). The distribution of graphite corrosion locations is more accurate but still shows significant discrepancies for the lower reflector, the middle reflector and the pebble area.

Interpretation of the modified model results

The results for this model are better than the blind model but still show discrepancies, especially around the lower reflector for the temperatures and the pebble region as well for the graphite mass loss. It seems that the graphite corrosion modeled is still too fast. However, studies showed that if this reaction is slowed further, then oxygen is not consumed in the lower part of the channel and can reach the

pebble bed area. This explains the overestimate of graphite corroded in the pebbles area. The reaction rate was reduced in order to optimize the distribution of the graphite corrosion and as a result, some oxygen had access to the pebbles. This discrepancy suggests therefore that the graphite corrosion rate is too low. There is a contradiction in these conclusions since the reaction rates cannot be too fast and too slow simultaneously. That leads us to believe that there is another reason for the mis-distribution of graphite corrosion mass loss.

Two explanations make sense in this case:

- The graphite corrosion specifications (stoichiometry and rate) are not the same for different geometries, surface reaction and graphite porosity (surface characteristics). These graphite specifications vary not only with the type of graphite but also with its configuration. For instance, there will be faster corrosion of the small channel reflectors due to the larger surface of reaction. Therefore a higher burn off is achieved in the small reflector than for the larger one. According to Fuller and Okoh [22], a burn off of 40% can lead to an increase in the corrosion rate by a factor 10. The reaction rate is also very sensitive to pore geometry and structural parameters. Therefore, this information and the comparison between computational and experimental data confirm that the reaction rate might be higher for the 96 channels reflectors than for the 12 channel one and the columns. This strengthens the need to perform experiments to measure graphite corrosion rates in specific PBMR like experimental conditions.
- The imperfection of the experimental configurations and more specifically the non-homogeneity of the channel heating is another explanation for the discrepancies recorded. Due to the inlet tube and other experimental settings, wires can not be homogeneously spread out around the channel in its lower section. The first wire temperature control device is located above the middle reflector. This one tends to be hotter and can be surrounded by more wires than the lower ones. There is no overheating of the entry space and lower reflector to account for this. Therefore, it makes sense to expect the entry space and lower reflector to be less heated and cooler. This will slow down the reactions in this

part of the channel, partly explaining the discrepancies between experimental and computational results.

Chapter 7

Results of the Benchmarking of the Return Chimney Test, July 2004

The return chimney experiment is very similar to the open chimney experiment. Both were described thoroughly in Chapter 2 and the general FLUENT model was described in Chapter 3. Therefore, this chapter solely presents the modifications made to the standard model. Unless specified otherwise, the model and experimental set up mentioned are the same as the open chimney model.

The return chimney experiment was run in July 2004. The main characteristics of the experiment are repeated here. The main experimental channel is heated to 850 C and closed at the top. A return duct is heated to around 200 C. The height of the large pebbles bed is 280 mm. It is also of importance to mention that the inlet and outlet ducts are all at the same level, providing a quick entry of air in the lower part of the channels. The test facility is initially filled with helium. At time $t=0s$, the inlet and outlet duct that were closed for the helium filling are open to the atmosphere. The experiment takes place for 25 hours. The complete sequence of events taking place in an air ingress accident occurs in this experiment: diffusion, onset of natural convection and graphite corrosion.

The procedure to model this experiment is slightly different than the open chimney one. Running just a steady state model would not account for the initial diffusion process and the onset of natural convection which are highly time dependent. But as it was mentioned earlier, it would be too computationally expensive to run a

full transient model. Therefore, a staged modeling strategy was adopted. First, the diffusion process is modeled time dependently without activating the chemistry options. This provides an approximation of the time of onset of natural convection and allows a good understanding of the diffusion process. This model is then used to calculate an estimate of the mass flow rate in the channels. The second stage consists in running the modified model at a temperature of 850C, using results from the open chimney benchmark. Modifications are added in particular to the chemistry model in order to take in account the change of temperature and insights gained from the open chimney modeling. In this second model, the mass flow is imposed to be the natural convection one calculated with the transient model. This second model is run steady state and provides results on the final state of the experiment. A third stage of the complete modeling would be to check this approximation by running the full return duct transient model with chemical reactions activated. This work was not performed in this thesis and will be carried on in collaboration with PBMR. Shown in Chapter 9 are also the main variables for this model.

This chapter describes the blind benchmarking of the return duct experiments in two stages. Based on the results analysis, a modified model and further work is proposed.

The blind benchmarking of the return duct experiment was developed after the blind benchmarking of the open chimney experiment. As a result, one could call this benchmarking not as blind. Indeed, some knowledge was gained from the first experiment on the scales and range of parameters to expect. Moreover, it provided a better understanding of the discrepancies between experiment and modeling. However, the diffusion process, the flow with a return duct, the chemical reaction at 850 C with addition of the Boudouard reaction are new to this experiment. As a consequence, the main lessons that can be learned from this experiment are the result of a truly blind modeling.

7.1 Stage one of Blind Benchmarking : the diffusion process and onset of natural convection

This stage of modeling aims at studying the diffusion process after the inlet and outlet ducts were open to the atmosphere, as well as the time of onset of convection. The results obtained from this model are an approximation of the experiment. In addition to the uncertainties and approximations due to modeling, which is a idealized representation of real conditions, there are two other sources of inaccuracy in the modeling stage of this experiment.

The first source of error is due to lack of chemistry modeling in this model. Therefore, there is no rise in the temperature due to the exothermic graphite corrosion. Higher temperatures enhance the diffusion process and provide a lower density to the incoming air. Therefore, not taking in account the chemical reactions in the return duct transient model induces an over estimate of the time of onset of natural convection.

The second source of error is due to uncertainties in the experimental configuration. The inlet and outlet tubes are at the same heights, but their length and configuration is not accurately known. This might have a very small impact on the result. A bigger source of uncertainty is the state of temperatures of the main channel and return duct. As mentioned in the previous chapter, the heating of the channels walls is not be totally homogeneous. Moreover, the NACOK scientists mentioned that chaotic reactions in the entry of the channels required them to lower the temperatures after 8 hours. This procedure was not documented in the experimental configuration description provided. As a result, it was not known for the blind benchmarking process. This lack of knowledge on the experimental procedure adds a large uncertainty to the model and to the time of onset of natural convection computed.

7.1.1 The transient diffusion model

Sensitivity studies described in Chapter 5, section 3 showed that in order to model correctly the exchange of species at the outlet of the experimental channels, the surrounding medium should be modeled as well. Doing so provides the ability to model the interface between atmosphere and ducts by a FLUENT interior condition. As opposed to pressure boundary conditions, this type of interface allows one to take in account the exit of helium in the atmosphere. Figure 7-1 presents the geometry meshed of this model. The diffusion process was studied using nitrogen and not air. Since the chemical reactions are not modeled, The approximation in the modeling of diffusion process induced by using only nitrogen is smaller than the fact that the chemical reactions are not modeled and the temperature variations not taken in account. Moreover, all the oxygen that diffuses reacts early with the graphite and therefore, only nitrogen will play a major role in the onset of natural convection.

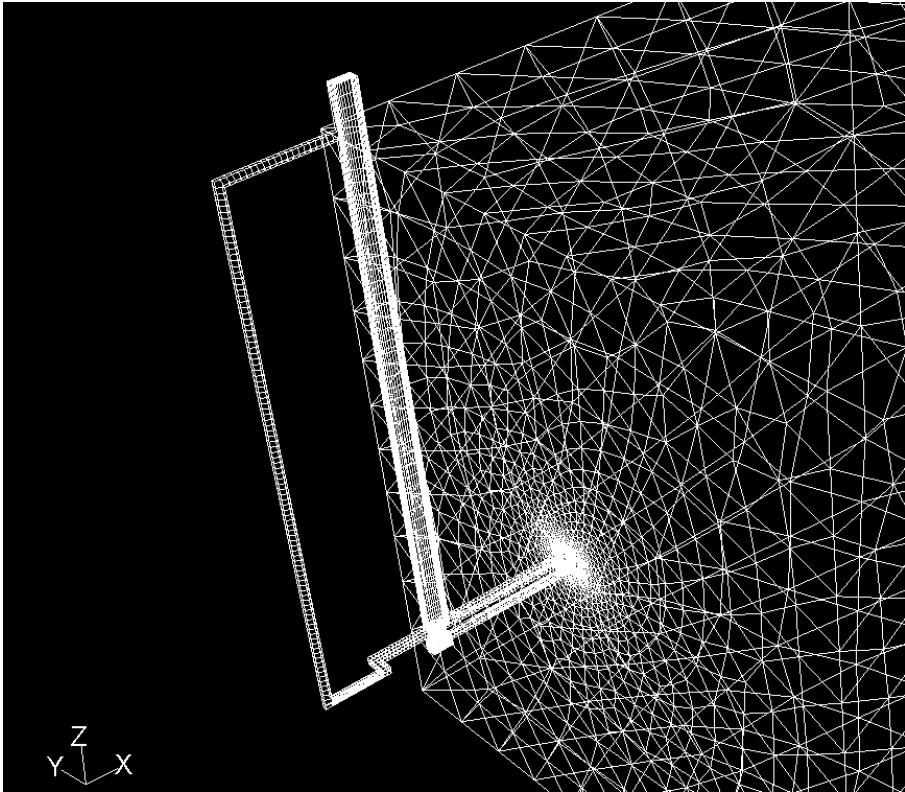


Figure 7-1: Geometry and mesh and of the main channel, return ducts and surroundings

The overall model is initialized with the following conditions:

- Main channel at 850C, return duct at 200C and surroundings at 20C.
- Main channel and Return duct helium mass fraction = 1, Surroundings nitrogen mass fraction = 1.
- Time steps range between 0.01s and 5s.

7.1.2 Results

Diffusion process

As predicted, the diffusion occurs as follows:

- The helium in the horizontal inlet and outlet pipes exits rapidly and is replaced by nitrogen (approximately 70s). (Figure 7-2)

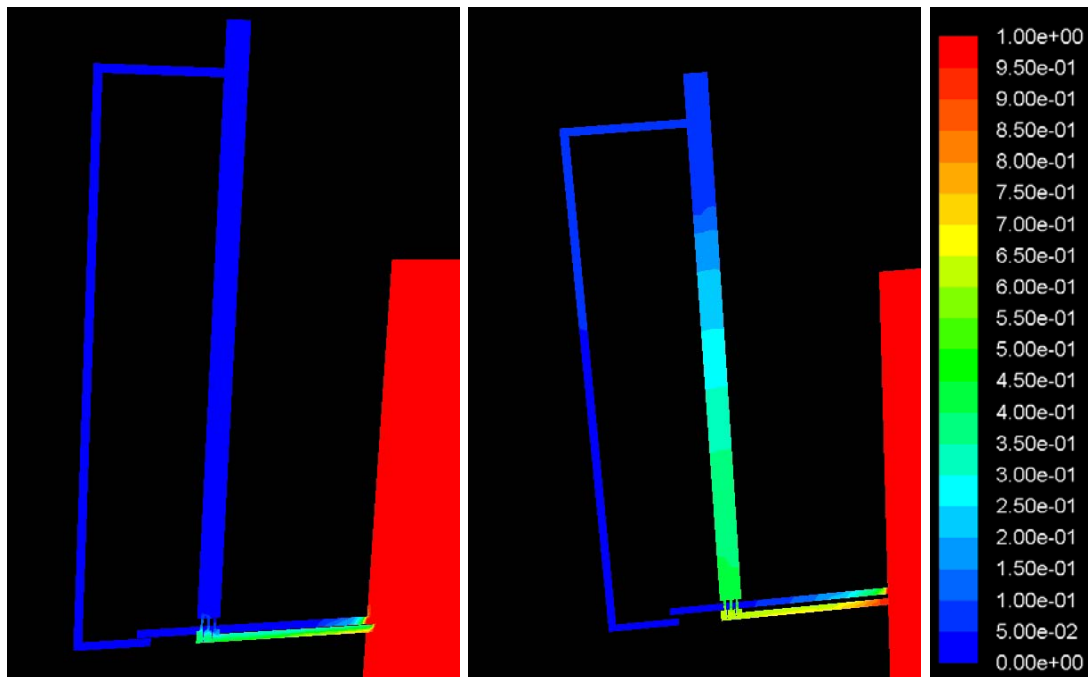


Figure 7-2: Diffusion process in the return duct experiment at 80 seconds and 163 min. The scale represents the nitrogen mass fraction.

- This process is followed by a slight natural convection of the helium itself in the reverse U tube configuration due to the fact that there is a lighter density of the helium in the hot leg compared to the cold leg. This natural convection

cannot be completely initiated because the air at the inlet and outlet is of higher density than the helium. It does create a slight over pressure that slows down the entry of air in the outlet duct compared to the speed of entry of air by diffusion and convection process in the inlet duct.

- Diffusion takes place in both channels, and is enhanced in the main hot channel by the temperature. (Figure 7-2 and 7-3)
- Sufficient air reached the top of the experimental set up. Natural convection then takes place very rapidly. (Figure 7-3)

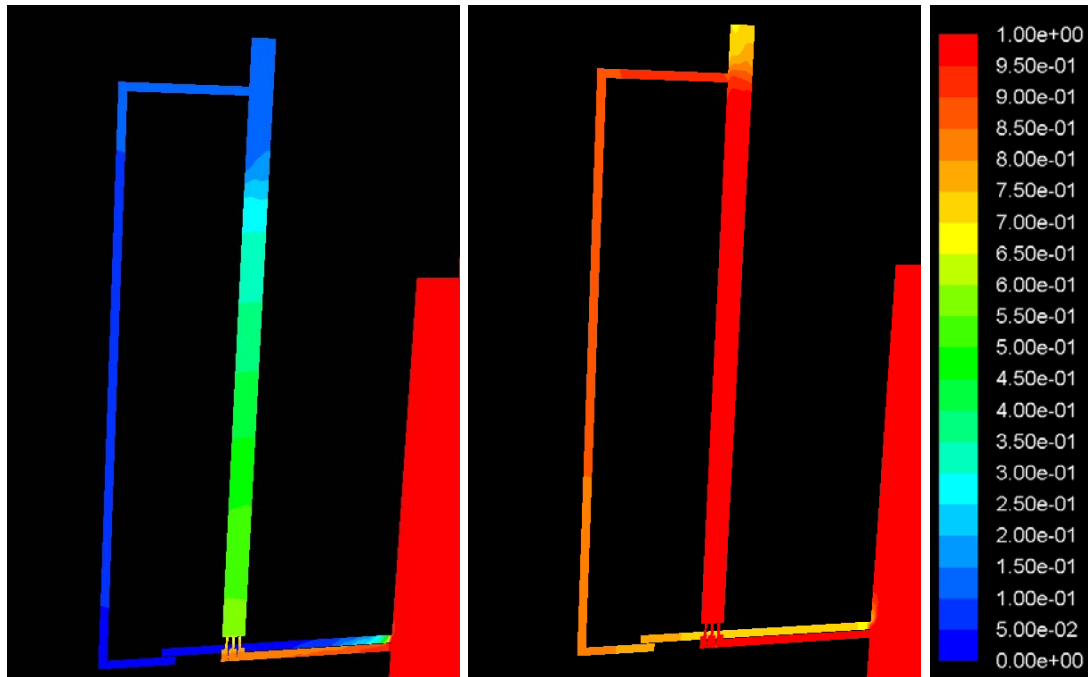


Figure 7-3: Diffusion process in the return duct experiment at 4.4 hours and onset of natural convection. The scale represents the nitrogen mass fraction.

Onset of natural convection

The time of onset of convection, that is, the time at which the channel is filled up with air and all helium expelled, is calculated by FLUENT to be approximately 22800s or 6.3 hours. The data provided by the Jülich center gives a time of onset of natural convection of 5h30min, that is 19800s. The blind FLUENT prediction is

therefore off by 15% and slightly over predicts this time, as it was expected due to no chemical reactions modeled in stage 1 of this analysis.

Once the natural circulation takes place, the mass flow rate stabilizes at $0.00168Kg.s^{-1}$. The NACOK flow data is given as a quantity of air entering over the entire experiment during 25 hours: 3515 mol of air. This is equivalent, over 19.5 hours of flow, to an average mass flow rate of $0.00145Kg.s^{-1}$. The FLUENT computed prediction is off by 15.8% but does not account for the lowering of temperature. The natural convection flow rate might actually be higher in the experiment. Since the temperature was lowered after 9 hours as described in the next section, the flow might have slowed down and the mass flow rate is not a constant over the remaining 19.5 hours.

7.2 Stage two of Blind Benchmarking: Steady state calculation of the hot channel final state

7.2.1 The steady state model

Once natural convection has started, the phenomena taking place in the hot channel are similar to the ones in the open chimney experiment. Therefore, the model developed for the open chimney benchmarking is used with the return duct experiment boundary conditions and different chemical reactions:

- The pressure inlet is replaced by a mass flow inlet with a specified mass flow rate of $1.68g.s^{-1}$.
- The Arrhenius constant for the graphite corrosion by oxygen is set to $5 * 10^{10}$ based on the previous open chimney experiment.
- The Arrhenius constant for the Boudouard corrosion is set to be equal to 1000, with the activation energy equal to $2.6 * 10^8$.
- The height of the 60 mm diameter pebble bed is set to 280 mm.
- The hot leg walls are set to have a fixed temperature of 850C.

7.2.2 Results

The temperature distributions and the graphite corrosion are the main results of interest in the benchmarking process of FLUENT as a code able to predict the final state of the return duct experiment.

Word on the results provided by the Jülich center

After having received results from the blind benchmarking computations, the Jülich center provided experimental data on this experiment. These results were provided in several forms: a power point presentation giving the outline of the main results (Temperature distribution over time, mass flow, graphite corrosion) and Excel files presenting data recorded by sensors during the experiment. These files and results showed discrepancies between the announced experimental and boundary conditions and the real conditions. More particularly, the temperature of the main channel was supposedly maintained at 850 C over the whole period of the experiment. Results show that this temperature was lowered to 650 C after 9 hours, that is, approximately 3.5 hours after the onset of natural convection. For the lower parts of the channel particularly, the change in experimental settings is quite important compared to what was used for the blind benchmarking. As a result, the final state of the experiment does not correspond to the computed final state. Since the change in experimental conditions was done only after the onset of natural convection, the first part of the blind benchmarking (stage one) is valid.

In order to be able to use the results from the stage 2 of the blind benchmarking, the computational FLUENT results were compared with the state of the system at time 8 hours for the temperature distribution. The time of 8 hours is chosen because a steady state seems to have been reached at that point and the experimental conditions have not been yet modified. The graphite corrosion is experimentally measured over the total experimental time. Therefore, the graphite loss comparison does not yield much useful information due to the change of experimental conditions. It will be necessary to rely on the open chimney experiment for the evaluation of the FLUENT's ability in this domain.

Explanations for this experimental procedure modification was provided by PBMR. The main goal of the return duct experiment was to measure the onset of natural convection and the flow under natural convection. Therefore, after 5.5 hours, the first goal of the experiment had been reached. At 9 hours, flow and temperatures distributions were at steady state. Therefore, the experiment was stopped and the temperatures allowed to come down. The reason for this is that at that time, given the loss of carbon in the system, more corrosion could have caused movements in the structure and thus jeopardized the evaluation of the test. Figure 7-4 shows the experimental temperature profile as a function of time with the wire heaters on the exterior walls of the channel.

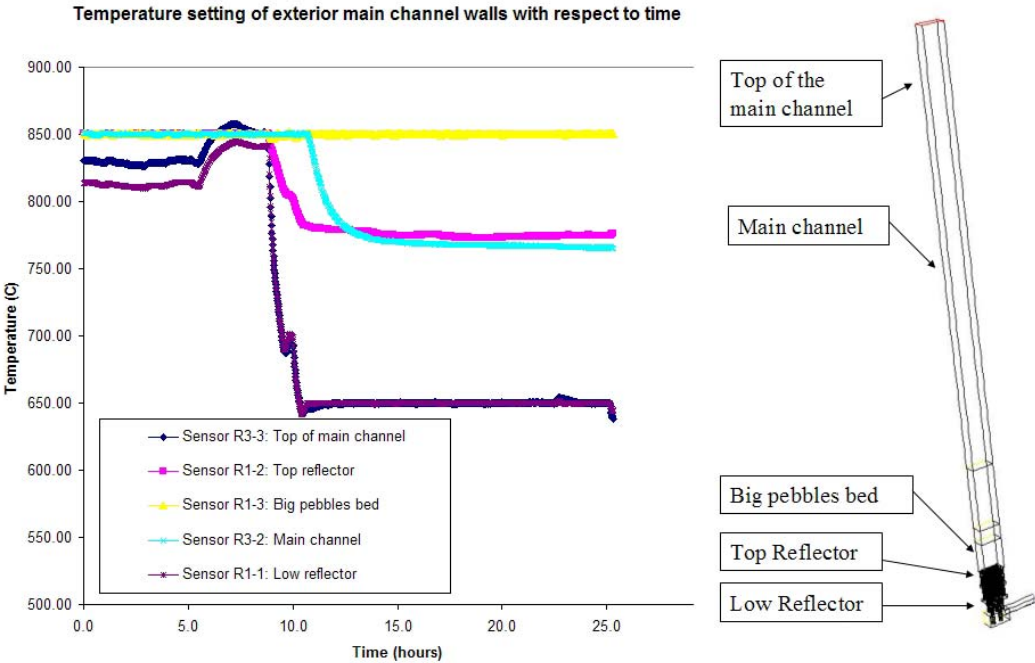


Figure 7-4: Temperature Experimental conditions of the external walls of the main channel

Temperature distributions

Figure 7-5 shows results provided by the Jülich center for the temperature distribution in the channel. [13]. The comparison between experimental data at 8 hours and the steady state blind benchmark model results is presented in Table 7-1 and

Figure 7-6. The experimental temperatures are point measures. The FLUENT data are also point measures except for the entry space. The temperature gradient there is quite important and the temperatures range from 20 to 870C. Therefore, the experimental point estimate was compared with the computed temperature average in this volume.

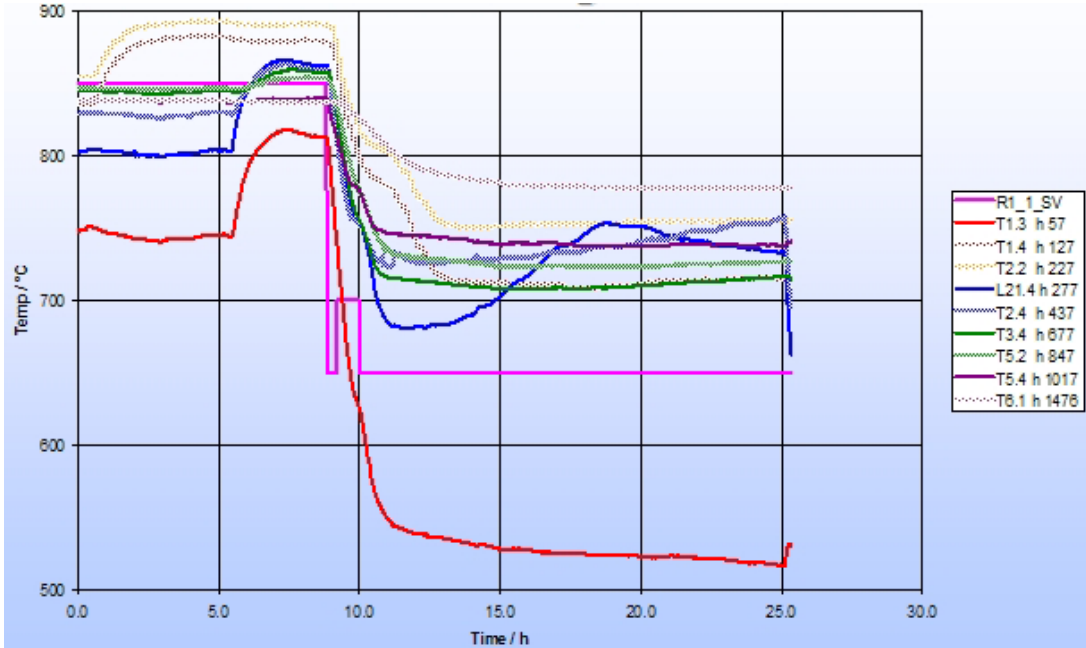


Figure 7-5: **Experimental Gas Temperature at different height levels. hXXX corresponds to the height in mm and the names refer to the instruments in the return duct experiment.**

The maximum temperature was well predicted to be around 900 C. The temperatures computed with FLUENT are however too low compared to the experimental data in the lower region of the channel and in the upper region as well.

Interpretation of the results

The underestimate of the temperature in the lower section of the main channel can be easily explained by the fact that the graphite corrosion rate was set to low. The blind model was launched after the reception of results from the open chimney experiment but before the correction to the reaction rate model. The Arrhenius constant in this model is $5 * 10^{10}$ but it should be more around $5 * 10^{11}$ (As the open chimney

Table 7.1: Comparison of computed and experimental temperatures for the blind FLUENT return duct experiment

Location	FLUENT blind temperature (C) point measures from steady state calculations	NACOK temperature (C) point measure after 8 hours
Entry space	494 C (average)	820 C
Low section of the lower reflector	780 C	880 C
High section of the low reflector	901 C	890 C
Empty chamber between low and middle reflector	878 C	870 C
High section of the middle reflector	850 C	860 C
High section of the top reflector	850 C	850 C
Big pebble bed	750 C	850 C
Above first pebble bed	760 C	840 C
Small pebble bed	800 C	840 C
Top chimney	850 C	840 C

modified model recommended a value of 10^{11} for a temperature of 650C). Concerning the higher part of the main channel, the cooling down in the FLUENT model is due to a high reaction rate for the Boudouard reaction (endothermic). Therefore, the important fraction of carbon dioxide in the pebble bed (21%) allows for the Boudouard reaction to take place in a non negligible manner at this temperature. This phenomenon accounts for the cooling of this area in the FLUENT model. The experimental data suggests that the impact of the Boudouard reaction at this temperature should not be as strong and the model needs to be modified.

7.3 The modified model

A modified model is run after having compared the blind results with the experimental data. As a result of the interpretation of the discrepancies, the Arrhenius

Comparison of computed and experimental temperatures for the blind return duct experiment

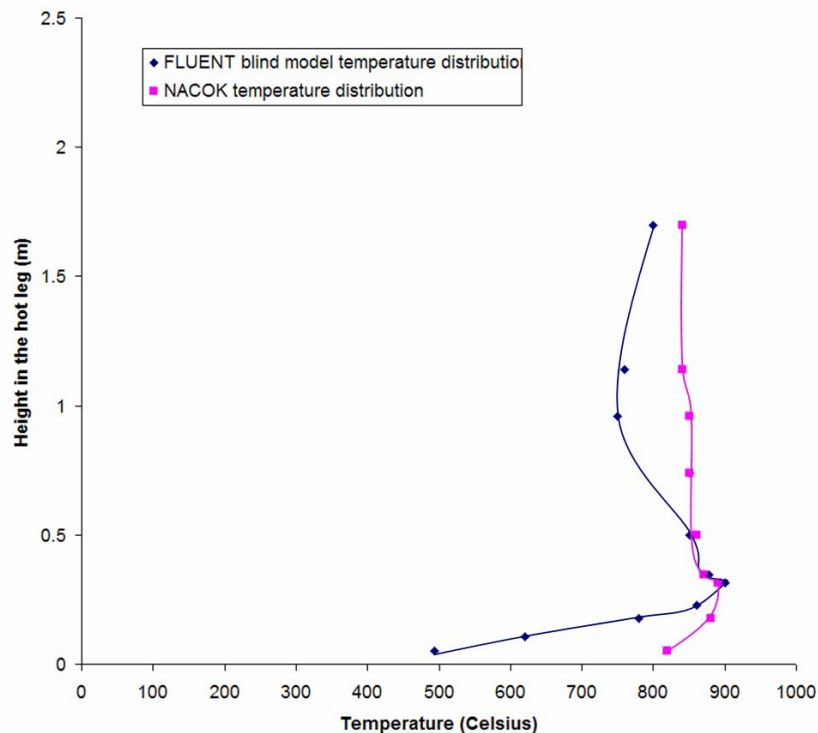


Figure 7-6: Comparison of computed and experimental temperatures for the blind FLUENT return duct experiment at 8 hours

constant for the graphite oxidation is set to 10^{12} to take in account the higher temperatures in the hot leg due to reactions during the diffusion. The Boudouard reaction's Arrhenius constant is set to 200. The results are compared with the experimental data at 8 hours after the start of the experiment.

Temperature distributions

Table 7-2 presents the comparison of the temperatures measured or computed in different parts of the main channel. The computed results appear to have a better agreement with the experimental data. The maximum of temperature is over predicted (as in the open chimney test). This can be explained once again by the fact that the channel exterior walls temperatures may be less than 850 C in the lower part of the experiment set up. Also, the corrosion rate might be slightly over predicted and should be different for different types of geometries and reflectors due to complex chemistry parameters (diffusion processes, atomistic surface area, burn

off of the graphite, etc.). Once again, as in the open chimney experiment modeling, specific experiments are needed to develop a good knowledge of the graphite corrosion rate for these experimental conditions.

The blind under estimate of the temperature in the higher parts of the main channel are corrected with this model thanks to the Boudouard reaction rate correction.

Table 7.2: Comparison of computed and experimental temperatures for the blind FLUENT return duct experiment

Location	FLUENT blind temperature (C), steady state calculations	NACOK temperature (C) after 8 hours
Entry space	847 C (average)	820 C
Low section of the lower reflector	877 C	880 C
High section of the low reflector	928 C	890 C
Empty chamber between low and middle reflector	903 C	870 C
High section of the middle reflector	850 C	860 C
High section of the top reflector	850 C	850 C
Big pebble bed	846 C	850 C
Above first pebble bed	848 C	840 C
Small pebble bed	850 C	840 C
Top chimney	850 C	840 C

Graphite corrosion and species fractions

The molar fraction of species at the top of the chimney (before entering the return duct) is: 0.1% O_2 , 0.46% CO and 20.5% CO_2 . Therefore, even though the Boudouard reaction produces CO while consuming carbon dioxide, there will be a very small fraction of carbon monoxide exiting the experimental channel.

It was mentioned that the graphite corrosion comparison can not be made since

the experimental conditions were changed after 9 hours but the experiment went on for another 16 hours. The graphite corrosion is measured by weighing the graphite pieces at the end of the experiment. Therefore, only the whole corrosion process occurring during the experiment can be compared. The computed data is obtained by multiplying the rate of graphite corrosion by the time length of the experiment. This procedure assumes a constant rate which was not the case in this experiment. Due to these reasons, this data comparison is mainly qualitative and quantitative benchmarking conclusions can't be drawn from it.

Table 7-3 presents the graphite loss distribution. The total graphite loss is over estimated by 6.2%. This can be understood by the fact that the temperature have been taken down after 9 hours. Therefore, the corrosion rates must have slowed down and less graphite was corroded. Overall, the graphite loss prediction is in the right order of magnitude. As it was the case for the open chimney experiment, the graphite corrosion location is more distributed in the FLUENT model than in the experiment while still being in the right order of magnitude. The same explanations can be proposed (different rates and corrosion behavior for different geometries).

Table 7.3: Graphite corrosion location for the adapted model of the return duct experiment

Location	FLUENT mass loss (Kg)	NACOK mass loss (Kg)
lower columns	1.07	0.606
Lower reflector	3.21	2.534
Middle reflector	3.47	8.03
Upper reflector	1.738	0.385
Pebbles	0.717	0.055
Crumbly pieces	NA	1.998
Total	10.21	9.612

Chapter 8

Conclusions and Future Work

Summary and conclusions

The purpose of the work presented in this thesis was to develop an analytical capability to model NACOK air ingress corrosion experiments run in March and July 2004 at the Jülich Research Center in Germany using the FLUENT CFD tool in a blind benchmarking process.

The Chapter 1 of the thesis described the progression of an air ingress event in a pebble bed reactor and provided a summary of previous benchmarking work of the JAERI experiments conducted at MIT. The NACOK experimental facility was then described for both the open chimney and return duct experiments. Information from several sources was assembled in order to develop a good understanding of the experimental characteristics (materials used and experimental procedures) and the experimental data acquired. The FLUENT code and the standard FLUENT model used in this project were then explained in detail. Chapter 4 focused on the chemistry models used to model the experiments. The reactions and theory were introduced as well as a discussion on the many reaction rate correlations that are available. Chapter 5 discussed insights on the different phenomena taking place during an air ingress event. Sensitivity studies on pressure loss correlations, porous media modeling, diffusion and chemistry modeling were detailed. Chapters 6 and 7 present the results of the blind benchmarking of the open chimney and return duct experiment. Blind computed results were then compared to experimental data. The initial results of the blind benchmark for the open chimney showed quite good agree-

ment on peak temperature and amount of graphite consumed. For the return duct experiment, the comparative results were not as good due in part to significant but unknown changes in the experimental procedure which were not identified until the benchmark analysis was completed. Discrepancies were interpreted and recommendations for improvement were made. An updated model was developed based on the comparison of the experimental results to obtain a better agreement with the experimental data as appropriate. It was found that FLUENT can accurately represent the fundamental processes in air ingress phenomena: diffusion, onset of natural convection, chemical reactions and flow.

It was found that the system undergoing an air ingress event eventually reaches a steady state. This final state can be computed using FLUENT in steady state mode. The diffusion process and onset of natural convection can be modeled with FLUENT in transient mode. It appears that approximations employed to reduce computation time in the chemistry and the geometry of the structures still yield good results.

The main source of uncertainty in the analysis of an air ingress event and more particularly in the benchmarking process of the NACOK experiments, is the uncertainty on graphite corrosion behavior and rates. This corrosion phenomenon is very sensitive to many parameters such as the type of graphite used, the degree of burn off, the temperature, diffusion flow layers. etc. Therefore, in order to accurately predict the rate of corrosion and the ratio of species (CO/CO_2) produced in different parts of the reactor, specific experiments under reactor conditions must be carried out.

It was observed that the temperature in the 650 C channel reaches a peak of 860 C. The rise is proportionally smaller for a hotter channel (900C) which rises to 1150C. Therefore, one can expect the temperature rise in the case of an air ingress event to be lower at higher initial temperatures. At 650 C and 850 C, the main gas exiting the experimental channel is carbon dioxide. Carbon monoxide is released but in small quantities. The ratio of CO released increases with increasing temperature due to the Boudouard reaction.

Less computationally expensive ways to model the NACOK experiments were investigated. Geometry simplifications by modeling fine reflectors as porous media were validated. Fixed stoichiometric coefficients were shown to yield a good approximation compared to more temperature dependent coefficients implemented with user defined functions.

The most significant findings were the importance of graphite characterization on the in-situ corrosion of graphite. Without good specific data, the correlations available in the literature vary so widely, that good predictions of the results of air ingress events will be difficult at best. The other important factor to assess, which was beyond the scope of this thesis but evidenced in the results, is the effect of the loss of graphite as a structural support due to the corrosion taking place at high temperature in a localized phenomenon. It was found that little air reached the fuel pebbles due to aggressive attack in the lower reflector regions and the peak temperature reached in the pebble zone was well below the limiting temperatures for the silicon carbide degradation (neglecting decay heat). Finally, computational fluid dynamics tools such as FLUENT can be used to effectively benchmark air ingress events using approximations confirmed by this work.

8.0.1 Future work

Experimental characterization of the graphite corrosion behavior in very specific situations must be conducted. Correlations developed can then be applied with confidence to FLUENT models. The pebble bed modular reactor should then be modeled with FLUENT in order to predict the consequences of air ingress events. This work will require modeling simplifications of the PBMR geometry and modeling such factors as decay heat, radiative heat transfer in the reflectors and in the fuel.

Chapter 9

Summary of the main variables in FLUENT models

Table 9.1: Modifiable variables in FLUENT models

Variable/Model	Blind model for open chimney	Modified model for open chimney	Blind model for return duct	Modified model for return duct
k Graphite Corrosion	$3.6 * 10^{12}$	10^{11}	$5 * 10^{10}$	10^{12}
E_A Graphite corrosion	$2.09 * 10^*$	$2.09 * 10^*$	$2.09 * 10^*$	$2.09 * 10^*$
x/y Stoichiometry	0.86	1.86	1.5	1.5
k Boudouard reaction	N.A.	N.A.	1000	200
E_A Boudouard reaction	N.A.	N.A.	$2.6 * 10^8$	$2.6 * 10^8$
Pressure outlet pressure gauge	-27.4 Pa	-27.4 Pa	0 Pa	0 Pa
k CO oxidation	$2.8 * 10^{12}$	$2.8 * 10^{12}$	$2.8 * 10^{12}$	$2.8 * 10^{12}$
E_A CO oxidation	$1.7 * 10^8$	$1.7 * 10^8$	$1.7 * 10^8$	$1.7 * 10^8$

Nomenclature Table

Parameter	Meaning	Units
A	Cross sectional flow area	m^2
A_r	Arrhenius constant	Consistent units
C_0 and C_1	Porous media pressure loss coefficients	N.A.
C_p	Heat capacity	$J.Kg^{-1}.K^{-1}$
$C_{j,r}$	Molar concentration of species j in reaction r	$kmol.m^{-3}$
d	Pebble diameter	mm
D_{eff}	Effective gas diffusivity	$m^2.s^{-1}$
E_A	Activation Energy	$J.kmol^{-1}$
f_n	Fan boundary pressure loss coefficient	N.A.
f_{regime}	Function giving the dependance on graphite burn off	N.A.
h	Height of pebble bed	mm
H	Enthalpy	$J.Kg^{-1}$
J	Diffusion flux	$Kg.m^{-2}.s^{-1}$
k	Arrhenius constant	Consistent units
M	Molecular weight	$kmol$
\dot{m}	Mass flow rate	$kg.s^{-1}$
P	Pressure	Pa
Q_X	Quantity of species X entering the channel during a time t	mol
R	Universal gas constant	$J.kgmol^{-1}.K^{-1}$
S	Source term (variation of Pressure, species quantity, etc...)	N.A.

Parameter	Meaning	Units
S_X	Rate of creation of species X by other means than reactions	<i>mol</i>
$\overline{R_X}$	Net production of species X	<i>mol.s⁻¹</i> or <i>Kg.m⁻².s⁻¹</i> or <i>Kg.s⁻¹</i>
$\overline{R_{X,r}}$	Molar production of a species X due to the reaction r	<i>mol</i>
$R_{X,mass}$	Mass production of X	<i>Kg</i>
Re	Reynolds Number	N.A.
t	time	<i>s</i> or hours
T	Temperature	Kelvin or Celsius
v	Flow velocity	<i>m.s⁻¹</i>
X	Mole quantity of the species X	<i>mol</i>
x, y and z	Stoichiometric coefficients of <i>O₂</i> , <i>CO</i> and <i>CO₂</i> in graphite corrosion	N.A.
<i>eta</i>	Fluid dynamic viscosity	<i>Pa.s</i>
$\eta_{j,r}$	Rate exponent for the species j in reaction r	N.A.
ϵ	Porosity	N.A.
ν_X	Stoichiometric coefficient of X	N.A.
ψ	Khulmann correlation parameter	N.A.
ρ	Density of gas mixture	<i>kg.m⁻³</i>

Bibliography

- [1] T. ZHAI, A. KADAK and H-C. NO, *LOCA and Air Ingress Accident Analysis of a Pebble Bed Reactor*, CANES MIT, MIT-ANP-TR-102, (March 2004)
- [2] H. S. LIM and H. C .NO, *GAMMA Multidimensional Mixture Analysis to Predict Air Ingress Phenomena in an HTGR*, Nuclear Science and Engineering: 152, 87-97 (2006)
- [3] H. S. LIM and H. C .NO, *Transient Multicomponent Mixture Analysis based on Ice Numerical Scheme for Predicting an Air Ingress Phenomena in an HTGR*, 10th Int. Top. Meet. on Nuclear Reactor Thermal Hydraulics (NURETH-10), Korea, (October 2003)
- [4] T. TAKEDA and M. HISHIDA, *Studies on molecular diffusion and natural convection in a multicomponent gas system*, Int. J. Heat Mass Transfer, Vol 39 No 3 pp 527-536. (1996)
- [5] *PBMR*, www.pbmr.com, (2006)
- [6] A. KADAK, T. ZHAI, *Air Ingress Benchmarking with Computational Fluid dynamics Analysis*, 2nd Int. Topical Meet. on High Temperature Reactor Technology, Beijing China, (September 2004)
- [7] US DOE Nuclear Energy Research Advisory Committee and the Generation IV International Forum, *A Technology Roadmap for Generation IV Nuclear Energy Systems*, (December 2002)
- [8] M. B. KUHLMANN, *Experimente zu Gastransport und Graphitkorrosion bei Luftteinbruchstörfällen im Hochtemperaturreaktor*, Forschungszentrum Jülich, Jül-4003, (2002)

- [9] M. L. DAMS, *Simulation of the pebble bed modular reactor natural air convection passive heat removal system*, Integrator of System Technology Ltd, Waterkloof South Africa
- [10] US Nuclear Regulatory Commission, *NUREG-0800 Review of transients and accident analysis methods*
- [11] M. WEIGHTMAN, *Containment: validation of computer codes and calculational methods*, Nuclear Safety Directorate, T/AST/042, (2003)
- [12] FLUENT Inc 2006, *FLUENT 6.0 User's guide*
- [13] Hans F. NIESEN, *NACOK experimentalist*, JULICH center, Germany
- [14] A. BLANCHARD, *The Thermal Oxidation of Graphite*, IAEA-TECDOC-1154, Appendix 2, (April 2000)
- [15] R. MOORMANN and H. HINSENN, *Transport and Reaction of gaseous oxidants in porous nuclear carbons*, Proceedings Int. CIMTEC conf on Mass and Charge Transport in Inorganics Solids, Italy, (2002)
- [16] . FROHLING and J. ROES, *Zur chemischen Stabilität bei innovativen Kernreaktoren*, Forschungszentrum Jülich, Jül-3118, (1995)
- [17] . ROES, *Experimentelle Untersuchungen zur Graphitkorrosion und Aerosolentstehung beim Lufteinbruch in das Core eines Kugelhaufen-Hochtemperaturreaktors*, Forschungszentrum Jülich, Jül-2956, (1994)
- [18] R. MOORMANN , *Phenomenology of graphite burning in massive air ingress accidents*, 3rd Int. Topical Meeting on High Temperature Reactor Technology, Johannesburg South Africa, (October 2006)
- [19] S. J. BALL, *NGNP Depressurized Loss of Forced Circulation (D-LOFC) Accidents with Air Ingress*, ORNL/GEN4/LTR-06-026, (2006)
- [20] . B BIRD, C. F CURTISS and J. O. HIRSCHFELDER, *Molecular theory of gases and liquids*, John Wiley and Sons Inc., (1964)
- [21] German Nuclear Safety Standards Commission, *German Safety Guide*, KTA 3102.2 and KTA 3102.3 (1983)

- [22] E. L. FULLER and J. M. OKOH, *Kinetics and mechanisms of the reaction of air with nuclear grade graphites: IG-110*, J. of Nuclear Materials, Vol 240 pp 241-250, (1997)
- [23] R. BACKREEDY, A. WILLIAMS et al. *A study of the reaction of oxygen with graphite: Model chemistry*, Faraday Discuss, vol 119 pp 385-394, (2001)
- [24] L. C. BLACKMAN, *Modern Aspects of Graphite Technology*, Academic Press BCURA Industrial Laboratories, (1970)
- [25] . E. IDELCHIK, *Handbook of Hydraulic Resistance*, 3rd edition, Begell House Publishers, (2001)
- [26] FLUENT Inc 2006, *GAMBIT 2.0 User's guide*
- [27] . E. NIGHTINGALE, *Nuclear Graphite*, Handford Laboratory GE company, (1962)
- [28] Health and Safety Laboratory, *Guidance for NSD on the assesment of CFD simulations in safety cases*, FR/08/004/1997
- [29] R. MOORMANN and H. HINSENN, *Advanced Graphite Oxidation Models*, Proceedings 2nd Information Exchange Meet. on Basic Studies in the Field of High Temperature Engineering, Paris France, (2001)
- [30] R. MOORMANN, S. ALBERICI et al., *Oxidation behaviour of carbon based materials used for high temperature gas cooled reactors and fusion reactors*, Proceedings 9th CIMTEC, Florence Italy, (June 1998)
- [31] R. MOORMANN, *Some comments on the term graphite burning and graphite fire in connection to a massive air ingress in HTRs*, Jülich Center, (2006)
- [32] B. PARKS, *Using the FLUENT computational dynamics codeto model the NA-COK long term corrosion test*, MIT, (2004)
- [33] Walter SCHMITZ, *Computational Fluid dynamics Expert*, PBMR, South Africa
- [34] W. SCHMITZ and A. KOSTER, *Air Ingress Simulations using CFD*, 3rd Int. Topical Meet. on High Temperature Reactor Technology, Johannesburg South Africa, (October 2006)

- [35] . D. SMOOT and P. J. SMITH, *Coal combustion and gasification*, Plenum press, (1985)
- [36] M. TAKAHASHI, M KOTAKA and H. SEKIMOTO, *Burn off and Production of CO and CO2 in the Oxidation of Nuclear Reactor Grade Graphites in a Flow System*, J. of Nuclear Science and Technology, Vol 31 No 12 pp1275-1286, (December 1994)
- [37] US Nuclear Regulatory Commission, *Regulatory Guide 1.203: Transients and accident analysis methods*, (2002)
- [38] R. P. WICHNER, *Graphite burning characteristics*, Technology Insights for Oak Ridge Laboratory, (September 2001)
- [39] L. XIAOWEI et al. *Effect of temperature on graphite oxidation behavior*, Nuclear Engineering and Design, Vol 227 pp 273-280, (2004)

Appendices

APPENDIX 1: Open Chimney Blind Model

FLUENT

Version: 3d, dp, segregated, spe, lam (3d, double precision, segregated, species, laminar)

Release: 6.2.16

Title:

Models

Model	Settings
Space	3D
Time	Steady
Viscous	Laminar
Heat Transfer	Enabled
Solidification and Melting	Disabled
Radiation	None
Species Transport	Reacting (5 species)
Coupled Dispersed Phase	Disabled
Pollutants	Disabled
Soot	Disabled

Boundary Conditions

Zones

name	id	type
chimney	2	fluid
entree_reflektor	3	fluid
entree_bas	4	fluid
inlet	5	fluid
solid.47	6	solid
peb2	7	fluid
intpeb	8	fluid
peb1	9	fluid
ref2	10	fluid
interref	11	fluid
ref1	12	fluid
porous_jump.63	14	fan
wall-shadow	61	wall
wall_entree:047-shadow	60	wall
wall	13	wall
symmetry	15	symmetry
pressure_outlet.61	16	pressure-outlet
pressure_inlet.60	17	pressure-inlet
interior_	18	interior
wall_chimey	19	wall
wall_peb2	20	wall
wall_interpeb	21	wall
wall_peb1	22	wall
wall_ref2	23	wall
wall_interef	24	wall
wall_ref1	25	wall
wall_libre_1	26	wall
wall_ref_bas	27	wall
wall_entree	28	wall
wall_inlet	29	wall
default-interior	31	interior
symmetry:001	1	symmetry
symmetry:030	30	symmetry
symmetry:032	32	symmetry

```

symmetry:033      33  symmetry
symmetry:034      34  symmetry
symmetry:035      35  symmetry
symmetry:036      36  symmetry
symmetry:037      37  symmetry
symmetry:038      38  symmetry
interior_:039     39  interior
interior_:040     40  interior
interior_:041     41  interior
interior_:042     42  interior
interior_:043     43  interior
interior_:044     44  interior
interior_:045     45  interior
wall_entree:046   46  wall
wall_entree:047   47  wall
default-interior:048 48  interior
default-interior:049 49  interior
default-interior:050 50  interior
default-interior:051 51  interior
default-interior:052 52  interior
default-interior:053 53  interior
default-interior:054 54  interior
default-interior:055 55  interior
default-interior:056 56  interior
default-interior:057 57  interior
default-interior:058 58  interior

```

Boundary Conditions

chimney

Condition	Value
Material Name	mixture-template
Specify source terms?	no
Source Terms	((mass (inactive . #f) (constant . 0) (profile)) (x-momentum (inactive . #f) (constant . 0) (profile)) (y-momentum (inactive . #f) (constant . 0) (profile)) (z-momentum (inactive . #f) (constant . 0) (profile)) (species-0 (inactive . #f) (constant . 0) (profile)) (species-1 (inactive . #f) (constant . 0) (profile)) (species-2 (inactive . #f) (constant . 0) (profile)) (species-3 (inactive . #f) (constant . 0) (profile)) (energy (inactive . #f) (constant . 0) (profile)))
Specify fixed values?	no
Local Coordinate System for Fixed Velocities	no
Fixed Values	((x-velocity (inactive . #f) (constant . 0) (profile)) (y-velocity (inactive . #f) (constant . 0) (profile)) (z-velocity (inactive . #f) (constant . 0) (profile)) (species-0 (inactive . #f) (constant . 0) (profile)) (species-1 (inactive . #f) (constant . 0) (profile)) (species-2 (inactive . #f) (constant . 0) (profile)) (species-3 (inactive . #f) (constant . 0) (profile)) (temperature (inactive . #f) (constant . 0) (profile)))
Motion Type	0
X-Velocity Of Zone	0
Y-Velocity Of Zone	0
Z-Velocity Of Zone	0
Rotation speed	0
X-Origin of Rotation-Axis	0
Y-Origin of Rotation-Axis	0
Z-Origin of Rotation-Axis	0
X-Component of Rotation-Axis	0
Y-Component of Rotation-Axis	0
Z-Component of Rotation-Axis	1
Deactivated Thread	no
Porous zone?	no
Conical porous zone?	no
X-Component of Direction-1 Vector	1

Y-Component of Direction-1 Vector	0
Z-Component of Direction-1 Vector	0
X-Component of Direction-2 Vector	0
Y-Component of Direction-2 Vector	1
Z-Component of Direction-2 Vector	0
X-Coordinate of Point on Cone Axis	1
Y-Coordinate of Point on Cone Axis	0
Z-Coordinate of Point on Cone Axis	0
Half Angle of Cone Relative to its Axis	0
Direction-1 Viscous Resistance	0
Direction-2 Viscous Resistance	0
Direction-3 Viscous Resistance	0
Direction-1 Inertial Resistance	0
Direction-2 Inertial Resistance	0
Direction-3 Inertial Resistance	0
C0 Coefficient for Power-Law	0
C1 Coefficient for Power-Law	0
Porosity	1
Solid Material Name	aluminum
Reaction Mechanism	0
Activate reaction mechanisms?	yes
Surface-Volume-Ratio	0

entree_reflektor

Condition	Value
-----	-----
-----	-----
-----	-----
Material Name	mixture-template
Specify source terms?	no
Source Terms	((mass (inactive . #f) (constant . 0) (profile)) (x-momentum (inactive . #f) (constant . 0) (profile)) (y-momentum (inactive . #f) (constant . 0) (profile)) (z-momentum (inactive . #f) (constant . 0) (profile)) (energy (inactive . #f) (constant . 0) (profile)))
Specify fixed values?	no
Local Coordinate System for Fixed Velocities	no
Fixed Values	((x-velocity (inactive . #f) (constant . 0) (profile)) (y-velocity (inactive . #f) (constant . 0) (profile)) (z-velocity (inactive . #f) (constant . 0) (profile)) (temperature (inactive . #f) (constant . 0) (profile)))
Motion Type	0
X-Velocity Of Zone	0
Y-Velocity Of Zone	0
Z-Velocity Of Zone	0
Rotation speed	0
X-Origin of Rotation-Axis	0
Y-Origin of Rotation-Axis	0
Z-Origin of Rotation-Axis	0
X-Component of Rotation-Axis	0
Y-Component of Rotation-Axis	0
Z-Component of Rotation-Axis	1
Deactivated Thread	no
Porous zone?	no
Conical porous zone?	no
X-Component of Direction-1 Vector	1
Y-Component of Direction-1 Vector	0
Z-Component of Direction-1 Vector	0
X-Component of Direction-2 Vector	0
Y-Component of Direction-2 Vector	1
Z-Component of Direction-2 Vector	0
X-Coordinate of Point on Cone Axis	1
Y-Coordinate of Point on Cone Axis	0
Z-Coordinate of Point on Cone Axis	0
Half Angle of Cone Relative to its Axis	0
Direction-1 Viscous Resistance	0
Direction-2 Viscous Resistance	0
Direction-3 Viscous Resistance	0
Direction-1 Inertial Resistance	0
Direction-2 Inertial Resistance	0

Direction-3 Inertial Resistance	0
C0 Coefficient for Power-Law	0
C1 Coefficient for Power-Law	0
Porosity	1
Solid Material Name	aluminum
Reaction Mechanism	0
Activate reaction mechanisms?	yes
Surface-Volume-Ratio	0

entree_bas

Condition	Value

Material Name	mixture-template
Specify source terms?	no
Source Terms	((mass (inactive . #f) (constant . 0) (profile)) (x-momentum (inactive . #f) (constant . 0) (profile)) (y-momentum (inactive . #f) (constant . 0) (profile)) (z-momentum (inactive . #f) (constant . 0) (profile)) (species-0 (inactive . #f) (constant . 0) (profile)) (species-1 (inactive . #f) (constant . 0) (profile)) (species-2 (inactive . #f) (constant . 0) (profile)) (species-3 (inactive . #f) (constant . 0) (profile)) (energy (inactive . #f) (constant . 0) (profile)))
Specify fixed values?	no
Local Coordinate System for Fixed Velocities	no
Fixed Values	((x-velocity (inactive . #f) (constant . 0) (profile)) (y-velocity (inactive . #f) (constant . 0) (profile)) (z-velocity (inactive . #f) (constant . 0) (profile)) (species-0 (inactive . #f) (constant . 0) (profile)) (species-1 (inactive . #f) (constant . 0) (profile)) (species-2 (inactive . #f) (constant . 0) (profile)) (species-3 (inactive . #f) (constant . 0) (profile)) (temperature (inactive . #f) (constant . 0) (profile)))
Motion Type	0
X-Velocity Of Zone	0
Y-Velocity Of Zone	0
Z-Velocity Of Zone	0
Rotation speed	0
X-Origin of Rotation-Axis	0
Y-Origin of Rotation-Axis	0
Z-Origin of Rotation-Axis	0
X-Component of Rotation-Axis	0
Y-Component of Rotation-Axis	0
Z-Component of Rotation-Axis	1
Deactivated Thread	no
Porous zone?	no
Conical porous zone?	no
X-Component of Direction-1 Vector	1
Y-Component of Direction-1 Vector	0
Z-Component of Direction-1 Vector	0
X-Component of Direction-2 Vector	0
Y-Component of Direction-2 Vector	1
Z-Component of Direction-2 Vector	0
X-Coordinate of Point on Cone Axis	1
Y-Coordinate of Point on Cone Axis	0
Z-Coordinate of Point on Cone Axis	0
Half Angle of Cone Relative to its Axis	0
Direction-1 Viscous Resistance	0
Direction-2 Viscous Resistance	0
Direction-3 Viscous Resistance	0
Direction-1 Inertial Resistance	0
Direction-2 Inertial Resistance	0
Direction-3 Inertial Resistance	0
C0 Coefficient for Power-Law	0
C1 Coefficient for Power-Law	0
Porosity	1
Solid Material Name	aluminum
Reaction Mechanism	0

Activate reaction mechanisms? yes
Surface-Volume-Ratio 0

inlet

Condition	Value
-----	-----
-----	-----
-----	-----
-----	-----
-----	-----
-----	-----

Material Name mixture-template
Specify source terms? no
Source Terms ((mass (inactive . #f) (constant . 0) (profile)) (x-momentum (inactive . #f) (constant . 0) (profile)) (y-momentum (inactive . #f) (constant . 0) (profile)) (z-momentum (inactive . #f) (constant . 0) (profile)) (species-0 (inactive . #f) (constant . 0) (profile)) (species-1 (inactive . #f) (constant . 0) (profile)) (species-2 (inactive . #f) (constant . 0) (profile)) (species-3 (inactive . #f) (constant . 0) (profile)) (energy (inactive . #f) (constant . 0) (profile)))
Specify fixed values? no
Local Coordinate System for Fixed Velocities no
Fixed Values ((x-velocity (inactive . #f) (constant . 0) (profile)) (y-velocity (inactive . #f) (constant . 0) (profile)) (z-velocity (inactive . #f) (constant . 0) (profile)) (species-0 (inactive . #f) (constant . 0) (profile)) (species-1 (inactive . #f) (constant . 0) (profile)) (species-2 (inactive . #f) (constant . 0) (profile)) (species-3 (inactive . #f) (constant . 0) (profile)) (temperature (inactive . #f) (constant . 0) (profile)))
Motion Type 0
X-Velocity Of Zone 0
Y-Velocity Of Zone 0
Z-Velocity Of Zone 0
Rotation speed 0
X-Origin of Rotation-Axis 0
Y-Origin of Rotation-Axis 0
Z-Origin of Rotation-Axis 0
X-Component of Rotation-Axis 0
Y-Component of Rotation-Axis 0
Z-Component of Rotation-Axis 1
Deactivated Thread no
Porous zone? no
Conical porous zone? no
X-Component of Direction-1 Vector 1
Y-Component of Direction-1 Vector 0
Z-Component of Direction-1 Vector 0
X-Component of Direction-2 Vector 0
Y-Component of Direction-2 Vector 1
Z-Component of Direction-2 Vector 0
X-Coordinate of Point on Cone Axis 1
Y-Coordinate of Point on Cone Axis 0
Z-Coordinate of Point on Cone Axis 0
Half Angle of Cone Relative to its Axis 0
Direction-1 Viscous Resistance 0
Direction-2 Viscous Resistance 0
Direction-3 Viscous Resistance 0
Direction-1 Inertial Resistance 0
Direction-2 Inertial Resistance 0
Direction-3 Inertial Resistance 0
C0 Coefficient for Power-Law 0
C1 Coefficient for Power-Law 0
Porosity 1
Solid Material Name aluminum
Reaction Mechanism 0
Activate reaction mechanisms? no
Surface-Volume-Ratio 0

solid.47

Condition Value

```

-----
----
Material Name                graphite-south-africa
Specify source terms?       no
Source Terms                 ((energy (inactive . #f) (constant . 0) (profile
)))
Specify fixed values?       no
Fixed Values                 ((temperature (constant . 900) (profile )))
Motion Type                  0
X-Velocity Of Zone          0
Y-Velocity Of Zone          0
Z-Velocity Of Zone          0
Rotation speed               0
X-Origin of Rotation-Axis    0
Y-Origin of Rotation-Axis    0
Z-Origin of Rotation-Axis    0
X-Component of Rotation-Axis 0
Y-Component of Rotation-Axis 0
Z-Component of Rotation-Axis 1
Deactivated Thread          no

```

peb2

Condition	Value
-----------	-------

```

-----
-----
-----
-----
-----
-----
-----
-----
-----
-----

```

```

-----
Material Name                mixture-template
Specify source terms?       no
Source Terms                 ((mass (inactive . #f) (constant
. 0) (profile )) (x-momentum (inactive . #f) (constant . 0) (profile )) (y-momentum
(inactive . #f) (constant . 0) (profile )) (z-momentum (inactive . #f) (constant . 0)
(profile )) (species-0 (inactive . #f) (constant . 0) (profile )) (species-1 (inactive
. #f) (constant . 0) (profile )) (species-2 (inactive . #f) (constant . 0) (profile ))
(species-3 (inactive . #f) (constant . 0) (profile )) (energy (inactive . #f) (constant
. 0) (profile )))
Specify fixed values?       no
Local Coordinate System for Fixed Velocities no
Fixed Values                 ((x-velocity (inactive . #f)
(constant . 0) (profile )) (y-velocity (inactive . #f) (constant . 0) (profile )) (z-
velocity (inactive . #f) (constant . 0) (profile )) (species-0 (inactive . #f) (constant
. 0) (profile )) (species-1 (inactive . #f) (constant . 0) (profile )) (species-2
(inactive . #f) (constant . 0) (profile )) (species-3 (inactive . #f) (constant . 0)
(profile )) (temperature (constant . 900) (profile )))
Motion Type                  0
X-Velocity Of Zone          0
Y-Velocity Of Zone          0
Z-Velocity Of Zone          0
Rotation speed               0
X-Origin of Rotation-Axis    0
Y-Origin of Rotation-Axis    0
Z-Origin of Rotation-Axis    0
X-Component of Rotation-Axis 0
Y-Component of Rotation-Axis 0
Z-Component of Rotation-Axis 1
Deactivated Thread          no
Porous zone?                 yes
Conical porous zone?        no
X-Component of Direction-1 Vector 1
Y-Component of Direction-1 Vector 0
Z-Component of Direction-1 Vector 0
X-Component of Direction-2 Vector 0
Y-Component of Direction-2 Vector 1
Z-Component of Direction-2 Vector 0
X-Coordinate of Point on Cone Axis 1
Y-Coordinate of Point on Cone Axis 0
Z-Coordinate of Point on Cone Axis 0

```

```

Half Angle of Cone Relative to its Axis      0
Direction-1 Viscous Resistance               0
Direction-2 Viscous Resistance               0
Direction-3 Viscous Resistance               0
Direction-1 Inertial Resistance              0
Direction-2 Inertial Resistance              0
Direction-3 Inertial Resistance              0
C0 Coefficient for Power-Law                 341
C1 Coefficient for Power-Law                 1.6107
Porosity                                     0.39500001
Solid Material Name                          graphite-south-africa
Reaction Mechanism                            0
Activate reaction mechanisms?                 yes
Surface-Volume-Ratio                         363

```

intpeb

Condition	Value
Material Name	mixture-template
Specify source terms?	no
Source Terms	((mass (inactive . #f) (constant . 0) (profile)) (x-momentum (inactive . #f) (constant . 0) (profile)) (y-momentum (inactive . #f) (constant . 0) (profile)) (z-momentum (inactive . #f) (constant . 0) (profile)) (species-0 (inactive . #f) (constant . 0) (profile)) (species-1 (inactive . #f) (constant . 0) (profile)) (species-2 (inactive . #f) (constant . 0) (profile)) (species-3 (inactive . #f) (constant . 0) (profile)) (energy (inactive . #f) (constant . 0) (profile)))
Specify fixed values?	no
Local Coordinate System for Fixed Velocities	no
Fixed Values	((x-velocity (inactive . #f) (constant . 0) (profile)) (y-velocity (inactive . #f) (constant . 0) (profile)) (z-velocity (inactive . #f) (constant . 0) (profile)) (species-0 (inactive . #f) (constant . 0) (profile)) (species-1 (inactive . #f) (constant . 0) (profile)) (species-2 (inactive . #f) (constant . 0) (profile)) (species-3 (inactive . #f) (constant . 0) (profile)) (temperature (inactive . #f) (constant . 0) (profile)))
Motion Type	0
X-Velocity Of Zone	0
Y-Velocity Of Zone	0
Z-Velocity Of Zone	0
Rotation speed	0
X-Origin of Rotation-Axis	0
Y-Origin of Rotation-Axis	0
Z-Origin of Rotation-Axis	0
X-Component of Rotation-Axis	0
Y-Component of Rotation-Axis	0
Z-Component of Rotation-Axis	1
Deactivated Thread	no
Porous zone?	no
Conical porous zone?	no
X-Component of Direction-1 Vector	1
Y-Component of Direction-1 Vector	0
Z-Component of Direction-1 Vector	0
X-Component of Direction-2 Vector	0
Y-Component of Direction-2 Vector	1
Z-Component of Direction-2 Vector	0
X-Coordinate of Point on Cone Axis	1
Y-Coordinate of Point on Cone Axis	0
Z-Coordinate of Point on Cone Axis	0
Half Angle of Cone Relative to its Axis	0
Direction-1 Viscous Resistance	0
Direction-2 Viscous Resistance	0
Direction-3 Viscous Resistance	0
Direction-1 Inertial Resistance	0
Direction-2 Inertial Resistance	0

Direction-3 Inertial Resistance	0
C0 Coefficient for Power-Law	0
C1 Coefficient for Power-Law	0
Porosity	1
Solid Material Name	aluminum
Reaction Mechanism	0
Activate reaction mechanisms?	yes
Surface-Volume-Ratio	0

pebl

Condition	Value

Material Name	mixture-template
Specify source terms?	no
Source Terms	((mass (inactive . #f) (constant . 0) (profile)) (x-momentum (inactive . #f) (constant . 0) (profile)) (y-momentum (inactive . #f) (constant . 0) (profile)) (z-momentum (profile udf big_inzmom_source) (constant . 0)) (species-0 (inactive . #f) (constant . 0) (profile)) (species-1 (inactive . #f) (constant . 0) (profile)) (species-2 (inactive . #f) (constant . 0) (profile)) (species-3 (inactive . #f) (constant . 0) (profile)) (energy (inactive . #f) (constant . 0) (profile))))
Specify fixed values?	no
Local Coordinate System for Fixed Velocities	no
Fixed Values	((x-velocity (inactive . #f) (constant . 0) (profile)) (y-velocity (inactive . #f) (constant . 0) (profile)) (z-velocity (inactive . #f) (constant . 0) (profile)) (species-0 (inactive . #f) (constant . 0) (profile)) (species-1 (inactive . #f) (constant . 0) (profile)) (species-2 (inactive . #f) (constant . 0) (profile)) (species-3 (inactive . #f) (constant . 0) (profile)) (temperature (constant . 900) (profile))))
Motion Type	0
X-Velocity Of Zone	0
Y-Velocity Of Zone	0
Z-Velocity Of Zone	0
Rotation speed	0
X-Origin of Rotation-Axis	0
Y-Origin of Rotation-Axis	0
Z-Origin of Rotation-Axis	0
X-Component of Rotation-Axis	0
Y-Component of Rotation-Axis	0
Z-Component of Rotation-Axis	1
Deactivated Thread	no
Porous zone?	yes
Conical porous zone?	no
X-Component of Direction-1 Vector	0
Y-Component of Direction-1 Vector	0
Z-Component of Direction-1 Vector	1
X-Component of Direction-2 Vector	0
Y-Component of Direction-2 Vector	1
Z-Component of Direction-2 Vector	0
X-Coordinate of Point on Cone Axis	1
Y-Coordinate of Point on Cone Axis	0
Z-Coordinate of Point on Cone Axis	0
Half Angle of Cone Relative to its Axis	0
Direction-1 Viscous Resistance	0
Direction-2 Viscous Resistance	0
Direction-3 Viscous Resistance	0
Direction-1 Inertial Resistance	0
Direction-2 Inertial Resistance	0
Direction-3 Inertial Resistance	0
C0 Coefficient for Power-Law	36.688
C1 Coefficient for Power-Law	1.7599
Porosity	0.39500001
Solid Material Name	graphite-south-africa
Reaction Mechanism	0

Activate reaction mechanisms? yes
Surface-Volume-Ratio 60.5

ref2

Condition	Value
-----	-----
-----	-----
-----	-----
-----	-----
-----	-----
-----	-----

Material Name mixture-template
Specify source terms? no
Source Terms ((mass (inactive . #f) (constant . 0) (profile)) (x-momentum (inactive . #f) (constant . 0) (profile)) (y-momentum (inactive . #f) (constant . 0) (profile)) (z-momentum (inactive . #f) (constant . 0) (profile)) (species-0 (inactive . #f) (constant . 0) (profile)) (species-1 (inactive . #f) (constant . 0) (profile)) (species-2 (inactive . #f) (constant . 0) (profile)) (species-3 (inactive . #f) (constant . 0) (profile)) (energy (inactive . #f) (constant . 0) (profile)))
Specify fixed values? no
Local Coordinate System for Fixed Velocities no
Fixed Values ((x-velocity (inactive . #f) (constant . 0) (profile)) (y-velocity (inactive . #f) (constant . 0) (profile)) (z-velocity (inactive . #f) (constant . 0) (profile)) (species-0 (inactive . #f) (constant . 0) (profile)) (species-1 (inactive . #f) (constant . 0) (profile)) (species-2 (inactive . #f) (constant . 0) (profile)) (species-3 (inactive . #f) (constant . 0) (profile)) (temperature (constant . 900) (profile)))
Motion Type 0
X-Velocity Of Zone 0
Y-Velocity Of Zone 0
Z-Velocity Of Zone 0
Rotation speed 0
X-Origin of Rotation-Axis 0
Y-Origin of Rotation-Axis 0
Z-Origin of Rotation-Axis 0
X-Component of Rotation-Axis 0
Y-Component of Rotation-Axis 0
Z-Component of Rotation-Axis 1
Deactivated Thread no
Porous zone? yes
Conical porous zone? no
X-Component of Direction-1 Vector 0
Y-Component of Direction-1 Vector 0
Z-Component of Direction-1 Vector 1
X-Component of Direction-2 Vector 0
Y-Component of Direction-2 Vector 1
Z-Component of Direction-2 Vector 0
X-Coordinate of Point on Cone Axis 1
Y-Coordinate of Point on Cone Axis 0
Z-Coordinate of Point on Cone Axis 0
Half Angle of Cone Relative to its Axis 0
Direction-1 Viscous Resistance 0
Direction-2 Viscous Resistance 0
Direction-3 Viscous Resistance 0
Direction-1 Inertial Resistance 0
Direction-2 Inertial Resistance 0
Direction-3 Inertial Resistance 0
C0 Coefficient for Power-Law 63
C1 Coefficient for Power-Law 1.72
Porosity 0.13
Solid Material Name graphite-south-africa
Reaction Mechanism 0
Activate reaction mechanisms? yes
Surface-Volume-Ratio 53.580002

interref

Condition	Value
-----------	-------


```

Material Name                mixture-template
Specify source terms?       no
Source Terms                 ((mass (inactive . #f) (constant
. 0) (profile )) (x-momentum (inactive . #f) (constant . 0) (profile )) (y-momentum
(inactive . #f) (constant . 0) (profile )) (z-momentum (inactive . #f) (constant . 0)
(profile )) (species-0 (inactive . #f) (constant . 0) (profile )) (species-1 (inactive
. #f) (constant . 0) (profile )) (species-2 (inactive . #f) (constant . 0) (profile ))
(species-3 (inactive . #f) (constant . 0) (profile )) (energy (inactive . #f) (constant
. 0) (profile )))
Specify fixed values?       no
Local Coordinate System for Fixed Velocities no
Fixed Values                 ((x-velocity (inactive . #f)
(constant . 0) (profile )) (y-velocity (inactive . #f) (constant . 0) (profile )) (z-
velocity (inactive . #f) (constant . 0) (profile )) (species-0 (inactive . #f) (constant
. 0) (profile )) (species-1 (inactive . #f) (constant . 0) (profile )) (species-2
(inactive . #f) (constant . 0) (profile )) (species-3 (inactive . #f) (constant . 0)
(profile )) (temperature (inactive . #f) (constant . 0) (profile )))
Motion Type                  0
X-Velocity Of Zone          0
Y-Velocity Of Zone          0
Z-Velocity Of Zone          0
Rotation speed              0
X-Origin of Rotation-Axis   0
Y-Origin of Rotation-Axis   0
Z-Origin of Rotation-Axis   0
X-Component of Rotation-Axis 0
Y-Component of Rotation-Axis 0
Z-Component of Rotation-Axis 1
Deactivated Thread          no
Porous zone?                no
Conical porous zone?       no
X-Component of Direction-1 Vector 1
Y-Component of Direction-1 Vector 0
Z-Component of Direction-1 Vector 0
X-Component of Direction-2 Vector 0
Y-Component of Direction-2 Vector 1
Z-Component of Direction-2 Vector 0
X-Coordinate of Point on Cone Axis 1
Y-Coordinate of Point on Cone Axis 0
Z-Coordinate of Point on Cone Axis 0
Half Angle of Cone Relative to its Axis 0
Direction-1 Viscous Resistance 0
Direction-2 Viscous Resistance 0
Direction-3 Viscous Resistance 0
Direction-1 Inertial Resistance 0
Direction-2 Inertial Resistance 0
Direction-3 Inertial Resistance 0
C0 Coefficient for Power-Law 0
C1 Coefficient for Power-Law 0
Porosity                    1
Solid Material Name         aluminum
Reaction Mechanism          0
Activate reaction mechanisms? yes
Surface-Volume-Ratio        0

```

ref1

Condition	Value

```

-----
Material Name                               mixture-template
Specify source terms?                       no
Source Terms                                ((mass (inactive . #f) (constant
. 0) (profile )) (x-momentum (inactive . #f) (constant . 0) (profile )) (y-momentum
(inactive . #f) (constant . 0) (profile )) (z-momentum (inactive . #f) (constant . 0)
(profile )) (species-0 (inactive . #f) (constant . 0) (profile )) (species-1 (inactive
. #f) (constant . 0) (profile )) (species-2 (inactive . #f) (constant . 0) (profile ))
(species-3 (inactive . #f) (constant . 0) (profile )) (energy (inactive . #f) (constant
. 0) (profile )))
Specify fixed values?                       no
Local Coordinate System for Fixed Velocities no
Fixed Values                                ((x-velocity (inactive . #f)
(constant . 0) (profile )) (y-velocity (inactive . #f) (constant . 0) (profile )) (z-
velocity (inactive . #f) (constant . 0) (profile )) (species-0 (inactive . #f) (constant
. 0) (profile )) (species-1 (inactive . #f) (constant . 0) (profile )) (species-2
(inactive . #f) (constant . 0) (profile )) (species-3 (inactive . #f) (constant . 0)
(profile )) (temperature (constant . 900) (profile )))
Motion Type                                 0
X-Velocity Of Zone                          0
Y-Velocity Of Zone                          0
Z-Velocity Of Zone                          0
Rotation speed                              0
X-Origin of Rotation-Axis                   0
Y-Origin of Rotation-Axis                   0
Z-Origin of Rotation-Axis                   0
X-Component of Rotation-Axis                0
Y-Component of Rotation-Axis                0
Z-Component of Rotation-Axis                1
Deactivated Thread                          no
Porous zone?                                yes
Conical porous zone?                        no
X-Component of Direction-1 Vector           0
Y-Component of Direction-1 Vector           0
Z-Component of Direction-1 Vector           1
X-Component of Direction-2 Vector           0
Y-Component of Direction-2 Vector           1
Z-Component of Direction-2 Vector           0
X-Coordinate of Point on Cone Axis          1
Y-Coordinate of Point on Cone Axis          0
Z-Coordinate of Point on Cone Axis          0
Half Angle of Cone Relative to its Axis     0
Direction-1 Viscous Resistance              0
Direction-2 Viscous Resistance              0
Direction-3 Viscous Resistance              0
Direction-1 Inertial Resistance             0
Direction-2 Inertial Resistance             0
Direction-3 Inertial Resistance             0
C0 Coefficient for Power-Law                63
C1 Coefficient for Power-Law                1.72
Porosity                                    0.13
Solid Material Name                         graphite-south-africa
Reaction Mechanism                          0
Activate reaction mechanisms?                yes
Surface-Volume-Ratio                        53.580002

```

porous_jump.63

Condition	Value
Flow Direction (-1,0,1)	1
Calculate Pressure-Jump from Average Conditions?	yes
Pressure-Jump	((polynomial normal-velocity
0 0 30))	
Limit Polynomial Velocity Range?	no
Polynomial Range: Minimum Velocity Magnitude	0
Polynomial Range: Maximum Velocity Magnitude	1e+10
Profile Specification of Pressure-Jump?	no
Pressure Jump Profile	0

Swirl-Velocity Specification?	no
Radial-Velocity Polynomial Coefficient	()
Tangential-Velocity Polynomial Coefficient	()
Fan Hub Radius	1e-06
X-Coordinate of Fan Origin	0
Y-Coordinate of Fan Origin	0
Z-Coordinate of Fan Origin	0
X-Component of Fan Axis	1
Y-Component of Fan Axis	0
Z-Component of Fan Axis	0
Profile Specification of Tangential Velocity?	no
Tangential Velocity Profile	0
Profile Specification of Radial Velocity?	no
Radial Velocity Profile	0

wall-shadow

Condition	Value
-----	-----
Wall Thickness	0
Heat Generation Rate	0
Material Name	graphite-south-africa
Thermal BC Type	3
Temperature	900
Heat Flux	0
Convective Heat Transfer Coefficient	0
Free Stream Temperature	300
Enable shell conduction?	no
Wall Motion	0
Shear Boundary Condition	0
Define wall motion relative to adjacent cell zone?	yes
Apply a rotational velocity to this wall?	no
Velocity Magnitude	0
X-Component of Wall Translation	1
Y-Component of Wall Translation	0
Z-Component of Wall Translation	0
Define wall velocity components?	no
X-Component of Wall Translation	0
Y-Component of Wall Translation	0
Z-Component of Wall Translation	0
External Emissivity	1
External Radiation Temperature	300
Activate Reaction Mechanisms	no
Rotation Speed	0
X-Position of Rotation-Axis Origin	0
Y-Position of Rotation-Axis Origin	0
Z-Position of Rotation-Axis Origin	0
X-Component of Rotation-Axis Direction	0
Y-Component of Rotation-Axis Direction	0
Z-Component of Rotation-Axis Direction	1
X-component of shear stress	0
Y-component of shear stress	0
Z-component of shear stress	0
Surface tension gradient	0
Reaction Mechanisms	0
Specularity Coefficient	0

wall_entree:047-shadow

Condition	Value
-----	-----
Wall Thickness	0
Heat Generation Rate	0
Material Name	graphite-south-africa
Thermal BC Type	3
Temperature	300
Heat Flux	0
Convective Heat Transfer Coefficient	0
Free Stream Temperature	300
Enable shell conduction?	no
Wall Motion	0


```

Shear Boundary Condition 0
Define wall motion relative to adjacent cell zone? yes
Apply a rotational velocity to this wall? no
Velocity Magnitude 0
X-Component of Wall Translation 1
Y-Component of Wall Translation 0
Z-Component of Wall Translation 0
Define wall velocity components? no
X-Component of Wall Translation 0
Y-Component of Wall Translation 0
Z-Component of Wall Translation 0
External Emissivity 1
External Radiation Temperature 300
Activate Reaction Mechanisms no
Rotation Speed 0
X-Position of Rotation-Axis Origin 0
Y-Position of Rotation-Axis Origin 0
Z-Position of Rotation-Axis Origin 0
X-Component of Rotation-Axis Direction 0
Y-Component of Rotation-Axis Direction 0
Z-Component of Rotation-Axis Direction 1
X-component of shear stress 0
Y-component of shear stress 0
Z-component of shear stress 0
Surface tension gradient 0
Reaction Mechanisms 0
Specularity Coefficient 0

```

wall

Condition	Value
Wall Thickness	0
Heat Generation Rate	0
Material Name	graphite-south-africa
Thermal BC Type	3
Temperature	900
Heat Flux	0
Convective Heat Transfer Coefficient	0
Free Stream Temperature	300
Enable shell conduction?	no
Wall Motion	0
Shear Boundary Condition	0
Define wall motion relative to adjacent cell zone?	yes
Apply a rotational velocity to this wall?	no
Velocity Magnitude	0
X-Component of Wall Translation	1
Y-Component of Wall Translation	0
Z-Component of Wall Translation	0
Define wall velocity components?	no
X-Component of Wall Translation	0
Y-Component of Wall Translation	0
Z-Component of Wall Translation	0
External Emissivity	1
External Radiation Temperature	300
Activate Reaction Mechanisms	yes
	(0 0 0 0)
	((constant . 0) (profile
)) ((constant . 0) (profile)) ((constant . 0) (profile)) ((constant . 0) (profile	
))	
Rotation Speed	0
X-Position of Rotation-Axis Origin	0
Y-Position of Rotation-Axis Origin	0
Z-Position of Rotation-Axis Origin	0
X-Component of Rotation-Axis Direction	0
Y-Component of Rotation-Axis Direction	0
Z-Component of Rotation-Axis Direction	1
X-component of shear stress	0
Y-component of shear stress	0

```

Z-component of shear stress          0
Surface tension gradient             0
Reaction Mechanisms                  0
Specularity Coefficient              0

```

symmetry

```

Condition  Value
-----

```

pressure_outlet.61

```

Condition                                     Value
-----

```

```

-----
Gauge Pressure                               -30
Radial Equilibrium Pressure Distribution     no
Backflow Total Temperature                   923
Backflow Direction Specification Method      1
Coordinate System                            0
X-Component of Flow Direction                1
Y-Component of Flow Direction                0
Z-Component of Flow Direction                0
X-Component of Axis Direction                1
Y-Component of Axis Direction                0
Z-Component of Axis Direction                0
X-Coordinate of Axis Origin                  0
Y-Coordinate of Axis Origin                  0
Z-Coordinate of Axis Origin                  0
Backflow                                     (((constant . 0.0043000001) (profile
)) ((constant . 0.233) (profile )) ((constant . 0) (profile )) ((constant . 0) (profile
)))
is zone used in mixing-plane model?         no
Specify targeted mass-flow rate              no
Targeted mass-flow                           1

```

pressure_inlet.60

```

Condition                                     Value
-----

```

```

-----
Gauge Total Pressure                          0
Supersonic/Initial Gauge Pressure             0
Total Temperature                             293.14999
Direction Specification Method                 1
Coordinate System                              0
X-Component of Flow Direction                  1
Y-Component of Flow Direction                  0
Z-Component of Flow Direction                  0
X-Component of Axis Direction                  1
Y-Component of Axis Direction                  0
Z-Component of Axis Direction                  0
X-Coordinate of Axis Origin                    0
Y-Coordinate of Axis Origin                    0
Z-Coordinate of Axis Origin                    0
(((constant . 0.0043000001) (profile ))
((constant . 0.23) (profile )) ((constant . 0) (profile )) ((constant . 0) (profile
)))
is zone used in mixing-plane model?           no

```

interior_

```

Condition  Value
-----

```

wall_chimey

```

Condition                                     Value

```

```

-----
-
Wall Thickness 0
Heat Generation Rate 0
Material Name aluminum
Thermal BC Type 0
Temperature 923.15002
Heat Flux 0
Convective Heat Transfer Coefficient 0
Free Stream Temperature 300
Enable shell conduction? no
Wall Motion 0
Shear Boundary Condition 0
Define wall motion relative to adjacent cell zone? yes
Apply a rotational velocity to this wall? no
Velocity Magnitude 0
X-Component of Wall Translation 1
Y-Component of Wall Translation 0
Z-Component of Wall Translation 0
Define wall velocity components? no
X-Component of Wall Translation 0
Y-Component of Wall Translation 0
Z-Component of Wall Translation 0
External Emissivity 1
External Radiation Temperature 300
Activate Reaction Mechanisms no
(0 0 0 0)
(((constant . 0) (profile
)) ((constant . 0) (profile )) ((constant . 0) (profile )) ((constant . 0) (profile
)))

```

```

Rotation Speed 0
X-Position of Rotation-Axis Origin 0
Y-Position of Rotation-Axis Origin 0
Z-Position of Rotation-Axis Origin 0
X-Component of Rotation-Axis Direction 0
Y-Component of Rotation-Axis Direction 0
Z-Component of Rotation-Axis Direction 1
X-component of shear stress 0
Y-component of shear stress 0
Z-component of shear stress 0
Surface tension gradient 0
Reaction Mechanisms 0
Specularity Coefficient 0

```

wall_peg2

Condition	Value
-----------	-------

```

-----
-
Wall Thickness 0
Heat Generation Rate 0
Material Name aluminum
Thermal BC Type 0
Temperature 923.15002
Heat Flux 0
Convective Heat Transfer Coefficient 0
Free Stream Temperature 300
Enable shell conduction? no
Wall Motion 0
Shear Boundary Condition 0
Define wall motion relative to adjacent cell zone? yes
Apply a rotational velocity to this wall? no
Velocity Magnitude 0
X-Component of Wall Translation 1
Y-Component of Wall Translation 0
Z-Component of Wall Translation 0
Define wall velocity components? no
X-Component of Wall Translation 0
Y-Component of Wall Translation 0

```

```

Z-Component of Wall Translation      0
External Emissivity                  1
External Radiation Temperature      300
Activate Reaction Mechanisms        no
                                     (0 0 0 0)
                                     (((constant . 0) (profile
)) ((constant . 0) (profile )) ((constant . 0) (profile )) ((constant . 0) (profile
)))

```

```

Rotation Speed                       0
X-Position of Rotation-Axis Origin   0
Y-Position of Rotation-Axis Origin   0
Z-Position of Rotation-Axis Origin   0
X-Component of Rotation-Axis Direction 0
Y-Component of Rotation-Axis Direction 0
Z-Component of Rotation-Axis Direction 1
X-component of shear stress          0
Y-component of shear stress          0
Z-component of shear stress          0
Surface tension gradient              0
Reaction Mechanisms                  0
Specularity Coefficient               0

```

wall_interpeb

Condition	Value
-----------	-------

```

-----
-
Wall Thickness                       0
Heat Generation Rate                 0
Material Name                        aluminum
Thermal BC Type                      0
Temperature                          923.15002
Heat Flux                             0
Convective Heat Transfer Coefficient 0
Free Stream Temperature              300
Enable shell conduction?             no
Wall Motion                          0
Shear Boundary Condition              0
Define wall motion relative to adjacent cell zone? yes
Apply a rotational velocity to this wall? no
Velocity Magnitude                   0
X-Component of Wall Translation       1
Y-Component of Wall Translation       0
Z-Component of Wall Translation       0
Define wall velocity components?     no
X-Component of Wall Translation       0
Y-Component of Wall Translation       0
Z-Component of Wall Translation       0
External Emissivity                  1
External Radiation Temperature      300
Activate Reaction Mechanisms        no
                                     (0 0 0 0)
                                     (((constant . 0) (profile
)) ((constant . 0) (profile )) ((constant . 0) (profile )) ((constant . 0) (profile
)))

```

```

Rotation Speed                       0
X-Position of Rotation-Axis Origin   0
Y-Position of Rotation-Axis Origin   0
Z-Position of Rotation-Axis Origin   0
X-Component of Rotation-Axis Direction 0
Y-Component of Rotation-Axis Direction 0
Z-Component of Rotation-Axis Direction 1
X-component of shear stress          0
Y-component of shear stress          0
Z-component of shear stress          0
Surface tension gradient              0
Reaction Mechanisms                  0
Specularity Coefficient               0

```

wall_peb1

Condition	Value
Wall Thickness	0
Heat Generation Rate	0
Material Name	aluminum
Thermal BC Type	0
Temperature	923.15002
Heat Flux	0
Convective Heat Transfer Coefficient	0
Free Stream Temperature	300
Enable shell conduction?	no
Wall Motion	0
Shear Boundary Condition	0
Define wall motion relative to adjacent cell zone?	yes
Apply a rotational velocity to this wall?	no
Velocity Magnitude	0
X-Component of Wall Translation	1
Y-Component of Wall Translation	0
Z-Component of Wall Translation	0
Define wall velocity components?	no
X-Component of Wall Translation	0
Y-Component of Wall Translation	0
Z-Component of Wall Translation	0
External Emissivity	1
External Radiation Temperature	300
Activate Reaction Mechanisms	no
	(0 0 0 0)
	((constant . 0) (profile
)) ((constant . 0) (profile)) ((constant . 0) (profile)) ((constant . 0) (profile	
)))	
Rotation Speed	0
X-Position of Rotation-Axis Origin	0
Y-Position of Rotation-Axis Origin	0
Z-Position of Rotation-Axis Origin	0
X-Component of Rotation-Axis Direction	0
Y-Component of Rotation-Axis Direction	0
Z-Component of Rotation-Axis Direction	1
X-component of shear stress	0
Y-component of shear stress	0
Z-component of shear stress	0
Surface tension gradient	0
Reaction Mechanisms	0
Specularity Coefficient	0

wall_ref2

Condition	Value
Wall Thickness	0
Heat Generation Rate	0
Material Name	aluminum
Thermal BC Type	0
Temperature	923.15002
Heat Flux	0
Convective Heat Transfer Coefficient	0
Free Stream Temperature	300
Enable shell conduction?	no
Wall Motion	0
Shear Boundary Condition	0
Define wall motion relative to adjacent cell zone?	yes
Apply a rotational velocity to this wall?	no
Velocity Magnitude	0
X-Component of Wall Translation	1
Y-Component of Wall Translation	0
Z-Component of Wall Translation	0
Define wall velocity components?	no

```

X-Component of Wall Translation      0
Y-Component of Wall Translation      0
Z-Component of Wall Translation      0
External Emissivity                  1
External Radiation Temperature       300
Activate Reaction Mechanisms         no
                                     (0 0 0 0)
                                     (((constant . 0) (profile
)) ((constant . 0) (profile )) ((constant . 0) (profile )) ((constant . 0) (profile
)))

```

```

Rotation Speed                       0
X-Position of Rotation-Axis Origin    0
Y-Position of Rotation-Axis Origin    0
Z-Position of Rotation-Axis Origin    0
X-Component of Rotation-Axis Direction 0
Y-Component of Rotation-Axis Direction 0
Z-Component of Rotation-Axis Direction 1
X-component of shear stress           0
Y-component of shear stress           0
Z-component of shear stress           0
Surface tension gradient              0
Reaction Mechanisms                   0
Specularity Coefficient               0

```

wall_interef

Condition	Value
-----------	-------

-

Wall Thickness	0
Heat Generation Rate	0
Material Name	aluminum
Thermal BC Type	0
Temperature	923.15002
Heat Flux	0
Convective Heat Transfer Coefficient	0
Free Stream Temperature	300
Enable shell conduction?	no
Wall Motion	0
Shear Boundary Condition	0
Define wall motion relative to adjacent cell zone?	yes
Apply a rotational velocity to this wall?	no
Velocity Magnitude	0
X-Component of Wall Translation	1
Y-Component of Wall Translation	0
Z-Component of Wall Translation	0
Define wall velocity components?	no
X-Component of Wall Translation	0
Y-Component of Wall Translation	0
Z-Component of Wall Translation	0
External Emissivity	1
External Radiation Temperature	300
Activate Reaction Mechanisms	no

```

                                     (0 0 0 0)
                                     (((constant . 0) (profile
)) ((constant . 0) (profile )) ((constant . 0) (profile )) ((constant . 0) (profile
)))

```

```

Rotation Speed                       0
X-Position of Rotation-Axis Origin    0
Y-Position of Rotation-Axis Origin    0
Z-Position of Rotation-Axis Origin    0
X-Component of Rotation-Axis Direction 0
Y-Component of Rotation-Axis Direction 0
Z-Component of Rotation-Axis Direction 1
X-component of shear stress           0
Y-component of shear stress           0
Z-component of shear stress           0
Surface tension gradient              0
Reaction Mechanisms                   0
Specularity Coefficient               0

```

```

wall_refl
-----
Condition                                     Value
-----
-
Wall Thickness                                0
Heat Generation Rate                          0
Material Name                                 graphite-south-africa
Thermal BC Type                               0
Temperature                                   923.15002
Heat Flux                                      0
Convective Heat Transfer Coefficient          0
Free Stream Temperature                       300
Enable shell conduction?                      no
Wall Motion                                   0
Shear Boundary Condition                     0
Define wall motion relative to adjacent cell zone? yes
Apply a rotational velocity to this wall?     no
Velocity Magnitude                            0
X-Component of Wall Translation               1
Y-Component of Wall Translation               0
Z-Component of Wall Translation               0
Define wall velocity components?              no
X-Component of Wall Translation               0
Y-Component of Wall Translation               0
Z-Component of Wall Translation               0
External Emissivity                           1
External Radiation Temperature                300
Activate Reaction Mechanisms                  no
                                                (0 0 0 0)
                                                (((constant . 0) (profile
)) ((constant . 0) (profile )) ((constant . 0) (profile )) ((constant . 0) (profile
)))
Rotation Speed                                0
X-Position of Rotation-Axis Origin            0
Y-Position of Rotation-Axis Origin            0
Z-Position of Rotation-Axis Origin            0
X-Component of Rotation-Axis Direction        0
Y-Component of Rotation-Axis Direction        0
Z-Component of Rotation-Axis Direction        1
X-component of shear stress                   0
Y-component of shear stress                   0
Z-component of shear stress                   0
Surface tension gradient                      0
Reaction Mechanisms                           0
Specularity Coefficient                       0

wall_libre_1
-----
Condition                                     Value
-----
-
Wall Thickness                                0
Heat Generation Rate                          0
Material Name                                 aluminum
Thermal BC Type                               0
Temperature                                   923.15002
Heat Flux                                      0
Convective Heat Transfer Coefficient          0
Free Stream Temperature                       300
Enable shell conduction?                      no
Wall Motion                                   0
Shear Boundary Condition                     0
Define wall motion relative to adjacent cell zone? yes
Apply a rotational velocity to this wall?     no
Velocity Magnitude                            0
X-Component of Wall Translation               1
Y-Component of Wall Translation               0

```

```

Z-Component of Wall Translation      0
Define wall velocity components?    no
X-Component of Wall Translation      0
Y-Component of Wall Translation      0
Z-Component of Wall Translation      0
External Emissivity                  1
External Radiation Temperature       300
Activate Reaction Mechanisms         no
                                     (0 0 0 0)
                                     (((constant . 0) (profile
)) ((constant . 0) (profile )) ((constant . 0) (profile
)))

```

```

Rotation Speed                       0
X-Position of Rotation-Axis Origin    0
Y-Position of Rotation-Axis Origin    0
Z-Position of Rotation-Axis Origin    0
X-Component of Rotation-Axis Direction 0
Y-Component of Rotation-Axis Direction 0
Z-Component of Rotation-Axis Direction 1
X-component of shear stress           0
Y-component of shear stress           0
Z-component of shear stress           0
Surface tension gradient              0
Reaction Mechanisms                   0
Specularity Coefficient                0

```

wall_ref_bas

Condition	Value
-----------	-------

```

-----
-
Wall Thickness                       0
Heat Generation Rate                 0
Material Name                         graphite-south-africa
Thermal BC Type                       0
Temperature                           923.15002
Heat Flux                             0
Convective Heat Transfer Coefficient  0
Free Stream Temperature               300
Enable shell conduction?              no
Wall Motion                           0
Shear Boundary Condition               0
Define wall motion relative to adjacent cell zone? yes
Apply a rotational velocity to this wall? no
Velocity Magnitude                    0
X-Component of Wall Translation        1
Y-Component of Wall Translation        0
Z-Component of Wall Translation        0
Define wall velocity components?      no
X-Component of Wall Translation        0
Y-Component of Wall Translation        0
Z-Component of Wall Translation        0
External Emissivity                    1
External Radiation Temperature         300
Activate Reaction Mechanisms           yes
                                     (0 0 0 0)
                                     (((constant . 0) (profile
)) ((constant . 0) (profile )) ((constant . 0) (profile
)))

```

```

Rotation Speed                       0
X-Position of Rotation-Axis Origin    0
Y-Position of Rotation-Axis Origin    0
Z-Position of Rotation-Axis Origin    0
X-Component of Rotation-Axis Direction 0
Y-Component of Rotation-Axis Direction 0
Z-Component of Rotation-Axis Direction 1
X-component of shear stress           0
Y-component of shear stress           0
Z-component of shear stress           0
Surface tension gradient              0

```



```

Reaction Mechanisms          0
Specularity Coefficient      0

```

wall_entree

```

-----
Condition                      Value
-----
-
Wall Thickness                  0
Heat Generation Rate           0
Material Name                   aluminum
Thermal BC Type                0
Temperature                     923.15002
Heat Flux                       0
Convective Heat Transfer Coefficient 0
Free Stream Temperature        300
Enable shell conduction?       no
Wall Motion                     0
Shear Boundary Condition       0
Define wall motion relative to adjacent cell zone? yes
Apply a rotational velocity to this wall? no
Velocity Magnitude             0
X-Component of Wall Translation 1
Y-Component of Wall Translation 0
Z-Component of Wall Translation 0
Define wall velocity components? no
X-Component of Wall Translation 0
Y-Component of Wall Translation 0
Z-Component of Wall Translation 0
External Emissivity             1
External Radiation Temperature 300
Activate Reaction Mechanisms    no
                                (0 0 0 0)
                                (((constant . 0) (profile
)) ((constant . 0) (profile )) ((constant . 0) (profile
)))
Rotation Speed                 0
X-Position of Rotation-Axis Origin 0
Y-Position of Rotation-Axis Origin 0
Z-Position of Rotation-Axis Origin 0
X-Component of Rotation-Axis Direction 0
Y-Component of Rotation-Axis Direction 0
Z-Component of Rotation-Axis Direction 1
X-component of shear stress     0
Y-component of shear stress     0
Z-component of shear stress     0
Surface tension gradient        0
Reaction Mechanisms             0
Specularity Coefficient         0

```

wall_inlet

```

-----
Condition                      Value
-----
-
Wall Thickness                  0
Heat Generation Rate           0
Material Name                   aluminum
Thermal BC Type                0
Temperature                     293.14999
Heat Flux                       0
Convective Heat Transfer Coefficient 0
Free Stream Temperature        300
Enable shell conduction?       no
Wall Motion                     0
Shear Boundary Condition       0
Define wall motion relative to adjacent cell zone? yes
Apply a rotational velocity to this wall? no
Velocity Magnitude             0

```

```

X-Component of Wall Translation      1
Y-Component of Wall Translation      0
Z-Component of Wall Translation      0
Define wall velocity components?     no
X-Component of Wall Translation      0
Y-Component of Wall Translation      0
Z-Component of Wall Translation      0
External Emissivity                  1
External Radiation Temperature       300
Activate Reaction Mechanisms         no
                                     (0 0 0 0)
                                     (((constant . 0) (profile
)) ((constant . 0) (profile )) ((constant . 0) (profile )) ((constant . 0) (profile
)))

```

```

Rotation Speed                       0
X-Position of Rotation-Axis Origin    0
Y-Position of Rotation-Axis Origin    0
Z-Position of Rotation-Axis Origin    0
X-Component of Rotation-Axis Direction 0
Y-Component of Rotation-Axis Direction 0
Z-Component of Rotation-Axis Direction 1
X-component of shear stress           0
Y-component of shear stress           0
Z-component of shear stress           0
Surface tension gradient              0
Reaction Mechanisms                   0
Specularity Coefficient               0

```

default-interior

```

Condition  Value
-----

```

symmetry:001

```

Condition  Value
-----

```

symmetry:030

```

Condition  Value
-----

```

symmetry:032

```

Condition  Value
-----

```

symmetry:033

```

Condition  Value
-----

```

symmetry:034

```

Condition  Value
-----

```

symmetry:035

```

Condition  Value
-----

```

symmetry:036

```

Condition  Value
-----

```

symmetry:037

```

Condition  Value

```

symmetry:038

Condition Value

interior_:039

Condition Value

interior_:040

Condition Value

interior_:041

Condition Value

interior_:042

Condition Value

interior_:043

Condition Value

interior_:044

Condition Value

interior_:045

Condition Value

wall_entree:046

Condition	Value

Wall Thickness	0
Heat Generation Rate	0
Material Name	aluminum
Thermal BC Type	1
Temperature	300
Heat Flux	0
Convective Heat Transfer Coefficient	0
Free Stream Temperature	300
Enable shell conduction?	no
Wall Motion	0
Shear Boundary Condition	0
Define wall motion relative to adjacent cell zone?	yes
Apply a rotational velocity to this wall?	no
Velocity Magnitude	0
X-Component of Wall Translation	1
Y-Component of Wall Translation	0
Z-Component of Wall Translation	0
Define wall velocity components?	no
X-Component of Wall Translation	0
Y-Component of Wall Translation	0
Z-Component of Wall Translation	0
External Emissivity	1
External Radiation Temperature	300
Activate Reaction Mechanisms	no
Rotation Speed	0

```

X-Position of Rotation-Axis Origin      0
Y-Position of Rotation-Axis Origin      0
Z-Position of Rotation-Axis Origin      0
X-Component of Rotation-Axis Direction  0
Y-Component of Rotation-Axis Direction  0
Z-Component of Rotation-Axis Direction  1
X-component of shear stress              0
Y-component of shear stress              0
Z-component of shear stress              0
Surface tension gradient                 0
Reaction Mechanisms                     0
Specularity Coefficient                  0

```

wall_entree:047

```

Condition                               Value
-----
Wall Thickness                           0
Heat Generation Rate                     0
Material Name                            graphite-south-africa
Thermal BC Type                          3
Temperature                               300
Heat Flux                                0
Convective Heat Transfer Coefficient     0
Free Stream Temperature                   300
Enable shell conduction?                 no
Wall Motion                              0
Shear Boundary Condition                  0
Define wall motion relative to adjacent cell zone? yes
Apply a rotational velocity to this wall? no
Velocity Magnitude                       0
X-Component of Wall Translation           1
Y-Component of Wall Translation           0
Z-Component of Wall Translation           0
Define wall velocity components?         no
X-Component of Wall Translation           0
Y-Component of Wall Translation           0
Z-Component of Wall Translation           0
External Emissivity                      1
External Radiation Temperature            300
Activate Reaction Mechanisms             yes
                                           (0 0 0 0)
                                           (((constant . 0) (profile
)) ((constant . 0) (profile )) ((constant . 0) (profile
)))
Rotation Speed                           0
X-Position of Rotation-Axis Origin        0
Y-Position of Rotation-Axis Origin        0
Z-Position of Rotation-Axis Origin        0
X-Component of Rotation-Axis Direction    0
Y-Component of Rotation-Axis Direction    0
Z-Component of Rotation-Axis Direction    1
X-component of shear stress                0
Y-component of shear stress                0
Z-component of shear stress                0
Surface tension gradient                   0
Reaction Mechanisms                       0
Specularity Coefficient                   0

```

default-interior:048

```

Condition  Value
-----

```

default-interior:049

```

Condition  Value
-----

```

default-interior:050

Condition	Value
-----------	-------

default-interior:051

Condition	Value
-----------	-------

default-interior:052

Condition	Value
-----------	-------

default-interior:053

Condition	Value
-----------	-------

default-interior:054

Condition	Value
-----------	-------

default-interior:055

Condition	Value
-----------	-------

default-interior:056

Condition	Value
-----------	-------

default-interior:057

Condition	Value
-----------	-------

default-interior:058

Condition	Value
-----------	-------

Solver Controls

Equations

Equation	Solved
Flow	yes
h2o	yes
o2	yes
co	yes
co2	yes
Energy	yes

Numerics

Numeric	Enabled
Absolute Velocity Formulation	no

Relaxation

Variable	Relaxation Factor
Pressure	0.60000002
Density	0.40000001

(arrhenius 0.145 2.0785e+08 0) (mixing-rate 4 0.5) (use-third-body-efficiencies? . #f)
 (surface-reaction? . #t))

Mechanism		reaction-mechs	(mechanism-1
(reaction-type . all)	(reaction-list	reaction-3 reaction-2 reaction-1)	(site-info))
Density	kg/m3	ideal-gas	#f
Cp (Specific Heat)	j/kg-k	mixing-law	#f
Thermal Conductivity	w/m-k	ideal-gas-mixing-law	#f
Viscosity	kg/m-s	mass-weighted-mixing-law	#f
Mass Diffusivity	m2/s	kinetic-theory	#f
Thermal Diffusion Coefficient	kg/m-s	kinetic-theory	#f
Thermal Expansion Coefficient	1/k	constant	0

Material: (carbon-solid . boudouard) (fluid)

Property	Units	Method	Value(s)
Cp (Specific Heat)	j/kg-k	constant	1220
Thermal Conductivity	w/m-k	constant	0.045400001
Viscosity	kg/m-s	constant	1.72e-05
Molecular Weight	kg/kgmol	constant	12.01115
Standard State Enthalpy	j/kgmol	constant	-101.268
Standard State Entropy	j/kgmol-k	constant	5731.7471
Reference Temperature	c	constant	24.85
L-J Characteristic Length	angstrom	constant	2
L-J Energy Parameter	c	constant	-263.15
Degrees of Freedom		constant	0
Speed of Sound	m/s	none	#f

Material: (nitrogen . boudouard) (fluid)

Property	Units	Method	Value(s)
Cp (Specific Heat)	j/kg-k	constant	1040.67
Thermal Conductivity	w/m-k	constant	0.0242
Viscosity	kg/m-s	constant	1.663e-05
Molecular Weight	kg/kgmol	constant	28.013399
Standard State Enthalpy	j/kgmol	constant	0
Standard State Entropy	j/kgmol-k	constant	191494.78
Reference Temperature	c	constant	24.99999
L-J Characteristic Length	angstrom	constant	3.7490001
L-J Energy Parameter	c	constant	-193.35
Degrees of Freedom		constant	0
Speed of Sound	m/s	none	#f

Material: (carbon-dioxide . boudouard) (fluid)

Property	Units	Method	Value(s)
Cp (Specific Heat)	j/kg-k	constant	840.37
Thermal Conductivity	w/m-k	constant	0.0145
Viscosity	kg/m-s	constant	1.37e-05
Molecular Weight	kg/kgmol	constant	44.009949
Standard State Enthalpy	j/kgmol	constant	-3.9353235e+08
Standard State Entropy	j/kgmol-k	constant	213720.2
Reference Temperature	c	constant	24.99999
L-J Characteristic Length	angstrom	constant	3.941
L-J Energy Parameter	c	constant	-77.95
Degrees of Freedom		constant	0
Speed of Sound	m/s	none	#f

Material: (carbon-monoxide . boudouard) (fluid)

Property	Units	Method	Value(s)
Cp (Specific Heat)	j/kg-k	constant	1043
Thermal Conductivity	w/m-k	constant	0.025
Viscosity	kg/m-s	constant	1.75e-05
Molecular Weight	kg/kgmol	constant	28.01055
Standard State Enthalpy	j/kgmol	constant	-1.1053956e+08
Standard State Entropy	j/kgmol-k	constant	197531.64
Reference Temperature	c	constant	24.99999

L-J Characteristic Length	angstrom	constant	3.5899999
L-J Energy Parameter	c	constant	-185.15
Degrees of Freedom		constant	0
Speed of Sound	m/s	none	#f

Material: (oxygen . boudouard) (fluid)

Property	Units	Method	Value (s)
Cp (Specific Heat)	j/kg-k	constant	919.31
Thermal Conductivity	w/m-k	constant	0.024599999
Viscosity	kg/m-s	constant	1.919e-05
Molecular Weight	kg/kgmol	constant	31.9988
Standard State Enthalpy	j/kgmol	constant	0
Standard State Entropy	j/kgmol-k	constant	205026.86
Reference Temperature	c	constant	24.99999
L-J Characteristic Length	angstrom	constant	3.5409999
L-J Energy Parameter	c	constant	-185.15
Degrees of Freedom		constant	0
Speed of Sound	m/s	none	#f

Material: (water-vapor . boudouard) (fluid)

Property	Units	Method	Value (s)
Cp (Specific Heat)	j/kg-k	constant	2014
Thermal Conductivity	w/m-k	constant	0.0261
Viscosity	kg/m-s	constant	1.34e-05
Molecular Weight	kg/kgmol	constant	18.01534
Standard State Enthalpy	j/kgmol	constant	-2.418379e+08
Standard State Entropy	j/kgmol-k	constant	188696.44
Reference Temperature	c	constant	25
L-J Characteristic Length	angstrom	constant	2.605
L-J Energy Parameter	c	constant	299.25
Degrees of Freedom		constant	0
Speed of Sound	m/s	none	#f

Material: (carbon-solid . mixture-template) (fluid)

Property	Units	Method	Value (s)
Cp (Specific Heat)	j/kg-k	constant	1220
Thermal Conductivity	w/m-k	constant	0.045400001
Viscosity	kg/m-s	constant	1.72e-05
Molecular Weight	kg/kgmol	constant	12.01115
Standard State Enthalpy	j/kgmol	constant	-101.268
Standard State Entropy	j/kgmol-k	constant	5731.7471
Reference Temperature	c	constant	24.85
L-J Characteristic Length	angstrom	constant	2
L-J Energy Parameter	c	constant	-263
Degrees of Freedom		constant	0
Speed of Sound	m/s	none	#f

Material: (carbon-dioxide . mixture-template) (fluid)

Property	Units	Method	Value (s)
Cp (Specific Heat)	j/kg-k	constant	840.37
Thermal Conductivity	w/m-k	constant	0.0145
Viscosity	kg/m-s	constant	1.37e-05
Molecular Weight	kg/kgmol	constant	44.009949
Standard State Enthalpy	j/kgmol	constant	-3.9353235e+08
Standard State Entropy	j/kgmol-k	constant	213720.2
Reference Temperature	c	constant	24.99999
L-J Characteristic Length	angstrom	constant	3.8970001
L-J Energy Parameter	c	constant	-60.15
Degrees of Freedom		constant	0
Speed of Sound	m/s	none	#f

Material: (carbon-monoxide . mixture-template) (fluid)

Property	Units	Method	Value (s)
Cp (Specific Heat)	j/kg-k	constant	1043
Thermal Conductivity	w/m-k	constant	0.025
Viscosity	kg/m-s	constant	1.75e-05
Molecular Weight	kg/kgmol	constant	28.01055
Standard State Enthalpy	j/kgmol	constant	-1.1053956e+08
Standard State Entropy	j/kgmol-k	constant	197531.64
Reference Temperature	c	constant	24.99999
L-J Characteristic Length	angstrom	constant	3.5899999
L-J Energy Parameter	c	constant	-185.15
Degrees of Freedom		constant	0
Speed of Sound	m/s	none	#f

Material: carbon-dioxide (fluid)

Property	Units	Method	Value (s)
Density	kg/m3	constant	1.7878
Cp (Specific Heat)	j/kg-k	constant	840.37
Thermal Conductivity	w/m-k	constant	0.0145
Viscosity	kg/m-s	constant	1.37e-05
Molecular Weight	kg/kgmol	constant	44.00995
Standard State Enthalpy	j/kgmol	constant	-3.9353235e+08
Standard State Entropy	j/kgmol-k	constant	213720.2
Reference Temperature	c	constant	25
L-J Characteristic Length	angstrom	constant	3.941
L-J Energy Parameter	c	constant	-77.95
Thermal Expansion Coefficient	1/k	constant	0
Degrees of Freedom		constant	0
Speed of Sound	m/s	none	#f

Material: carbon-monoxide (fluid)

Property	Units	Method	Value (s)
Density	kg/m3	constant	1.1233
Cp (Specific Heat)	j/kg-k	constant	1043
Thermal Conductivity	w/m-k	constant	0.025
Viscosity	kg/m-s	constant	1.75e-05
Molecular Weight	kg/kgmol	constant	28.01055
Standard State Enthalpy	j/kgmol	constant	-1.1053956e+08
Standard State Entropy	j/kgmol-k	constant	197531.64
Reference Temperature	c	constant	25
L-J Characteristic Length	angstrom	constant	0
L-J Energy Parameter	c	constant	-273.15
Thermal Expansion Coefficient	1/k	constant	0
Degrees of Freedom		constant	0
Speed of Sound	m/s	none	#f

Material: carbon-solid (fluid)

Property	Units	Method	Value (s)
Density	kg/m3	constant	2000
Cp (Specific Heat)	j/kg-k	constant	1220
Thermal Conductivity	w/m-k	constant	0.0454
Viscosity	kg/m-s	constant	1.72e-05
Molecular Weight	kg/kgmol	constant	12.01115
Standard State Enthalpy	j/kgmol	constant	-101.268
Standard State Entropy	j/kgmol-k	constant	5731.747
Reference Temperature	c	constant	24.85
L-J Characteristic Length	angstrom	constant	0
L-J Energy Parameter	c	constant	-273.15
Thermal Expansion Coefficient	1/k	constant	0
Degrees of Freedom		constant	0
Speed of Sound	m/s	none	#f

Material: mixture-template (mixture)

Property	Units	Method	Value (s)
----------	-------	--------	-----------

```
-----  
-----  
-----  
-----  
-----  
-----  
-----  
-----  
-----  
-----  
-----  
  
Mixture Species                        names                  ((h2o o2 co co2  
n2) (c<s>) ( ))  
Reaction                               finite-rate           ((reaction-1  
((o2 0.76999998 1 1) (c<s> 1 0 1)) ((co 0.46000001 0 1) (co2 0.54000002 0 1)) ((h2o 0 1)  
(n2 0 1)) (stoichiometry 0.76999998o2 + 1c<s> --> 0.46000001co + 0.54000002co2)  
(arrhenius 3.6e+12 2.09e+08 0) (mixing-rate 4 0.5) (use-third-body-efficiencies? . #f)  
(surface-reaction? . #t)) (reaction-2 ((o2 0.5 0.25 1) (co 1 1 1)) ((co2 1 0 1) (h2o 0  
0.5 1)) ((n2 0 1)) (stoichiometry 0.5o2 + 1co --> 1co2 + 0h2o) (arrhenius 2.24e+12  
1.674e+08 0) (mixing-rate 4 0.5) (use-third-body-efficiencies? . #f)) (reaction-3 ((co2 1  
1 1)) ((co 1 0 1) (o2 0.5 0 1)) ((h2o 0 1) (n2 0 1)) (stoichiometry 1co2 --> 1co + 0.5o2)  
(arrhenius 45000000 1.674e+08 0) (mixing-rate 4 0.5) (use-third-body-efficiencies? . #f))  
(reaction-4 ((c<s> 1 0 1) (co2 1 1 1)) ((co 2 0 1)) ((h2o 0 1) (o2 0 1) (n2 0 1))  
(stoichiometry 1c<s> + 1co2 --> 2co) (arrhenius 0.145 2e+08 0) (mixing-rate 4 0.5) (use-  
third-body-efficiencies? . #f) (surface-reaction? . #t))  
Mechanism                               reaction-mechs        ((mechanism-1  
(reaction-type . all) (reaction-list reaction-4 reaction-3 reaction-2 reaction-1) (site-  
info)))  
Density                                kg/m3                ideal-gas            #f  
Cp (Specific Heat)                     j/kg-k              mixing-law           #f  
Thermal Conductivity                    w/m-k               ideal-gas-mixing-law #f  
Viscosity                               kg/m-s              mass-weighted-mixing-law #f  
Mass Diffusivity                        m2/s                kinetic-theory       #f  
Thermal Diffusion Coefficient           kg/m-s              kinetic-theory       #f  
Thermal Expansion Coefficient            1/k                  constant              0
```

Material: (nitrogen . mixture-template) (fluid)

Property	Units	Method	Value(s)
Cp (Specific Heat)	j/kg-k	constant	1040.67
Thermal Conductivity	w/m-k	constant	0.0242
Viscosity	kg/m-s	constant	1.663e-05
Molecular Weight	kg/kgmol	constant	28.013399
Standard State Enthalpy	j/kgmol	constant	0
Standard State Entropy	j/kgmol-k	constant	191494.78
Reference Temperature	c	constant	24.99999
L-J Characteristic Length	angstrom	constant	3.7490001
L-J Energy Parameter	c	constant	-193.35
Degrees of Freedom		constant	0
Speed of Sound	m/s	none	#f

Material: nitrogen (fluid)

Property	Units	Method	Value(s)
Density	kg/m3	constant	1.138
Cp (Specific Heat)	j/kg-k	constant	1040.67
Thermal Conductivity	w/m-k	constant	0.0242
Viscosity	kg/m-s	constant	1.663e-05
Molecular Weight	kg/kgmol	constant	28.0134
Standard State Enthalpy	j/kgmol	constant	0
Standard State Entropy	j/kgmol-k	constant	191494.78
Reference Temperature	c	constant	25
L-J Characteristic Length	angstrom	constant	3.621
L-J Energy Parameter	c	constant	-175.62
Thermal Expansion Coefficient	1/k	constant	0
Degrees of Freedom		constant	0
Speed of Sound	m/s	none	#f

Material: (oxygen . mixture-template) (fluid)

Property	Units	Method	Value (s)
Cp (Specific Heat)	j/kg-k	constant	919.31
Thermal Conductivity	w/m-k	constant	0.024599999
Viscosity	kg/m-s	constant	1.919e-05
Molecular Weight	kg/kgmol	constant	31.9988
Standard State Enthalpy	j/kgmol	constant	0
Standard State Entropy	j/kgmol-k	constant	205026.86
Reference Temperature	c	constant	24.99999
L-J Characteristic Length	angstrom	constant	3.5409999
L-J Energy Parameter	c	constant	-185.15
Degrees of Freedom		constant	0
Speed of Sound	m/s	none	#f

Material: oxygen (fluid)

Property	Units	Method	Value (s)
Density	kg/m3	constant	1.2999
Cp (Specific Heat)	j/kg-k	constant	919.31
Thermal Conductivity	w/m-k	constant	0.0246
Viscosity	kg/m-s	constant	1.919e-05
Molecular Weight	kg/kgmol	constant	31.9988
Standard State Enthalpy	j/kgmol	constant	0
Standard State Entropy	j/kgmol-k	constant	205026.86
Reference Temperature	c	constant	25
L-J Characteristic Length	angstrom	constant	3.458
L-J Energy Parameter	c	constant	-165.75
Thermal Expansion Coefficient	1/k	constant	0
Degrees of Freedom		constant	0
Speed of Sound	m/s	none	#f

Material: (water-vapor . mixture-template) (fluid)

Property	Units	Method	Value (s)
Cp (Specific Heat)	j/kg-k	constant	2014
Thermal Conductivity	w/m-k	constant	0.0261
Viscosity	kg/m-s	constant	1.34e-05
Molecular Weight	kg/kgmol	constant	18.01534
Standard State Enthalpy	j/kgmol	constant	-2.418379e+08
Standard State Entropy	j/kgmol-k	constant	188696.44
Reference Temperature	c	constant	25
L-J Characteristic Length	angstrom	constant	2.605
L-J Energy Parameter	c	constant	299.25
Degrees of Freedom		constant	0
Speed of Sound	m/s	none	#f

Material: water-vapor (fluid)

Property	Units	Method	Value (s)
Density	kg/m3	constant	0.5542
Cp (Specific Heat)	j/kg-k	constant	2014
Thermal Conductivity	w/m-k	constant	0.0261
Viscosity	kg/m-s	constant	1.34e-05
Molecular Weight	kg/kgmol	constant	18.01534
Standard State Enthalpy	j/kgmol	constant	-2.418379e+08
Standard State Entropy	j/kgmol-k	constant	188696.44
Reference Temperature	c	constant	25
L-J Characteristic Length	angstrom	constant	2.605
L-J Energy Parameter	c	constant	299.25
Thermal Expansion Coefficient	1/k	constant	0
Degrees of Freedom		constant	0
Speed of Sound	m/s	none	#f

Material: graphite-south-africa (solid)

Property	Units	Method	Value (s)
----------	-------	--------	-----------

```

-----
Density          kg/m3      constant  2240
Cp (Specific Heat)  j/kg-k    constant  710
Thermal Conductivity w/m-k     constant  168

```

Material: air (fluid)

```

Property          Units      Method      Value(s)
-----
-----
Density          kg/m3      ideal-gas   #f
Cp (Specific Heat)  j/kg-k    polynomial  (-0.15 1005) (199.85 1026)
(399.85 1068) (599.85 1114) (799.85 1156) (1099.85 1197)
Thermal Conductivity w/m-k     polynomial  (-0.15 0.0244) (199.85
0.039299998) (399.85 0.052099999) (599.85 0.062199999) (799.85 0.071800001) (1099.85
0.085000001)
Viscosity        kg/m-s     polynomial  (-0.15 1.7e-05) (199.85
2.6e-05) (399.85 3.3e-05) (599.85 3.9099999e-05) (799.85 4.4299999e-05) (1099.85
5.1200001e-05)
Molecular Weight  kg/kgmol   constant    28.966
Standard State Enthalpy  j/kgmol    constant    0
Standard State Entropy  j/kgmol-k  constant    0
Reference Temperature  c           constant    25
L-J Characteristic Length  angstrom   constant    3.711
L-J Energy Parameter  c           constant    -194.55
Thermal Expansion Coefficient  1/k        constant    0
Degrees of Freedom  constant    0
Speed of Sound      m/s        none        #f

```

Material: aluminum (solid)

```

Property          Units      Method      Value(s)
-----
Density          kg/m3      constant    2719
Cp (Specific Heat)  j/kg-k    constant    871
Thermal Conductivity w/m-k     constant    202.4

```

APPENDIX 2: Return Duct Model

FLUENT

Version: 3d, dp, segregated, spe, lam, unsteady (3d, double precision, segregated, species, laminar, unsteady)

Release: 6.2.16

Title:

Models

Model	Settings
Space	3D
Time	Unsteady, 1st-Order Implicit
Viscous	Laminar
Heat Transfer	Enabled
Solidification and Melting	Disabled
Radiation	None
Species Transport	Reacting (6 species)
Coupled Dispersed Phase	Disabled
Pollutants	Disabled
Soot	Disabled

Boundary Conditions

Zones

name	id	type
outside	2	fluid
inlet2	3	fluid
outlet1	4	fluid
inlet1	5	fluid
outlet	6	fluid
chimney	7	fluid
return	8	fluid
entree_reflecttor	9	fluid
entree_bas	10	fluid
solid.47	11	solid
peb2	12	fluid
intpeb	13	fluid
peb1	14	fluid
ref2	15	fluid
interref	16	fluid
ref1	17	fluid
porous_jump.67	24	interior
porous_jump.63	25	interior
wallerreur-shadow	84	wall
wall-shadow	83	wall
wall_entree:061-shadow	82	wall
wall	18	wall
weallout	19	wall
walloutlet1	20	wall
wallerreur	21	wall
wall_outlet	22	wall
wall_return	23	wall
symmetry	26	symmetry
interior_	27	interior
wall_chimey	28	wall
wall_peb2	29	wall
wall_interpeb	30	wall
wall_peb1	31	wall
wall_ref2	32	wall
wall_interef	33	wall

wall_ref1	34	wall
wall_libre_1	35	wall
wall_ref_bas	36	wall
wall_entree	37	wall
wall_inlet	38	wall
default-interior	40	interior
symmetry:001	1	symmetry
symmetry:039	39	symmetry
symmetry:041	41	symmetry
symmetry:042	42	symmetry
symmetry:043	43	symmetry
symmetry:044	44	symmetry
symmetry:045	45	symmetry
symmetry:046	46	symmetry
symmetry:047	47	symmetry
symmetry:048	48	symmetry
symmetry:049	49	symmetry
symmetry:050	50	symmetry
interior_:051	51	interior
interior_:052	52	interior
interior_:053	53	interior
interior_:054	54	interior
interior_:055	55	interior
interior_:056	56	interior
interior_:057	57	interior
interior_:058	58	interior
interior_:059	59	interior
interior_:060	60	interior
wall_entree:061	61	wall
wall_entree:062	62	wall
wall_inlet:063	63	wall
default-interior:064	64	interior
default-interior:065	65	interior
default-interior:066	66	interior
default-interior:067	67	interior
default-interior:068	68	interior
default-interior:069	69	interior
default-interior:070	70	interior
default-interior:071	71	interior
default-interior:072	72	interior
default-interior:073	73	interior
default-interior:074	74	interior
default-interior:075	75	interior
default-interior:076	76	interior
default-interior:077	77	interior
default-interior:078	78	interior
default-interior:079	79	interior
default-interior:080	80	interior

Boundary Conditions

outside

Condition	Value

Material Name	mixture-template
Specify source terms?	no
Source Terms	((mass (inactive . #f) (constant . 0) (profile)) (x-momentum (inactive . #f) (constant . 0) (profile)) (y-momentum (inactive . #f) (constant . 0) (profile)) (z-momentum (inactive . #f) (constant . 0) (profile)) (species-0 (inactive . #f) (constant . 0) (profile)) (energy (inactive . #f) (constant . 0) (profile)))
Specify fixed values?	no
Local Coordinate System for Fixed Velocities	no
Fixed Values	((x-velocity (inactive . #f) (constant . 0) (profile)) (y-velocity (inactive . #f) (constant . 0) (profile)) (z-

```

velocity (inactive . #f) (constant . 0) (profile ) (species-0 (inactive . #f) (constant
. 0) (profile )) (temperature (inactive . #f) (constant . 0) (profile )))
Motion Type 0
X-Velocity Of Zone 0
Y-Velocity Of Zone 0
Z-Velocity Of Zone 0
Rotation speed 0
X-Origin of Rotation-Axis 0
Y-Origin of Rotation-Axis 0
Z-Origin of Rotation-Axis 0
X-Component of Rotation-Axis 0
Y-Component of Rotation-Axis 0
Z-Component of Rotation-Axis 1
Deactivated Thread no
Porous zone? no
Conical porous zone? no
X-Component of Direction-1 Vector 1
Y-Component of Direction-1 Vector 0
Z-Component of Direction-1 Vector 0
X-Component of Direction-2 Vector 0
Y-Component of Direction-2 Vector 1
Z-Component of Direction-2 Vector 0
X-Coordinate of Point on Cone Axis 1
Y-Coordinate of Point on Cone Axis 0
Z-Coordinate of Point on Cone Axis 0
Half Angle of Cone Relative to its Axis 0
Direction-1 Viscous Resistance 0
Direction-2 Viscous Resistance 0
Direction-3 Viscous Resistance 0
Direction-1 Inertial Resistance 0
Direction-2 Inertial Resistance 0
Direction-3 Inertial Resistance 0
C0 Coefficient for Power-Law 0
C1 Coefficient for Power-Law 0
Porosity 1
Solid Material Name aluminum
Reaction Mechanism 0
Activate reaction mechanisms? yes
Surface-Volume-Ratio 0

```

inlet2

Condition	Value
Material Name	mixture-template
Specify source terms?	no
Source Terms	((mass (inactive . #f) (constant . 0) (profile)) (x-momentum (inactive . #f) (constant . 0) (profile)) (y-momentum (inactive . #f) (constant . 0) (profile)) (z-momentum (inactive . #f) (constant . 0) (profile)) (species-0 (inactive . #f) (constant . 0) (profile)) (energy (inactive . #f) (constant . 0) (profile)))
Specify fixed values?	no
Local Coordinate System for Fixed Velocities	no
Fixed Values	((x-velocity (inactive . #f) (constant . 0) (profile)) (y-velocity (inactive . #f) (constant . 0) (profile)) (z-velocity (inactive . #f) (constant . 0) (profile)) (species-0 (inactive . #f) (constant . 0) (profile)) (temperature (inactive . #f) (constant . 0) (profile)))
Motion Type	0
X-Velocity Of Zone	0
Y-Velocity Of Zone	0
Z-Velocity Of Zone	0
Rotation speed	0
X-Origin of Rotation-Axis	0
Y-Origin of Rotation-Axis	0
Z-Origin of Rotation-Axis	0
X-Component of Rotation-Axis	0
Y-Component of Rotation-Axis	0

Z-Component of Rotation-Axis	1
Deactivated Thread	no
Porous zone?	no
Conical porous zone?	no
X-Component of Direction-1 Vector	1
Y-Component of Direction-1 Vector	0
Z-Component of Direction-1 Vector	0
X-Component of Direction-2 Vector	0
Y-Component of Direction-2 Vector	1
Z-Component of Direction-2 Vector	0
X-Coordinate of Point on Cone Axis	1
Y-Coordinate of Point on Cone Axis	0
Z-Coordinate of Point on Cone Axis	0
Half Angle of Cone Relative to its Axis	0
Direction-1 Viscous Resistance	0
Direction-2 Viscous Resistance	0
Direction-3 Viscous Resistance	0
Direction-1 Inertial Resistance	0
Direction-2 Inertial Resistance	0
Direction-3 Inertial Resistance	0
C0 Coefficient for Power-Law	0
C1 Coefficient for Power-Law	0
Porosity	1
Solid Material Name	aluminum
Reaction Mechanism	0
Activate reaction mechanisms?	yes
Surface-Volume-Ratio	0

outlet1

Condition	Value
-----	-----
Material Name	mixture-template
Specify source terms?	no
Source Terms	()
Specify fixed values?	no
Local Coordinate System for Fixed Velocities	no
Fixed Values	()
Motion Type	0
X-Velocity Of Zone	0
Y-Velocity Of Zone	0
Z-Velocity Of Zone	0
Rotation speed	0
X-Origin of Rotation-Axis	0
Y-Origin of Rotation-Axis	0
Z-Origin of Rotation-Axis	0
X-Component of Rotation-Axis	0
Y-Component of Rotation-Axis	0
Z-Component of Rotation-Axis	1
Deactivated Thread	no
Porous zone?	no
Conical porous zone?	no
X-Component of Direction-1 Vector	1
Y-Component of Direction-1 Vector	0
Z-Component of Direction-1 Vector	0
X-Component of Direction-2 Vector	0
Y-Component of Direction-2 Vector	1
Z-Component of Direction-2 Vector	0
X-Coordinate of Point on Cone Axis	1
Y-Coordinate of Point on Cone Axis	0
Z-Coordinate of Point on Cone Axis	0
Half Angle of Cone Relative to its Axis	0
Direction-1 Viscous Resistance	0
Direction-2 Viscous Resistance	0
Direction-3 Viscous Resistance	0
Direction-1 Inertial Resistance	0
Direction-2 Inertial Resistance	0
Direction-3 Inertial Resistance	0
C0 Coefficient for Power-Law	0
C1 Coefficient for Power-Law	0
Porosity	1

Solid Material Name	aluminum
Reaction Mechanism	0
Activate reaction mechanisms?	yes
Surface-Volume-Ratio	0

inlet1

Condition	Value
-----	-----
-----	-----
-----	-----

Material Name	mixture-template
Specify source terms?	no
Source Terms	((mass (inactive . #f) (constant . 0) (profile)) (x-momentum (inactive . #f) (constant . 0) (profile)) (y-momentum (inactive . #f) (constant . 0) (profile)) (z-momentum (inactive . #f) (constant . 0) (profile)) (species-0 (inactive . #f) (constant . 0) (profile)) (energy (inactive . #f) (constant . 0) (profile)))
Specify fixed values?	no
Local Coordinate System for Fixed Velocities	no
Fixed Values	((x-velocity (inactive . #f) (constant . 0) (profile)) (y-velocity (inactive . #f) (constant . 0) (profile)) (z-velocity (inactive . #f) (constant . 0) (profile)) (species-0 (inactive . #f) (constant . 0) (profile)) (temperature (inactive . #f) (constant . 0) (profile)))
Motion Type	0
X-Velocity Of Zone	0
Y-Velocity Of Zone	0
Z-Velocity Of Zone	0
Rotation speed	0
X-Origin of Rotation-Axis	0
Y-Origin of Rotation-Axis	0
Z-Origin of Rotation-Axis	0
X-Component of Rotation-Axis	0
Y-Component of Rotation-Axis	0
Z-Component of Rotation-Axis	1
Deactivated Thread	no
Porous zone?	no
Conical porous zone?	no
X-Component of Direction-1 Vector	1
Y-Component of Direction-1 Vector	0
Z-Component of Direction-1 Vector	0
X-Component of Direction-2 Vector	0
Y-Component of Direction-2 Vector	1
Z-Component of Direction-2 Vector	0
X-Coordinate of Point on Cone Axis	1
Y-Coordinate of Point on Cone Axis	0
Z-Coordinate of Point on Cone Axis	0
Half Angle of Cone Relative to its Axis	0
Direction-1 Viscous Resistance	0
Direction-2 Viscous Resistance	0
Direction-3 Viscous Resistance	0
Direction-1 Inertial Resistance	0
Direction-2 Inertial Resistance	0
Direction-3 Inertial Resistance	0
C0 Coefficient for Power-Law	0
C1 Coefficient for Power-Law	0
Porosity	1
Solid Material Name	aluminum
Reaction Mechanism	0
Activate reaction mechanisms?	yes
Surface-Volume-Ratio	0

outlet

Condition	Value
-----	-----
Material Name	mixture-template
Specify source terms?	no
Source Terms	()

Specify fixed values?	no
Local Coordinate System for Fixed Velocities	no
Fixed Values	()
Motion Type	0
X-Velocity Of Zone	0
Y-Velocity Of Zone	0
Z-Velocity Of Zone	0
Rotation speed	0
X-Origin of Rotation-Axis	0
Y-Origin of Rotation-Axis	0
Z-Origin of Rotation-Axis	0
X-Component of Rotation-Axis	0
Y-Component of Rotation-Axis	0
Z-Component of Rotation-Axis	1
Deactivated Thread	no
Porous zone?	no
Conical porous zone?	no
X-Component of Direction-1 Vector	1
Y-Component of Direction-1 Vector	0
Z-Component of Direction-1 Vector	0
X-Component of Direction-2 Vector	0
Y-Component of Direction-2 Vector	1
Z-Component of Direction-2 Vector	0
X-Coordinate of Point on Cone Axis	1
Y-Coordinate of Point on Cone Axis	0
Z-Coordinate of Point on Cone Axis	0
Half Angle of Cone Relative to its Axis	0
Direction-1 Viscous Resistance	0
Direction-2 Viscous Resistance	0
Direction-3 Viscous Resistance	0
Direction-1 Inertial Resistance	0
Direction-2 Inertial Resistance	0
Direction-3 Inertial Resistance	0
C0 Coefficient for Power-Law	0
C1 Coefficient for Power-Law	0
Porosity	1
Solid Material Name	aluminum
Reaction Mechanism	0
Activate reaction mechanisms?	yes
Surface-Volume-Ratio	0

chimney

Condition	Value
Material Name	mixture-template
Specify source terms?	no
Source Terms	()
Specify fixed values?	no
Local Coordinate System for Fixed Velocities	no
Fixed Values	()
Motion Type	0
X-Velocity Of Zone	0
Y-Velocity Of Zone	0
Z-Velocity Of Zone	0
Rotation speed	0
X-Origin of Rotation-Axis	0
Y-Origin of Rotation-Axis	0
Z-Origin of Rotation-Axis	0
X-Component of Rotation-Axis	0
Y-Component of Rotation-Axis	0
Z-Component of Rotation-Axis	1
Deactivated Thread	no
Porous zone?	no
Conical porous zone?	no
X-Component of Direction-1 Vector	1
Y-Component of Direction-1 Vector	0
Z-Component of Direction-1 Vector	0
X-Component of Direction-2 Vector	0
Y-Component of Direction-2 Vector	1
Z-Component of Direction-2 Vector	0

X-Coordinate of Point on Cone Axis	1
Y-Coordinate of Point on Cone Axis	0
Z-Coordinate of Point on Cone Axis	0
Half Angle of Cone Relative to its Axis	0
Direction-1 Viscous Resistance	0
Direction-2 Viscous Resistance	0
Direction-3 Viscous Resistance	0
Direction-1 Inertial Resistance	0
Direction-2 Inertial Resistance	0
Direction-3 Inertial Resistance	0
C0 Coefficient for Power-Law	0
C1 Coefficient for Power-Law	0
Porosity	1
Solid Material Name	aluminum
Reaction Mechanism	0
Activate reaction mechanisms?	yes
Surface-Volume-Ratio	0

return

Condition	Value
-----	-----
Material Name	mixture-template
Specify source terms?	no
Source Terms	()
Specify fixed values?	no
Local Coordinate System for Fixed Velocities	no
Fixed Values	()
Motion Type	0
X-Velocity Of Zone	0
Y-Velocity Of Zone	0
Z-Velocity Of Zone	0
Rotation speed	0
X-Origin of Rotation-Axis	0
Y-Origin of Rotation-Axis	0
Z-Origin of Rotation-Axis	0
X-Component of Rotation-Axis	0
Y-Component of Rotation-Axis	0
Z-Component of Rotation-Axis	1
Deactivated Thread	no
Porous zone?	no
Conical porous zone?	no
X-Component of Direction-1 Vector	1
Y-Component of Direction-1 Vector	0
Z-Component of Direction-1 Vector	0
X-Component of Direction-2 Vector	0
Y-Component of Direction-2 Vector	1
Z-Component of Direction-2 Vector	0
X-Coordinate of Point on Cone Axis	1
Y-Coordinate of Point on Cone Axis	0
Z-Coordinate of Point on Cone Axis	0
Half Angle of Cone Relative to its Axis	0
Direction-1 Viscous Resistance	0
Direction-2 Viscous Resistance	0
Direction-3 Viscous Resistance	0
Direction-1 Inertial Resistance	0
Direction-2 Inertial Resistance	0
Direction-3 Inertial Resistance	0
C0 Coefficient for Power-Law	0
C1 Coefficient for Power-Law	0
Porosity	1
Solid Material Name	aluminum
Reaction Mechanism	0
Activate reaction mechanisms?	yes
Surface-Volume-Ratio	0

entree_reflektor

Condition	Value
-----	-----
Material Name	mixture-template

Specify source terms?	no
Source Terms	()
Specify fixed values?	no
Local Coordinate System for Fixed Velocities	no
Fixed Values	()
Motion Type	0
X-Velocity Of Zone	0
Y-Velocity Of Zone	0
Z-Velocity Of Zone	0
Rotation speed	0
X-Origin of Rotation-Axis	0
Y-Origin of Rotation-Axis	0
Z-Origin of Rotation-Axis	0
X-Component of Rotation-Axis	0
Y-Component of Rotation-Axis	0
Z-Component of Rotation-Axis	1
Deactivated Thread	no
Porous zone?	no
Conical porous zone?	no
X-Component of Direction-1 Vector	1
Y-Component of Direction-1 Vector	0
Z-Component of Direction-1 Vector	0
X-Component of Direction-2 Vector	0
Y-Component of Direction-2 Vector	1
Z-Component of Direction-2 Vector	0
X-Coordinate of Point on Cone Axis	1
Y-Coordinate of Point on Cone Axis	0
Z-Coordinate of Point on Cone Axis	0
Half Angle of Cone Relative to its Axis	0
Direction-1 Viscous Resistance	0
Direction-2 Viscous Resistance	0
Direction-3 Viscous Resistance	0
Direction-1 Inertial Resistance	0
Direction-2 Inertial Resistance	0
Direction-3 Inertial Resistance	0
C0 Coefficient for Power-Law	0
C1 Coefficient for Power-Law	0
Porosity	1
Solid Material Name	aluminum
Reaction Mechanism	0
Activate reaction mechanisms?	yes
Surface-Volume-Ratio	0

entree_bas

Condition	Value
-----	-----
Material Name	mixture-template
Specify source terms?	no
Source Terms	()
Specify fixed values?	no
Local Coordinate System for Fixed Velocities	no
Fixed Values	()
Motion Type	0
X-Velocity Of Zone	0
Y-Velocity Of Zone	0
Z-Velocity Of Zone	0
Rotation speed	0
X-Origin of Rotation-Axis	0
Y-Origin of Rotation-Axis	0
Z-Origin of Rotation-Axis	0
X-Component of Rotation-Axis	0
Y-Component of Rotation-Axis	0
Z-Component of Rotation-Axis	1
Deactivated Thread	no
Porous zone?	no
Conical porous zone?	no
X-Component of Direction-1 Vector	1
Y-Component of Direction-1 Vector	0
Z-Component of Direction-1 Vector	0
X-Component of Direction-2 Vector	0

```

Y-Component of Direction-2 Vector      1
Z-Component of Direction-2 Vector      0
X-Coordinate of Point on Cone Axis     1
Y-Coordinate of Point on Cone Axis     0
Z-Coordinate of Point on Cone Axis     0
Half Angle of Cone Relative to its Axis 0
Direction-1 Viscous Resistance         0
Direction-2 Viscous Resistance         0
Direction-3 Viscous Resistance         0
Direction-1 Inertial Resistance        0
Direction-2 Inertial Resistance        0
Direction-3 Inertial Resistance        0
C0 Coefficient for Power-Law          0
C1 Coefficient for Power-Law          0
Porosity                               1
Solid Material Name                    aluminum
Reaction Mechanism                     0
Activate reaction mechanisms?          yes
Surface-Volume-Ratio                   0

```

solid.47

```

Condition                               Value
-----
Material Name                           aluminum
Specify source terms?                   no
Source Terms                            ()
Specify fixed values?                   no
Fixed Values                            ()
Motion Type                             0
X-Velocity Of Zone                     0
Y-Velocity Of Zone                     0
Z-Velocity Of Zone                     0
Rotation speed                          0
X-Origin of Rotation-Axis               0
Y-Origin of Rotation-Axis               0
Z-Origin of Rotation-Axis               0
X-Component of Rotation-Axis            0
Y-Component of Rotation-Axis            0
Z-Component of Rotation-Axis            1
Deactivated Thread                       no

```

peb2

```

Condition                               Value
-----
Material Name                           mixture-template
Specify source terms?                   no
Source Terms                            ((mass (inactive . #f) (constant
. 0) (profile )) (x-momentum (inactive . #f) (constant . 0) (profile )) (y-momentum
(inactive . #f) (constant . 0) (profile )) (z-momentum (inactive . #f) (constant . 0)
(profile )) (species-0 (inactive . #f) (constant . 0) (profile )) (species-1 (inactive
. #f) (constant . 0) (profile )) (species-2 (inactive . #f) (constant . 0) (profile ))
(species-3 (inactive . #f) (constant . 0) (profile )) (species-4 (inactive . #f)
(constant . 0) (profile )) (energy (inactive . #f) (constant . 0) (profile )))
Specify fixed values?                   no
Local Coordinate System for Fixed Velocities no
Fixed Values                            ((x-velocity (inactive . #f)
(constant . 0) (profile )) (y-velocity (inactive . #f) (constant . 0) (profile )) (z-
velocity (inactive . #f) (constant . 0) (profile )) (species-0 (inactive . #f) (constant
. 0) (profile )) (species-1 (inactive . #f) (constant . 0) (profile )) (species-2
(inactive . #f) (constant . 0) (profile )) (species-3 (inactive . #f) (constant . 0)
(profile )) (species-4 (inactive . #f) (constant . 0) (profile )) (temperature
(inactive . #f) (constant . 0) (profile )))
Motion Type                             0

```

X-Velocity Of Zone	0
Y-Velocity Of Zone	0
Z-Velocity Of Zone	0
Rotation speed	0
X-Origin of Rotation-Axis	0
Y-Origin of Rotation-Axis	0
Z-Origin of Rotation-Axis	0
X-Component of Rotation-Axis	0
Y-Component of Rotation-Axis	0
Z-Component of Rotation-Axis	1
Deactivated Thread	no
Porous zone?	yes
Conical porous zone?	no
X-Component of Direction-1 Vector	1
Y-Component of Direction-1 Vector	0
Z-Component of Direction-1 Vector	0
X-Component of Direction-2 Vector	0
Y-Component of Direction-2 Vector	1
Z-Component of Direction-2 Vector	0
X-Coordinate of Point on Cone Axis	1
Y-Coordinate of Point on Cone Axis	0
Z-Coordinate of Point on Cone Axis	0
Half Angle of Cone Relative to its Axis	0
Direction-1 Viscous Resistance	0
Direction-2 Viscous Resistance	0
Direction-3 Viscous Resistance	0
Direction-1 Inertial Resistance	0
Direction-2 Inertial Resistance	0
Direction-3 Inertial Resistance	0
C0 Coefficient for Power-Law	341
C1 Coefficient for Power-Law	1.6107
Porosity	0.39500001
Solid Material Name	aluminum
Reaction Mechanism	0
Activate reaction mechanisms?	no
Surface-Volume-Ratio	0

intpeb

Condition	Value
-----	-----
Material Name	mixture-template
Specify source terms?	no
Source Terms	()
Specify fixed values?	no
Local Coordinate System for Fixed Velocities	no
Fixed Values	()
Motion Type	0
X-Velocity Of Zone	0
Y-Velocity Of Zone	0
Z-Velocity Of Zone	0
Rotation speed	0
X-Origin of Rotation-Axis	0
Y-Origin of Rotation-Axis	0
Z-Origin of Rotation-Axis	0
X-Component of Rotation-Axis	0
Y-Component of Rotation-Axis	0
Z-Component of Rotation-Axis	1
Deactivated Thread	no
Porous zone?	no
Conical porous zone?	no
X-Component of Direction-1 Vector	1
Y-Component of Direction-1 Vector	0
Z-Component of Direction-1 Vector	0
X-Component of Direction-2 Vector	0
Y-Component of Direction-2 Vector	1
Z-Component of Direction-2 Vector	0
X-Coordinate of Point on Cone Axis	1
Y-Coordinate of Point on Cone Axis	0
Z-Coordinate of Point on Cone Axis	0
Half Angle of Cone Relative to its Axis	0

```

Direction-1 Viscous Resistance      0
Direction-2 Viscous Resistance      0
Direction-3 Viscous Resistance      0
Direction-1 Inertial Resistance     0
Direction-2 Inertial Resistance     0
Direction-3 Inertial Resistance     0
C0 Coefficient for Power-Law        0
C1 Coefficient for Power-Law        0
Porosity                             1
Solid Material Name                  aluminum
Reaction Mechanism                   0
Activate reaction mechanisms?        yes
Surface-Volume-Ratio                 0

```

peb1

Condition	Value
Material Name	mixture-template
Specify source terms?	no
Source Terms	((mass (inactive . #f) (constant . 0) (profile)) (x-momentum (inactive . #f) (constant . 0) (profile)) (y-momentum (inactive . #f) (constant . 0) (profile)) (z-momentum (inactive . #f) (constant . 0) (profile)) (species-0 (inactive . #f) (constant . 0) (profile)) (species-1 (inactive . #f) (constant . 0) (profile)) (species-2 (inactive . #f) (constant . 0) (profile)) (species-3 (inactive . #f) (constant . 0) (profile)) (species-4 (inactive . #f) (constant . 0) (profile)) (energy (inactive . #f) (constant . 0) (profile)))
Specify fixed values?	no
Local Coordinate System for Fixed Velocities	no
Fixed Values	((x-velocity (inactive . #f) (constant . 0) (profile)) (y-velocity (inactive . #f) (constant . 0) (profile)) (z-velocity (inactive . #f) (constant . 0) (profile)) (species-0 (inactive . #f) (constant . 0) (profile)) (species-1 (inactive . #f) (constant . 0) (profile)) (species-2 (inactive . #f) (constant . 0) (profile)) (species-3 (inactive . #f) (constant . 0) (profile)) (species-4 (inactive . #f) (constant . 0) (profile)) (temperature (inactive . #f) (constant . 0) (profile)))
Motion Type	0
X-Velocity Of Zone	0
Y-Velocity Of Zone	0
Z-Velocity Of Zone	0
Rotation speed	0
X-Origin of Rotation-Axis	0
Y-Origin of Rotation-Axis	0
Z-Origin of Rotation-Axis	0
X-Component of Rotation-Axis	0
Y-Component of Rotation-Axis	0
Z-Component of Rotation-Axis	1
Deactivated Thread	no
Porous zone?	yes
Conical porous zone?	no
X-Component of Direction-1 Vector	1
Y-Component of Direction-1 Vector	0
Z-Component of Direction-1 Vector	0
X-Component of Direction-2 Vector	0
Y-Component of Direction-2 Vector	1
Z-Component of Direction-2 Vector	0
X-Coordinate of Point on Cone Axis	1
Y-Coordinate of Point on Cone Axis	0
Z-Coordinate of Point on Cone Axis	0
Half Angle of Cone Relative to its Axis	0
Direction-1 Viscous Resistance	0
Direction-2 Viscous Resistance	0
Direction-3 Viscous Resistance	0
Direction-1 Inertial Resistance	0
Direction-2 Inertial Resistance	0

Direction-3 Inertial Resistance	0
C0 Coefficient for Power-Law	36.688
C1 Coefficient for Power-Law	1.7599
Porosity	0.39500001
Solid Material Name	aluminum
Reaction Mechanism	0
Activate reaction mechanisms?	yes
Surface-Volume-Ratio	60.5

ref2

Condition	Value

Material Name	mixture-template
Specify source terms?	no
Source Terms	((mass (inactive . #f) (constant . 0) (profile)) (x-momentum (inactive . #f) (constant . 0) (profile)) (y-momentum (inactive . #f) (constant . 0) (profile)) (z-momentum (inactive . #f) (constant . 0) (profile)) (species-0 (inactive . #f) (constant . 0) (profile)) (species-1 (inactive . #f) (constant . 0) (profile)) (species-2 (inactive . #f) (constant . 0) (profile)) (species-3 (inactive . #f) (constant . 0) (profile)) (species-4 (inactive . #f) (constant . 0) (profile)) (energy (inactive . #f) (constant . 0) (profile)))
Specify fixed values?	no
Local Coordinate System for Fixed Velocities	no
Fixed Values	((x-velocity (inactive . #f) (constant . 0) (profile)) (y-velocity (inactive . #f) (constant . 0) (profile)) (z-velocity (inactive . #f) (constant . 0) (profile)) (species-0 (inactive . #f) (constant . 0) (profile)) (species-1 (inactive . #f) (constant . 0) (profile)) (species-2 (inactive . #f) (constant . 0) (profile)) (species-3 (inactive . #f) (constant . 0) (profile)) (species-4 (inactive . #f) (constant . 0) (profile)) (temperature (inactive . #f) (constant . 0) (profile)))
Motion Type	0
X-Velocity Of Zone	0
Y-Velocity Of Zone	0
Z-Velocity Of Zone	0
Rotation speed	0
X-Origin of Rotation-Axis	0
Y-Origin of Rotation-Axis	0
Z-Origin of Rotation-Axis	0
X-Component of Rotation-Axis	0
Y-Component of Rotation-Axis	0
Z-Component of Rotation-Axis	1
Deactivated Thread	no
Porous zone?	yes
Conical porous zone?	no
X-Component of Direction-1 Vector	1
Y-Component of Direction-1 Vector	0
Z-Component of Direction-1 Vector	0
X-Component of Direction-2 Vector	0
Y-Component of Direction-2 Vector	1
Z-Component of Direction-2 Vector	0
X-Coordinate of Point on Cone Axis	1
Y-Coordinate of Point on Cone Axis	0
Z-Coordinate of Point on Cone Axis	0
Half Angle of Cone Relative to its Axis	0
Direction-1 Viscous Resistance	0
Direction-2 Viscous Resistance	0
Direction-3 Viscous Resistance	0
Direction-1 Inertial Resistance	0
Direction-2 Inertial Resistance	0
Direction-3 Inertial Resistance	0
C0 Coefficient for Power-Law	63
C1 Coefficient for Power-Law	1.72
Porosity	0.13
Solid Material Name	aluminum


```

Reaction Mechanism          0
Activate reaction mechanisms? yes
Surface-Volume-Ratio      53.580002

```

interref

```

Condition                      Value
-----
Material Name                  mixture-template
Specify source terms?         no
Source Terms                   ()
Specify fixed values?         no
Local Coordinate System for Fixed Velocities no
Fixed Values                   ()
Motion Type                    0
X-Velocity Of Zone            0
Y-Velocity Of Zone            0
Z-Velocity Of Zone            0
Rotation speed                 0
X-Origin of Rotation-Axis     0
Y-Origin of Rotation-Axis     0
Z-Origin of Rotation-Axis     0
X-Component of Rotation-Axis  0
Y-Component of Rotation-Axis  0
Z-Component of Rotation-Axis  1
Deactivated Thread            no
Porous zone?                  no
Conical porous zone?         no
X-Component of Direction-1 Vector 1
Y-Component of Direction-1 Vector 0
Z-Component of Direction-1 Vector 0
X-Component of Direction-2 Vector 0
Y-Component of Direction-2 Vector 1
Z-Component of Direction-2 Vector 0
X-Coordinate of Point on Cone Axis 1
Y-Coordinate of Point on Cone Axis 0
Z-Coordinate of Point on Cone Axis 0
Half Angle of Cone Relative to its Axis 0
Direction-1 Viscous Resistance 0
Direction-2 Viscous Resistance 0
Direction-3 Viscous Resistance 0
Direction-1 Inertial Resistance 0
Direction-2 Inertial Resistance 0
Direction-3 Inertial Resistance 0
C0 Coefficient for Power-Law   0
C1 Coefficient for Power-Law   0
Porosity                       1
Solid Material Name            aluminum
Reaction Mechanism              0
Activate reaction mechanisms?   yes
Surface-Volume-Ratio           0

```

ref1

```

Condition                      Value
-----
Material Name                  mixture-template
Specify source terms?         no
Source Terms                   ((mass (inactive . #f) (constant
. 0) (profile )) (x-momentum (inactive . #f) (constant . 0) (profile )) (y-momentum
(inactive . #f) (constant . 0) (profile )) (z-momentum (inactive . #f) (constant . 0)
(profile )) (species-0 (inactive . #f) (constant . 0) (profile )) (species-1 (inactive
. #f) (constant . 0) (profile )) (species-2 (inactive . #f) (constant . 0) (profile ))
(species-3 (inactive . #f) (constant . 0) (profile )) (species-4 (inactive . #f)
(constant . 0) (profile )) (energy (inactive . #f) (constant . 0) (profile )))

```

```

Specify fixed values? no
Local Coordinate System for Fixed Velocities no
Fixed Values ((x-velocity (inactive . #f)
(constant . 0) (profile )) (y-velocity (inactive . #f) (constant . 0) (profile )) (z-
velocity (inactive . #f) (constant . 0) (profile )) (species-0 (inactive . #f) (constant
. 0) (profile )) (species-1 (inactive . #f) (constant . 0) (profile )) (species-2
(inactive . #f) (constant . 0) (profile )) (species-3 (inactive . #f) (constant . 0)
(profile )) (species-4 (inactive . #f) (constant . 0) (profile )) (temperature
(inactive . #f) (constant . 0) (profile )))
Motion Type 0
X-Velocity Of Zone 0
Y-Velocity Of Zone 0
Z-Velocity Of Zone 0
Rotation speed 0
X-Origin of Rotation-Axis 0
Y-Origin of Rotation-Axis 0
Z-Origin of Rotation-Axis 0
X-Component of Rotation-Axis 0
Y-Component of Rotation-Axis 0
Z-Component of Rotation-Axis 1
Deactivated Thread no
Porous zone? yes
Conical porous zone? no
X-Component of Direction-1 Vector 1
Y-Component of Direction-1 Vector 0
Z-Component of Direction-1 Vector 0
X-Component of Direction-2 Vector 0
Y-Component of Direction-2 Vector 1
Z-Component of Direction-2 Vector 0
X-Coordinate of Point on Cone Axis 1
Y-Coordinate of Point on Cone Axis 0
Z-Coordinate of Point on Cone Axis 0
Half Angle of Cone Relative to its Axis 0
Direction-1 Viscous Resistance 0
Direction-2 Viscous Resistance 0
Direction-3 Viscous Resistance 0
Direction-1 Inertial Resistance 0
Direction-2 Inertial Resistance 0
Direction-3 Inertial Resistance 0
C0 Coefficient for Power-Law 63
C1 Coefficient for Power-Law 1.72
Porosity 0.13
Solid Material Name aluminum
Reaction Mechanism 0
Activate reaction mechanisms? yes
Surface-Volume-Ratio 53.580002

```

porous_jump.67

```

Condition Value
-----

```

porous_jump.63

```

Condition Value
-----

```

wallerreur-shadow

```

Condition Value
-----
Wall Thickness 0
Heat Generation Rate 0
Material Name aluminum
Thermal BC Type 3
Temperature 300
Heat Flux 0
Convective Heat Transfer Coefficient 0
Free Stream Temperature 300
Enable shell conduction? no
Wall Motion 0

```

Shear Boundary Condition	0
Define wall motion relative to adjacent cell zone?	yes
Apply a rotational velocity to this wall?	no
Velocity Magnitude	0
X-Component of Wall Translation	1
Y-Component of Wall Translation	0
Z-Component of Wall Translation	0
Define wall velocity components?	no
X-Component of Wall Translation	0
Y-Component of Wall Translation	0
Z-Component of Wall Translation	0
External Emissivity	1
External Radiation Temperature	300
Activate Reaction Mechanisms	no
Rotation Speed	0
X-Position of Rotation-Axis Origin	0
Y-Position of Rotation-Axis Origin	0
Z-Position of Rotation-Axis Origin	0
X-Component of Rotation-Axis Direction	0
Y-Component of Rotation-Axis Direction	0
Z-Component of Rotation-Axis Direction	1
X-component of shear stress	0
Y-component of shear stress	0
Z-component of shear stress	0
Surface tension gradient	0
Reaction Mechanisms	0
Specularity Coefficient	0

wall-shadow

Condition	Value
-----	-----
Wall Thickness	0
Heat Generation Rate	0
Material Name	aluminum
Thermal BC Type	3
Temperature	300
Heat Flux	0
Convective Heat Transfer Coefficient	0
Free Stream Temperature	300
Enable shell conduction?	no
Wall Motion	0
Shear Boundary Condition	0
Define wall motion relative to adjacent cell zone?	yes
Apply a rotational velocity to this wall?	no
Velocity Magnitude	0
X-Component of Wall Translation	1
Y-Component of Wall Translation	0
Z-Component of Wall Translation	0
Define wall velocity components?	no
X-Component of Wall Translation	0
Y-Component of Wall Translation	0
Z-Component of Wall Translation	0
External Emissivity	1
External Radiation Temperature	300
Activate Reaction Mechanisms	no
Rotation Speed	0
X-Position of Rotation-Axis Origin	0
Y-Position of Rotation-Axis Origin	0
Z-Position of Rotation-Axis Origin	0
X-Component of Rotation-Axis Direction	0
Y-Component of Rotation-Axis Direction	0
Z-Component of Rotation-Axis Direction	1
X-component of shear stress	0
Y-component of shear stress	0
Z-component of shear stress	0
Surface tension gradient	0
Reaction Mechanisms	0
Specularity Coefficient	0

wall_entree:061-shadow

Condition	Value
Wall Thickness	0
Heat Generation Rate	0
Material Name	aluminum
Thermal BC Type	3
Temperature	300
Heat Flux	0
Convective Heat Transfer Coefficient	0
Free Stream Temperature	300
Enable shell conduction?	no
Wall Motion	0
Shear Boundary Condition	0
Define wall motion relative to adjacent cell zone?	yes
Apply a rotational velocity to this wall?	no
Velocity Magnitude	0
X-Component of Wall Translation	1
Y-Component of Wall Translation	0
Z-Component of Wall Translation	0
Define wall velocity components?	no
X-Component of Wall Translation	0
Y-Component of Wall Translation	0
Z-Component of Wall Translation	0
External Emissivity	1
External Radiation Temperature	300
Activate Reaction Mechanisms	no
Rotation Speed	0
X-Position of Rotation-Axis Origin	0
Y-Position of Rotation-Axis Origin	0
Z-Position of Rotation-Axis Origin	0
X-Component of Rotation-Axis Direction	0
Y-Component of Rotation-Axis Direction	0
Z-Component of Rotation-Axis Direction	1
X-component of shear stress	0
Y-component of shear stress	0
Z-component of shear stress	0
Surface tension gradient	0
Reaction Mechanisms	0
Specularity Coefficient	0

wall

Condition	Value
Wall Thickness	0
Heat Generation Rate	0
Material Name	aluminum
Thermal BC Type	3
Temperature	300
Heat Flux	0
Convective Heat Transfer Coefficient	0
Free Stream Temperature	300
Enable shell conduction?	no
Wall Motion	0
Shear Boundary Condition	0
Define wall motion relative to adjacent cell zone?	yes
Apply a rotational velocity to this wall?	no
Velocity Magnitude	0
X-Component of Wall Translation	1
Y-Component of Wall Translation	0
Z-Component of Wall Translation	0
Define wall velocity components?	no
X-Component of Wall Translation	0
Y-Component of Wall Translation	0
Z-Component of Wall Translation	0
External Emissivity	1
External Radiation Temperature	300
Activate Reaction Mechanisms	no
	(0)

```

)))
Rotation Speed 0
X-Position of Rotation-Axis Origin 0
Y-Position of Rotation-Axis Origin 0
Z-Position of Rotation-Axis Origin 0
X-Component of Rotation-Axis Direction 0
Y-Component of Rotation-Axis Direction 0
Z-Component of Rotation-Axis Direction 1
X-component of shear stress 0
Y-component of shear stress 0
Z-component of shear stress 0
Surface tension gradient 0
Reaction Mechanisms 0
Specularity Coefficient 0

```

```

weallout
Condition Value
-----
Wall Thickness 0
Heat Generation Rate 0
Material Name aluminum
Thermal BC Type 1
Temperature 300
Heat Flux 0
Convective Heat Transfer Coefficient 0
Free Stream Temperature 300
Enable shell conduction? no
Wall Motion 0
Shear Boundary Condition 0
Define wall motion relative to adjacent cell zone? yes
Apply a rotational velocity to this wall? no
Velocity Magnitude 0
X-Component of Wall Translation 1
Y-Component of Wall Translation 0
Z-Component of Wall Translation 0
Define wall velocity components? no
X-Component of Wall Translation 0
Y-Component of Wall Translation 0
Z-Component of Wall Translation 0
External Emissivity 1
External Radiation Temperature 300
Activate Reaction Mechanisms no
(0 0 0 0 0)

```

```

)) ((constant . 0) (profile )) ((constant . 0) (profile )) ((constant . 0) (profile ))
((constant . 0) (profile ))
Rotation Speed 0
X-Position of Rotation-Axis Origin 0
Y-Position of Rotation-Axis Origin 0
Z-Position of Rotation-Axis Origin 0
X-Component of Rotation-Axis Direction 0
Y-Component of Rotation-Axis Direction 0
Z-Component of Rotation-Axis Direction 1
X-component of shear stress 0
Y-component of shear stress 0
Z-component of shear stress 0
Surface tension gradient 0
Reaction Mechanisms 0
Specularity Coefficient 0

```

```

walloutlet1
Condition Value
-----
Wall Thickness 0

```

```

Heat Generation Rate 0
Material Name aluminum
Thermal BC Type 1
Temperature 300
Heat Flux 0
Convective Heat Transfer Coefficient 0
Free Stream Temperature 300
Enable shell conduction? no
Wall Motion 0
Shear Boundary Condition 0
Define wall motion relative to adjacent cell zone? yes
Apply a rotational velocity to this wall? no
Velocity Magnitude 0
X-Component of Wall Translation 1
Y-Component of Wall Translation 0
Z-Component of Wall Translation 0
Define wall velocity components? no
X-Component of Wall Translation 0
Y-Component of Wall Translation 0
Z-Component of Wall Translation 0
External Emissivity 1
External Radiation Temperature 300
Activate Reaction Mechanisms no
(0 0 0 0 0)
((constant . 0) (profile )) ((constant . 0) (profile )) ((constant . 0) (profile ))
((constant . 0) (profile )))
Rotation Speed 0
X-Position of Rotation-Axis Origin 0
Y-Position of Rotation-Axis Origin 0
Z-Position of Rotation-Axis Origin 0
X-Component of Rotation-Axis Direction 0
Y-Component of Rotation-Axis Direction 0
Z-Component of Rotation-Axis Direction 1
X-component of shear stress 0
Y-component of shear stress 0
Z-component of shear stress 0
Surface tension gradient 0
Reaction Mechanisms 0
Specularity Coefficient 0

```

wallerreur

Condition	Value
Wall Thickness	0
Heat Generation Rate	0
Material Name	aluminum
Thermal BC Type	3
Temperature	300
Heat Flux	0
Convective Heat Transfer Coefficient	0
Free Stream Temperature	300
Enable shell conduction?	no
Wall Motion	0
Shear Boundary Condition	0
Define wall motion relative to adjacent cell zone?	yes
Apply a rotational velocity to this wall?	no
Velocity Magnitude	0
X-Component of Wall Translation	1
Y-Component of Wall Translation	0
Z-Component of Wall Translation	0
Define wall velocity components?	no
X-Component of Wall Translation	0
Y-Component of Wall Translation	0
Z-Component of Wall Translation	0
External Emissivity	1
External Radiation Temperature	300
Activate Reaction Mechanisms	no
	(0)

```

)))
Rotation Speed 0
X-Position of Rotation-Axis Origin 0
Y-Position of Rotation-Axis Origin 0
Z-Position of Rotation-Axis Origin 0
X-Component of Rotation-Axis Direction 0
Y-Component of Rotation-Axis Direction 0
Z-Component of Rotation-Axis Direction 1
X-component of shear stress 0
Y-component of shear stress 0
Z-component of shear stress 0
Surface tension gradient 0
Reaction Mechanisms 0
Specularity Coefficient 0

wall_outlet
Condition Value
-----
Wall Thickness 0
Heat Generation Rate 0
Material Name aluminum
Thermal BC Type 0
Temperature 300
Heat Flux 0
Convective Heat Transfer Coefficient 0
Free Stream Temperature 300
Enable shell conduction? no
Wall Motion 0
Shear Boundary Condition 0
Define wall motion relative to adjacent cell zone? yes
Apply a rotational velocity to this wall? no
Velocity Magnitude 0
X-Component of Wall Translation 1
Y-Component of Wall Translation 0
Z-Component of Wall Translation 0
Define wall velocity components? no
X-Component of Wall Translation 0
Y-Component of Wall Translation 0
Z-Component of Wall Translation 0
External Emissivity 1
External Radiation Temperature 300
Activate Reaction Mechanisms no
(0 0 0 0 0)
)) ((constant . 0) (profile )) ((constant . 0) (profile )) ((constant . 0) (profile ))
((constant . 0) (profile ))
Rotation Speed 0
X-Position of Rotation-Axis Origin 0
Y-Position of Rotation-Axis Origin 0
Z-Position of Rotation-Axis Origin 0
X-Component of Rotation-Axis Direction 0
Y-Component of Rotation-Axis Direction 0
Z-Component of Rotation-Axis Direction 1
X-component of shear stress 0
Y-component of shear stress 0
Z-component of shear stress 0
Surface tension gradient 0
Reaction Mechanisms 0
Specularity Coefficient 0

wall_return
Condition Value
-----
Wall Thickness 0

```

```

Heat Generation Rate 0
Material Name aluminum
Thermal BC Type 0
Temperature 500
Heat Flux 0
Convective Heat Transfer Coefficient 0
Free Stream Temperature 300
Enable shell conduction? no
Wall Motion 0
Shear Boundary Condition 0
Define wall motion relative to adjacent cell zone? yes
Apply a rotational velocity to this wall? no
Velocity Magnitude 0
X-Component of Wall Translation 1
Y-Component of Wall Translation 0
Z-Component of Wall Translation 0
Define wall velocity components? no
X-Component of Wall Translation 0
Y-Component of Wall Translation 0
Z-Component of Wall Translation 0
External Emissivity 1
External Radiation Temperature 300
Activate Reaction Mechanisms no
(0 0 0 0 0)
(((constant . 0) (profile
)) ((constant . 0) (profile )) ((constant . 0) (profile ))
((constant . 0) (profile )))
Rotation Speed 0
X-Position of Rotation-Axis Origin 0
Y-Position of Rotation-Axis Origin 0
Z-Position of Rotation-Axis Origin 0
X-Component of Rotation-Axis Direction 0
Y-Component of Rotation-Axis Direction 0
Z-Component of Rotation-Axis Direction 1
X-component of shear stress 0
Y-component of shear stress 0
Z-component of shear stress 0
Surface tension gradient 0
Reaction Mechanisms 0
Specularity Coefficient 0

symmetry

Condition Value
-----

interior_

Condition Value
-----

wall_chimey

Condition Value
-----
-----
Wall Thickness 0
Heat Generation Rate 0
Material Name aluminum
Thermal BC Type 0
Temperature 1123
Heat Flux 0
Convective Heat Transfer Coefficient 0
Free Stream Temperature 300
Enable shell conduction? no
Wall Motion 0
Shear Boundary Condition 0
Define wall motion relative to adjacent cell zone? yes
Apply a rotational velocity to this wall? no
Velocity Magnitude 0

```



```

X-Component of Wall Translation      1
Y-Component of Wall Translation      0
Z-Component of Wall Translation      0
Define wall velocity components?     no
X-Component of Wall Translation      0
Y-Component of Wall Translation      0
Z-Component of Wall Translation      0
External Emissivity                  1
External Radiation Temperature       300
Activate Reaction Mechanisms         no
                                     (0 0 0 0 0)
                                     (((constant . 0) (profile
)) ((constant . 0) (profile )) ((constant . 0) (profile )) ((constant . 0) (profile ))
((constant . 0) (profile )))
Rotation Speed                       0
X-Position of Rotation-Axis Origin    0
Y-Position of Rotation-Axis Origin    0
Z-Position of Rotation-Axis Origin    0
X-Component of Rotation-Axis Direction 0
Y-Component of Rotation-Axis Direction 0
Z-Component of Rotation-Axis Direction 1
X-component of shear stress           0
Y-component of shear stress           0
Z-component of shear stress           0
Surface tension gradient              0
Reaction Mechanisms                   0
Specularity Coefficient               0

wall_peg2

Condition                             Value
-----
Wall Thickness                        0
Heat Generation Rate                  0
Material Name                         aluminum
Thermal BC Type                      0
Temperature                          1123
Heat Flux                             0
Convective Heat Transfer Coefficient  0
Free Stream Temperature               300
Enable shell conduction?              no
Wall Motion                           0
Shear Boundary Condition              0
Define wall motion relative to adjacent cell zone? yes
Apply a rotational velocity to this wall? no
Velocity Magnitude                   0
X-Component of Wall Translation        1
Y-Component of Wall Translation        0
Z-Component of Wall Translation        0
Define wall velocity components?     no
X-Component of Wall Translation        0
Y-Component of Wall Translation        0
Z-Component of Wall Translation        0
External Emissivity                   1
External Radiation Temperature        300
Activate Reaction Mechanisms          no
                                     (0 0 0 0 0)
                                     (((constant . 0) (profile
)) ((constant . 0) (profile )) ((constant . 0) (profile )) ((constant . 0) (profile ))
((constant . 0) (profile )))
Rotation Speed                       0
X-Position of Rotation-Axis Origin    0
Y-Position of Rotation-Axis Origin    0
Z-Position of Rotation-Axis Origin    0
X-Component of Rotation-Axis Direction 0
Y-Component of Rotation-Axis Direction 0
Z-Component of Rotation-Axis Direction 1
X-component of shear stress           0
Y-component of shear stress           0

```

Z-component of shear stress	0
Surface tension gradient	0
Reaction Mechanisms	0
Specularity Coefficient	0

wall_interpeb

Condition	Value
Wall Thickness	0
Heat Generation Rate	0
Material Name	aluminum
Thermal BC Type	0
Temperature	1123
Heat Flux	0
Convective Heat Transfer Coefficient	0
Free Stream Temperature	300
Enable shell conduction?	no
Wall Motion	0
Shear Boundary Condition	0
Define wall motion relative to adjacent cell zone?	yes
Apply a rotational velocity to this wall?	no
Velocity Magnitude	0
X-Component of Wall Translation	1
Y-Component of Wall Translation	0
Z-Component of Wall Translation	0
Define wall velocity components?	no
X-Component of Wall Translation	0
Y-Component of Wall Translation	0
Z-Component of Wall Translation	0
External Emissivity	1
External Radiation Temperature	300
Activate Reaction Mechanisms	no
	(0 0 0 0 0)
	((constant . 0) (profile))
) ((constant . 0) (profile)) ((constant . 0) (profile)) ((constant . 0) (profile))	
((constant . 0) (profile))	
Rotation Speed	0
X-Position of Rotation-Axis Origin	0
Y-Position of Rotation-Axis Origin	0
Z-Position of Rotation-Axis Origin	0
X-Component of Rotation-Axis Direction	0
Y-Component of Rotation-Axis Direction	0
Z-Component of Rotation-Axis Direction	1
X-component of shear stress	0
Y-component of shear stress	0
Z-component of shear stress	0
Surface tension gradient	0
Reaction Mechanisms	0
Specularity Coefficient	0

wall_peb1

Condition	Value
Wall Thickness	0
Heat Generation Rate	0
Material Name	aluminum
Thermal BC Type	0
Temperature	1123
Heat Flux	0
Convective Heat Transfer Coefficient	0
Free Stream Temperature	300
Enable shell conduction?	no
Wall Motion	0
Shear Boundary Condition	0
Define wall motion relative to adjacent cell zone?	yes

```

Apply a rotational velocity to this wall?      no
Velocity Magnitude                            0
X-Component of Wall Translation                1
Y-Component of Wall Translation                0
Z-Component of Wall Translation                0
Define wall velocity components?              no
X-Component of Wall Translation                0
Y-Component of Wall Translation                0
Z-Component of Wall Translation                0
External Emissivity                           1
External Radiation Temperature                300
Activate Reaction Mechanisms                  no
                                                (0 0 0 0 0)
                                                (((constant . 0) (profile
)) ((constant . 0) (profile )) ((constant . 0) (profile )) ((constant . 0) (profile ))
((constant . 0) (profile )))
Rotation Speed                                0
X-Position of Rotation-Axis Origin            0
Y-Position of Rotation-Axis Origin            0
Z-Position of Rotation-Axis Origin            0
X-Component of Rotation-Axis Direction        0
Y-Component of Rotation-Axis Direction        0
Z-Component of Rotation-Axis Direction        1
X-component of shear stress                   0
Y-component of shear stress                   0
Z-component of shear stress                   0
Surface tension gradient                      0
Reaction Mechanisms                           0
Specularity Coefficient                       0

```

wall_ref2

Condition	Value
Wall Thickness	0
Heat Generation Rate	0
Material Name	aluminum
Thermal BC Type	0
Temperature	1123
Heat Flux	0
Convective Heat Transfer Coefficient	0
Free Stream Temperature	300
Enable shell conduction?	no
Wall Motion	0
Shear Boundary Condition	0
Define wall motion relative to adjacent cell zone?	yes
Apply a rotational velocity to this wall?	no
Velocity Magnitude	0
X-Component of Wall Translation	1
Y-Component of Wall Translation	0
Z-Component of Wall Translation	0
Define wall velocity components?	no
X-Component of Wall Translation	0
Y-Component of Wall Translation	0
Z-Component of Wall Translation	0
External Emissivity	1
External Radiation Temperature	300
Activate Reaction Mechanisms	no
	(0 0 0 0 0)
	(((constant . 0) (profile
)) ((constant . 0) (profile)) ((constant . 0) (profile)) ((constant . 0) (profile))
	((constant . 0) (profile)))
Rotation Speed	0
X-Position of Rotation-Axis Origin	0
Y-Position of Rotation-Axis Origin	0
Z-Position of Rotation-Axis Origin	0
X-Component of Rotation-Axis Direction	0
Y-Component of Rotation-Axis Direction	0
Z-Component of Rotation-Axis Direction	1

X-component of shear stress	0
Y-component of shear stress	0
Z-component of shear stress	0
Surface tension gradient	0
Reaction Mechanisms	0
Specularity Coefficient	0

wall_interef

Condition	Value
Wall Thickness	0
Heat Generation Rate	0
Material Name	aluminum
Thermal BC Type	0
Temperature	1123
Heat Flux	0
Convective Heat Transfer Coefficient	0
Free Stream Temperature	300
Enable shell conduction?	no
Wall Motion	0
Shear Boundary Condition	0
Define wall motion relative to adjacent cell zone?	yes
Apply a rotational velocity to this wall?	no
Velocity Magnitude	0
X-Component of Wall Translation	1
Y-Component of Wall Translation	0
Z-Component of Wall Translation	0
Define wall velocity components?	no
X-Component of Wall Translation	0
Y-Component of Wall Translation	0
Z-Component of Wall Translation	0
External Emissivity	1
External Radiation Temperature	300
Activate Reaction Mechanisms	no
	(0 0 0 0 0)
	((constant . 0) (profile))
	((constant . 0) (profile)) ((constant . 0) (profile)) ((constant . 0) (profile))
	((constant . 0) (profile))
Rotation Speed	0
X-Position of Rotation-Axis Origin	0
Y-Position of Rotation-Axis Origin	0
Z-Position of Rotation-Axis Origin	0
X-Component of Rotation-Axis Direction	0
Y-Component of Rotation-Axis Direction	0
Z-Component of Rotation-Axis Direction	1
X-component of shear stress	0
Y-component of shear stress	0
Z-component of shear stress	0
Surface tension gradient	0
Reaction Mechanisms	0
Specularity Coefficient	0

wall_ref1

Condition	Value
Wall Thickness	0
Heat Generation Rate	0
Material Name	aluminum
Thermal BC Type	0
Temperature	1123
Heat Flux	0
Convective Heat Transfer Coefficient	0
Free Stream Temperature	300
Enable shell conduction?	no
Wall Motion	0

```

Shear Boundary Condition 0
Define wall motion relative to adjacent cell zone? yes
Apply a rotational velocity to this wall? no
Velocity Magnitude 0
X-Component of Wall Translation 1
Y-Component of Wall Translation 0
Z-Component of Wall Translation 0
Define wall velocity components? no
X-Component of Wall Translation 0
Y-Component of Wall Translation 0
Z-Component of Wall Translation 0
External Emissivity 1
External Radiation Temperature 300
Activate Reaction Mechanisms no
(0 0 0 0 0)
((constant . 0) (profile )) ((constant . 0) (profile )) ((constant . 0) (profile ))
((constant . 0) (profile ))
Rotation Speed 0
X-Position of Rotation-Axis Origin 0
Y-Position of Rotation-Axis Origin 0
Z-Position of Rotation-Axis Origin 0
X-Component of Rotation-Axis Direction 0
Y-Component of Rotation-Axis Direction 0
Z-Component of Rotation-Axis Direction 1
X-component of shear stress 0
Y-component of shear stress 0
Z-component of shear stress 0
Surface tension gradient 0
Reaction Mechanisms 0
Specularity Coefficient 0

wall_libre_1

Condition Value
-----
-----
Wall Thickness 0
Heat Generation Rate 0
Material Name aluminum
Thermal BC Type 0
Temperature 1123
Heat Flux 0
Convective Heat Transfer Coefficient 0
Free Stream Temperature 300
Enable shell conduction? no
Wall Motion 0
Shear Boundary Condition 0
Define wall motion relative to adjacent cell zone? yes
Apply a rotational velocity to this wall? no
Velocity Magnitude 0
X-Component of Wall Translation 1
Y-Component of Wall Translation 0
Z-Component of Wall Translation 0
Define wall velocity components? no
X-Component of Wall Translation 0
Y-Component of Wall Translation 0
Z-Component of Wall Translation 0
External Emissivity 1
External Radiation Temperature 300
Activate Reaction Mechanisms no
(0 0 0 0 0)
((constant . 0) (profile )) ((constant . 0) (profile )) ((constant . 0) (profile ))
((constant . 0) (profile ))
Rotation Speed 0
X-Position of Rotation-Axis Origin 0
Y-Position of Rotation-Axis Origin 0
Z-Position of Rotation-Axis Origin 0
X-Component of Rotation-Axis Direction 0

```

Y-Component of Rotation-Axis Direction	0
Z-Component of Rotation-Axis Direction	1
X-component of shear stress	0
Y-component of shear stress	0
Z-component of shear stress	0
Surface tension gradient	0
Reaction Mechanisms	0
Specularity Coefficient	0

wall_ref_bas

Condition	Value
-----	-----
-----	-----
Wall Thickness	0
Heat Generation Rate	0
Material Name	aluminum
Thermal BC Type	0
Temperature	1123
Heat Flux	0
Convective Heat Transfer Coefficient	0
Free Stream Temperature	300
Enable shell conduction?	no
Wall Motion	0
Shear Boundary Condition	0
Define wall motion relative to adjacent cell zone?	yes
Apply a rotational velocity to this wall?	no
Velocity Magnitude	0
X-Component of Wall Translation	1
Y-Component of Wall Translation	0
Z-Component of Wall Translation	0
Define wall velocity components?	no
X-Component of Wall Translation	0
Y-Component of Wall Translation	0
Z-Component of Wall Translation	0
External Emissivity	1
External Radiation Temperature	300
Activate Reaction Mechanisms	yes
	(0 0 0 0 0)
	((constant . 0) (profile
)) ((constant . 0) (profile)) ((constant . 0) (profile)) ((constant . 0) (profile))	
((constant . 0) (profile)))	
Rotation Speed	0
X-Position of Rotation-Axis Origin	0
Y-Position of Rotation-Axis Origin	0
Z-Position of Rotation-Axis Origin	0
X-Component of Rotation-Axis Direction	0
Y-Component of Rotation-Axis Direction	0
Z-Component of Rotation-Axis Direction	1
X-component of shear stress	0
Y-component of shear stress	0
Z-component of shear stress	0
Surface tension gradient	0
Reaction Mechanisms	0
Specularity Coefficient	0

wall_entree

Condition	Value
-----	-----
-----	-----
Wall Thickness	0
Heat Generation Rate	0
Material Name	aluminum
Thermal BC Type	0
Temperature	900
Heat Flux	0
Convective Heat Transfer Coefficient	0
Free Stream Temperature	300

```

Enable shell conduction?          no
Wall Motion                       0
Shear Boundary Condition          0
Define wall motion relative to adjacent cell zone?  yes
Apply a rotational velocity to this wall?  no
Velocity Magnitude               0
X-Component of Wall Translation   1
Y-Component of Wall Translation   0
Z-Component of Wall Translation   0
Define wall velocity components?  no
X-Component of Wall Translation   0
Y-Component of Wall Translation   0
Z-Component of Wall Translation   0
External Emissivity               1
External Radiation Temperature    300
Activate Reaction Mechanisms      no
                                (0 0 0 0 0)
                                (((constant . 0) (profile
)) ((constant . 0) (profile )) ((constant . 0) (profile )) ((constant . 0) (profile ))
((constant . 0) (profile )))
Rotation Speed                    0
X-Position of Rotation-Axis Origin 0
Y-Position of Rotation-Axis Origin 0
Z-Position of Rotation-Axis Origin 0
X-Component of Rotation-Axis Direction 0
Y-Component of Rotation-Axis Direction 0
Z-Component of Rotation-Axis Direction 1
X-component of shear stress        0
Y-component of shear stress        0
Z-component of shear stress        0
Surface tension gradient           0
Reaction Mechanisms                0
Specularity Coefficient            0

```

wall_inlet

Condition	Value
Wall Thickness	0
Heat Generation Rate	0
Material Name	aluminum
Thermal BC Type	0
Temperature	300
Heat Flux	0
Convective Heat Transfer Coefficient	0
Free Stream Temperature	300
Enable shell conduction?	no
Wall Motion	0
Shear Boundary Condition	0
Define wall motion relative to adjacent cell zone?	yes
Apply a rotational velocity to this wall?	no
Velocity Magnitude	0
X-Component of Wall Translation	1
Y-Component of Wall Translation	0
Z-Component of Wall Translation	0
Define wall velocity components?	no
X-Component of Wall Translation	0
Y-Component of Wall Translation	0
Z-Component of Wall Translation	0
External Emissivity	1
External Radiation Temperature	300
Activate Reaction Mechanisms	no
	(0 0 0 0 0)
	(((constant . 0) (profile
)) ((constant . 0) (profile)) ((constant . 0) (profile)) ((constant . 0) (profile))
	((constant . 0) (profile)))
Rotation Speed	0
X-Position of Rotation-Axis Origin	0
Y-Position of Rotation-Axis Origin	0

Z-Position of Rotation-Axis Origin	0
X-Component of Rotation-Axis Direction	0
Y-Component of Rotation-Axis Direction	0
Z-Component of Rotation-Axis Direction	1
X-component of shear stress	0
Y-component of shear stress	0
Z-component of shear stress	0
Surface tension gradient	0
Reaction Mechanisms	0
Specularity Coefficient	0

default-interior

Condition	Value
-----	-----

symmetry:001

Condition	Value
-----	-----

symmetry:039

Condition	Value
-----	-----

symmetry:041

Condition	Value
-----	-----

symmetry:042

Condition	Value
-----	-----

symmetry:043

Condition	Value
-----	-----

symmetry:044

Condition	Value
-----	-----

symmetry:045

Condition	Value
-----	-----

symmetry:046

Condition	Value
-----	-----

symmetry:047

Condition	Value
-----	-----

symmetry:048

Condition	Value
-----	-----

symmetry:049

Condition	Value
-----	-----

symmetry:050

Condition Value

interior_:051

Condition Value

interior_:052

Condition Value

interior_:053

Condition Value

interior_:054

Condition Value

interior_:055

Condition Value

interior_:056

Condition Value

interior_:057

Condition Value

interior_:058

Condition Value

interior_:059

Condition Value

interior_:060

Condition Value

wall_entree:061

Condition Value

Wall Thickness	0
Heat Generation Rate	0
Material Name	aluminum
Thermal BC Type	3
Temperature	300
Heat Flux	0
Convective Heat Transfer Coefficient	0
Free Stream Temperature	300
Enable shell conduction?	no
Wall Motion	0

```

Shear Boundary Condition 0
Define wall motion relative to adjacent cell zone? yes
Apply a rotational velocity to this wall? no
Velocity Magnitude 0
X-Component of Wall Translation 1
Y-Component of Wall Translation 0
Z-Component of Wall Translation 0
Define wall velocity components? no
X-Component of Wall Translation 0
Y-Component of Wall Translation 0
Z-Component of Wall Translation 0
External Emissivity 1
External Radiation Temperature 300
Activate Reaction Mechanisms yes
(0 0 0 0 0)
((constant . 0) (profile )) ((constant . 0) (profile )) ((constant . 0) (profile ))
((constant . 0) (profile ))
Rotation Speed 0
X-Position of Rotation-Axis Origin 0
Y-Position of Rotation-Axis Origin 0
Z-Position of Rotation-Axis Origin 0
X-Component of Rotation-Axis Direction 0
Y-Component of Rotation-Axis Direction 0
Z-Component of Rotation-Axis Direction 1
X-component of shear stress 0
Y-component of shear stress 0
Z-component of shear stress 0
Surface tension gradient 0
Reaction Mechanisms 0
Specularity Coefficient 0

```

wall_entree:062

Condition	Value
Wall Thickness	0
Heat Generation Rate	0
Material Name	aluminum
Thermal BC Type	0
Temperature	900
Heat Flux	0
Convective Heat Transfer Coefficient	0
Free Stream Temperature	300
Enable shell conduction?	no
Wall Motion	0
Shear Boundary Condition	0
Define wall motion relative to adjacent cell zone?	yes
Apply a rotational velocity to this wall?	no
Velocity Magnitude	0
X-Component of Wall Translation	1
Y-Component of Wall Translation	0
Z-Component of Wall Translation	0
Define wall velocity components?	no
X-Component of Wall Translation	0
Y-Component of Wall Translation	0
Z-Component of Wall Translation	0
External Emissivity	1
External Radiation Temperature	300
Activate Reaction Mechanisms	no
Rotation Speed	0
X-Position of Rotation-Axis Origin	0
Y-Position of Rotation-Axis Origin	0
Z-Position of Rotation-Axis Origin	0
X-Component of Rotation-Axis Direction	0
Y-Component of Rotation-Axis Direction	0
Z-Component of Rotation-Axis Direction	1
X-component of shear stress	0
Y-component of shear stress	0
Z-component of shear stress	0
Surface tension gradient	0

```

Reaction Mechanisms          0
Specularity Coefficient     0

```

wall_inlet:063

Condition	Value
Wall Thickness	0
Heat Generation Rate	0
Material Name	aluminum
Thermal BC Type	0
Temperature	300
Heat Flux	0
Convective Heat Transfer Coefficient	0
Free Stream Temperature	300
Enable shell conduction?	no
Wall Motion	0
Shear Boundary Condition	0
Define wall motion relative to adjacent cell zone?	yes
Apply a rotational velocity to this wall?	no
Velocity Magnitude	0
X-Component of Wall Translation	1
Y-Component of Wall Translation	0
Z-Component of Wall Translation	0
Define wall velocity components?	no
X-Component of Wall Translation	0
Y-Component of Wall Translation	0
Z-Component of Wall Translation	0
External Emissivity	1
External Radiation Temperature	300
Activate Reaction Mechanisms	no
	(0 0 0 0 0)
	((constant . 0) (profile))
	((constant . 0) (profile)) ((constant . 0) (profile)) ((constant . 0) (profile))
Rotation Speed	0
X-Position of Rotation-Axis Origin	0
Y-Position of Rotation-Axis Origin	0
Z-Position of Rotation-Axis Origin	0
X-Component of Rotation-Axis Direction	0
Y-Component of Rotation-Axis Direction	0
Z-Component of Rotation-Axis Direction	1
X-component of shear stress	0
Y-component of shear stress	0
Z-component of shear stress	0
Surface tension gradient	0
Reaction Mechanisms	0
Specularity Coefficient	0

default-interior:064

```

Condition  Value
-----

```

default-interior:065

```

Condition  Value
-----

```

default-interior:066

```

Condition  Value
-----

```

default-interior:067

```

Condition  Value
-----

```

default-interior:068

Condition Value

default-interior:069

Condition Value

default-interior:070

Condition Value

default-interior:071

Condition Value

default-interior:072

Condition Value

default-interior:073

Condition Value

default-interior:074

Condition Value

default-interior:075

Condition Value

default-interior:076

Condition Value

default-interior:077

Condition Value

default-interior:078

Condition Value

default-interior:079

Condition Value

default-interior:080

Condition Value

Solver Controls

Equations

Equation Solved

```

-----
Flow      yes
n2        yes
co2       yes
co        yes
o2        yes
h2o       yes
Energy    yes

```

Numerics

```

Numeric                                     Enabled
-----
Absolute Velocity Formulation  yes

```

Unsteady Calculation Parameters

```

-----
Time Step (s)                            1
Max. Iterations Per Time Step            55

```

Relaxation

```

Variable      Relaxation Factor
-----
Pressure      0.30000001
Density       1
Body Forces   1
Momentum      0.050000001
n2            0.1
co2           1
co            1
o2            1
h2o           1
Energy        0.001

```

Linear Solver

Variable	Solver Type	Termination Criterion	Residual Reduction Tolerance
Pressure	V-Cycle	0.1	
X-Momentum	Flexible	0.1	0.7
Y-Momentum	Flexible	0.1	0.7
Z-Momentum	Flexible	0.1	0.7
n2	Flexible	0.1	0.7
co2	Flexible	0.1	0.7
co	Flexible	0.1	0.7
o2	Flexible	0.1	0.7
h2o	Flexible	0.1	0.7
Energy	Flexible	0.1	0.7

Discretization Scheme

```

Variable  Scheme
-----
Pressure  Second Order
Density   First Order Upwind
Momentum  First Order Upwind
n2        First Order Upwind
co2       First Order Upwind
co        First Order Upwind
o2        First Order Upwind
h2o       First Order Upwind
Energy    First Order Upwind

```

Solution Limits

```

Quantity                                     Limit
-----

```

Minimum Absolute Pressure	1
Maximum Absolute Pressure	5e+10
Minimum Temperature	1
Maximum Temperature	5000

Material Properties

Material: (carbon-solid . mixture-template) (fluid)

Property	Units	Method	Value (s)
Cp (Specific Heat)	j/kg-k	constant	1220
Molecular Weight	kg/kgmol	constant	12.01115
Standard State Enthalpy	j/kgmol	constant	-101.268
Standard State Entropy	j/kgmol-k	constant	5731.7471
Reference Temperature	k	constant	298
L-J Characteristic Length	angstrom	constant	2
L-J Energy Parameter	k	constant	10
Degrees of Freedom		constant	0
Speed of Sound	m/s	none	#f

Material: (water-vapor . mixture-template) (fluid)

Property	Units	Method	Value (s)
Cp (Specific Heat)	j/kg-k	constant	2014
Molecular Weight	kg/kgmol	constant	18.01534
Standard State Enthalpy	j/kgmol	constant	-2.418379e+08
Standard State Entropy	j/kgmol-k	constant	188696.44
Reference Temperature	k	constant	298.15
L-J Characteristic Length	angstrom	constant	2.605
L-J Energy Parameter	k	constant	572.4
Degrees of Freedom		constant	0
Speed of Sound	m/s	none	#f

Material: (oxygen . mixture-template) (fluid)

Property	Units	Method	Value (s)
Cp (Specific Heat)	j/kg-k	constant	919.31
Molecular Weight	kg/kgmol	constant	31.9988
Standard State Enthalpy	j/kgmol	constant	0
Standard State Entropy	j/kgmol-k	constant	205026.86
Reference Temperature	k	constant	298.15
L-J Characteristic Length	angstrom	constant	3.458
L-J Energy Parameter	k	constant	107.4
Degrees of Freedom		constant	0
Speed of Sound	m/s	none	#f

Material: (carbon-monoxide . mixture-template) (fluid)

Property	Units	Method	Value (s)
Cp (Specific Heat)	j/kg-k	constant	1043
Molecular Weight	kg/kgmol	constant	28.01055
Standard State Enthalpy	j/kgmol	constant	-1.1053956e+08
Standard State Entropy	j/kgmol-k	constant	197531.64
Reference Temperature	k	constant	298.14999
L-J Characteristic Length	angstrom	constant	3.5899999
L-J Energy Parameter	k	constant	88
Degrees of Freedom		constant	0
Speed of Sound	m/s	none	#f

Material: (carbon-dioxide . mixture-template) (fluid)

Property	Units	Method	Value (s)
Cp (Specific Heat)	j/kg-k	constant	840.37
Molecular Weight	kg/kgmol	constant	44.00995
Standard State Enthalpy	j/kgmol	constant	-3.9353235e+08

Standard State Entropy	j/kgmol-k	constant	213720.2
Reference Temperature	k	constant	298.15
L-J Characteristic Length	angstrom	constant	3.941
L-J Energy Parameter	k	constant	195.2
Degrees of Freedom		constant	0
Speed of Sound	m/s	none	#f

Material: carbon-solid (fluid)

Property	Units	Method	Value(s)
Density	kg/m3	constant	2000
Cp (Specific Heat)	j/kg-k	constant	1220
Thermal Conductivity	w/m-k	constant	0.0454
Viscosity	kg/m-s	constant	1.72e-05
Molecular Weight	kg/kgmol	constant	12.01115
Standard State Enthalpy	j/kgmol	constant	-101.268
Standard State Entropy	j/kgmol-k	constant	5731.747
Reference Temperature	k	constant	298
L-J Characteristic Length	angstrom	constant	0
L-J Energy Parameter	k	constant	0
Thermal Expansion Coefficient	1/k	constant	0
Degrees of Freedom		constant	0
Speed of Sound	m/s	none	#f

Material: carbon-monoxide (fluid)

Property	Units	Method	Value(s)
Density	kg/m3	constant	1.1233
Cp (Specific Heat)	j/kg-k	constant	1043
Thermal Conductivity	w/m-k	constant	0.025
Viscosity	kg/m-s	constant	1.75e-05
Molecular Weight	kg/kgmol	constant	28.01055
Standard State Enthalpy	j/kgmol	constant	-1.1053956e+08
Standard State Entropy	j/kgmol-k	constant	197531.64
Reference Temperature	k	constant	298.15
L-J Characteristic Length	angstrom	constant	0
L-J Energy Parameter	k	constant	0
Thermal Expansion Coefficient	1/k	constant	0
Degrees of Freedom		constant	0
Speed of Sound	m/s	none	#f

Material: carbon-dioxide (fluid)

Property	Units	Method	Value(s)
Density	kg/m3	constant	1.7878
Cp (Specific Heat)	j/kg-k	constant	840.37
Thermal Conductivity	w/m-k	constant	0.0145
Viscosity	kg/m-s	constant	1.37e-05
Molecular Weight	kg/kgmol	constant	44.00995
Standard State Enthalpy	j/kgmol	constant	-3.9353235e+08
Standard State Entropy	j/kgmol-k	constant	213720.2
Reference Temperature	k	constant	298.15
L-J Characteristic Length	angstrom	constant	3.941
L-J Energy Parameter	k	constant	195.2
Thermal Expansion Coefficient	1/k	constant	0
Degrees of Freedom		constant	0
Speed of Sound	m/s	none	#f

Material: (oxygen . mixture-template-new) (fluid)

Property	Units	Method	Value(s)
Density	kg/m3	constant	1.2999
Cp (Specific Heat)	j/kg-k	constant	919.31
Thermal Conductivity	w/m-k	constant	0.0246
Viscosity	kg/m-s	constant	1.919e-05
Molecular Weight	kg/kgmol	constant	31.9988
Standard State Enthalpy	j/kgmol	constant	0


```

-----
Mixture Species                                names                ((n2 co2 co o2 h2o he)
(c<s>) ())
Reaction                                         finite-rate          ((reaction-1 ((c<s> 1 0
1) (o2 0.69999999 1 1)) ((co2 0.40000001 0 1) (co 0.60000002 0 1)) ((n2 0 1) (h2o 0 1)
(he 0 1)) (stoichiometry 1c<s> + 0.69999999o2 --> 0.40000001co2 + 0.60000002co)
(arrhenius 9.9999998e+10 2.09e+08 0) (mixing-rate 4 0.5) (use-third-body-efficiencies? .
#f) (surface-reaction? . #t)) (reaction-2 ((o2 0.5 0.25 1) (co 1 1 1)) ((co2 1 0 1) (h2o
0 0.5 1)) ((n2 0 1) (he 0 1)) (stoichiometry 0.5o2 + 1co --> 1co2 + 0h2o) (arrhenius
2.24e+12 1.7e+08 0) (mixing-rate 4 0.5) (use-third-body-efficiencies? . #f)) (reaction-3
((co2 1 1 1)) ((co 1 0 1) (o2 0.5 0 1)) ((n2 0 1) (h2o 0 1) (he 0 1)) (stoichiometry 1co2
--> 1co + 0.5o2) (arrhenius 45000000 1.7e+08 0) (mixing-rate 4 0.5) (use-third-body-
efficiencies? . #f)) (reaction-4 ((c<s> 1 0 1) (co2 1 1 1)) ((co 2 0 1)) ((n2 0 1) (o2 0
1) (h2o 0 1) (he 0 1)) (stoichiometry 1c<s> + 1co2 --> 2co) (arrhenius 200 2.6e+08 0)
(mixing-rate 4 0.5) (use-third-body-efficiencies? . #f) (surface-reaction? . #t)))
Mechanism                                         reaction-mechs      ((mechanism-1 (reaction-
type . all) (reaction-list reaction-4 reaction-3 reaction-2 reaction-1) (site-info)))
Density                                           kg/m3               ideal-gas           #f
Cp (Specific Heat)                               j/kg-k              mixing-law          #f
Thermal Conductivity                             w/m-k               constant            0.045400001
Viscosity                                         kg/m-s              constant            1.72e-05
Mass Diffusivity                                 m2/s                kinetic-theory     #f
Thermal Expansion Coefficient                    1/k                 constant            0

```

Appendix 3: Model for UDF chemistry sensitivity study

Material Properties

Material: udf (mixture)

Property	Units	Method	Value(s)
Mixture Species		names	(h2o o2
co co2 n2) (c<s> ())			
Reaction		finite-rate	((r650 ((o2
0.76999998 1 1) (c<s> 1 0 1)) ((co 0.46000001 0 1) (co2 0.54000002 0 1)) ((h2o 0 1) (n2 0 1)) (stoichiometry 0.76999998o2 + 1c<s> --> 0.46000001co + 0.54000002co2) (arrhenius 2.9999999e+11 2.09e+08 0) (mixing-rate 4 0.5) (use-third-body-efficiencies? . #f) (surface-reaction? . #t)) (reaction-2 ((o2 0.5 0.25 1) (co 1 1 1)) ((co2 1 0 1) (h2o 0 0.5 1)) ((n2 0 1)) (stoichiometry 0.5o2 + 1co --> 1co2 + 0h2o) (arrhenius 2.24e+12 1.674e+08 0) (mixing-rate 4 0.5) (use-third-body-efficiencies? . #f) (reaction-3 ((co2 1 1 1)) ((co 1 0 1) (o2 0.5 0 1)) ((h2o 0 1) (n2 0 1)) (stoichiometry 1co2 --> 1co + 0.5o2) (arrhenius 45000000 1.674e+08 0) (mixing-rate 4 0.5) (use-third-body-efficiencies? . #f) (r675 ((o2 0.74000001 1 1) (c<s> 1 0 1)) ((co 0.51999998 0 1) (co2 0.47999999 0 1)) ((h2o 0 1) (n2 0 1)) (stoichiometry 0.74000001o2 + 1c<s> --> 0.51999998co + 0.47999999co2) (arrhenius 2.9999999e+11 2.09e+08 0) (mixing-rate 4 0.5) (use-third-body-efficiencies? . #f) (surface-reaction? . #t)) (r700 ((o2 0.71249998 1 1) (c<s> 1 0 1)) ((co 0.57499999 0 1) (co2 0.42500001 0 1)) ((h2o 0 1) (n2 0 1)) (stoichiometry 0.71249998o2 + 1c<s> --> 0.57499999co + 0.42500001co2) (arrhenius 2.9999999e+11 2.09e+08 0) (mixing-rate 4 0.5) (use-third-body-efficiencies? . #f) (surface-reaction? . #t)) (r725 ((o2 0.685 1 1) (c<s> 1 0 1)) ((co 0.63 0 1) (co2 0.37 0 1)) ((h2o 0 1) (n2 0 1)) (stoichiometry 0.685o2 + 1c<s> --> 0.63co + 0.37co2) (arrhenius 2.9999999e+11 2.09e+08 0) (mixing-rate 4 0.5) (use-third-body-efficiencies? . #f) (surface-reaction? . #t)) (r750 ((o2 0.66000003 1 1) (c<s> 1 0 1)) ((co2 0.32499999 0 1) (co 0.67000002 0 1)) ((h2o 0 1) (n2 0 1)) (stoichiometry 0.66000003o2 + 1c<s> --> 0.32499999co2 + 0.67000002co) (arrhenius 2.9999999e+11 2.09e+08 0) (mixing-rate 4 0.5) (use-third-body-efficiencies? . #f) (surface-reaction? . #t)) (r775 ((o2 0.64249998 1 1) (c<s> 1 0 1)) ((co 0.71499997 0 1) (co2 0.285 0 1)) ((h2o 0 1) (n2 0 1)) (stoichiometry 0.64249998o2 + 1c<s> --> 0.71499997co + 0.285co2) (arrhenius 2.9999999e+11 2.09e+08 0) (mixing-rate 4 0.5) (use-third-body-efficiencies? . #f) (surface-reaction? . #t)) (r800 ((o2 0.625 1 1) (c<s> 1 0 1)) ((co 0.75 0 1) (co2 0.25 0 1)) ((h2o 0 1) (n2 0 1)) (stoichiometry 0.625o2 + 1c<s> --> 0.75co + 0.25co2) (arrhenius 2.9999999e+11 1e+08 0) (mixing-rate 4 0.5) (use-third-body-efficiencies? . #f) (surface-reaction? . #t)) (r825 ((o2 0.60500002 0 1) (c<s> 1 0 1)) ((co2 0.215 0 1) (co 0.77999997 0 1)) ((h2o 0 1) (n2 0 1)) (stoichiometry 0.60500002o2 + 1c<s> --> 0.215co2 + 0.77999997co) (arrhenius 2.9999999e+11 2.09e+08 0) (mixing-rate 4 0.5) (use-third-body-efficiencies? . #f) (surface-reaction? . #t)) (r850 ((o2 0.59500003 1 1) (c<s> 1 0 1)) ((co 0.81 0 1) (co2 0.19 0 1)) ((h2o 0 1) (n2 0 1)) (stoichiometry 0.59500003o2 + 1c<s> --> 0.81co + 0.19co2) (arrhenius 2.9999999e+11 2.09e+08 0) (mixing-rate 4 0.5) (use-third-body-efficiencies? . #f) (surface-reaction? . #t)) (r875 ((o2 0.58249998 1 1) (c<s> 1 0 1)) ((co 0.83499998 0 1) (co2 0.16500001 0 1)) ((h2o 0 1) (n2 0 1)) (stoichiometry 0.58249998o2 + 1c<s> --> 0.83499998co + 0.16500001co2) (arrhenius 2.9999999e+11 2.09e+08 0) (mixing-rate 4 0.5) (use-third-body-efficiencies? . #f) (surface-reaction? . #t)) (r900 ((o2 0.57249999 1 1) (c<s> 1 0 1)) ((co 0.85500002 0 1) (co2 0.145 0 1)) ((h2o 0 1) (n2 0 1)) (stoichiometry 0.57249999o2 + 1c<s> --> 0.85500002co + 0.145co2) (arrhenius 2.9999999e+11 2.09e+08 0) (mixing-rate 4 0.5) (use-third-body-efficiencies? . #f) (surface-reaction? . #t))			
Mechanism		reaction-mechs	((mechanism-1
(reaction-type . all) (reaction-list r850 r825 r800 r775 r750 r725 r700 r675 r650 reaction-2 reaction-3 r875 r900) (site-info))			
Density	kg/m3	ideal-gas	#f
Cp (Specific Heat)	j/kg-k	mixing-law	#f
Thermal Conductivity	w/m-k	ideal-gas-mixing-law	#f
Viscosity	kg/m-s	mass-weighted-mixing-law	#f
Mass Diffusivity	m2/s	constant-dilute-appx	(2.88e-05)
Thermal Expansion Coefficient	1/k	constant	0

Material: (carbon-solid . udf) (fluid)

Property	Units	Method	Value(s)
----------	-------	--------	----------

Property	Units	Method	Value (s)
Cp (Specific Heat)	j/kg-k	constant	1220
Thermal Conductivity	w/m-k	constant	0.0454
Viscosity	kg/m-s	constant	1.72e-05
Molecular Weight	kg/kgmol	constant	12.01115
Standard State Enthalpy	j/kgmol	constant	-101.268
Standard State Entropy	j/kgmol-k	constant	5731.747
Reference Temperature	k	constant	298
L-J Characteristic Length	angstrom	constant	0
L-J Energy Parameter	k	constant	0
Degrees of Freedom		constant	0
Speed of Sound	m/s	none	#f

Material: (nitrogen . udf) (fluid)

Property	Units	Method	Value (s)
Cp (Specific Heat)	j/kg-k	constant	1040.67
Thermal Conductivity	w/m-k	constant	0.0242
Viscosity	kg/m-s	constant	1.663e-05
Molecular Weight	kg/kgmol	constant	28.0134
Standard State Enthalpy	j/kgmol	constant	0
Standard State Entropy	j/kgmol-k	constant	191494.78
Reference Temperature	k	constant	298.15
L-J Characteristic Length	angstrom	constant	3.621
L-J Energy Parameter	k	constant	97.53
Degrees of Freedom		constant	0
Speed of Sound	m/s	none	#f

Material: (carbon-dioxide . udf) (fluid)

Property	Units	Method	Value (s)
Cp (Specific Heat)	j/kg-k	constant	840.37
Thermal Conductivity	w/m-k	constant	0.0145
Viscosity	kg/m-s	constant	1.37e-05
Molecular Weight	kg/kgmol	constant	44.00995
Standard State Enthalpy	j/kgmol	constant	-3.9353235e+08
Standard State Entropy	j/kgmol-k	constant	213720.2
Reference Temperature	k	constant	298.15
L-J Characteristic Length	angstrom	constant	3.941
L-J Energy Parameter	k	constant	195.2
Degrees of Freedom		constant	0
Speed of Sound	m/s	none	#f

Material: (carbon-monoxide . udf) (fluid)

Property	Units	Method	Value (s)
Cp (Specific Heat)	j/kg-k	constant	1043
Thermal Conductivity	w/m-k	constant	0.025
Viscosity	kg/m-s	constant	1.75e-05
Molecular Weight	kg/kgmol	constant	28.01055
Standard State Enthalpy	j/kgmol	constant	-1.1053956e+08
Standard State Entropy	j/kgmol-k	constant	197531.64
Reference Temperature	k	constant	298.14999
L-J Characteristic Length	angstrom	constant	2
L-J Energy Parameter	k	constant	10
Degrees of Freedom		constant	0
Speed of Sound	m/s	none	#f

Material: (oxygen . udf) (fluid)

Property	Units	Method	Value (s)
Cp (Specific Heat)	j/kg-k	constant	919.31
Thermal Conductivity	w/m-k	constant	0.0246
Viscosity	kg/m-s	constant	1.919e-05
Molecular Weight	kg/kgmol	constant	31.9988
Standard State Enthalpy	j/kgmol	constant	0
Standard State Entropy	j/kgmol-k	constant	205026.86

Reference Temperature	k	constant	298.15
L-J Characteristic Length	angstrom	constant	3.458
L-J Energy Parameter	k	constant	107.4
Degrees of Freedom		constant	0
Speed of Sound	m/s	none	#f

Material: (water-vapor . udf) (fluid)

Property	Units	Method	Value (s)
Cp (Specific Heat)	j/kg-k	constant	2014
Thermal Conductivity	w/m-k	constant	0.0261
Viscosity	kg/m-s	constant	1.34e-05
Molecular Weight	kg/kgmol	constant	18.01534
Standard State Enthalpy	j/kgmol	constant	-2.418379e+08
Standard State Entropy	j/kgmol-k	constant	188696.44
Reference Temperature	k	constant	298.15
L-J Characteristic Length	angstrom	constant	2.605
L-J Energy Parameter	k	constant	572.4
Degrees of Freedom		constant	0
Speed of Sound	m/s	none	#f

Material: (carbon-solid . mixture-template) (fluid)

Property	Units	Method	Value (s)
Cp (Specific Heat)	j/kg-k	constant	1220
Molecular Weight	kg/kgmol	constant	12.01115
Standard State Enthalpy	j/kgmol	constant	-101.268
Standard State Entropy	j/kgmol-k	constant	5731.7471
Reference Temperature	k	constant	298
L-J Characteristic Length	angstrom	constant	2
L-J Energy Parameter	k	constant	10
Degrees of Freedom		constant	0
Speed of Sound	m/s	none	#f

Material: (carbon-dioxide . mixture-template) (fluid)

Property	Units	Method	Value (s)
Cp (Specific Heat)	j/kg-k	constant	840.37
Molecular Weight	kg/kgmol	constant	44.00995
Standard State Enthalpy	j/kgmol	constant	-3.9353235e+08
Standard State Entropy	j/kgmol-k	constant	213720.2
Reference Temperature	k	constant	298.15
L-J Characteristic Length	angstrom	constant	3.941
L-J Energy Parameter	k	constant	195.2
Degrees of Freedom		constant	0
Speed of Sound	m/s	none	#f

Material: (carbon-monoxide . mixture-template) (fluid)

Property	Units	Method	Value (s)
Cp (Specific Heat)	j/kg-k	constant	1043
Molecular Weight	kg/kgmol	constant	28.01055
Standard State Enthalpy	j/kgmol	constant	-1.1053956e+08
Standard State Entropy	j/kgmol-k	constant	197531.64
Reference Temperature	k	constant	298.14999
L-J Characteristic Length	angstrom	constant	3.5899999
L-J Energy Parameter	k	constant	88
Degrees of Freedom		constant	0
Speed of Sound	m/s	none	#f

Material: carbon-solid (fluid)

Property	Units	Method	Value (s)
Density	kg/m3	constant	2000
Cp (Specific Heat)	j/kg-k	constant	1220
Thermal Conductivity	w/m-k	constant	0.0454

Viscosity	kg/m-s	constant	1.72e-05
Molecular Weight	kg/kgmol	constant	12.01115
Standard State Enthalpy	j/kgmol	constant	-101.268
Standard State Entropy	j/kgmol-k	constant	5731.747
Reference Temperature	k	constant	298
L-J Characteristic Length	angstrom	constant	0
L-J Energy Parameter	k	constant	0
Thermal Expansion Coefficient	1/k	constant	0
Degrees of Freedom		constant	0
Speed of Sound	m/s	none	#f

Material: carbon-monoxide (fluid)

Property	Units	Method	Value(s)
Density	kg/m3	constant	1.1233
Cp (Specific Heat)	j/kg-k	constant	1043
Thermal Conductivity	w/m-k	constant	0.025
Viscosity	kg/m-s	constant	1.75e-05
Molecular Weight	kg/kgmol	constant	28.01055
Standard State Enthalpy	j/kgmol	constant	-1.1053956e+08
Standard State Entropy	j/kgmol-k	constant	197531.64
Reference Temperature	k	constant	298.15
L-J Characteristic Length	angstrom	constant	0
L-J Energy Parameter	k	constant	0
Thermal Expansion Coefficient	1/k	constant	0
Degrees of Freedom		constant	0
Speed of Sound	m/s	none	#f

Material: carbon-dioxide (fluid)

Property	Units	Method	Value(s)
Density	kg/m3	constant	1.7878
Cp (Specific Heat)	j/kg-k	constant	840.37
Thermal Conductivity	w/m-k	constant	0.0145
Viscosity	kg/m-s	constant	1.37e-05
Molecular Weight	kg/kgmol	constant	44.00995
Standard State Enthalpy	j/kgmol	constant	-3.9353235e+08
Standard State Entropy	j/kgmol-k	constant	213720.2
Reference Temperature	k	constant	298.15
L-J Characteristic Length	angstrom	constant	3.941
L-J Energy Parameter	k	constant	195.2
Thermal Expansion Coefficient	1/k	constant	0
Degrees of Freedom		constant	0
Speed of Sound	m/s	none	#f

Appendix 4: UDF for chemistry sensitivity study

```

/*****
Multiple reaction UDF that specifies different reaction rates
for different volumetric or surface chemical reactions
*****/
#include "udf.h"
#define W_O2 32.
#define W_C 12.
#define W_CO2 44.
#define W_CO 28.
#define W_H2O 18.
#define W_N2 28.
#define CONST_R 8.3144

/* ARRHENIUS CONSTANTS */
#define PRE_EXP 3.6e+12
#define ACTIVE 2.09e+08
#define BETA 0.0
double nO2, nH2O, nCO, nCO2, nN2;
double Mtot;
double rho;
real concenO2;

/* assume that :
* 0 = H2O
* 1 = O2
* 2 = CO
* 3 = CO2
* 4 = N2
* 5 = C solid
*/
/* Reaction Exponents */
#define O2_EXP 1.0

DEFINE_SR_RATE( name,f,t,r,mw,yi,rr)
{
/*If more than one reaction is defined, it is necessary to distinguish
between these using the names of the reactions. */
if (!strcmp(r->name, "r650"))
{
if ( F_T(f,t) < 948 )
{
/* Calculate Arrhenius reaction rate */

/*molar fractions of each specie*/
nO2 = ( yi[1] / W_O2 ) * ( 1 / ( ( yi[1] / W_O2 ) + ( yi[2] / W_CO ) +
(yi[3] / W_CO2 ) + ( yi[1] / W_H2O ) + ( yi[4] / W_N2 ) ) );
nH2O = ( yi[0] / W_H2O ) * ( 1 / ( ( yi[1] / W_O2 ) + ( yi[2] / W_CO ) +
(yi[3] / W_CO2 ) + ( yi[1] / W_H2O ) + ( yi[4] / W_N2 ) ) );
nCO = ( yi[2] / W_CO ) * ( 1 / ( ( yi[1] / W_O2 ) + ( yi[2] / W_CO ) +
(yi[3] / W_CO2 ) + ( yi[1] / W_H2O ) + ( yi[4] / W_N2 ) ) );
nCO2 = ( yi[3] / W_CO2 ) * ( 1 / ( ( yi[1] / W_O2 ) + ( yi[2] / W_CO ) +
(yi[3] / W_CO2 ) + ( yi[1] / W_H2O ) + ( yi[4] / W_N2 ) ) );
nN2 = ( yi[4] / W_N2 ) * ( 1 / ( ( yi[1] / W_O2 ) + ( yi[2] / W_CO ) +
(yi[3] / W_CO2 ) + ( yi[1] / W_H2O ) + ( yi[4] / W_N2 ) ) );

/* Mtot is the molar weight of the mixture*/
Mtot = (nO2 * W_O2) + (nCO * W_CO) + (nN2 * W_N2) + (nH2O * W_H2O) + (nCO2
* W_CO2);

/* rho is the density*/
rho = 288.16/F_T(f,t)*pow(10, (-1/18000))*1.2255;

```

```

        concenO2 = rho*yi[1]/mw[1];

        *rr = PRE_EXP*exp((-1*ACTIVE)/(8314.*F_T(f,t)))*pow(concenO2,O2_EXP);
    }
    else
    {
        *rr = 0 ;
    }
}
else if (!strcmp(r->name, "r675"))
{
    if (F_T(f,t) >= 50)
    {
/* Calculate Arrhenius reaction rate */

        /*molar fractions of each specie*/
        nO2 = ( yi[1] / W_O2 ) * ( 1 / ( ( yi[1] / W_O2 ) + ( yi[2] / W_CO ) +
(yi[3] / W_CO2 ) + ( yi[1] / W_H2O ) + ( yi[4] / W_N2 ) ) );
        nH2O = ( yi[0] / W_H2O ) * ( 1 / ( ( yi[1] / W_O2 ) + ( yi[2] / W_CO ) +
(yi[3] / W_CO2 ) + ( yi[1] / W_H2O ) + ( yi[4] / W_N2 ) ) );
        nCO = ( yi[2] / W_CO ) * ( 1 / ( ( yi[1] / W_O2 ) + ( yi[2] / W_CO ) +
(yi[3] / W_CO2 ) + ( yi[1] / W_H2O ) + ( yi[4] / W_N2 ) ) );
        nCO2 = ( yi[3] / W_CO2 ) * ( 1 / ( ( yi[1] / W_O2 ) + ( yi[2] / W_CO ) +
(yi[3] / W_CO2 ) + ( yi[1] / W_H2O ) + ( yi[4] / W_N2 ) ) );
        nN2 = ( yi[4] / W_N2 ) * ( 1 / ( ( yi[1] / W_O2 ) + ( yi[2] / W_CO ) +
(yi[3] / W_CO2 ) + ( yi[1] / W_H2O ) + ( yi[4] / W_N2 ) ) );

        /* Mtot is the molar weight of the mixture*/
        Mtot = (nO2 * W_O2) + (nCO * W_CO) + (nN2 * W_N2) + (nH2O * W_H2O) + (nCO2
* W_CO2);

        /* rho is the density*/
        rho = 288.16/F_T(f,t)*pow(10, (-1/18000))*1.2255;

        concenO2 = rho*yi[1]/mw[1];

        *rr = PRE_EXP*exp((-1*ACTIVE)/(8314.*F_T(f,t)))*pow(concenO2,O2_EXP);
    }
    else
    {
        *rr = 0;
    }
}
else if (!strcmp(r->name, "r700"))
{
    if (F_T(f,t) >= 973 && F_T(f,t) < 998)
    {
/* Calculate Arrhenius reaction rate */

        /*molar fractions of each specie*/
        nO2 = ( yi[1] / W_O2 ) * ( 1 / ( ( yi[1] / W_O2 ) + ( yi[2] / W_CO ) +
(yi[3] / W_CO2 ) + ( yi[1] / W_H2O ) + ( yi[4] / W_N2 ) ) );
        nH2O = ( yi[0] / W_H2O ) * ( 1 / ( ( yi[1] / W_O2 ) + ( yi[2] / W_CO ) +
(yi[3] / W_CO2 ) + ( yi[1] / W_H2O ) + ( yi[4] / W_N2 ) ) );
        nCO = ( yi[2] / W_CO ) * ( 1 / ( ( yi[1] / W_O2 ) + ( yi[2] / W_CO ) +
(yi[3] / W_CO2 ) + ( yi[1] / W_H2O ) + ( yi[4] / W_N2 ) ) );
        nCO2 = ( yi[3] / W_CO2 ) * ( 1 / ( ( yi[1] / W_O2 ) + ( yi[2] / W_CO ) +
(yi[3] / W_CO2 ) + ( yi[1] / W_H2O ) + ( yi[4] / W_N2 ) ) );
        nN2 = ( yi[4] / W_N2 ) * ( 1 / ( ( yi[1] / W_O2 ) + ( yi[2] / W_CO ) +
(yi[3] / W_CO2 ) + ( yi[1] / W_H2O ) + ( yi[4] / W_N2 ) ) );

        /* Mtot is the molar weight of the mixture*/
        Mtot = (nO2 * W_O2) + (nCO * W_CO) + (nN2 * W_N2) + (nH2O * W_H2O) + (nCO2
* W_CO2);

        /* rho is the density*/
        rho = 288.16/F_T(f,t)*pow(10, (-1/18000))*1.2255;

        concenO2 = rho*yi[1]/mw[1];

```

```

*rr = PRE_EXP*exp((-1*ACTIVE)/(8314.*F_T(f,t)))*pow(concenO2,O2_EXP);
}
else
{
*rr = 0;
}
}
else if (!strcmp(r->name, "r725"))
{
if (F_T(f,t) >= 998 && F_T(f,t) < 1023)
{
/* Calculate Arrhenius reaction rate */

/*molar fractions of each specie*/
nO2 = ( yi[1] / W_O2 ) * ( 1 / ( ( yi[1] / W_O2 ) + ( yi[2] / W_CO ) +
(yi[3] / W_CO2 ) + ( yi[1] / W_H2O ) + ( yi[4] / W_N2 ) ) );
nH2O = ( yi[0] / W_H2O ) * ( 1 / ( ( yi[1] / W_O2 ) + ( yi[2] / W_CO ) +
(yi[3] / W_CO2 ) + ( yi[1] / W_H2O ) + ( yi[4] / W_N2 ) ) );
nCO = ( yi[2] / W_CO ) * ( 1 / ( ( yi[1] / W_O2 ) + ( yi[2] / W_CO ) +
(yi[3] / W_CO2 ) + ( yi[1] / W_H2O ) + ( yi[4] / W_N2 ) ) );
nCO2 = ( yi[3] / W_CO2 ) * ( 1 / ( ( yi[1] / W_O2 ) + ( yi[2] / W_CO ) +
(yi[3] / W_CO2 ) + ( yi[1] / W_H2O ) + ( yi[4] / W_N2 ) ) );
nN2 = ( yi[4] / W_N2 ) * ( 1 / ( ( yi[1] / W_O2 ) + ( yi[2] / W_CO ) +
(yi[3] / W_CO2 ) + ( yi[1] / W_H2O ) + ( yi[4] / W_N2 ) ) );

/* Mtot is the molar weight of the mixture*/
Mtot = (nO2 * W_O2) + (nCO * W_CO) + (nN2 * W_N2) + (nH2O * W_H2O) + (nCO2
* W_CO2);

/* rho is the density*/
rho = 288.16/F_T(f,t)*pow(10, (-1/18000))*1.2255;

concenO2 = rho*yi[1]/mw[1];

*rr = PRE_EXP*exp((-1*ACTIVE)/(8314.*F_T(f,t)))*pow(concenO2,O2_EXP);
}
else
{
*rr = 0;
}
}
else if (!strcmp(r->name, "r750"))
{
if (F_T(f,t) >= 1023 && F_T(f,t) < 1048)
{
/* Calculate Arrhenius reaction rate */

/*molar fractions of each specie*/
nO2 = ( yi[1] / W_O2 ) * ( 1 / ( ( yi[1] / W_O2 ) + ( yi[2] / W_CO ) +
(yi[3] / W_CO2 ) + ( yi[1] / W_H2O ) + ( yi[4] / W_N2 ) ) );
nH2O = ( yi[0] / W_H2O ) * ( 1 / ( ( yi[1] / W_O2 ) + ( yi[2] / W_CO ) +
(yi[3] / W_CO2 ) + ( yi[1] / W_H2O ) + ( yi[4] / W_N2 ) ) );
nCO = ( yi[2] / W_CO ) * ( 1 / ( ( yi[1] / W_O2 ) + ( yi[2] / W_CO ) +
(yi[3] / W_CO2 ) + ( yi[1] / W_H2O ) + ( yi[4] / W_N2 ) ) );
nCO2 = ( yi[3] / W_CO2 ) * ( 1 / ( ( yi[1] / W_O2 ) + ( yi[2] / W_CO ) +
(yi[3] / W_CO2 ) + ( yi[1] / W_H2O ) + ( yi[4] / W_N2 ) ) );
nN2 = ( yi[4] / W_N2 ) * ( 1 / ( ( yi[1] / W_O2 ) + ( yi[2] / W_CO ) +
(yi[3] / W_CO2 ) + ( yi[1] / W_H2O ) + ( yi[4] / W_N2 ) ) );

/* Mtot is the molar weight of the mixture*/
Mtot = (nO2 * W_O2) + (nCO * W_CO) + (nN2 * W_N2) + (nH2O * W_H2O) + (nCO2
* W_CO2);

/* rho is the density*/
rho = 288.16/F_T(f,t)*pow(10, (-1/18000))*1.2255;

concenO2 = rho*yi[1]/mw[1];

*rr = PRE_EXP*exp((-1*ACTIVE)/(8314.*F_T(f,t)))*pow(concenO2,O2_EXP);
}
}
}
}

```



```

else
{
    *rr = 0;
}

else if (!strcmp(r->name, "r775"))
{
    if (F_T(f,t) >= 1048 && F_T(f,t) < 1073)
    {
/* Calculate Arrhenius reaction rate */

        /*molar fractions of each specie*/
        nO2 = ( yi[1] / W_O2 ) * ( 1 / ( ( yi[1] / W_O2 ) + ( yi[2] / W_CO ) +
(yi[3] / W_CO2 ) + ( yi[1] / W_H2O ) + ( yi[4] / W_N2 ) ) );
        nH2O = ( yi[0] / W_H2O ) * ( 1 / ( ( yi[1] / W_O2 ) + ( yi[2] / W_CO ) +
(yi[3] / W_CO2 ) + ( yi[1] / W_H2O ) + ( yi[4] / W_N2 ) ) );
        nCO = ( yi[2] / W_CO ) * ( 1 / ( ( yi[1] / W_O2 ) + ( yi[2] / W_CO ) +
(yi[3] / W_CO2 ) + ( yi[1] / W_H2O ) + ( yi[4] / W_N2 ) ) );
        nCO2 = ( yi[3] / W_CO2 ) * ( 1 / ( ( yi[1] / W_O2 ) + ( yi[2] / W_CO ) +
(yi[3] / W_CO2 ) + ( yi[1] / W_H2O ) + ( yi[4] / W_N2 ) ) );
        nN2 = ( yi[4] / W_N2 ) * ( 1 / ( ( yi[1] / W_O2 ) + ( yi[2] / W_CO ) +
(yi[3] / W_CO2 ) + ( yi[1] / W_H2O ) + ( yi[4] / W_N2 ) ) );

        /* Mtot is the molar weight of the mixture*/
        Mtot = (nO2 * W_O2) + (nCO * W_CO) + (nN2 * W_N2) + (nH2O * W_H2O) + (nCO2
* W_CO2);

        /* rho is the density*/
        rho = 288.16/F_T(f,t)*pow(10, (-1/18000))*1.2255;

        concenO2 = rho*yi[1]/mw[1];

        *rr = PRE_EXP*exp((-1*ACTIVE)/(8314.*F_T(f,t)))*pow(concenO2,O2_EXP);
    }
else
{
    *rr = 0;
}

else if (!strcmp(r->name, "r800"))
{
    if (F_T(f,t) >= 1073 && F_T(f,t) < 1098)
    {
/* Calculate Arrhenius reaction rate */

        /*molar fractions of each specie*/
        nO2 = ( yi[1] / W_O2 ) * ( 1 / ( ( yi[1] / W_O2 ) + ( yi[2] / W_CO ) +
(yi[3] / W_CO2 ) + ( yi[1] / W_H2O ) + ( yi[4] / W_N2 ) ) );
        nH2O = ( yi[0] / W_H2O ) * ( 1 / ( ( yi[1] / W_O2 ) + ( yi[2] / W_CO ) +
(yi[3] / W_CO2 ) + ( yi[1] / W_H2O ) + ( yi[4] / W_N2 ) ) );
        nCO = ( yi[2] / W_CO ) * ( 1 / ( ( yi[1] / W_O2 ) + ( yi[2] / W_CO ) +
(yi[3] / W_CO2 ) + ( yi[1] / W_H2O ) + ( yi[4] / W_N2 ) ) );
        nCO2 = ( yi[3] / W_CO2 ) * ( 1 / ( ( yi[1] / W_O2 ) + ( yi[2] / W_CO ) +
(yi[3] / W_CO2 ) + ( yi[1] / W_H2O ) + ( yi[4] / W_N2 ) ) );
        nN2 = ( yi[4] / W_N2 ) * ( 1 / ( ( yi[1] / W_O2 ) + ( yi[2] / W_CO ) +
(yi[3] / W_CO2 ) + ( yi[1] / W_H2O ) + ( yi[4] / W_N2 ) ) );

        /* Mtot is the molar weight of the mixture*/
        Mtot = (nO2 * W_O2) + (nCO * W_CO) + (nN2 * W_N2) + (nH2O * W_H2O) + (nCO2
* W_CO2);

        /* rho is the density*/
        rho = 288.16/F_T(f,t)*pow(10, (-1/18000))*1.2255;

        concenO2 = rho*yi[1]/mw[1];

        *rr = PRE_EXP*exp((-1*ACTIVE)/(8314.*F_T(f,t)))*pow(concenO2,O2_EXP);
    }
else

```

```

        {
            *rr = 0;
        }
    }

    else if (!strcmp(r->name, "r825"))
    {
        if (F_T(f,t) >= 1098 && F_T(f,t) < 1123)
        {
/* Calculate Arrhenius reaction rate */

            /*molar fractions of each specie*/
            nO2 = ( yi[1] / W_O2 ) * ( 1 / ( ( yi[1] / W_O2 ) + ( yi[2] / W_CO ) +
(yi[3] / W_CO2 ) + ( yi[1] / W_H2O ) + ( yi[4] / W_N2 ) ) );
            nH2O = ( yi[0] / W_H2O ) * ( 1 / ( ( yi[1] / W_O2 ) + ( yi[2] / W_CO ) +
(yi[3] / W_CO2 ) + ( yi[1] / W_H2O ) + ( yi[4] / W_N2 ) ) );
            nCO = ( yi[2] / W_CO ) * ( 1 / ( ( yi[1] / W_O2 ) + ( yi[2] / W_CO ) +
(yi[3] / W_CO2 ) + ( yi[1] / W_H2O ) + ( yi[4] / W_N2 ) ) );
            nCO2 = ( yi[3] / W_CO2 ) * ( 1 / ( ( yi[1] / W_O2 ) + ( yi[2] / W_CO ) +
(yi[3] / W_CO2 ) + ( yi[1] / W_H2O ) + ( yi[4] / W_N2 ) ) );
            nN2 = ( yi[4] / W_N2 ) * ( 1 / ( ( yi[1] / W_O2 ) + ( yi[2] / W_CO ) +
(yi[3] / W_CO2 ) + ( yi[1] / W_H2O ) + ( yi[4] / W_N2 ) ) );

            /* Mtot is the molar weight of the mixture*/
            Mtot = (nO2 * W_O2) + (nCO * W_CO) + (nN2 * W_N2) + (nH2O * W_H2O) + (nCO2
* W_CO2);

            /* rho is the density*/
            rho = 288.16/F_T(f,t)*pow(10, (-1/18000))*1.2255;

            concenO2 = rho*yi[1]/mw[1];

            *rr = PRE_EXP*exp((-1*ACTIVE)/(8314.*F_T(f,t)))*pow(concenO2,O2_EXP);
        }
    }
    else
    {
        *rr = 0;
    }
}

else if (!strcmp(r->name, "r850"))
{
    if (F_T(f,t) >= 1123 && F_T(f,t) < 1148)
    {
/* Calculate Arrhenius reaction rate */

            /*molar fractions of each specie*/
            nO2 = ( yi[1] / W_O2 ) * ( 1 / ( ( yi[1] / W_O2 ) + ( yi[2] / W_CO ) +
(yi[3] / W_CO2 ) + ( yi[1] / W_H2O ) + ( yi[4] / W_N2 ) ) );
            nH2O = ( yi[0] / W_H2O ) * ( 1 / ( ( yi[1] / W_O2 ) + ( yi[2] / W_CO ) +
(yi[3] / W_CO2 ) + ( yi[1] / W_H2O ) + ( yi[4] / W_N2 ) ) );
            nCO = ( yi[2] / W_CO ) * ( 1 / ( ( yi[1] / W_O2 ) + ( yi[2] / W_CO ) +
(yi[3] / W_CO2 ) + ( yi[1] / W_H2O ) + ( yi[4] / W_N2 ) ) );
            nCO2 = ( yi[3] / W_CO2 ) * ( 1 / ( ( yi[1] / W_O2 ) + ( yi[2] / W_CO ) +
(yi[3] / W_CO2 ) + ( yi[1] / W_H2O ) + ( yi[4] / W_N2 ) ) );
            nN2 = ( yi[4] / W_N2 ) * ( 1 / ( ( yi[1] / W_O2 ) + ( yi[2] / W_CO ) +
(yi[3] / W_CO2 ) + ( yi[1] / W_H2O ) + ( yi[4] / W_N2 ) ) );

            /* Mtot is the molar weight of the mixture*/
            Mtot = (nO2 * W_O2) + (nCO * W_CO) + (nN2 * W_N2) + (nH2O * W_H2O) + (nCO2
* W_CO2);

            /* rho is the density*/
            rho = 288.16/F_T(f,t)*pow(10, (-1/18000))*1.2255;

            concenO2 = rho*yi[1]/mw[1];

            *rr = PRE_EXP*exp((-1*ACTIVE)/(8314.*F_T(f,t)))*pow(concenO2,O2_EXP);
        }
    }
    else
    {

```

```

        *rr = 0;
    }
}

else if (!strcmp(r->name, "r875"))
{
    if (F_T(f,t) >= 1148 && F_T(f,t) < 1173)
    {
/* Calculate Arrhenius reaction rate */

        /*molar fractions of each specie*/
        nO2 = ( yi[1] / W_O2 ) * ( 1 / ( ( yi[1] / W_O2 ) + ( yi[2] / W_CO ) +
(yi[3] / W_CO2 ) + ( yi[1] / W_H2O ) + ( yi[4] / W_N2 ) ) );
        nH2O = ( yi[0] / W_H2O ) * ( 1 / ( ( yi[1] / W_O2 ) + ( yi[2] / W_CO ) +
(yi[3] / W_CO2 ) + ( yi[1] / W_H2O ) + ( yi[4] / W_N2 ) ) );
        nCO = ( yi[2] / W_CO ) * ( 1 / ( ( yi[1] / W_O2 ) + ( yi[2] / W_CO ) +
(yi[3] / W_CO2 ) + ( yi[1] / W_H2O ) + ( yi[4] / W_N2 ) ) );
        nCO2 = ( yi[3] / W_CO2 ) * ( 1 / ( ( yi[1] / W_O2 ) + ( yi[2] / W_CO ) +
(yi[3] / W_CO2 ) + ( yi[1] / W_H2O ) + ( yi[4] / W_N2 ) ) );
        nN2 = ( yi[4] / W_N2 ) * ( 1 / ( ( yi[1] / W_O2 ) + ( yi[2] / W_CO ) +
(yi[3] / W_CO2 ) + ( yi[1] / W_H2O ) + ( yi[4] / W_N2 ) ) );

        /* Mtot is the molar weight of the mixture*/
        Mtot = (nO2 * W_O2) + (nCO * W_CO) + (nN2 * W_N2) + (nH2O * W_H2O) + (nCO2
* W_CO2);

        /* rho is the density*/
        rho = 288.16/F_T(f,t)*pow(10, (-1/18000))*1.2255;

        concenO2 = rho*yi[1]/mw[1];

        *rr = PRE_EXP*exp((-1*ACTIVE)/(8314.*F_T(f,t)))*pow(concenO2,O2_EXP);
    }
else
    {
        *rr = 0;
    }
}
else if (!strcmp(r->name, "r900"))
{
    if (F_T(f,t) >= 1173)
    {
/* Calculate Arrhenius reaction rate */

        /*molar fractions of each specie*/
        nO2 = ( yi[1] / W_O2 ) * ( 1 / ( ( yi[1] / W_O2 ) + ( yi[2] / W_CO ) +
(yi[3] / W_CO2 ) + ( yi[1] / W_H2O ) + ( yi[4] / W_N2 ) ) );
        nH2O = ( yi[0] / W_H2O ) * ( 1 / ( ( yi[1] / W_O2 ) + ( yi[2] / W_CO ) +
(yi[3] / W_CO2 ) + ( yi[1] / W_H2O ) + ( yi[4] / W_N2 ) ) );
        nCO = ( yi[2] / W_CO ) * ( 1 / ( ( yi[1] / W_O2 ) + ( yi[2] / W_CO ) +
(yi[3] / W_CO2 ) + ( yi[1] / W_H2O ) + ( yi[4] / W_N2 ) ) );
        nCO2 = ( yi[3] / W_CO2 ) * ( 1 / ( ( yi[1] / W_O2 ) + ( yi[2] / W_CO ) +
(yi[3] / W_CO2 ) + ( yi[1] / W_H2O ) + ( yi[4] / W_N2 ) ) );
        nN2 = ( yi[4] / W_N2 ) * ( 1 / ( ( yi[1] / W_O2 ) + ( yi[2] / W_CO ) +
(yi[3] / W_CO2 ) + ( yi[1] / W_H2O ) + ( yi[4] / W_N2 ) ) );

        /* Mtot is the molar weight of the mixture*/
        Mtot = (nO2 * W_O2) + (nCO * W_CO) + (nN2 * W_N2) + (nH2O * W_H2O) + (nCO2
* W_CO2);

        /* rho is the density*/
        rho = 288.16/F_T(f,t)*pow(10, (-1/18000))*1.2255;

        concenO2 = rho*yi[1]/mw[1];

        *rr = PRE_EXP*exp((-1*ACTIVE)/(8314.*F_T(f,t)))*pow(concenO2,O2_EXP);
    }
else
    {
        *rr = 0;
    }
}
}

```

```
    }  
else  
{  
    /*      Message("Unknown Reaction\n"); */  
}  
/*  Message("Actual Reaction: %s\n", r->name); */  
  
}
```